CRC/ACI-Foundation Research Project

Optimization of Fiber-Reinforced Concrete using Data Mining

Final report

December 15th, 2023

Dr Emilio Garcia-Taengua
Associate Professor in Structures
University of Leeds
Leeds, England (United Kingdom)

UNIVERSITY OF LEEDS

Acknowledgments

I would like to express my gratitude, first of all, to the ACI Foundation for their generosity in funding this project and making it possible. Special thanks to Ann Masek for her kind support and understanding when things needed a bit more time.

I am forever grateful to my fellow members of the ACI Committee 544 Fiber-reinforced concrete for their support, the thought-provoking questions, the comments, suggestions, and words of encouragement in ACI conventions and so many videocalls.

A special word of thanks goes Mehdi Bakhshi, Liberato Ferrara, Jose R. Marti-Vargas and Pedro Serna for accepting to be members of the advisory panel for this project and for all their detailed feedback on progress reports and publications.

And thanks to my students, past and present, of the School of Civil Engineering at the University of Leeds, who inspire me so much. Special thanks to Ciaran Ryan and Rufus Burridge, whom I had the pleasure of supervising and contributed significantly to the first part of this project.

Table of contents

1. Descriptive analysis of the database of SFRC mixtures

1.1 Introduction

1.1.1 Context and scope of this chapter. The first part of this project was concerned with the compilation of a database of steel fiber reinforced concrete (SFRC) mixtures from papers published between the years 2000 and 2019. This chapter reports on the description and statistical analysis of the different variables included in said database, focusing on the relative amounts of the different constituents and those characteristics relevant to the proportioning of the mixtures, such as cement type, maximum aggregate size, and dimensions of the steel fibers.

1.1.2 Size and structure of the database. After an initial version of the database was completed, a preliminary analysis was carried out to detect and discard cases where the information was either clearly flawed or not consistent with most of the rest of the mixtures. Cases where most of the information regarding the mix proportions was missing were also discarded. The resulting, final database comprises 766 different cases. The list of all the sources from which this information was extracted is provided in appendix A.

The SFRC mixtures database is structured so that each row corresponds to a different SFRC mixture, and the columns correspond to the parameters describing the mixture proportions and other characteristics describing each mixture, including the characteristics of the fibers. Following the custom in data science, throughout this report the rows of the database (i.e. mixtures) are often referred to as 'cases', whilst the columns (i.e. mix proportions, type of cement, characteristics and dimensions of the fibers) are referred to as 'variables'.

1.1.3 Definition of variables. All variables concerned with the proportioning of the different mixture constituents are expressed in terms of the relative weight of the constituent per unit volume of concrete, in SI units (i.e. kg/m^3). These include the contents of: cement, water, limestone powder or filler, GGBS or slag, silica fume, fly ash, fine aggregate (particle size not higher than 4 mm), coarse aggregate (particle size higher than 4 mm), superplasticizer or high-range water-reducing admixture, air entrainer, retarder, and VMA. Additionally, the sum of cement, limestone powder, GGBS, silica fume and fly ash contents is stored in a variable called 'binder', and the difference between the binder content and the cement content is stored in a variable called 'SCMs', which stands for 'supplementary cementitious materials'.

The maximum aggregate size is expressed in millimeters (mm), and the type of cement is stored in a categorical variable, codified as CEM I, II, III, or IV in correspondence with the main categories as per European standards.

The fiber content of each mixture is expressed in terms of fiber volume fraction (V_f), in percentage. In addition to the fiber volume fraction, the following variables describing the characteristics of the fibers are also included in the database: fiber length and fiber diameter in millimeters (mm), aspect ratio, fiber strength (expressed in MPa), and fiber shape (using broadly descriptive terms such as hooked, or straight).

1.2 Treatment of missing values

1.2.1 Missing values in the database. The presence of missing data was inevitable because retrieving the values of all variables was not always possible, mostly due to the source of the data not reporting all the information. However, the prevalence of missing values in this database was low: 56.6% of the cases were complete, and overall only 7.8% of the information was missing, which was mostly concentrated on two variables: cement type and maximum aggregate size, as can be seen in Table 1.

Table 1. Percentage of missing values for selected variables.

Variable	Proportion of missing values
Cement type	42.1%
Maximum aggregate size	23.9%
Superplasticizer dosage	4.8%
Fine aggregate content	3.2%
Coarse aggregate content	3.2%
SCMs content	2.6%
Cement content	2.6%

1.2.2 Imputation of missing values. Imputation is the process by which missing values in a dataset are 'filled in' with estimates based on the exploitation of the correlations between variables, known relationships between them, characteristics of the information they represent, or a combination of the above.

Missing data regarding the cement type could not be remedied, due to the relatively high missingness percentage (42.1%) in addition to the categorical (non-quantitative) nature of the variable: correlations were not evident and no clear patterns of association with other variables were found.

On the other hand, the imputation of missing maximum aggregate size values was possible in most cases, and was done in different ways:

- Mixtures with no coarse aggregate. After the source papers were checked, it was found that some of these cases corresponded to UHPFRC mixtures, and in consequence the maximum aggregate size was set to 1 mm. On the other hand, mixtures which contained no coarse aggregate but were not reported as UHPFRC were assigned a maximum aggregate size of 4 mm, as this is the maximum aggregate size of fine aggregates.
- Mixtures with both fine and coarse aggregates. In these cases, a regression equation was used to estimate the maximum aggregate size as a function of the relative amounts of the other constituents. To that end, the subset of complete cases was considered, and the following equation was obtained, which was deemed sufficiently good for the purpose of imputation of missing values (R-squared=0.75):

$$Ln(m) = 25.72 - 117.7\frac{w}{c} + 126.7\left(\frac{w}{c}\right)^2 - 0.025G - 0.00001G^2 - 0.0094B + 0.0076S \qquad (1)$$

Where m is the maximum aggregate size (mm), S is the fine aggregate content, G is the coarse aggregate content, and B is the total binder content, all in kg/m^3.

The small percentage of cases (3.2%) where neither the fine aggregate nor the coarse aggregate contents were reported corresponded to papers which contained sufficient information to approximate such values as follows. The volumes of water, cement and SCMs in 1 m^3 of concrete were determined by dividing their relative amounts by their respective densities. Then, the volume of aggregates in 1 m^3 of concrete was determined by subtraction: 1,025 l/m^3 minus the volume of water, cement and SCMs. The volume of aggregates was then used to estimate the proportions of fine and coarse aggregates assuming Bolomey's curve for the combined grading of particles (aggregates, cement and SCMs), adopting a value of 12 for Bolomey's parameter. The fine aggregate content was calculated based on the proportion of particles up to 4 mm after excluding cement and SCMs. The coarse aggregate content was estimated as the difference between the total aggregates content and the fine aggregate content. A specific weight of 2.7 was assumed for both fine and coarse aggregates.

1.3 Composition of the binder

1.3.1 Type of cement. In almost 42% of the cases, the original sources did not report the type of cement. However, in 94% of the cases for which this information was available, the cement type was either CEM I or CEM II, and CEM I in particular was the most prevalent (Figure 1). In compiling this database, cement types were recorded according to the classification as per EN197-1. In some instances, cement types to different standards were reported, and where possible this information was assimilated to the EN197-1 framework for consistency. Often papers reporting the cement type also reported its strength class. However, due to the limited availability of this information, it was not possible to analyze the prevalence of cement types and strength classes in more detail.

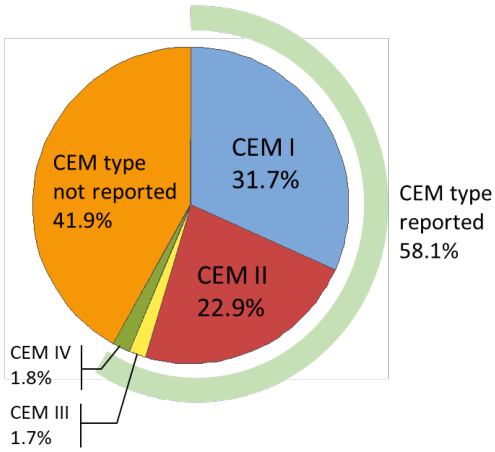

Figure 1. Pie chart showing the prevalence of cement types in the database.

1.3.2 Binder content. Figure 2 provides a graphical summary of the distribution of the binder content values in the database. The histogram in Figure 2 (the vertical axis shows number of cases) suggests that there are two subpopulations in the dataset: mixtures which have binder contents up to approximately 800 kg/m^3, and a second, less prominent set of mixtures, in which the binder content is very high.

The cumulative frequency diagram (CFD), on the right-hand side of Figure 2, shows the percentage of cases in which a particular value of the binder content is not exceeded. Horizontal

dashed lines corresponding to different cumulative percentages are shown for reference. The median is 450 kg/m^3, that is: the binder content is equal to or lower than 450 kg/m^3 in 50% of the cases. In 90% of the cases, the binder content is lower than 710 kg/m^3.

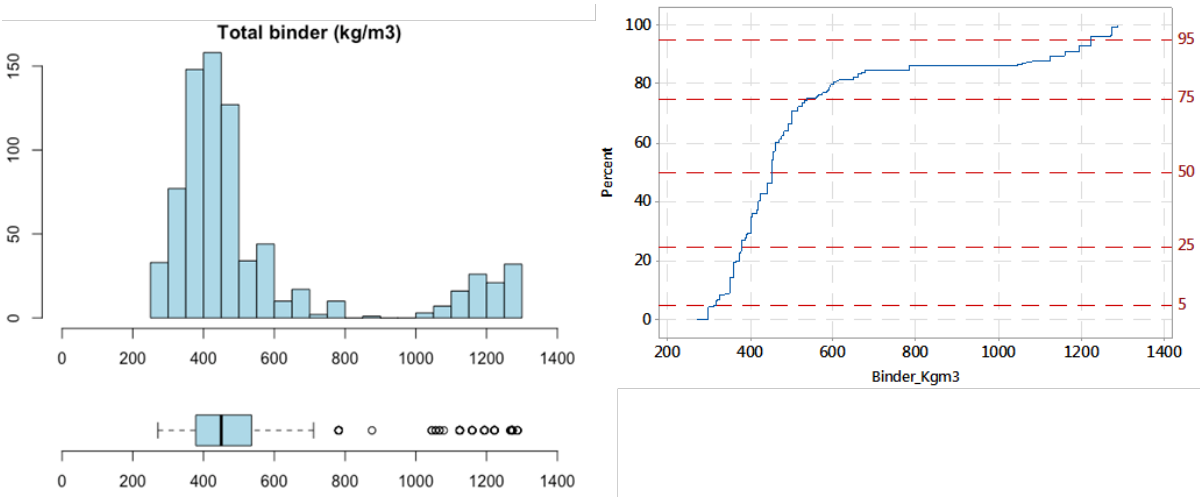

Figure 2. Histogram, CFD and boxplot for binder content (kg/m^3).

The boxplot in Figure 2 (on the left-hand side, below the histogram) shows whiskers extending to 271 and 711 kg/m^3. Binder contents outside that range can be tagged as potential outliers. Excluding those, the median is 440 kg/m^3, and in 90% of cases the binder content takes values between 300 and 638 kg/m^3.

1.3.3 Cement content. The distribution of the cement content values is shown in Figure 3. The median is 400 kg/m^3. In 90% of the cases in the database, the cement content ranges from 325 kg/m^3 to 678 kg/m^3. Considering the central 75% of the cases, the range is 360-485 kg/m^3. From the boxplot in Figure 3, it can be observed that the whiskers extend to 225 and 657 kg/m^3, which means that cement contents above 657 kg/m^3 are potential outliers as far as SFRC mixtures are concerned.

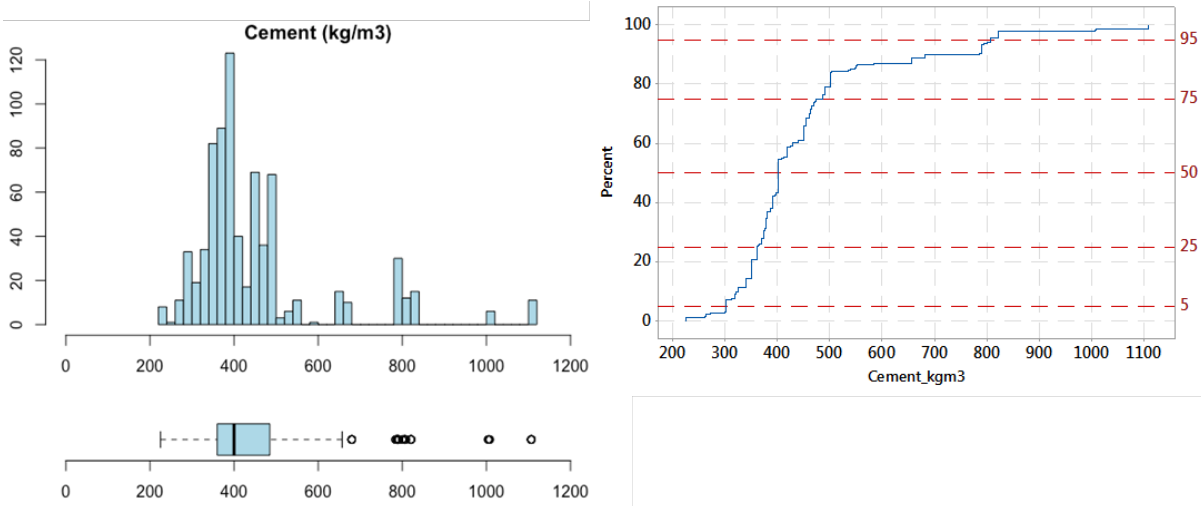

Figure 3. Histogram, CFD and boxplot for cement content (kg/m^3).

1.3.4 SCMs content. The distribution of the total SCMs content values is presented in Figure 4. Overall, 52.7% of the cases in the database corresponded to mixtures which incorporated no SCMs in addition to cement, and as a result the median is zero. A more representative median of the total amount of SCMs is obtained when only mixtures with SCMs are considered, and

that is 100kg/m^3. In fact, SCMs contents below 100kg/m^3 are the most prevalent in the SFRC database (in 75% of the cases in the database). In 90% of the cases, the total amount of SCMs is lower than 230 kg/m^3, and the boxplot in Figure 4 shows that, because of their skewed distribution, SCMs contents higher than 230 kg/m^3 can be considered outliers.

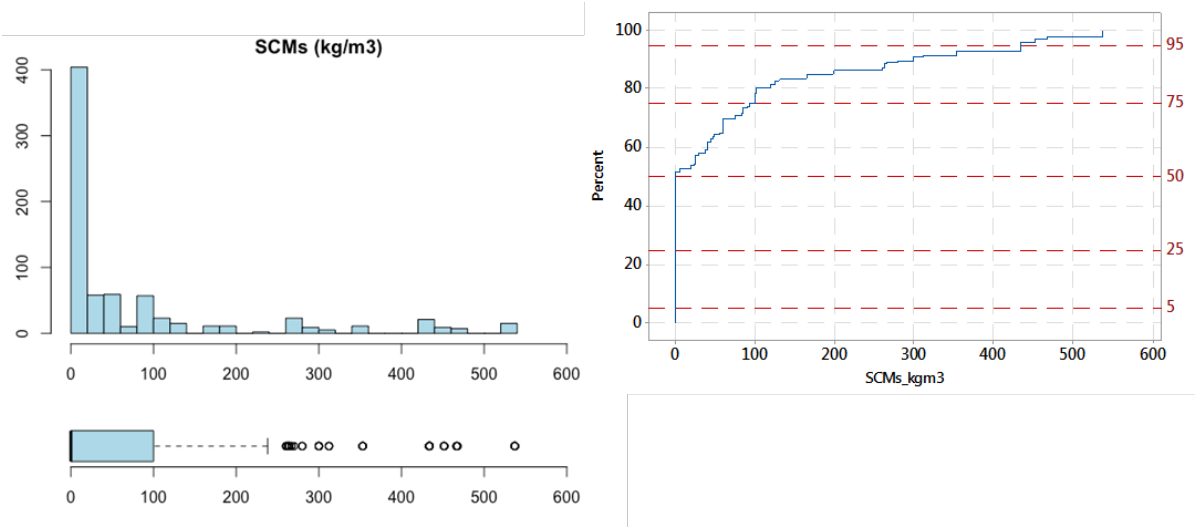

Figure 4. Histogram, CFD and boxplot for the total SCMs content (kg/m^3).

1.3.5 Water content. The values of the water content of the mixtures in the SFRC database are normally distributed, as shown by the histogram in Figure 5. The median water content is 180 kg/m^3. Since the whiskers in the boxplot extend to 125 and 252 kg/m^3, water contents higher than 252 kg/m^3 are outliers. In 90% of the SFRC mixtures in the database, the water content ranges from 140 to 237 kg/m^3.

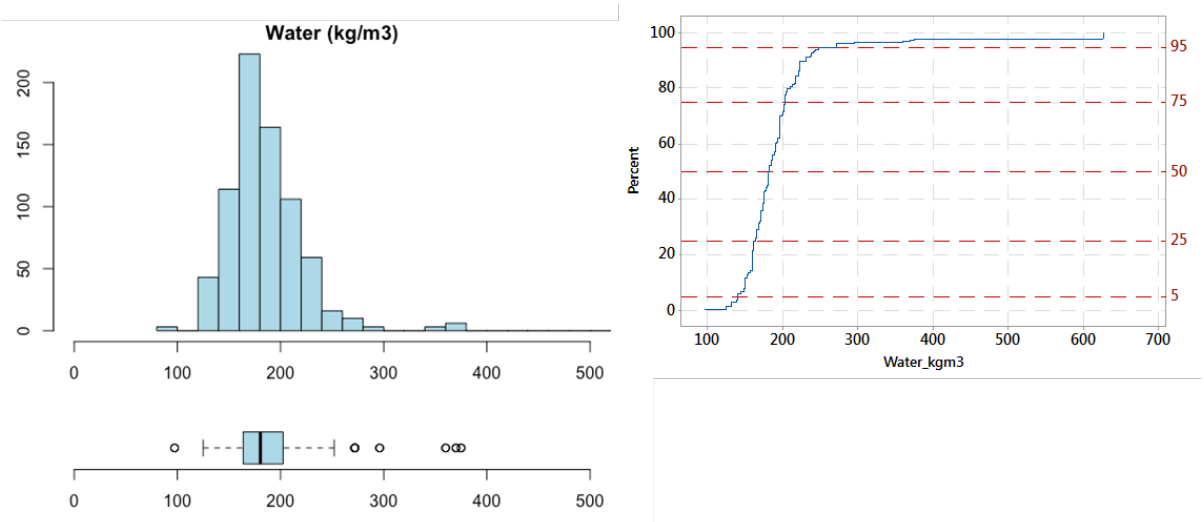

Figure 5. Histogram, CFD and boxplot for the water content (kg/m^3).

1.3.6 Water/Cement ratio. The plots in Figure 6 show the distribution of the values of the water/cement (*w/c*) ratio of the SFRC mixtures in the database. The histogram, on the left-hand side, shows that *w/c* values follow a normal distribution, except for some values higher than 0.7. The median *w/c* ratio is 0.45, and in 90% of the cases it takes values between 0.22 and 0.60. Values of the *w/c* ratio equal to or higher than 0.7 are potential outliers, as the whiskers in the boxplot below the histogram show.

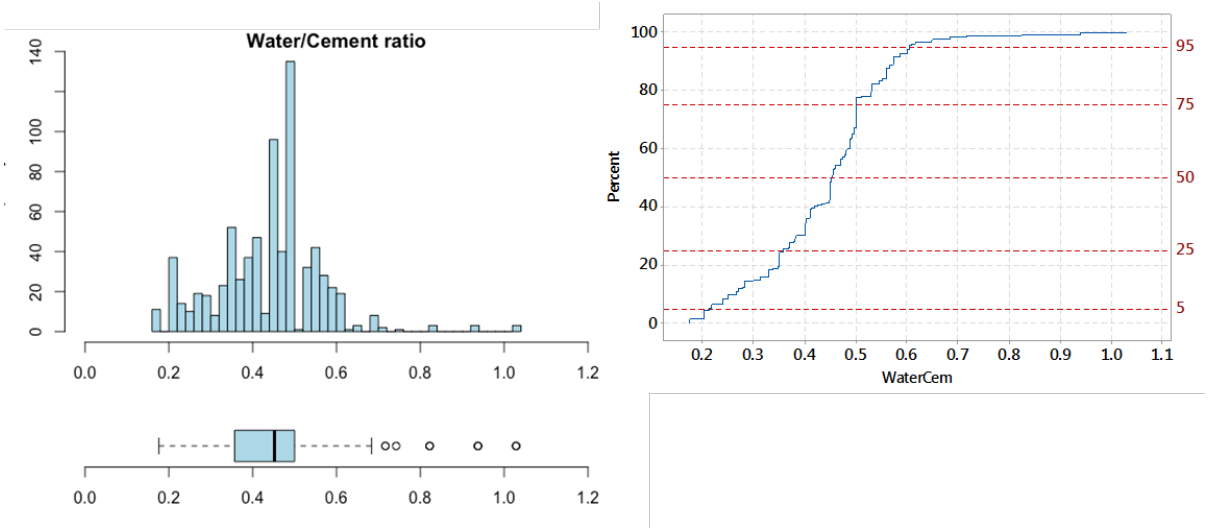

Figure 6. Histogram, CFD and boxplot for the water/cement ratio.

1.3.7 Superplasticizer content. The distribution of the values of superplasticizer content, in kg/m^3, is summarized in Figure 7. The histogram and the CFD plot show that 80% of the SFRC mixtures in the database include some amount of superplasticizers, indicating that this family of chemical admixtures is commonly used in the proportioning of SFRC mixtures to achieve good workability. The overall median is 3.5 kg/m^3, or 4.5 kg/m^3 if the cases with no superplasticizer are excluded. Superplasticizer contents higher than 16 kg/m^3 are outliers, as the boxplot shows.

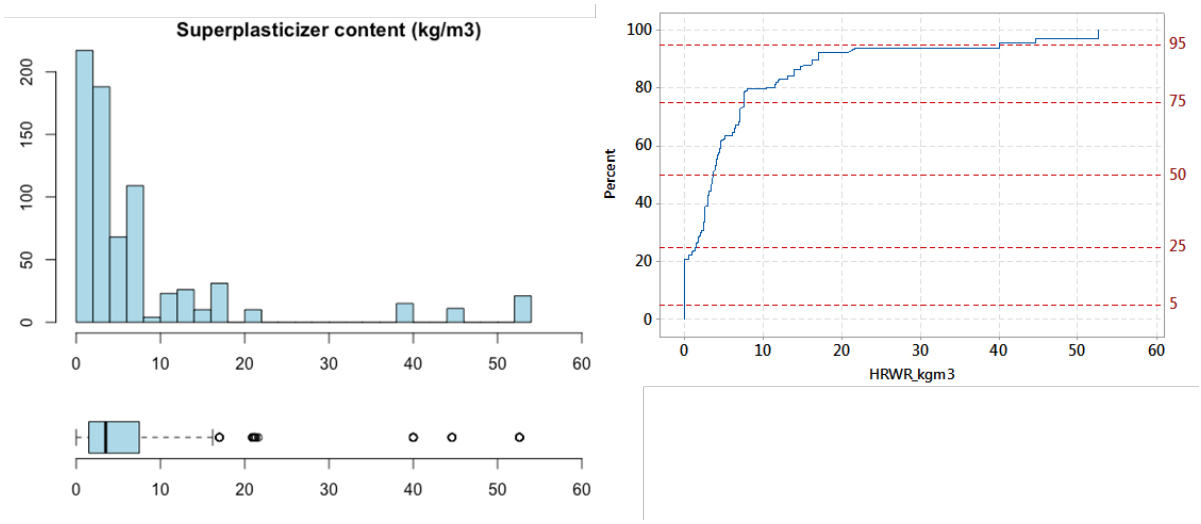

Figure 7. Histogram, CFD and boxplot for the superplasticizer content (kg/m^3).

As the histogram shows, the distribution is markedly skewed, confirming that small values are far more common than high values. This can be attributed to the fact that favoring minimal superplasticizer contents to control workability is advantageous for different reasons, such as: the risk of stability issues when superplasticizers are dosed in excess, their relatively high cost, or the diminishing returns when they are dosed beyond the saturation point. In fact, the ratio between superplasticizer and cement contents, taking the median values, is 4.5/400 = 1.125% over the weight of cement (o/cem), which is consistent with the typical values of the saturation point, which is generally between 1 and 1.5% o/cem.

1.4 Aggregates

1.4.1 Fine aggregate content. The relative amounts of fine aggregate in the SFRC mixtures in the database are normally distributed, as shown in Figure 8, apart from a few unusually high and low values. The median is 862 kg/m^3. Based on the 5th and 95th percentiles, fine aggregate contents range from 555kg/m^3 to 1539kg/m^3 in 90% of the cases. However, the boxplot of these values shows that fine aggregate contents outside of the range between 325 kg/m^3 and 1230 kg/m^3 are unusual and therefore potential outliers.

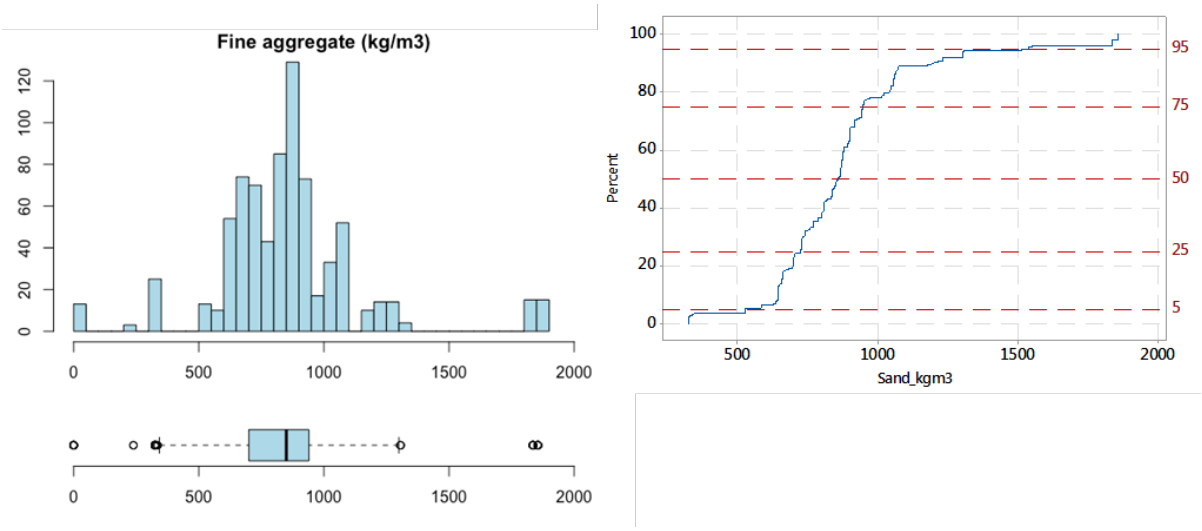

Figure 8. Histogram, CFD and boxplot for the fine aggregate content (kg/m^3).

1.4.2 Coarse aggregate content. The median coarse aggregate content is 821 kg/m^3. In 95% of the cases in the database, it takes values not higher than 1157 kg/m^3. As Figure 9 shows, 17.2% of the SFRC mixtures in the database had no coarse aggregate, which is consistent with the percentage of cases where the maximum aggregate size is 4 mm or lower (as shown in 1.4.3 and Figure 10). Considering only the SFRC mixtures which incorporate both fine and coarse aggregates, the median coarse aggregate content is 882 kg/m^3, and in 90% of the cases it ranges from 400 to 1157 kg/m^3. As per the boxplot in Figure 9, coarse aggregate contents equal to or higher than 1340 kg/m^3 are highly unusual and therefore can be considered outliers.

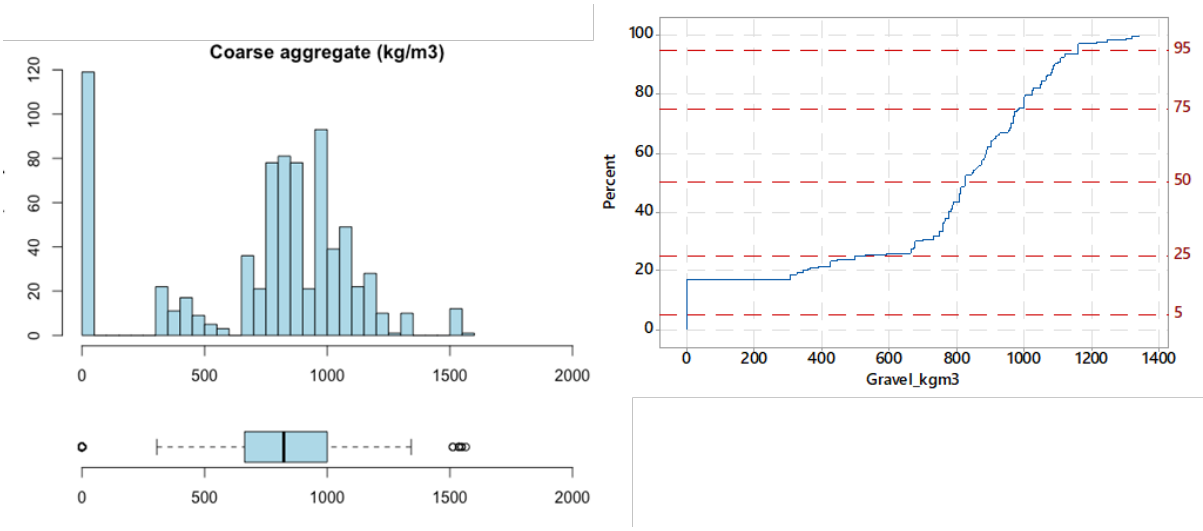

Figure 9. Histogram, CFD and boxplot for the coarse aggregate content (kg/m^3).

1.4.3 Maximum aggregate size (mm). Figure 10 summarizes the distribution of the maximum aggregate size values of the SFRC mixtures in the database. The median maximum aggregate size is 15 mm. In 95% of the cases, it is not higher than 20 mm. It is also relevant to note that, in 50% of the cases centered around the median value, the maximum aggregate size ranges from 10 mm to 16 mm. As the boxplot shows, values outside the range of 1 to 25 mm are outliers.

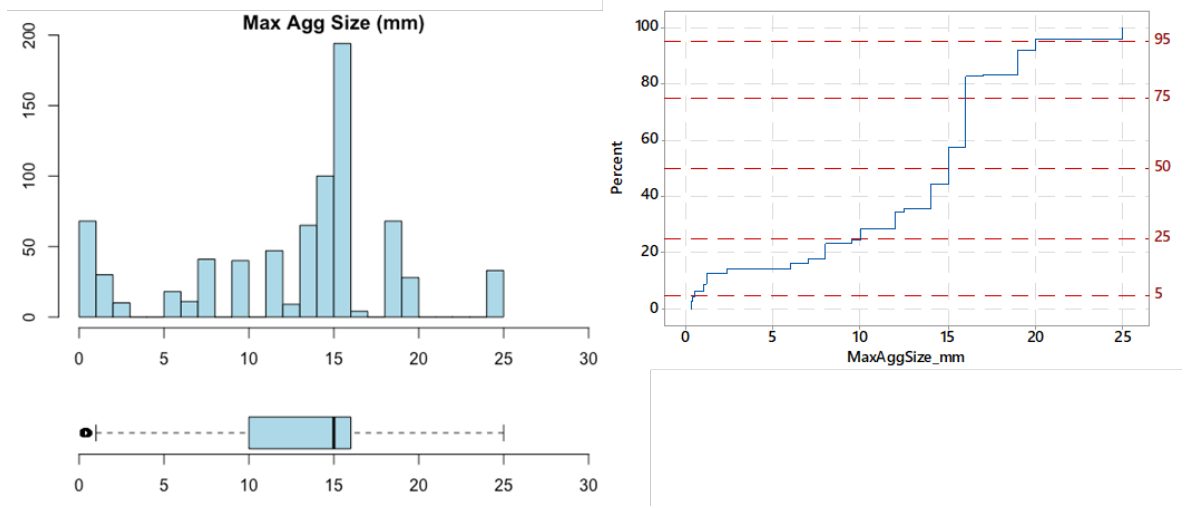

Figure 10. Histogram, CFD and boxplot for the maximum aggregate size (mm).

1.5 Steel fibers

1.5.1 Fiber volume fraction, V_f**.** Figure 11 shows that the distribution of the V_f values in the database is skewed, confirming that relatively low to moderate values are much more common than values on the higher end. The median is 0.51%, which means that the steel fiber volume fraction is not higher than 0.51% in 50% of the cases included the SFRC database. In 75% of the cases, V_f takes values between 0.38% and 1.0%, and in 90% of the cases it is lower than 1.6%. In those cases where the fiber volume fraction is higher than 1.6%, it very rarely exceeds 2%. As the boxplot in Figure 11 shows, values of the fiber volume fraction higher than 1.6% are potential outliers.

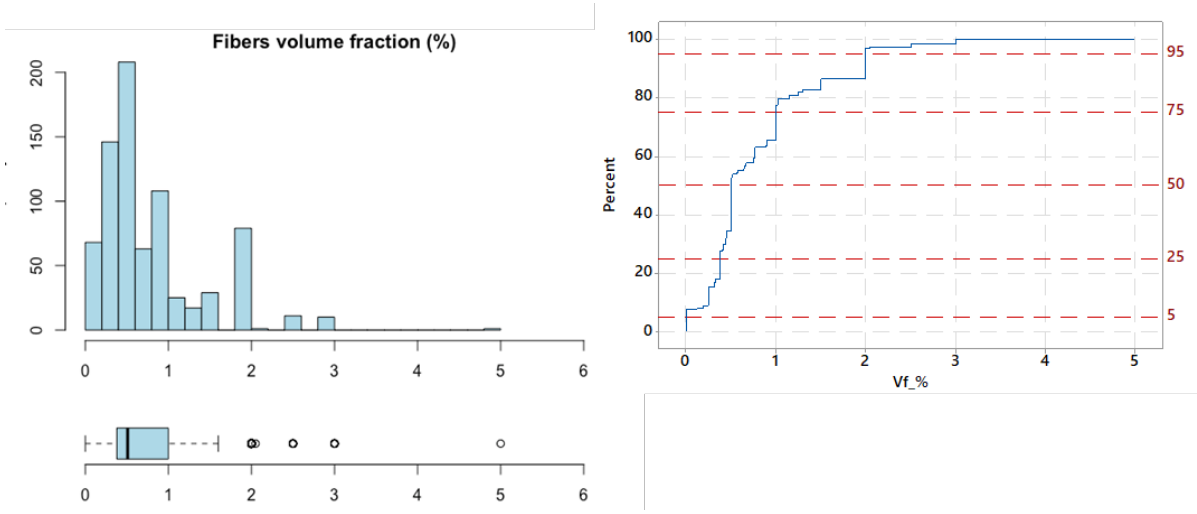

Figure 11. Histogram, CFD and boxplot for the steel fiber volume fraction.

1.5.2 Fiber length. The range of the fiber length values is shown in Figure 12. The apparent discontinuities suggested by the presence of peaks in the histogram and the corresponding steps in the CFD plot are simply due to the length of steel fibers being conditioned by the typical lengths which are commercially available. The typical fiber lengths are 30, 35, 50, and 60 mm, in correspondence with the peaks in the histogram, and the two most prevalent values in the SFRC database are 30 mm and 60 mm. The median fiber length is 45mm. Furthermore, the plots in Figure 12 also show that longer lengths are more prevalent: in 75% of the SFRC mixtures in the database, the steel fibers used are 30 mm-long or longer.

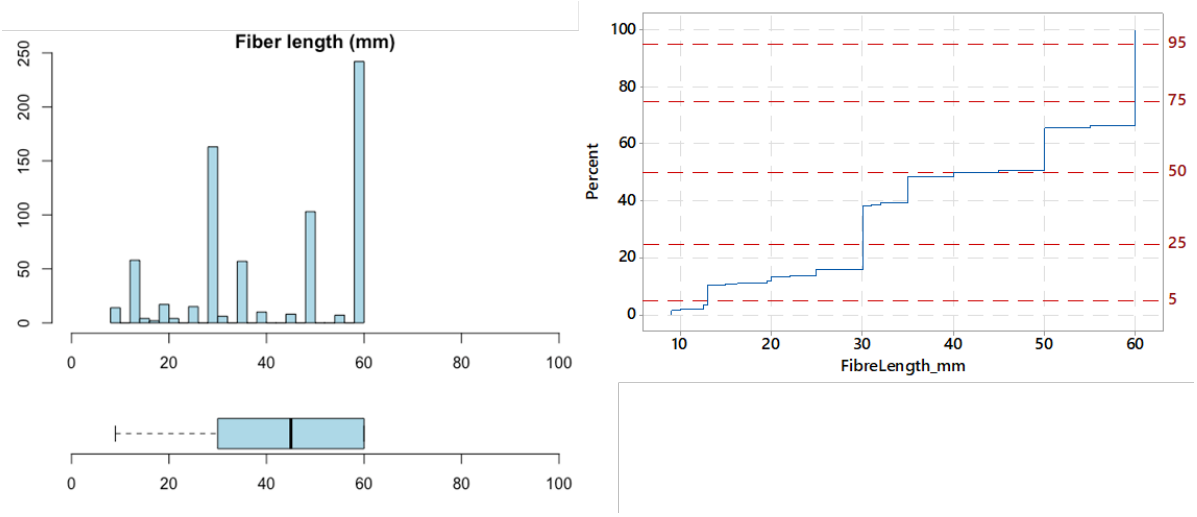

Figure 12. Histogram, CFD and boxplot for steel fiber length (mm).

1.5.3 Fiber aspect ratio. As shown in Figure 13, the aspect ratio of the steel fibers ranges from 45 to 80 in 90% of the SFRC mixtures in the database compiled in this study. The median aspect ratio is 65. Similarly to the fiber length, the apparent discontinuities in the histogram and CFD plot in Figure 13 are due to the commercially available steel fibers being set to certain values of the aspect ratio. In 90% of the cases, the aspect ratio takes values between 38 and 85. The whiskers of the boxplot indicate that aspect ratios outside of the 45-85 range are unusual.

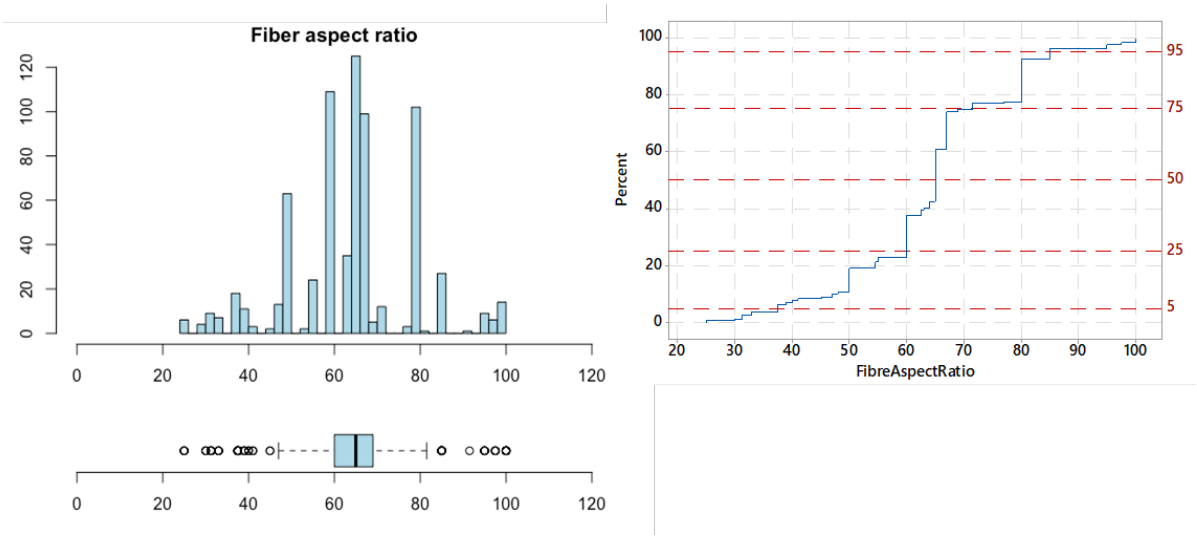

Figure 13. Histogram, CFD and boxplot for the aspect ratio of steel fibers.

2. Meta-analysis of SFRC mixtures and equations to guide the proportioning of SFRC

2.1 Introduction

The following sections are concerned with the analysis of the relationships that exist between the different variables describing the SFRC mixtures in the database in terms of the relative amounts of their constituents and the fundamental descriptors of such constituents. The exploration of the relationships between these and the residual flexural strength parameters is discussed separately, in chapter 5.

The methodological approach adopted for this analysis relies on the statistical technique known as multiple linear regression in order to obtain *explicit* equations that estimate some mix design variables as a function of others, with two (and equally relevant) objectives. Firstly, to be able to use these equations as guidance when proportioning SFRC mixtures. Secondly, to use them to produce different plots that can be used to interpret how the variation of some mix variables is associated with changes in others, and to quantify such variations.

Various attempts at the specification of the regression models were carried out until the best and most useful equations were identified., Although an overview of such preliminary analyses is given in some sections, this chapter does not present a detailed account of all the alternative specifications and modeling steps that. Rather, it focuses on those that turned out to be most useful in constituting a structured, coherent set of equations that can produce reasonable estimates to guide the proportioning of SFRC mixtures without being excessively complex.

2.2 Coarse-to-fine aggregate ratio

2.2.1 Justification. The coarse-to-fine aggregate ratio (*G/S*) was considered one of the key variables as it acts as a proxy for the combined grading of the aggregates in the SFRC mixture, which is in turn relevant to its cohesiveness. Initially, efforts were made to identify a relationship between the *G/S* ratio and the fiber dimensions and dosage, as it was thought that these parameters would directly affect the cohesiveness requirements for the fresh mixtures. However, it was found that there is little correlation between these variables and the *G/S* ratio, and the resulting equations had poor goodness-of-fit values. After exploring different options, the only two variables which showed a clear correlation with the *G/S* ratio turned out to be the maximum aggregate size and the coarse aggregate content.

2.2.2 General trends in the data and outliers. Figure 14 shows the scatterplot of the *G/S* ratios of the SFRC mixtures in the database against the corresponding coarse aggregate contents. A clear trend is observed, showing a direct, increasing relationship between the two variables. There were a few potential outliers, which are marked with an X in Figure 14, all overlapped under the same blue marker. These were identified as corresponding to fifteen cases in the database which had an unusually high binder content (1200 kg/m^3) and very low fine and coarse aggregate contents as a result (300 kg/m^3 and 600 kg/m^3, respectively). Having confirmed that they were indeed outliers, these cases were discarded before proceeding with the analysis.

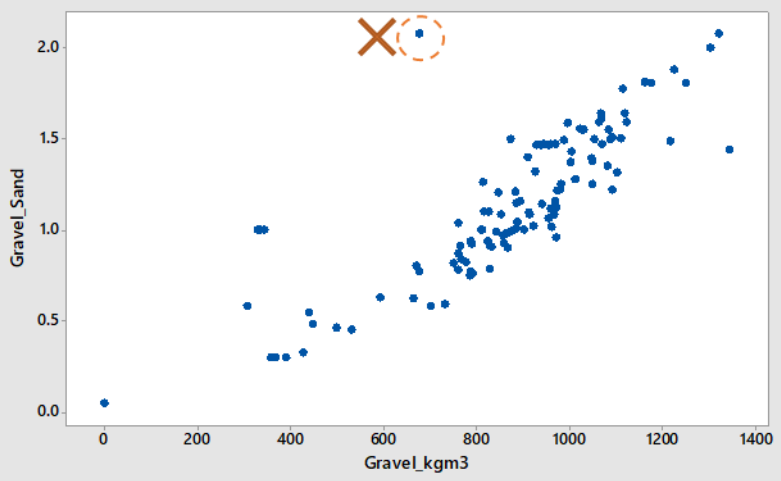

Figure 14. Coarse-to-fine aggregate ratio vs coarse aggregate content (kg/m^3).

2.2.3 Regression analysis and fitted equation. A multiple regression analysis was performed to find an expression relating the coarse-to-fine aggregate ratio to the coarse aggregate content and the maximum aggregate size. All quadratic terms and pairwise interactions (i.e. the coarse aggregate content times the maximum aggregate size) were initially considered. The equation was simplified by sequentially removing from the equation those terms that were not statistically significant, until an equation consisting of only statistically significant terms was obtained. This is the equation for the *G/S* ratio (R-squared = 0.92), with an error term of ±0.10:

$$\frac{G}{S} = (20.3 + 22.27\, m + 0.269\, G + 0.001\, G^2 - 0.029\, m\, G) \times 10^{-3} \pm 0.10 \qquad (2)$$

Where G and S are the coarse and fine aggregate contents respectively (in kg/m^3), and m is the maximum aggregate size (in mm).

Figure 15 shows the response surface obtained by plotting equation (2) against the coarse aggregate content and the maximum aggregate size.

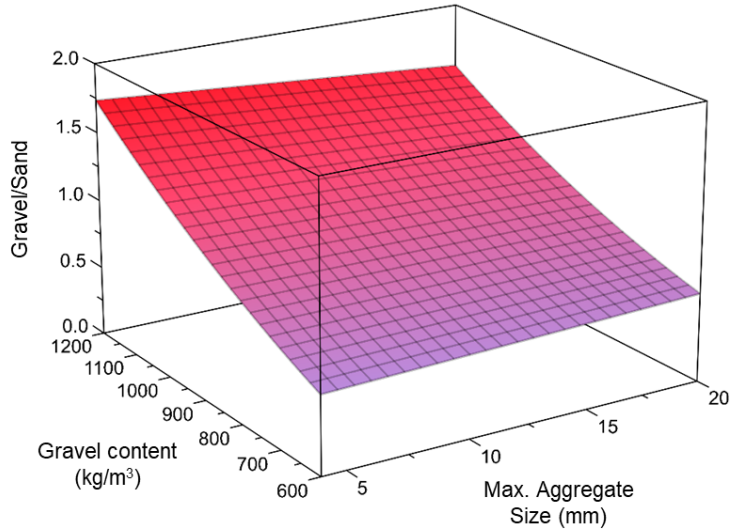

Figure 15. G/S ratio vs coarse aggregate content (kg/m^3) and maximum aggregate size (mm).

2.3 Coarse aggregate content

2.3.1 Justification and rationale. After modeling the *G/S* ratio, an investigation into the relative amounts of coarse and fine aggregate in the SFRC mixtures was necessary. The importance of the total aggregates content in relation to fresh and hardened state performance is evident, as it determines the relative volume of paste. Furthermore, the interaction between fibers and aggregates, given the marked difference between the shape and dimensions of aggregates and fibers, seemed to support the hypothesis that fibers would affect the aggregate contents, therefore indirectly affecting the *G/S* ratio.

Preliminary analyses were conducted to try and model the relative amounts of fine and coarse aggregate separately, as well as the total aggregate content, as a function of the other mix design variables, paying particular attention to the role of fibers. As an alternative modeling avenue, a modified total aggregate content was also considered where the coarse aggregate was weighted according to the maximum aggregate size. Regression analyses were carried out to model each of these parameters as a function of different subsets of the mix design variables, including interactions and quadratic terms. Stepwise regression and Box-Cox transformations were also trialed.

After all these efforts, it was concluded that the most satisfactory model (in terms of goodness of fit, parsimony, and avoidance of multicollinearity) was obtained for the coarse aggregate content.

2.3.2 Regression analysis and fitted equation. The regression analysis to model the coarse aggregate content as a function of the maximum aggregate size, fiber dimensions, and the fiber volume fraction, after considering all quadratic terms and interactions and removing all the statistically non-significant terms, yielded the following equation (R-squared = 0.76), with an error term of ±129 kg/m^3 for the estimate:

$$G = -95 - 2.21m^2 + V_f\left(4.15l_f - 1.35\lambda_f - 6.44m\right) + m(120 - 0.15l_f - 0.22\lambda_f) \pm 129 \qquad (3)$$

Where G is the coarse aggregate content (kg/m^3), m is the maximum aggregate size (mm), V_f is the fiber volume fraction (percentage), l_f is the fiber length (mm), and λ_f is the fiber aspect ratio.

The following sections are concerned with the interpretation of the trends followed by the coarse aggregate contents in the SFRC mixtures in the database as described by equation (3), with respect to the maximum aggregate size and the fiber length, aspect ratio and volume fraction.

2.3.3 Fiber dimensions and coarse aggregate content. Figure 16 shows the contour plots for the coarse aggregate content against the fiber length and aspect ratio, obtained by plotting equation (3) assuming four different values for the fiber volume fraction: 0.25%, 0.5%, 1.0% and 1.5%.

It can be observed that the effect of the fiber length and aspect ratio on the coarse aggregate content changes with the fiber volume fraction. In SFRC mixtures with low or moderate fiber contents (Figure 16, a and b), the fiber aspect ratio is the determining factor: lower aspect ratios are associated with higher coarse aggregate contents. In SFRC mixtures with higher fiber

contents (Figure 16, c and d), both the length and the aspect ratio of fibers are associated with changes in the coarse aggregate content, and longer fibers are associated with higher coarse aggregate contents.

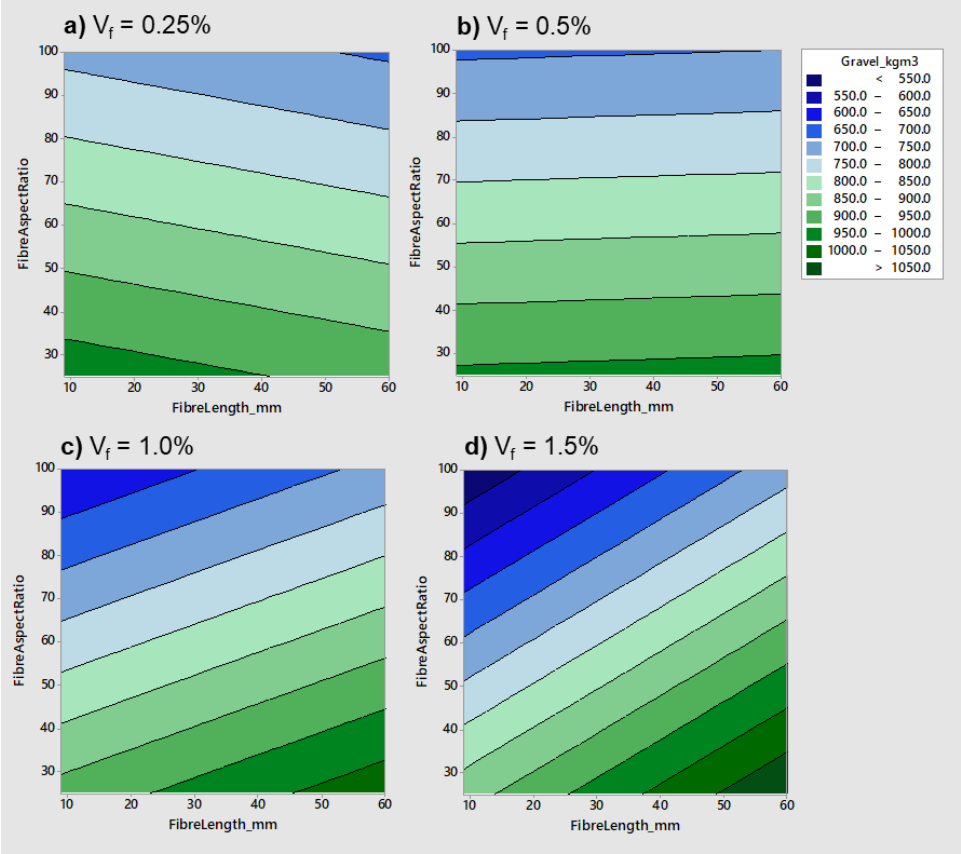

Figure 16. Contour plots for the coarse aggregate content against fiber length and aspect ratio, considering different fiber contents (max. aggregate size assumed as 14 mm).

The trends observed in Figure 16 can be explained in the following terms. Higher values of the fiber aspect ratio are associated with lower coarse aggregate contents, and therefore with a higher fine aggregate content and relative volume of paste in the SFRC mixture. This can be attributed to the fact that fibers with higher aspect ratios generally require the SFRC mixture to be more cohesive, which makes sense from the point of view of workability and fresh state stability (i.e. to prevent fiber balling and segregation). A similar reasoning is also applicable to the negative correlation between the fiber length and the coarse aggregate content: the use of shorter fibers, especially when in high contents, implies that the number of fibers per unit volume of concrete is high, hence requiring the mixture to be more cohesive, which translates into more fine aggregate and paste, thus less coarse aggregate.

In the discussion above, reference has been made to two intuitive scenarios: on one hand, 'low or moderate' fiber contents, and on the other hand, 'high' fiber contents. From Figure 16, the limit between the two seems to be at a a volume fraction of approximately 0.6-0.7%. A precise estimate for this value can be obtained by using equation (3). Finding out such value is equivalent to answering the following question: *above which V_f value does the effect of fiber length on the coarse aggregate content start to be more pronounced?* The answer to this question is obtained by differentiating the coarse aggregate content, as modeled by equation

(3), with respect to the variable fiber length, and equating this derivative to zero. The result, not surprisingly, depends on the maximum aggregate size (m):

$$\frac{\partial G}{\partial l_f} = 0 \;;\; 4.153V_f - 0.148m = 0 \rightarrow V_f = \begin{cases} 0.36\% \;\; if \; m = 10mm \\ 0.54\% \;\; if \; m = 15mm \\ 0.71\% \;\; if \; m = 20mm \end{cases} \quad (4)$$

2.3.4 Fiber dosage and coarse aggregate content. Equation (3) can be used to produce a different contour plot to examine the association between different values of the fiber dosage and the coarse aggregate content, for different fiber lengths. This contour plot is shown in Figure 17 (left). Two dashed lines are shown for reference. The horizontal line corresponds to the fiber volume fraction that is obtained by differentiating equation (3) with respect to the fiber length and then equating to zero, as per equation (4). The vertical line corresponds to the value of the fiber length that is obtained by differentiating equation (3) with respect to the fiber volume fraction and equating to zero. These two lines divide the contour plot into four quadrants or regions around the central saddle point, as shown in Figure 17 (right), which facilitates the interpretation of the contour plot in a detailed, systematic way. These regions have been numbered as 1, 2, 3, and 4.

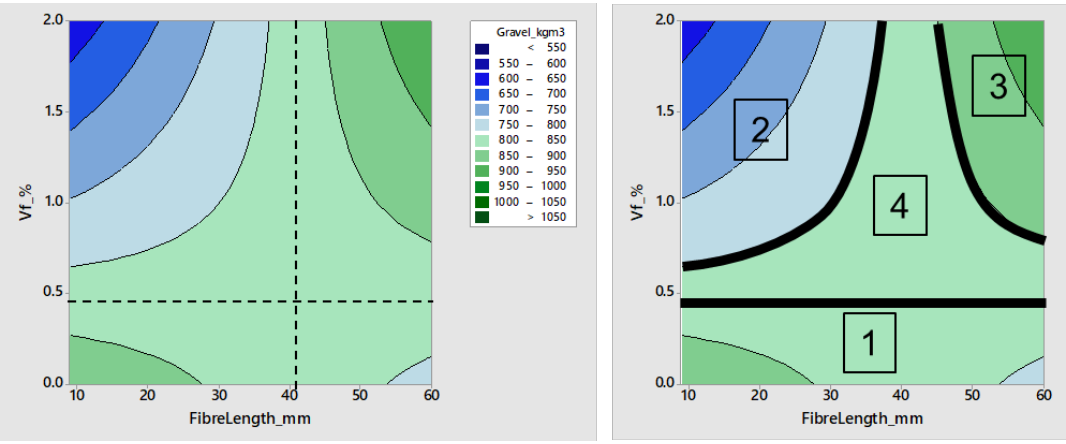

Figure 17. Coarse aggregate content against fiber length and volume fraction (aspect ratio assumed as 64, max. aggregate size assumed as 14 mm).

Region 1 includes those cases where the fiber volume fraction is below the threshold value as per equation (4). In Figure 17, a value of 14 mm has been assumed for the maximum aggregate size, and therefore the threshold fiber volume fraction is 0.49%. For fiber dosages up to that value, the coarse aggregate content is not very sensitive to changes in fiber length and takes values in the range of 800-850 kg/m^3. Coarse aggregate contents within this range are also compatible with higher fiber volume fractions when the fiber length is around 40 mm, which is region 4 in Figure 17. In summary, it can be concluded that coarse aggregate contents between 800 and 850 kg/m^3 are typical of SFRC mixtures with fibers of any length at low dosages, and also of SFRC mixtures with moderate to high fiber contents when the fibers used have a length of 35-45 mm.

On the other hand, region 2 shows that shorter fibers in moderate to high dosages are generally associated with coarse aggregate contents lower than 800 kg/m^3. This can be attributed to the fibers requiring the mixture to have a higher relative volume of fine aggregate and paste (and therefore less coarse aggregate content) in order to have sufficient cohesiveness. Finally, region 3 indicates that longer fibers, when incorporated in moderate to high dosages, are associated

with coarse aggregate contents higher than 850 kg/m^3. This can be interpreted in terms of longer fibers requiring higher values of the average particle size of the combined aggregates for better compatibility.

2.3.5 Coarse aggregate content and maximum aggregate size. The main effects plot for the coarse aggregate content with respect to the maximum aggregate size, as described by equation (3), is shown in Figure 18. This plot represents the mathematical expectation of the coarse aggregate content for different values of the maximum aggregate size, based on the information in the SFRC database. This is useful to illustrate the general trend in the relationship between these two mix design variables after having disaggregated the effect of the other variables in equation (3).

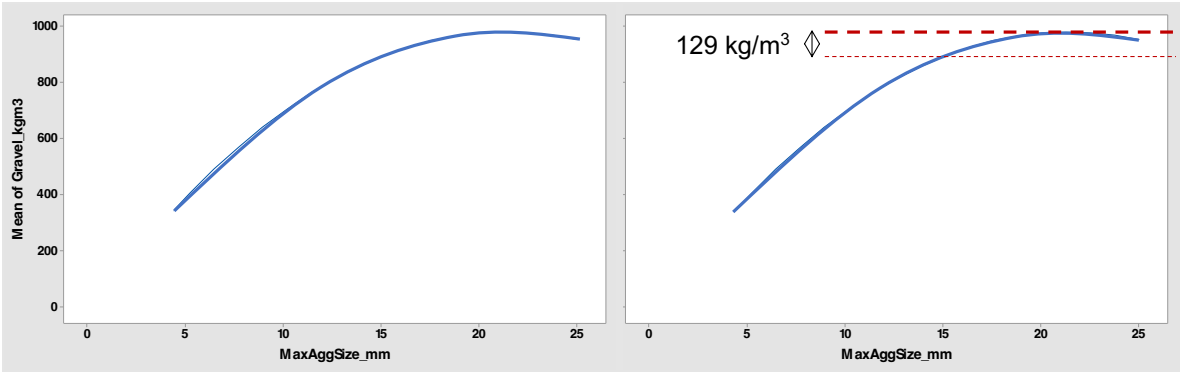

Figure 18. Coarse aggregate content vs maximum aggregate size.

It can be observed that higher values of the maximum aggregate size are associated with higher values of the coarse aggregate content, and that this relationship followed a quadratic trend. However, it is worth noting that, when the maximum aggregate size is 14 mm or higher, the curvature of this relationship is compatible with the coarse aggregate content not being affected by changes in the maximum aggregate size, as it falls within the margin of error associated with equation (3), as illustrated in Figure 18 (right). In consequence, it can be concluded that there is direct, although there is a clear positive correlation between the coarse aggregate content and the maximum aggregate size, changes in the maximum aggregate size when this is higher than 14 mm are not necessarily associated with changes in the coarse aggregate content.

2.4 Total binder content

2.4.1 Justification and rationale. After the statistical modeling and analysis of the relative proportions of aggregates, reported in 2.2 and 2.3, led to equations (2) and (3), it was realized that these expressions could be the first blocks of a data-driven set of equations that can guide the proportioning of SFRC mixtures. As per equation (3), the coarse aggregate content can be determined as a function of only the specified maximum aggregate size, the dimensions of the steel fibers and their volume fraction. Then, the coarse aggregate content and the maximum aggregate size can be used in equation (2) to estimate the coarse-to-fine aggregate ratio and, as a result, the fine aggregate content. Following on from these two equations, the next necessary step in this investigation was to try and obtain a model that allows for the determination of the amounts of cement and SCMs as a function of the maximum aggregate size, the dimensions and dosage of the steel fibers, and the fine aggregate and coarse aggregate contents.

Initially, the statistical modeling process was attempted for three response variables: total binder content, cement content only, and SCMs content only. In all three strategies, alternative models were trialed that initially considered all pairwise interactions and quadratic terms, followed by different model reduction procedures. The modeling of other parameters, such as the water-to-binder or water-to-cement ratios, was also explored. After these exploratory studies, it was concluded that the most satisfactory strategy in terms of goodness of fit, no multicollinearity and parsimony (e.g. simple specification) was to consider the total binder content, untransformed, as the response variable.

2.4.2 Regression analysis and fitted equation. The binder content (expressed in kg/m^3) was modeled by multiple linear regression analysis, initially as a function of the following variables: maximum aggregate size, fine and coarse aggregate contents, fiber length and aspect ratio, and fiber volume fraction. All quadratic and interaction terms were included in the first instance, and the model was simplified by stepwise regression. The following equation was obtained (R-squared = 0.90), with an error term of ±84 kg/m^3 for the binder content:

$$B = 262.1 - 6.11m + (19800S - 10.51S^2 - 4328G + 3.66G^2 - 7.45\,S \times G) \times 10^{-4} \pm 84 \quad (5)$$

Where B is the binder content (in kg/m^3), m is the maximum aggregate size (mm), and S, G are the fine aggregate and coarse aggregate contents (expressed in kg/m^3), respectively.

Interestingly, the variables related to the fibers (volume fraction, fiber length and aspect ratio) turned out not to have a statistically significant effect on the binder content, and that is the reason why they do not appear in equation (5). However, this does not mean that there is no association between the binder content of a SFRC mixture and the characteristics of the fibers: the effect of the fiber dimensions and dosage is already implicit in the other terms of equation (5), particularly the contents of fine and coarse aggregate. Firstly, the coarse aggregate content is a function of the fiber dimensions and dosage (equation (3), section 2.3). Secondly, the fine aggregate content depends on the coarse-to-fine aggregate content, which is a function of the coarse aggregate content (equation (2), section 2.2), which is, in turn, a function of the fiber dimensions and dosage (equation (3), section 2.3).

2.4.3 Model diagnosis and potential outliers. As mentioned in section 1.3.2, the descriptive analysis of the SFRC mixtures database identified as potential outliers those cases where the binder content is outside the 271-711 kg/m^3 range, and that these are not anomalous data but simply the result of there being a subset of cases with very high binder contents in the SFRC mixtures database. At this point in the analysis, it is necessary to check whether it is necessary to treat them separately in terms of the multiple linear regression analysis.

The plot of the binder content as per equation (5) against the actual binder contents of all the SFRC mixtures in the database is shown in Figure 19. For reference, the exact equivalence line (in blue) is also shown. This plot confirms that equation (5) estimates reasonably well the binder content in most cases, even when the binder content is outside the 271-711 kg/m^3 range. Therefore, none of the cases with unusually high binder contents were discarded.

The following sections are concerned with the discussion and interpretation of the sensitivity of binder contents with respect to the variables in equation (5), based on some contour plots in which the estimates produced by this equation are plotted against said variables.

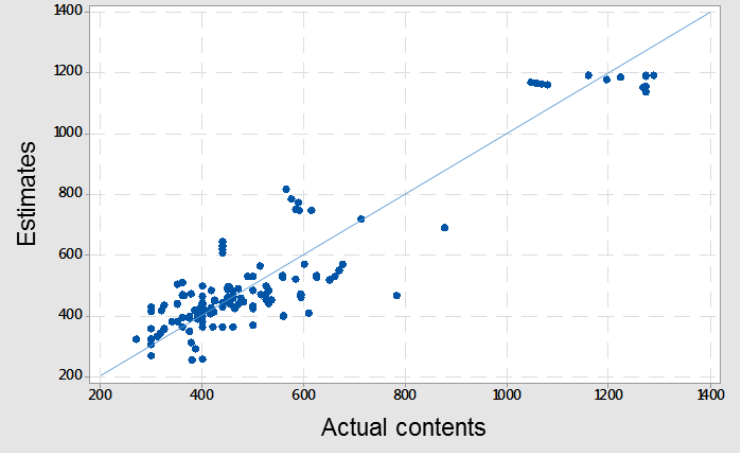

Figure 19. Binder content estimates vs actual binder contents (kg/m³).

2.4.4 Maximum aggregate size and binder content. Increasing the maximum aggregate size is associated with moderate reductions of the binder content. Interactions between the maximum aggregate size and other mix design variables do not have a statistically significant influence on the binder content. As a result, in equation (5) there is only one term that depends on the maximum aggregate size. As per equation (5), increasing the maximum aggregate size from 10 to 20 mm is associated with the binder content being, on average, 61 kg/m³ lower. For example, if a binder content of 450 kg/m³ is assumed, SFRC mixtures with a maximum aggregate size of 20 mm are expected to have a binder content that is 61/450 = 13.55% lower than that of SFRC mixtures with a maximum aggregate size of 10 mm.

2.4.5 Binder content and aggregate contents. Equation (5) can be used to produce contour plots that relate the binder content to the fine and coarse aggregate contents, as shown in Figure 20. In these plots, the same range has been considered for both fine and coarse aggregate contents: between 300 and 1200 kg/m³, based on the ranges identified as containing no potential outliers as per sections 1.4.1 and 1.4.2. However, not all combinations of fine aggregate and coarse aggregate contents in that plane are realistic. For example: it would be impossible for a SFRC mixture with normal density aggregates to contain 1200 kg/m³ of fine aggregate as well as 1200 kg/m³ of coarse aggregate.

Therefore, an additional condition needs to be imposed to equation (5). This is that the sum of the relative amounts of all SFRC mixture constituents has to be, on average, 2470 kg/m³. Assuming the median value for the water content –180 kg/m³ (see section 1.3.5)–, for the superplasticizer content –3.5 kg/m³ (see section 1.3.7)–, and for the fiber volume fraction – 0.51% (see section 1.5.1), meaning 40 kg/m³–, the above condition is as follows:

$$B + S + G = 2470 - 180 - 3.5 - 40 = (2246.5 \pm \varepsilon)\ kg/m^3 \quad (6)$$

Where B, S, and G are the binder, fine aggregate, and coarse aggregate contents respectively, and ε is half of the margin of variation for the sum of the contents of binder and aggregates, which based on the data from the SFRC database is +/- 150 kg/m³. As a result, the interpretation of the contour plots showing the binder content as per equation (5) on the fine aggregate – coarse aggregate plane must be restricted to the regions where the following is satisfied:

$$2096.5 \leq B + S + G \leq 2396.5 \quad (7)$$

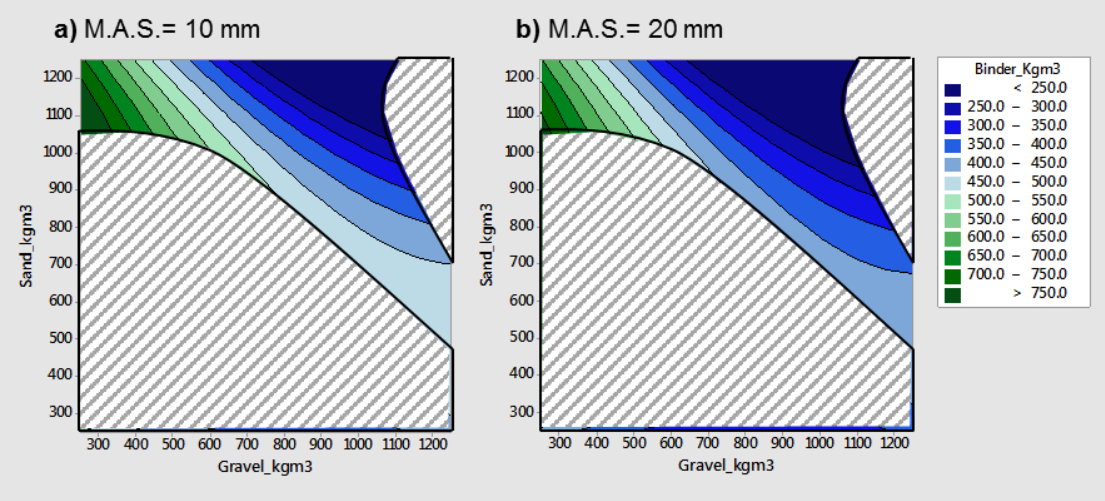

Figure 20. Contour plots of binder vs fine aggregate and coarse aggregate contents.

Figure 20 shows the contour plots derived from plotting equation (5) assuming two different values for the maximum aggregate size, and the greyed-out areas are those corresponding to combinations not compatible with condition (7). In both cases, higher binder contents are associated with the coarse aggregate content being lower than the fine aggregate content. In other words, the coarse-to-fine aggregate ratio decreases when the binder content is increased. On the other hand, lower binder contents correspond to mixtures where the fine aggregate and coarse aggregate contents are not too dissimilar, bringing the coarse-to-fine aggregate ratio close to 1. This can be explained in the following terms: when the binder content is low, it is necessary to improve the combined grading of the blend of fine and coarse aggregates so that this improves the cohesiveness of the mixture, therefore moving in the direction of coarse-to-fine aggregate ratios closer to 1.

An additional observation regarding the effect of the maximum aggregate is that the contour plots in Figure 20 have the same shape, the only difference being that contours are stepped down a bracket for a maximum aggregate size of 10 mm when compared to the 20 mm plot. In fact, it is stepped down by 61 kg/m^3, as discussed in section 2.4.4.

2.5 Superplasticizer content

2.5.1 Regression analysis and fitted equation. The regression analysis for the relative amount of superplasticizer (*SP*, kg/m^3) led to the following equation (R-squared = 0.77), with an error term of ±3.7 kg/m^3:

$$SP = (3930 + 27.53\,B + 0.032\,B^2 + 0.67\,W^2 - 0.42\,B \times W + 0.38\,B \times \lambda_f - 1.50\,W \times l_f - 0.68\,W \times \lambda_f + 17.23\,m \times l_f - 10.72\,m \times \lambda_f) \times 10^{-3} \pm 3.7 \quad (8)$$

Where *SP*, *B* and *W* are the relative contents of superplasticizer, total binder and water, respectively, all expressed in kg/m^3, and *m* is the maximum aggregate size (mm).

This model was particularly difficult to obtain. The superplasticizer dosages in the SFRC database constitute a particularly heterogeneous set of values (section 1.3.7), as different values correspond to different products from various manufacturers, each with different recommended dosage ranges. All this information was impossible to retrieve.

2.5.2 Model diagnosis and potential outliers. Figure 21 shows the scatterplot of values as estimated by equation (8) against the actual superplasticizer contents in the database. As per the discussion in 1.3.7, superplasticizer contents above 16 kg/m^3 were identified as potential outliers.

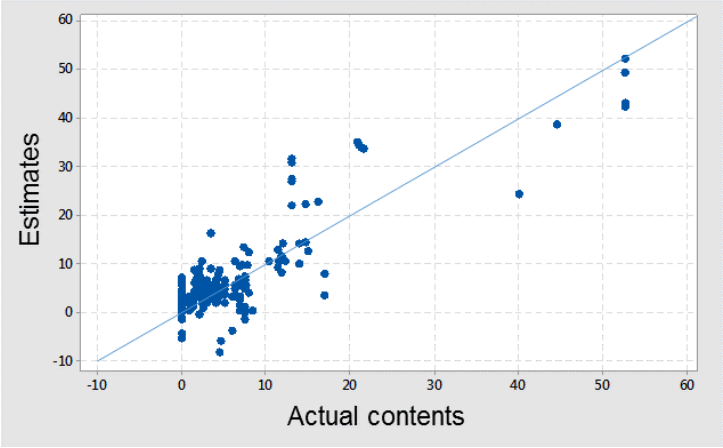

Figure 21. Scatterplot of estimated vs actual superplasticizer contents (kg/m^3).

2.5.3 Interpretation and discussion. Contour plots are shown in Figure 22, where the estimated superplasticizer content in kg/m^3 as per equation (8) is plotted against the water content and the total binder content. For comparison, two common sizes of steel fibers are considered (65/60 and 80/30), and two different values of the maximum aggregate size (13 mm and 20 mm). Unsurprisingly, low water contents and high binder contents are associated with high superplasticizer contents.

Those areas of the water-binder plane which correspond to unlikely combinations have been greyed out in Figure 21, considering the 5% and 95% percentiles to define the regions of the contour plots on which to focus. The water content (see 1.3.5) is higher than 140 kg/m^3 in 95% of SFRC mixtures in the database. Also, the 5th and 95th percentiles of the water-to-binder ratio are 0.15 and 0.56, respectively. The areas of the contour plots where these conditions are not met have been greyed out.

In line with the caveats highlighted in 2.5.1, any estimate of the superplasticizer content obtained by means of equation (8) should be interpreted as an indicative rather than a quantitative prediction. Therefore, when it comes to interpret the contour plots in Figure 21, the following aspects have been taken into consideration:

- Predicted values of 2.5 kg/m^3 and lower (the model can even yield negative estimates in some cases) are not necessarily different from zero, because the margin of error for this model is 3.7, which is obviously higher than 2.5 kg/m^3 (2.5.1). Therefore, when equation (8) gives an estimate for the superplasticizer content of 2.5 kg/m^3 or lower, this must be interpreted as meaning 'low superplasticizer dosage' or even 'no superplasticizer necessary'.
- As concluded in section 1.3.7, superplasticizer contents between 10-20 kg/m^3, or simply higher than 16 kg/m^3, are unusually high. Therefore, when equation (8) predicts the superplasticizer content as higher than 10 kg/m^3, this is to be interpreted as 'a high superplasticizer dosage is required', rather than the specific quantitative value.

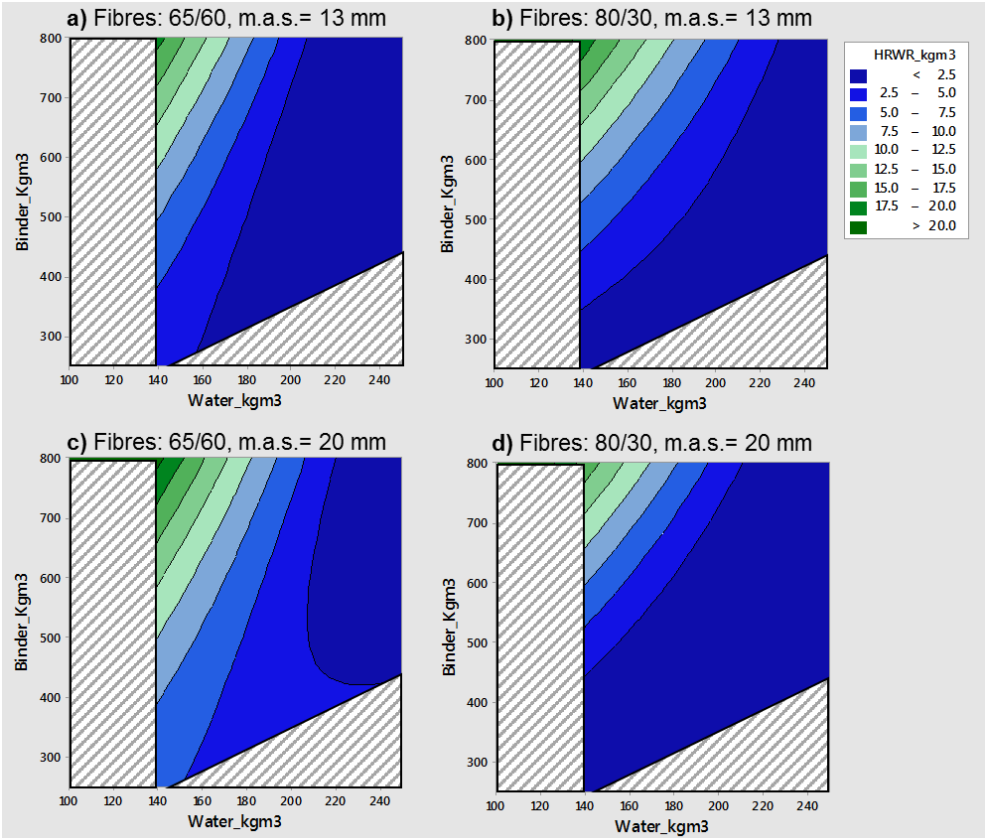

Figure 21. Contour plots for the superplasticizer content vs water and binder contents.

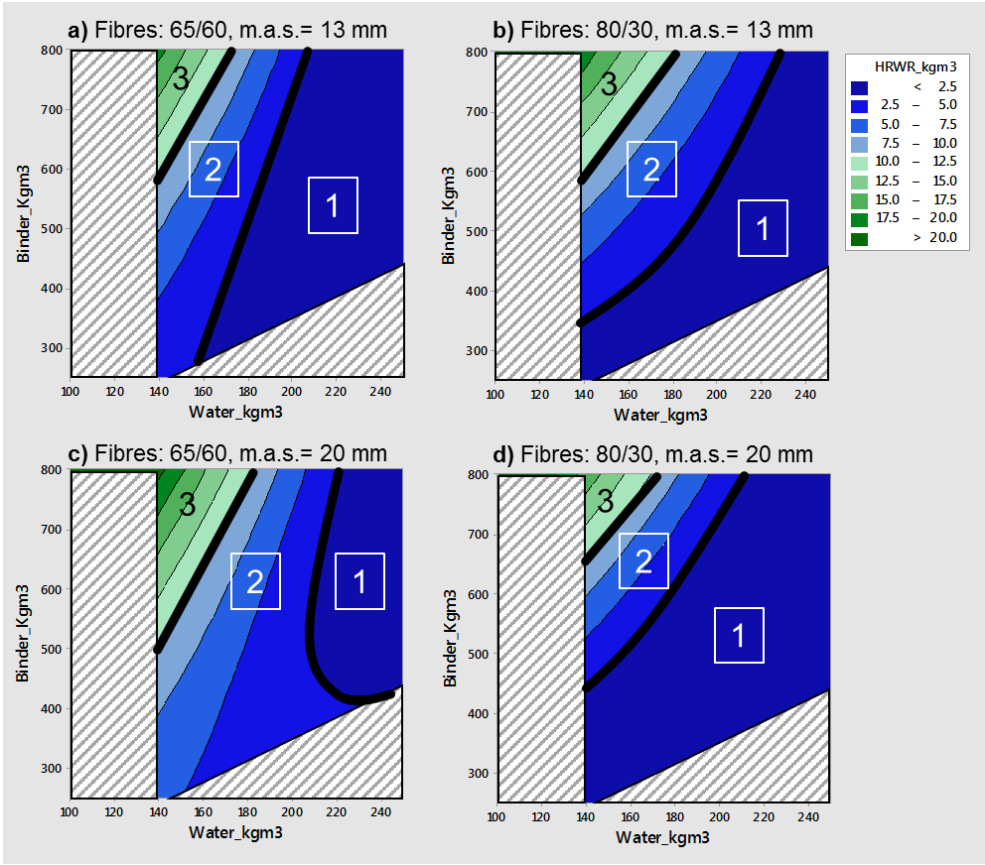

Figure 22. Contour plots for the superplasticizer content vs water and binder contents (2).

In light of the above considerations, it is useful to define three different zones in these contour plots in order to interpret them in broader, qualitative terms, taking as reference the estimates for superplasticizer content as per equation (8):

- Zone 1 comprises cases that are generally associated with low superplasticizer dosages or not even requiring the use of a superplasticizer. In such cases, the estimate for the superplasticizer content as per equation (8) is 2.5 kg/m^3 or lower.
- Zone 2 includes those cases where the estimate for the superplasticizer content as per equation (8) is between 2.5 and 10 kg/m^3, generally associated with the use of superplasticizer in non-negligible dosages.
- Zone 3, on the other hand, corresponds to those cases associated with superplasticizer contents on the higher end of the spectrum. In these cases, the estimate of superplasticizer content as per equation (8) is 10 kg/m^3 or higher.

Obviously, these are not clear-cut limits and values other than 2.5 and 10 kg/m^3 could be adopted. Nevertheless, the definition of these three zones can be superimposed to the contour plots, as shown in Figure 22, transforming them into a tool which can be used to inform a qualitative recommendation on the amount of superplasticizer.

For any given binder content, equation (8) and Figure 22 can be used to calculate the minimum values of the water-to-binder ratios that make superplasticizers either not necessary or used in relatively small amounts (i.e. below 2.5 kg/m^3). Some of these values are summarized in Table 2, for the fiber dimensions and maximum aggregate size values assumed in Figure 22.

Table 2. Minimum water-to-binder ratios for low superplasticizer content requirement.

Plot a), 65/60 and m.a.s. = 13 mm			Plot c), 65/60 and m.a.s. = 20 mm		
Water (kg/m^3)	Binder (kg/m^3)	Water-to-Binder ratio	Water (kg/m^3)	Binder (kg/m^3)	Water-to-Binder ratio
160	300	> 0.53	205	500	> 0.41
180	500	> 0.36	205	600	> 0.34
205	800	> 0.26	210	700	> 0.30

Similarly, the water-to-binder ratios associated with high amounts of superplasticizer (that is, 10 kg/m^3 or more) can also be determined. Table 3 presents a summary of some of these values, for the fiber dimensions and maximum aggregate size values assumed in Figure 22.

Table 3. Water-to-binder ratios associated with high superplasticizer contents.

Plot a), 65/60 and m.a.s. = 13 mm			Plot c), 65/60 and m.a.s. = 20 mm		
Water (kg/m^3)	Binder (kg/m^3)	Water-to-Binder ratio	Water (kg/m^3)	Binder (kg/m^3)	Water-to-Binder ratio
160	700	< 0.21	155	600	< 0.26
170	800	< 0.21	170	700	< 0.24
			180	800	< 0.23
Plot b), 80/30 and m.a.s. = 13 mm			Plot d), 80/30 and m.a.s. = 20 mm		
165	700	< 0.24	160	750	< 0.21
180	800	< 0.23	170	800	< 0.21

Some interesting observations can be made in relation to Tables 2 and 3 and Figure 22. For example, SFRC mixtures with 65/60 fibers and a maximum aggregate size of 20 mm are generally associated with the superplasticizer used in low to moderate amounts when the binder

content is not higher than 400 kg/m^3 (Figure 22, c). In fact, for such mixtures, the model estimates that the no-superplasticizer scenario is not an option unless the water content is on the higher end of the spectrum (around 205 kg/m^3) and the binder content around 500 kg/m^3, which corresponds to a water-to-binder ratio of 0.41.

It is also interesting to point out that the values in Table 3 demonstrate that, when the binder content is 700-800 kg/m^3, the water-to-binder ratios associated with high superplasticizer contents are relatively stable around 0.21-0.24. In other words, this seems to support a general recommendation that SFRC mixtures with binder contents above 700 kg/m^3 should be proportioned with water-to-binder ratios not lower than 0.25 in order to avoid excessively high superplasticizer contents.

2.6 Semi-empirical guidelines for proportioning SFRC mixtures

Following the analysis of individual variables, it became apparent that the equations reported in this chapter could be arranged into a structured methodology to guide the proportioning of SFRC mixtures. This methodology is summarized as a flowchart in Figure 23.

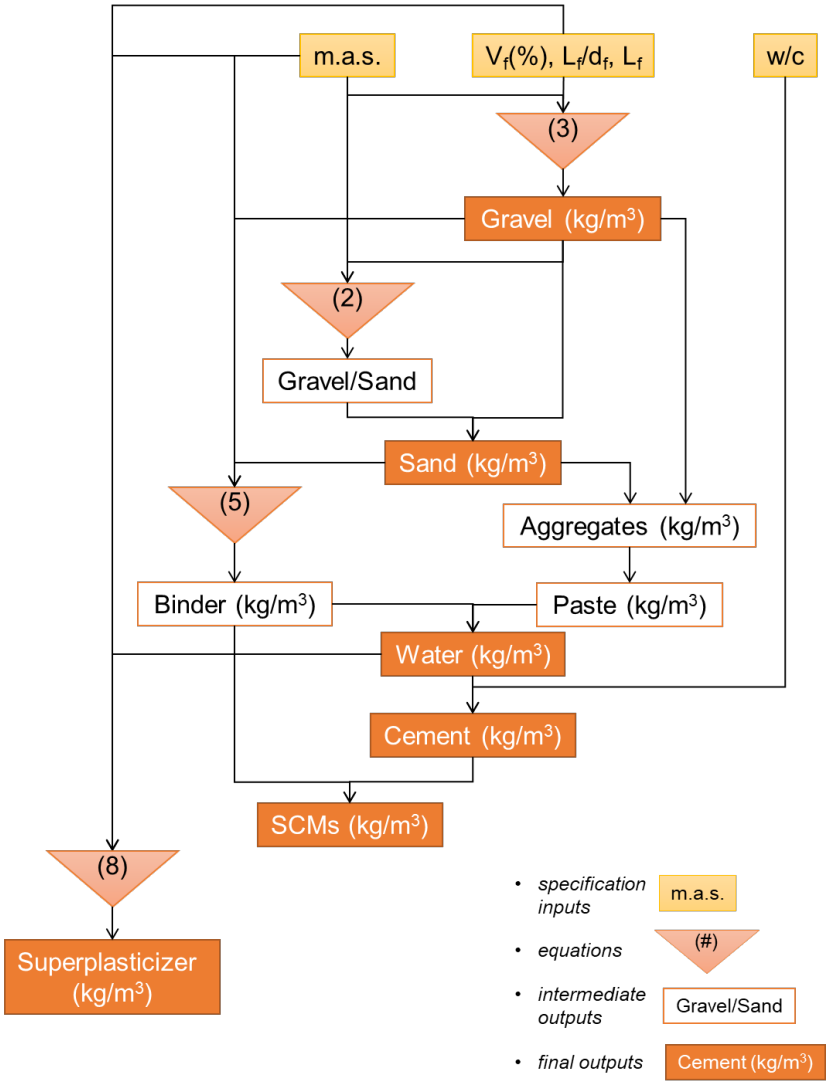

Figure 23. Flow chart of proposed mix proportioning methodology.

These equations can be used following the flowchart proposed in Figure 23 as follows:

- Based on the initial values of fiber volume fraction, fiber aspect ratio and length, together with the maximum aggregate size (m.a.s. in Figure 23), equation (3) can be used to determine the coarse aggregate content.
- The coarse aggregate content and the maximum aggregate size are the information needed to determine the coarse-to-fine aggregate ratio using equation (2).
- The fine aggregate content can be estimated based on the values of the coarse aggregate content and the coarse-to-fine aggregate ratio determined in the previous two steps.
- The total amount of paste in the mixture can be estimated by assuming a total weight per unit volume of 2470 kg/m^3 (the average of the SFRC mixtures in the database) and subtracting from that figure the contents of fine and coarse aggregate estimated in the previous steps.
- The binder content can be estimated by using equation (5) and the amounts estimated in the previous steps.
- By subtracting the binder content from the paste content, estimated in the two previous steps, the water content can be obtained.
- The cement content can be determined by dividing the water content by the water-to-cement ratio (*w/c*), which is assumed to be a given (or reasonably easy to estimate from the compressive strength specification).
- Subtracting the cement content from the total binder content gives an estimate of the total amount of supplementary cementitious materials (SCMs).
- Equation (8) can be used to get a preliminary idea of the requirements in terms of superplasticizer dosage (negligible, moderate, or high), based on the estimates obtained in the previous steps.

3. Descriptive analysis of the database of synthetic FRC mixtures

3.1 Introduction

3.1.1 Context and scope of this chapter. A database of synthetic fiber reinforced concrete mixtures was compiled from papers published between years 2000 and 2019. This chapter is concerned with the descriptive analysis of said database, focusing on the proportions and characteristics of the different mix constituents.

3.1.2 Size and structure of the database. A preliminary analysis of the data compiled in the database was carried out in order to identify cases where the information was clearly flawed, mostly incomplete, or inconsistent. These were either corrected, completed with estimates, or discarded. The resulting, final database comprised 1053 different cases. The list of the sources from which this information was extracted is provided in appendix B.

The database of synthetic FRC mixtures is structured in the same way as the SFRC database (see 1.1.2). The information compiled consisted of not only the synthetic FRC cases but also any complete data corresponding to SFRC mixtures reported in the same sources. This information was collected and incorporated to this database for different reasons: i) it made sense to extract all the information reported, not just in relation to synthetic FRC mixes; ii) in several sources, SFRC mixtures were also produced and tested as a reference against which to compare the synthetic FRC mixtures. In such cases, the rationale followed by the researchers was usually to proportion the synthetic FRC mixtures, which were then adjusted to incorporate steel rather than synthetic fibers. Therefore, it was considered appropriate to include them in the synthetic FRC database.

3.1.3 Definition of variables. All variables concerned with the proportioning of the different mixture constituents were expressed in terms of the relative weight of the constituent per unit volume of concrete, in SI units (i.e. kg/m^3). The definition of the variables in the synthetic FRC database was consistent with the SFRC database (see 1.1.3). Regarding the characteristics of the fibers, the following variables were added to the synthetic FRC database: fiber material, fiber tensile strength (MPa), and fiber elastic modulus (MPa), for the sake of information completeness. A piechart showing the makeup of the database of synthetic FRC mixtures in terms of the fiber material is presented in Figure 24.

3.2 Treatment of missing data

3.2.1 Missing data in the database. The prevalence of missing data in this database was low: 72.1% of the cases were complete. Overall, only 5.3% of the information was missing, which was mostly concentrated on three variables: cement type, fiber aspect ratio, and maximum aggregate size, as can be seen in Table 4.

3.2.2 Imputation of missing values. Imputation is the process by which missing data in a dataset are ‘filled in’ with estimates based on the exploitation of correlation with other

variables, known relationships between them or the underlying phenomena they represent, or a combination of both.

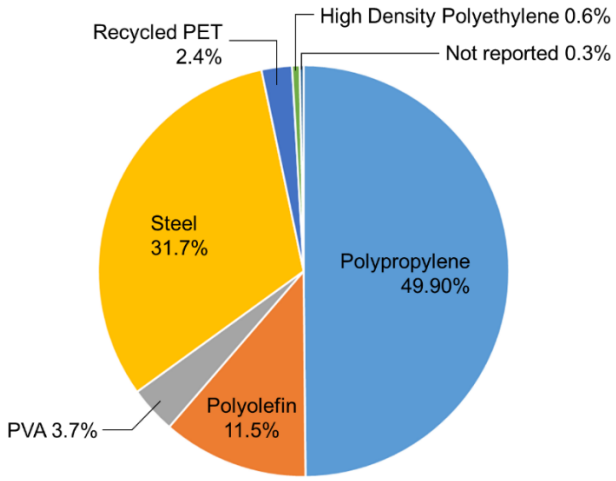

Figure 24. Piechart of fiber types in the synthetic FRC mixtures database.

Table 4. Percentage of missing values for selected variables.

Variable	**Missingness**
Cement type	24.0%
Fiber aspect ratio	13.4%
Maximum aggregate size	11.5%
Superplasticizer dosage	7.0%
Fine aggregate content	8.1%
Coarse aggregate content	8.1%
SCMs content	4.5%
Cement content	4.5%
Water content	4.5%

The missing values regarding the cement type (24.03%) could not be remedied by imputation, as this is a non-quantitative variable. Missing values were, in most of these cases, due to the cement type not being explicitly reported. There were some instances of it being reported with reference to different standards, and an effort was made, during the data collection process, to find an unambiguous equivalence in terms of EN standard classification whenever possible.

The aspect ratio of the fibers was not reported in 13.39% of the cases but, this being a relatively low percentage, the imputation of the missing fiber aspect ratio values was possible. Stepwise regression was used, starting with all the mixture proportioning variables, their quadratic terms and all pairwise interactions as covariates, to obtain a predictive equation for the fiber aspect ratio. This equation fitted the non-missing values reasonably well (R-squared = 0.73) and was therefore deemed appropriate for estimating the missing values. However, the imputation was not possible in those cases where the values of any of the other mix design variables were also missing. A total of 90 imputations were done, bringing the percentage of missing aspect ratio values down to 4.84%.

Maximum aggregate size values were missing in 11.49% of the cases in the database. In those cases where the relative amounts of fine and coarse aggregate, cement, SCMs and water were available, the maximum aggregate size was estimated by assuming Bolomey's curve as a good

approximation to the grading of the mixture, and assuming the same specific weight for both fine and coarse aggregates. A total of 81 imputations was done, reducing the missingness percentage to 3.8%.

The relative amounts of fine and coarse aggregates were missing in 8.07% of cases. When the maximum aggregate size was known and the total aggregate content could be approximated by subtraction, the proportion of fine to coarse aggregate was estimated following Bolomey's curve with a parameter of 12. A total of 38 imputations could be done this way, bringing the missingness percentage down to 4.46%. The missingness percentage was the same for cement, water, and SCMs contents (4.46%). All these cases corresponded to papers which did not report the amounts of aggregates either. In these cases, it was impossible to estimate the relative volume of paste or its composition, and therefore the imputation of missing values was not possible.

3.3 Composition of the binder

3.3.1 Type of cement. In 24% of the cases in the synthetic FRC database, the type of cement or the strength class are not known, as they were not reported in the original sources. The cement type is either CEM I or CEM II in 94% of the cases for which this information was available. The most prevalent type of cement is CEM I (Figure 25).

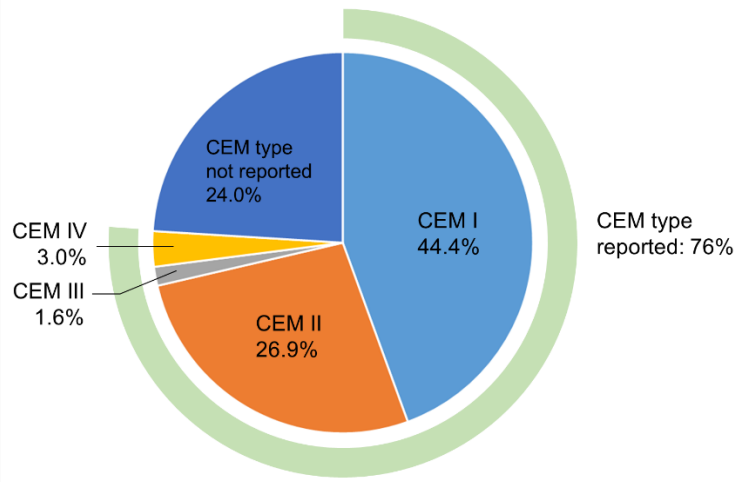

Figure 25. Pie chart showing the prevalence of cement types in the database.

3.3.2 Binder content. A graphical summary of the distribution of binder content values in the database is shown in Figure 26. In this and subsequent sections, the histograms, boxplots and CFD plots are first shown considering all the cases in the synthetic FRC database (as in Figure 26 a), followed by the same plots recalculated after excluding the information corresponding to control SFRC mixtures (as in Figure 26 b). Generally there are no major differences, but all the plots are provided for the sake of completeness. The discussion of representative values is concerned with the synthetic FRC mixtures only, unless otherwise stated.

Binder contents are distributed around a median of 400 kg/m^3. In 90% of the cases, the binder content ranges from 310 to 600 kg/m^3 (5% and 95% percentiles), which is a representative minimum-maximum range after excluding the most extreme cases. In 50% of the cases (that

is, considering the 25% and 75% percentiles), binder contents take values between 350 and 500 kg/m^3, which define what can be considered a 'typical' range.

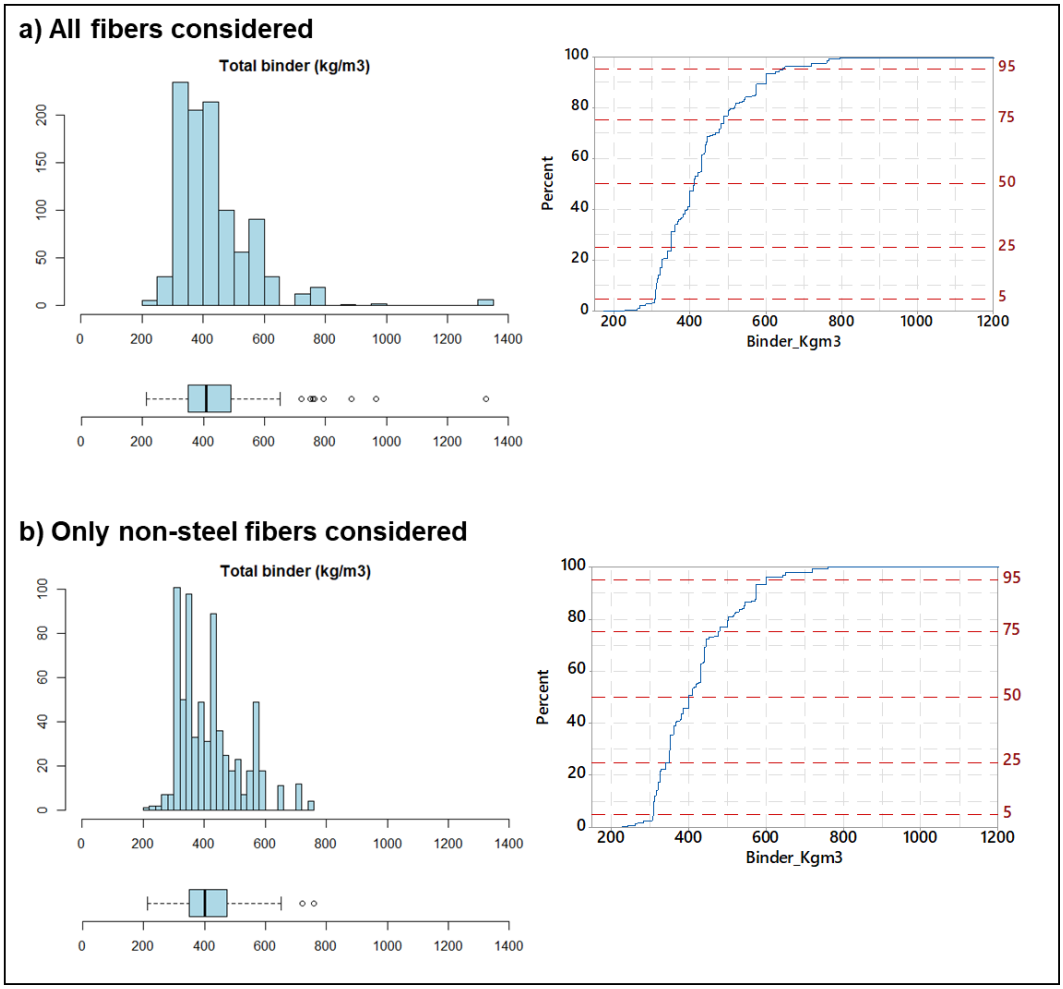

Figure 26. Histogram, CFD and boxplot for binder content (kg/m^3).

There is no evidence of peaks defining any subsets in the dataset of synthetic FRC mixtures, as opposed to the SFRC database, where there is a subset of mixtures with very high binder contents (see 1.3.2). However, as the boxplot in Figure 26 b shows, the whiskers based on the interquartile range extend to 213 and 650 kg/m^3, and therefore mixtures with a binder content outside of this range can be outliers.

3.3.3 Cement content. The cement content of the synthetic FRC mixtures in the database (Figure 27) takes values between 200 and 452 kg/m^3 in 90% of the cases (and, in the central 50% of the cases, between 309 and 400 kg/m^3), around a median of 360 kg/m^3. Compared to the SFRC dataset (see 1.3.3), the median cement content of the synthetic FRC mixtures is 40 kg/m^3 lower, and the 95% percentile is 208 kg/m^3 lower (452 instead of 660 kg/m^3). Therefore, it can be concluded that the cement content of synthetic FRC mixtures is generally lower than that of SFRC mixtures, and that its values are less scattered, closer to the median and the mean. This is also evidenced by the histograms in Figure 27 being narrower than their counterparts in section 1.3.3.

The whiskers of the boxplot in Figure 27 b show that values of the cement content outside the 180-520 kg/m^3 range are unusual and therefore can be tagged as outliers as far as synthetic FRC mixtures are concerned.

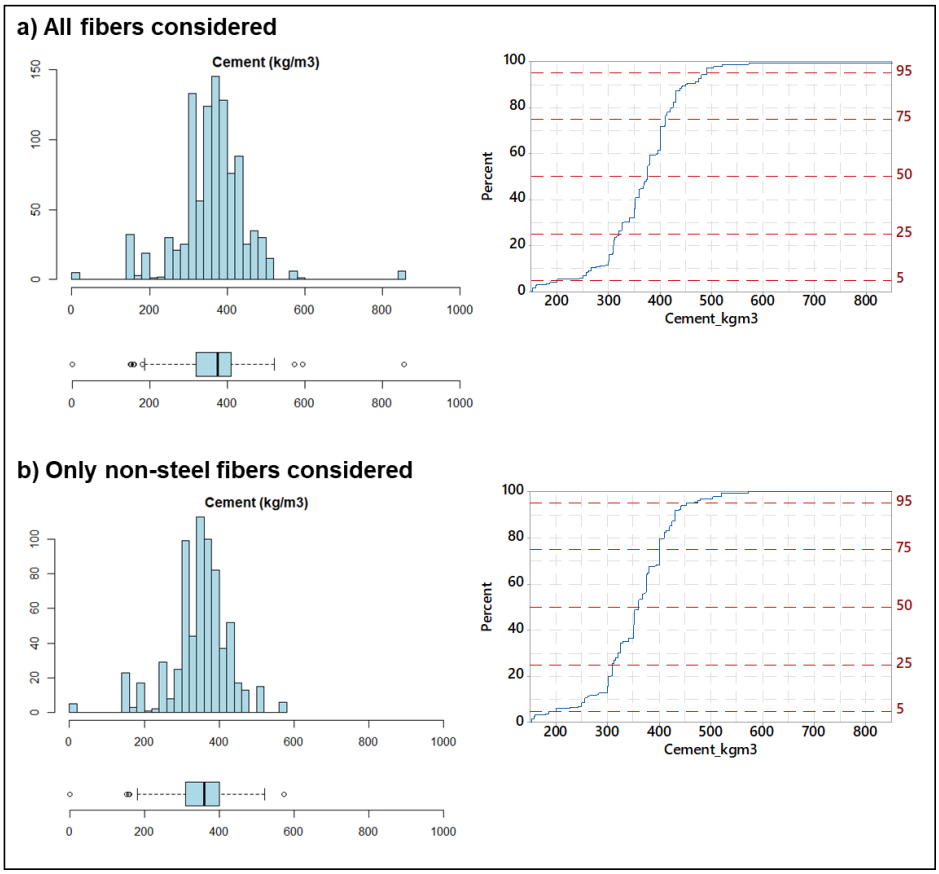

Figure 27. Histogram, CFD and boxplot for cement content (kg/m^3).

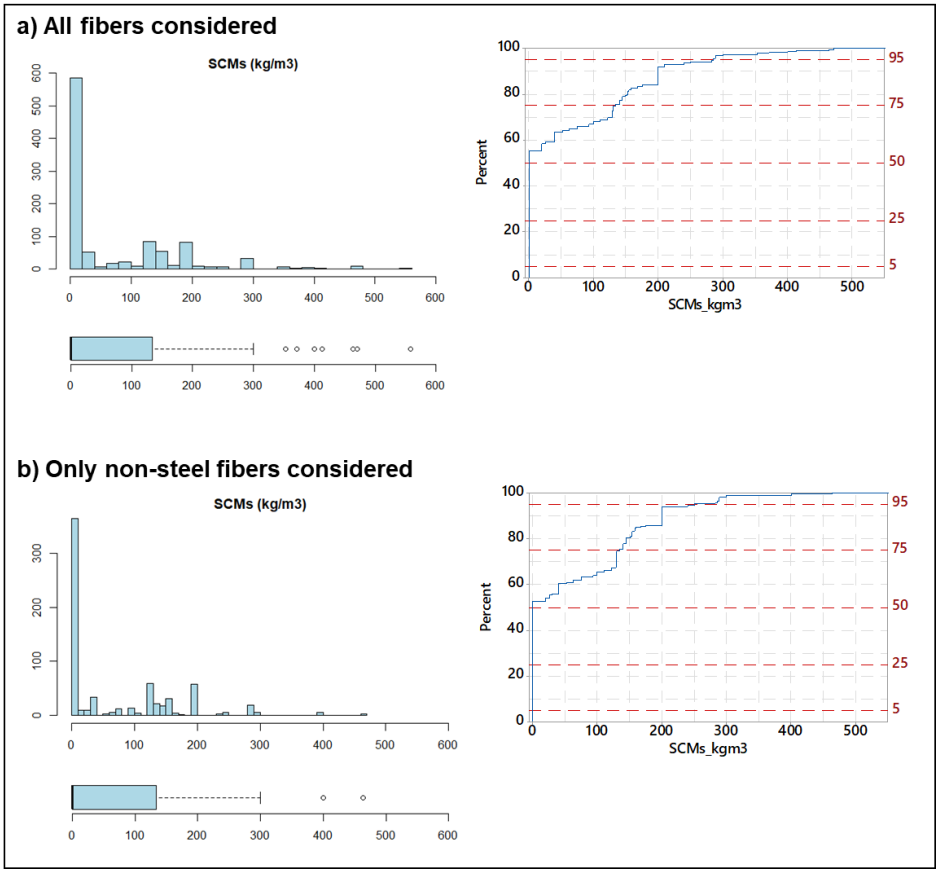

Figure 28. Histogram, CFD and boxplot for SCMs content (kg/m^3).

3.3.4 SCMs content. Figure 28 shows the graphical description of the variable grouping the relative amounts of any SCMs. Out of all the synthetic FRC mixtures in the database, 47.1% incorporate SCMs in addition to cement. This percentage is very similar to that observed in relation to the SFRC mixtures (see 1.3.4). In 95% of the syntehtic FRC mixtures in the database, the SCMs content is not higher than 249 kg/m^3, a representative maximum value which is also very similar to that observed in relation to SFRC mixtures. In 75% of the cases, the SCMs content is not higher than 134 kg/m^3. SCMs contents higher than 300 kg/m^3 are unusual and potential outliers, as the boxplot in Figure 28 b shows.

3.3.5 Water content. As the histograms in Figure 29 show, the median water content is 175 kg/m^3. In 90% of the synthetic FRC mixtures in the database, the water content takes values between 115 and 225 kg/m^3 (5% and 95% percentiles). If the 25% and 75% percentiles are considered, the water contents ranges from 162 to 198 kg/m^3, representative of the central 50% of the cases around the median. The whiskers of the boxplot shown in Figure 29 b comprise the values between 105 and 248 kg/m^3, and therefore synthetic FRC mixtures with a water content outside of this range are potential outliers.

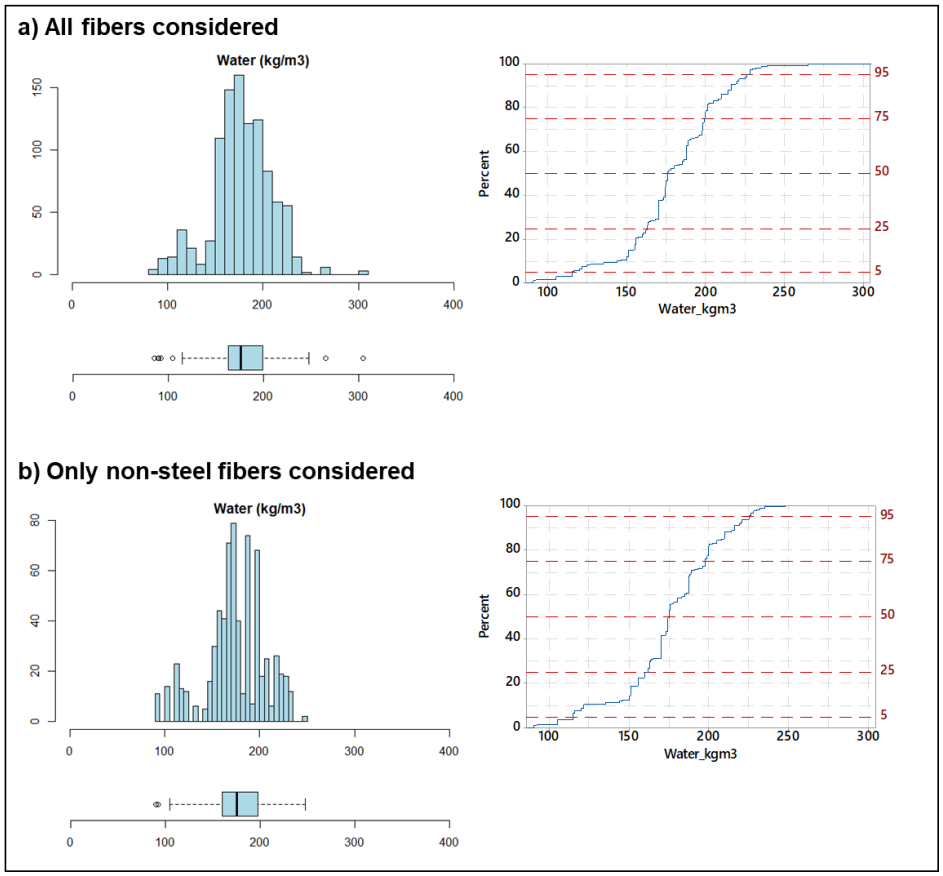

Figure 29. Histogram, CFD and boxplot for water content (kg/m^3).

3.3.6 Water/Cement ratio. The median water-to-cement ratio is 0.50. In 90% of the mixtures in the synthetic FRC database, the water-to-cement ratio takes values between 0.35 and 0.75. The distribution of values is shown in Figure 30. If the 25% and 75% percentiles are considered, the range they define is 0.45-0.55, which is representative of the most typical cases. Considering the range covered by the whiskers of the boxplot in Figure 30 b, synthetic FRC mixtures with a water content lower than 0.30 or higher than 0.70 are unusual.

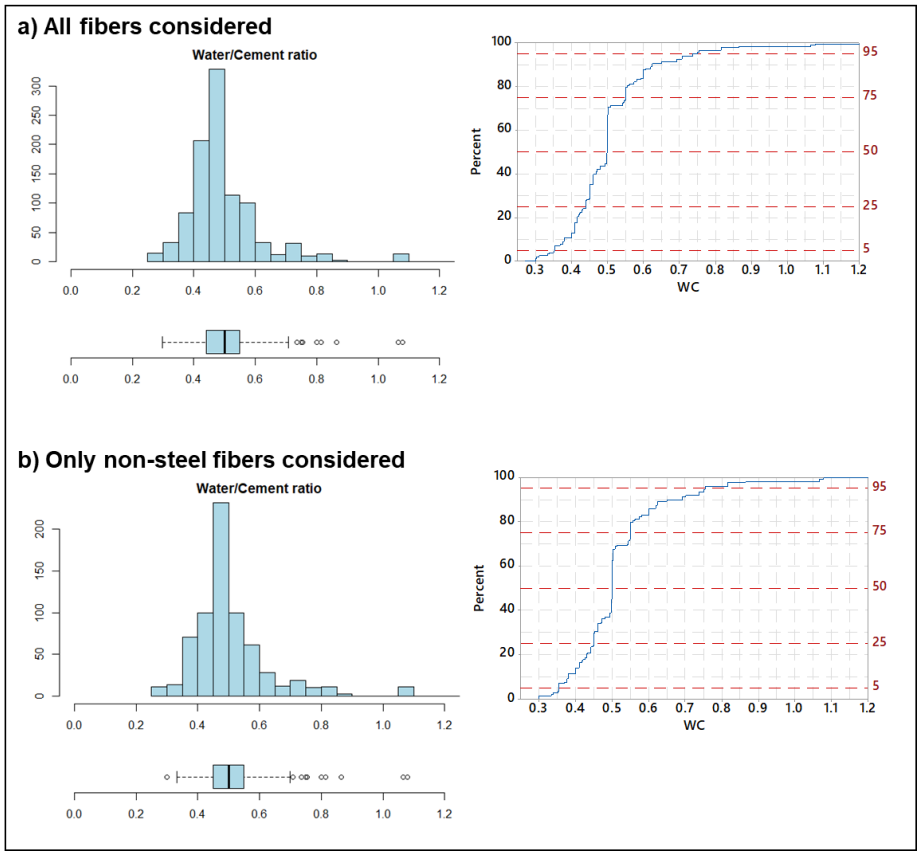

Figure 30. Histogram, CFD and boxplot for water-to-cement ratio (kg/m^3).

3.3.7 Superplasticizer content. As the histograms in Figure 31 show, the distribution of the superplasticizer contents in the synthetic FRC database is skewed, as low values are more common than high values. The skewness in the distribution of the values of superplasticizer content is shared with the SFRC mixtures (section 1.3.7). However, some interesting differences emerge when only the synthetic FRC mixtures are considered (that is, when the reference SFRC mixtures are excluded from the analysis).

Considering only the FRC mixtures with synthetic fibers (Figure 31 b), mixtures containing no superplasticizer represent 38.6% of the cases, which is higher than the corresponding percentage of 30.8% observed when SFRC data are also taken into account (Figure 31 a). In terms of the median superplasticizer content, this is 2.4 kg/m^3 when all mixtures are considered, but it lowers to 2 kg/m^3 when SFRC mixtures are excluded. These differences seem to suggest that superplasticizer is used less often in synthetic FRC mixtures than in their counterpart mixtures with steel fibers, and, on average, in lower amounts.

The conclusion mentioned above is also supported when this database is compared to the database of SFRC mixtures (section 1.3.7). Superplasticizer was found to be used in approximately 80% of the SFRC cases, as opposed to 61.4% of the mixtures with synthetic fibers. Also, the median superplasticizer content in the SFRC database was 6 kg/m^3, considerably higher than the median superplasticizer content for synthetic FRC mixtures, which is 2 kg/m^3. These observations seem to confirm that, generally speaking, the use of superplasticizer in SFRC mixtures is more common (and in higher amounts) than in synthetic FRC mixtures. This does not necessarily imply, however, that the use of steel fibers requires more superplasticizer to be added to the FRC mixture than synthetic fibers. It could be argued,

for example, that it signals significant differences in achieving the balance between workability and cohesiveness of the fresh mixture depending on the fiber material.

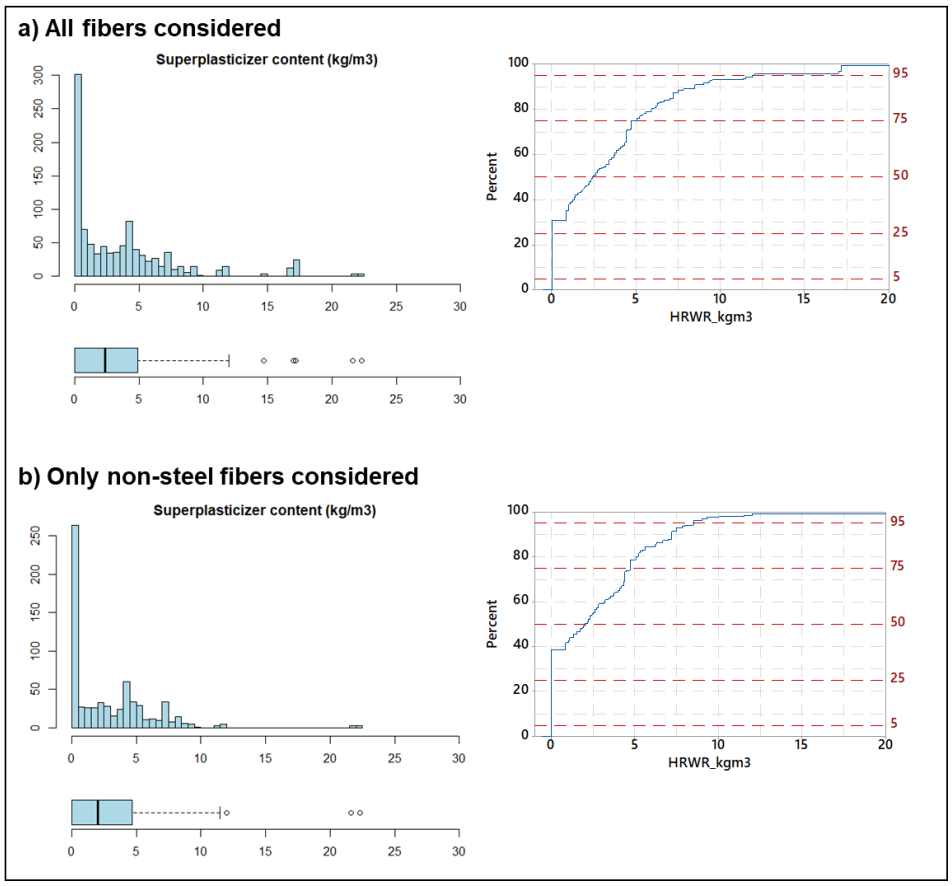

Figure 31. Histogram, CFD and boxplot for superplasticizer content (kg/m^3).

As per Figure 31, the superplasticizer content is less than 4.7 kg/m^3 in 50% of the cases. Only in 5% of the cases it is higher than 8.5 kg/m^3, and superplasticizer contents above 11.5 kg/m^3 are very unusual in the synthetic FRC mixtures in the database.

Taking the median values for the superplasticizer and cement contents in synthetic FRC mixtures are considered (2 kg/m^3 and 360 kg/m^3, respectively), an indicative dosage of superplasticizer is 0.56% over the weight of cement. Bearing in mind that the saturation point of superplasticizers is generally between 1% and 2%, this observation seems to support the claim that superplasticizers are dosed significantly below their saturation point when it comes to synthetic FRC mixtures.

3.4 Aggregates

3.4.1 Fine aggregate content. Figure 32 shows the descriptive graphs corresponding to the fine aggregate content of the synthetic FRC mixtures in the database compiled for this study. The median fine aggregate content is 849 kg/m^3. Fine aggregate contents range from 634 to 1042 kg/m^3 in 90% of the cases. These values represent the lower and upper limits of what can be referred to as the representative range of values for this variable. The 25% and 75% percentiles, on the other hand, can be considered as the limits between which the most typical values are found, and these are 751 and 916 kg/m^3 respectively. The whiskers in the boxplot based on the

interquartile range, shown below the histogram in Figure 32, cover the range from 510 to 1132 kg/m^3: values of the fine aggregate content outside of this range are very unusual and can therefore be tagged as outliers.

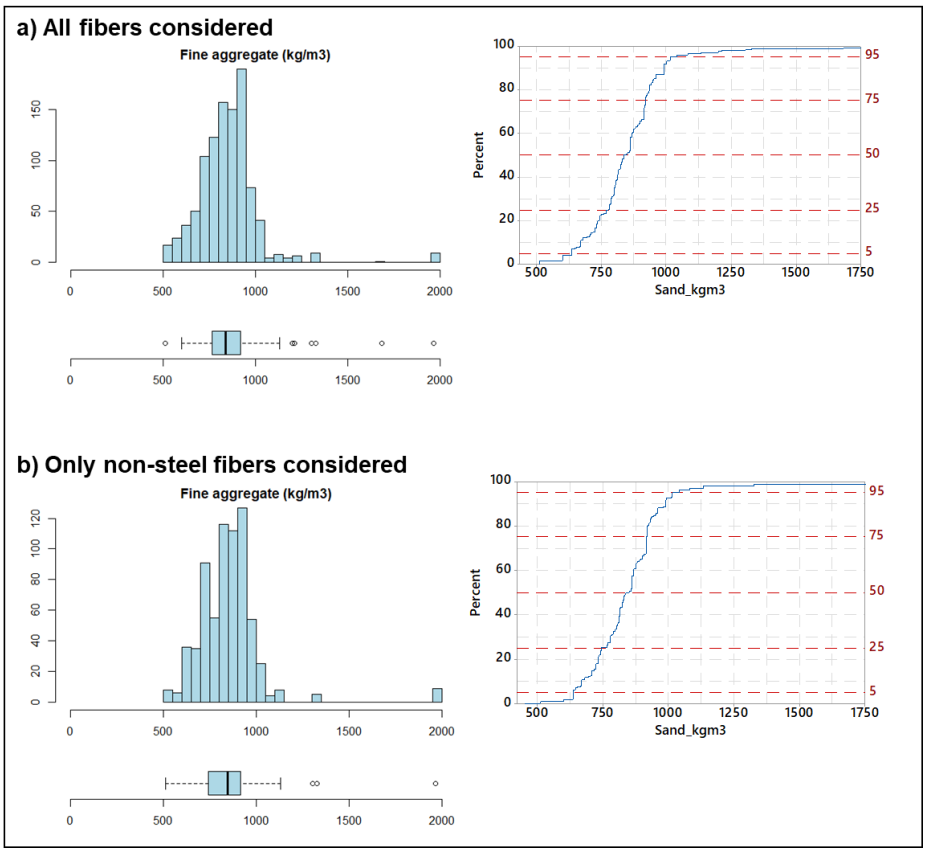

Figure 32. Histogram, CFD and boxplot for the fine aggregate content (kg/m^3).

3.4.2 Coarse aggregate content. The mixtures in the synthetic FRC database have coarse aggregate contents which are generally higher and more scattered than the values of the fine aggregate content, as can be seen if the histograms in Figure 33 are compared to those in Figure 32. The median coarse aggregate content of the synthetic FRC mixtures in the database is 954 kg/m^3 (which is 105 kg/m^3 higher than the median fine aggregate content, as detailed in 3.4.1). In 90% of the cases, the coarse aggregate content takes values between 532 and 1170 kg/m^3. In the 50% of the cases closest to the median, the range is 752-1077 kg/m^3. As the boxplot in Figure 33 b shows, coarse aggregate contents outside of the range between 330 and 1305 kg/m^3 are very unusual and can be considered as outliers.

3.4.3 Maximum aggregate size (mm). The graphs describing the distribution of the maximum aggregate size values in the synthetic FRC database are shown in Figure 34. The median maximum aggregate size is 16 mm. In 90% of the cases, values of the maximum aggregate size are between 9.5 and 25 mm. If the 25% and 75% percentiles are considered, the central 50% of the cases includes values between 12 and 20 mm. Values of the maximum aggregate size of 4 mm or less, corresponding to synthetic FRC mixtures without coarse aggregate, have a prevalence of only 2% in the database. This is consistent with the fact that coarse aggregate contents below 330 kg/m^3 are outliers (3.4.2). Also, as the boxplot in Figure 34 b shows, synthetic FRC mixtures with a maximum aggregate size higher than 26 mm can also be considered as potential outliers.

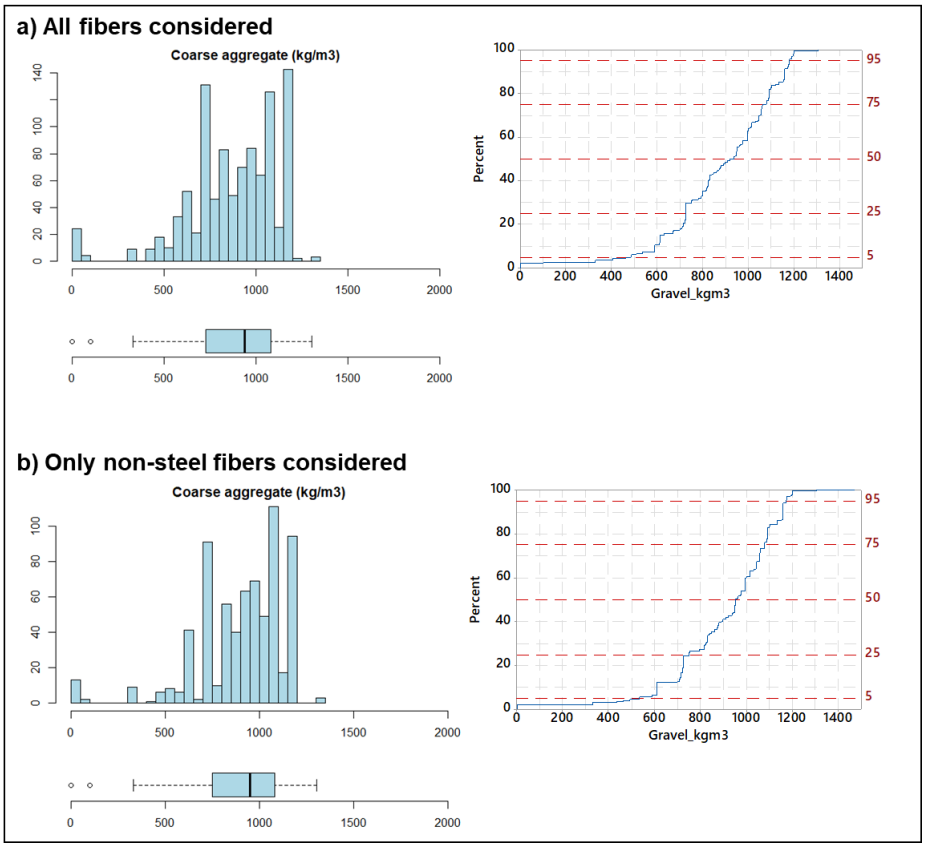

Figure 33. Histogram, CFD and boxplot for the coarse aggregate content (kg/m³).

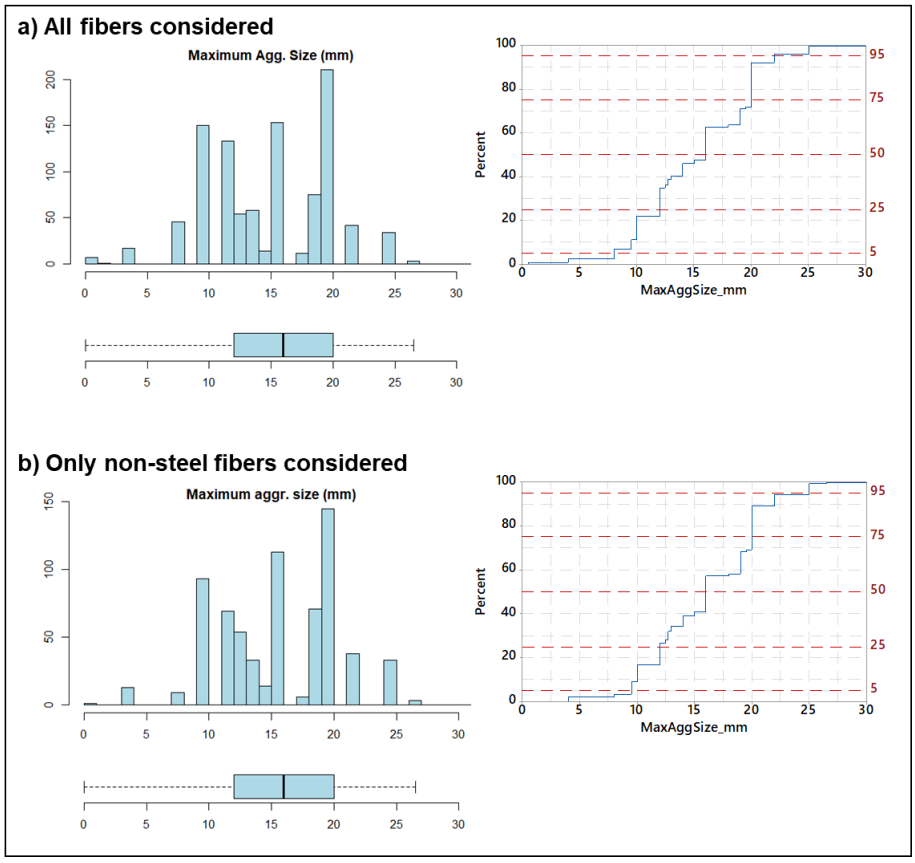

Figure 34. Histogram, CFD and boxplot for the maximum aggregate size (mm).

3.5 Fibers

3.5.1 Fiber volume fraction, $\mathbf{V_f}$ **.** The values of the fiber volume fraction in the database of synthetic FRC mixtures are distributed around a median of 0.50%, which is almost the same as the median fiber volume fraction of the SFRC database (which is 0.51%, section 1.5.1). If only the mixtures with polypropylene (PP) fibers are considered, the median is also 0.5%. On the other hand, when only cases with polyolefin (PO) fibers are considered, the median is 0.62%.

The distribution of the fiber content values in the synthetic FRC database is shown in Figure 35. In 95% of the cases, the fiber volume fraction is not higher than 1.35%. This representative maximum is lower than its equivalent for the SFRC database (which is 1.6%, see 1.5.1). Perhaps more interesting is the fact that the fiber volume fraction is lower than 1.0% in 87% of the cases.

If the 5% and 95% percentiles are considered as the representative minimum and maximum, as they comprise 90% of the cases in the database, the fiber volume fraction of synthetic FRC mixtures takes values between 0.14% and 1.35%. The more typical range, corresponding to the 50% of the cases closest to the mean and defined by the 25% and 75% percentiles, is between 0.41% and 0.75%.

The whiskers of the boxplot shown in Figure 35 b, which is based on the interquantile range, show that, when only the FRC mixtures with synthetic fibers are considered, cases with a fiber volume fraction higher than 1.25% are very rare and can be considered outliers.

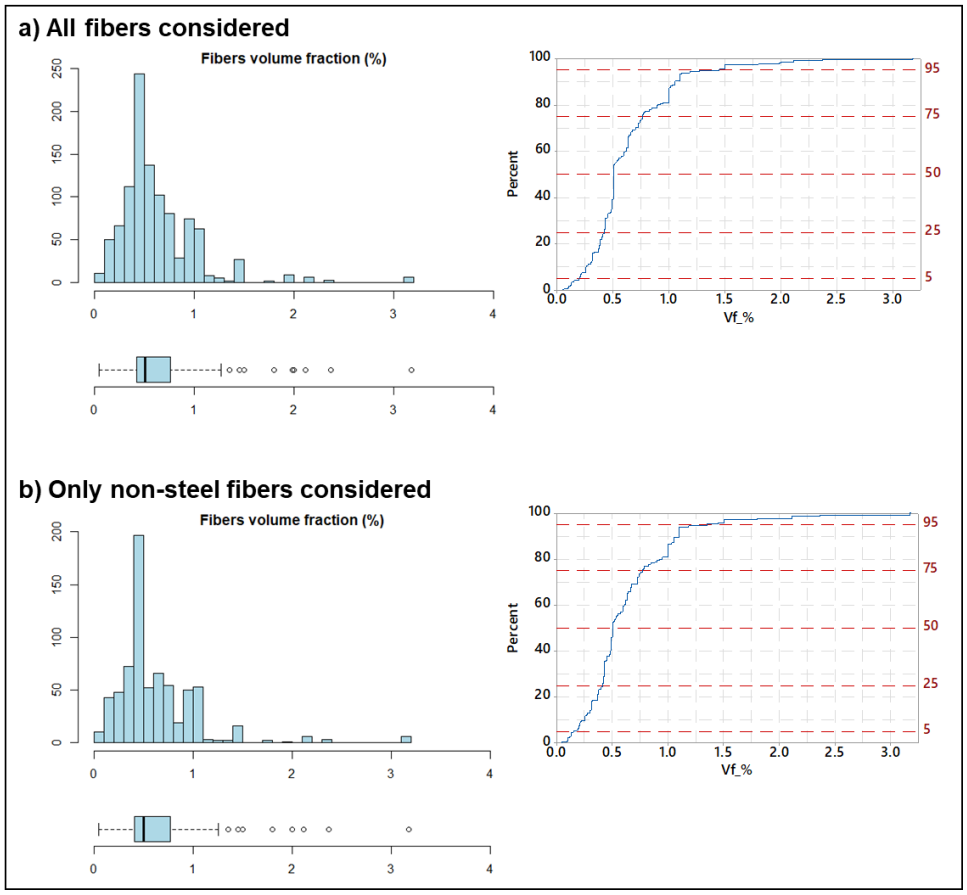

Figure 35. Histogram, CFD and boxplot for the synthetic fiber volume fraction.

3.5.2 Fiber length. Figure 36 shows the graphical summary of the distribution of fiber length values in the database of synthetic FRC mixtures. Peaks in the histograms and step-like jumps in the CDF plots are due to the most common fiber lengths commercially available and used by researchers in their studies. The most prominent peaks correspond to fiber lengths of 50, 55, 40, and 60 mm (Figure 36 b).

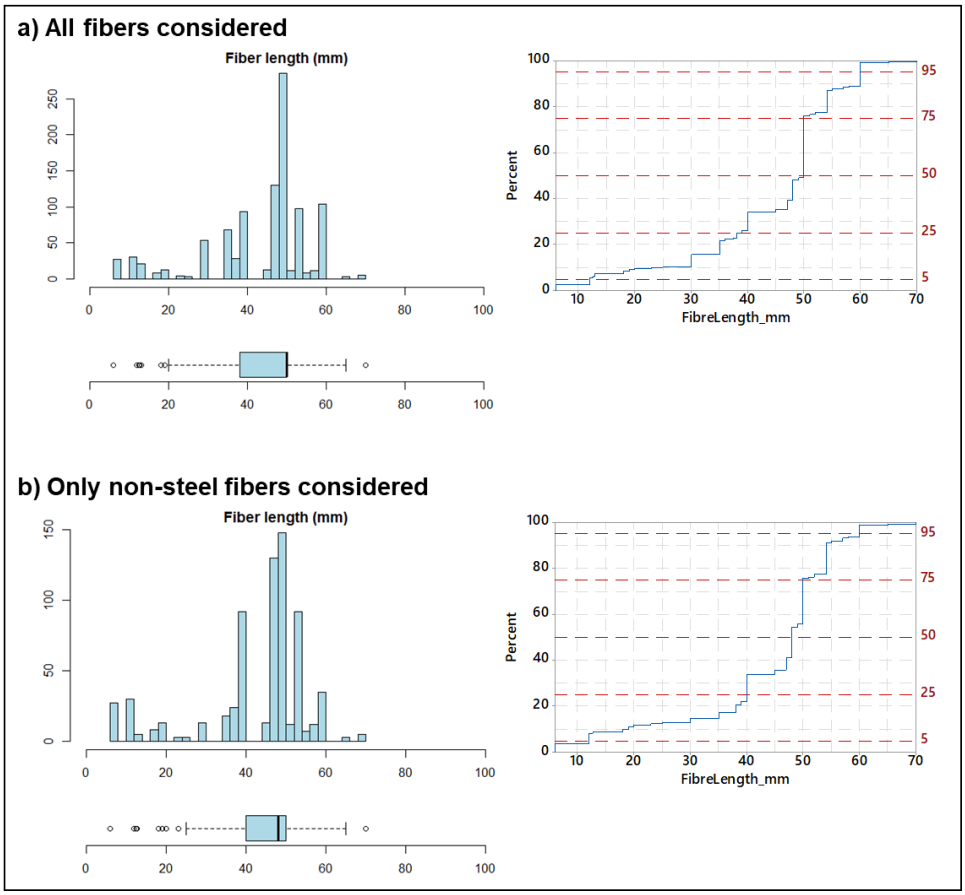

Figure 36. Histogram, CFD and boxplot for fiber length (mm).

The median fiber length is 48 mm. In 90% of the mixtures in the synthetic FRC database, the fiber length varies between 12 and 60 mm. In the 50% of the cases closest to the mean, as defined by the 25th and 75th percentiles, the fiber length ranges from 40 to 50 mm. It is also interesting to mention that the median, 90% and 50% ranges of the fiber length are significantly different in the case of PVA fibers, these being much shorter than the PP or PO fibers as far as the synthetic FRC mixtures in the database are concerned:

- PP: median=50 mm, between 12 and 58 mm in 90% of cases (40-52 in 50% of cases).
- PO: median=48 mm, between 35 and 60 mm in 90% of cases (48-50 in 50% of cases).
- PVA: median=12 mm, between 6 and 30 mm in 90% of cases (6-12 in 50% of cases).

Considering the width covered by the whiskers of the boxplot in Figure 36 b, values of the fiber length outside of the range between 25 mm and 65 mm are rare and therefore correspond to cases that are potential outliers. This would classify the FRC mixtures with PVA fibers as outliers. However, rather than being outliers, it is more appropriate to establish that FRC mixtures with PVA fibers cannot be regarded as part of the same population as FRC mixtures with either PP or PO fibers. In any case, cases with fibers longer than 65 mm are unusual and can be considered as potential outliers, regardless of the fiber material.

3.5.3 Fiber aspect ratio. As shown in Figure 37, the distribution of the values of the fiber aspect ratio was clearly skewed. This is due to a few synthetic FRC mixtures in the database produced with PVA fibers of very small diameters and therefore a very high aspect ratio compared to the rest of cases in the database. Such cases, however, represent less than 5% of the mixtures in the database (section 3.2.2).

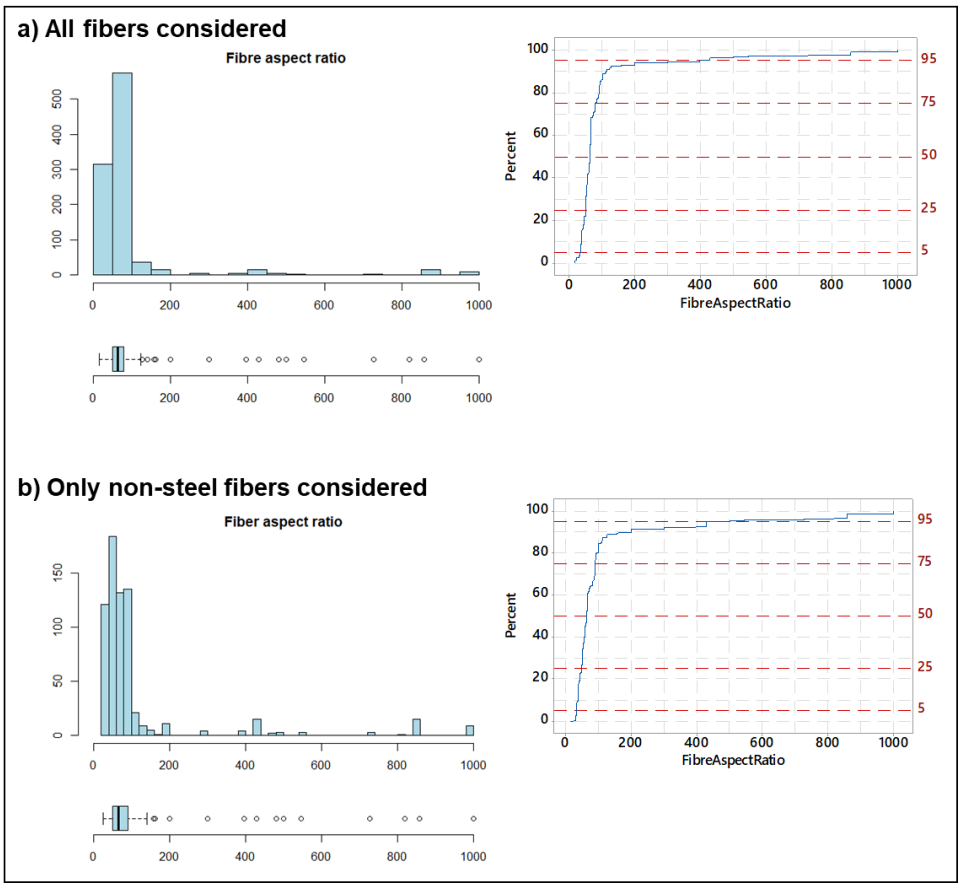

Figure 37. Histogram, CFD and boxplot for fiber aspect ratio.

The median fiber aspect ratio is 66 (specifically: 60 and 66, for PP and PO fibers, respectively). Considering only the mixtures with PP fibers, their aspect ratio takes values between 33 and 158 in 90% of the cases, and between 42-87 in 50% of the cases. If mixtures with PO fibers are considered instead, the fiber aspect ratio is between 53-200 in 90% of the cases, and between 53-100 in 50% of the cases.

Based on the boxplot in Figure 37 b, fiber aspect ratios above 140 are rare and can be considered as potential outliers. However, they represent approximately 11% of the cases in the database, which is not a small percentage. Similarly to what has been said in relation to the fiber length, they are not necessarily outliers but, rather, form a different group within the database. As these differences have been clearly attributed to differences in the fiber material (and particularly PVA fibers), the modeling and analysis reported in chapter 4 explicitly incorporates the fiber material as a variable that necessarily 'modifies' any terms that involve the fiber length and aspect ratio in the equations / models.

4. Meta-analysis of synthetic FRC mixtures: relationships between mix design variables

4.1 Preparation of the dataset

4.1.1 Introduction. This chapter is concerned with the relationships between the variables that describe synthetic FRC mixtures in terms of the relative amounts of their constituents and their characteristics. The approach followed to study these relationships is a semi-empirical modeling process applied to the database of synthetic FRC mixtures compiled as part of this project.

4.1.2 Dataset of synthetic FRC mixtures. In data science and, more generally, machine learning, it is important to ensure that the datasets used for modeling are reasonably coherent. The models discussed in the following sections are based on the dataset of synthetic FRC mixtures after excluding the cases corresponding to their steel fiber counterparts. Also, only mixtures with a density or specific weight compatible with conventional concrete have been considered, as lightweight concrete mixtures or those made with unconventional aggregates are substantially dissimilar to the majority of synthetic FRC mixtures.

Furthermore, during the data collection stages it was observed that some papers reported mixtures where the sum of the relative amounts of all constituents was either too high or two low, suggesting that some of the mixture proportions had been incorrectly reported. It was decided to use the sum of the relative amounts of binder, water, fine aggregate, coarse aggregate and admixtures as a criterion to identify mixtures which were not comparable to the rest of the synthetic FRC mixtures in the dataset, so they could be discarded.

The sum of the amounts of all constituents was calculated for all the mixtures in the database. A normal probability distribution was then fitted to these values, and the best fit corresponded to a normal distribution with a mean of 2364 kg/m^3 and a standard deviation = 111 kg/m^3. The lower and upper limits of the interval which contains 95% of the cases for such a normal distribution are 2146 and 2582 kg/m^3. Those cases for which the total weight of all constituents fell outside of this interval were discarded. Figure 38 shows a summary of the preparation of the dataset of synthetic FRC mixtures used in the analysis described in the subsequent sections of this chapter.

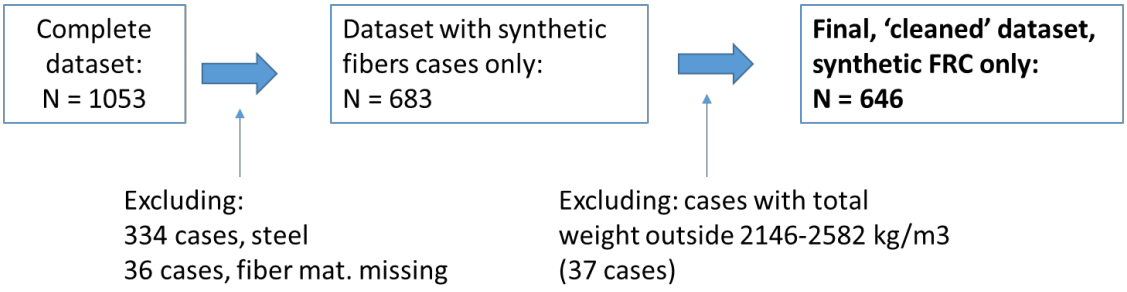

Figure 38. Summary of the preparation of synthetic FRC data for modelling.

4.2 Coarse-to-fine aggregate ratio

4.2.1 Justification. After several attempts at modeling the relationships between variables concerned with the aggregates and the other mix design variables, it was concluded that the most satisfactory strategy was to follow the same modeling rationale as in the case of SFRC mixtures (section 2.2.1). In consequence, the coarse-to-fine aggregate ratio is the first parameter discussed in relation to the synthetic FRC mixtures.

4.2.2 General trend and outliers. Figure 39 shows the scatterplot of the values of the coarse-to-fine aggregate ratio of the synthetic FRC mixtures in the dataset against their coarse aggregate content. This confirms a clear trend where a direct, positive correlation between the two parameters is obvious.

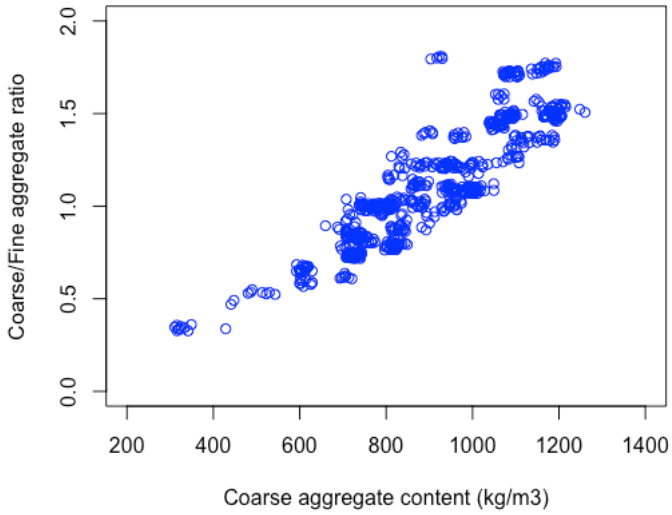

Figure 39. Coarse-to-fine aggregate ratio vs coarse aggregate content (kg/m³).

4.2.3 Regression analysis and fitted equation. A multiple linear regression analysis was performed to obtain an expression relating the coarse-to-fine aggregate ratio to the coarse aggregate content, the maximum aggregate size, and the fiber material. All the quadratic terms and pairwise interactions of these variables were initially included, and the equation was simplified by sequentially removing statistically non-significant terms. The following equation was obtained (R-squared = 0.87), with an error term of ±0.09 for the estimate:

$$\frac{G}{S} = (k - 8.53\, m + 0.831\, G + 0.001\, G^2) \times 10^{-3} \pm 0.09 \tag{9}$$

Where G and S are the the relative amounts of coarse aggregate and fine aggregate, respectively (kg/m³); m is the maximum aggregate size (mm); and k is a coefficient that depends on the fiber material, its different values as per equation (10):

$$k = \begin{cases} 40.0\ (PP) \\ 87.3\ (PO) \\ 338.9\ (PVA) \\ 187.1\ (HDPE) \\ 5.7\ (PET) \end{cases} \tag{10}$$

4.2.4 Significance of the fiber material. In equation (9), the coefficients multiplying the different terms that represent the maximum aggregate size and the coarse aggregate content do not vary with the fiber material. This is because the interactions between those two variables

and the fiber material were found to be statistically not significant as far as their relationship with the coarse-to-fine aggregate ratio is concerned. Therefore, the trend of the coarse-to-fine aggregate ratio with respect to the coarse aggregate content (or with respect to the maximum aggregate size) does not change with the fiber material. What changes is the baseline, as illustrated in Figure 40, where equation (9) is plotted for PP, PO, or PVA fibers, assuming a maximum aggregate size of 16 mm.

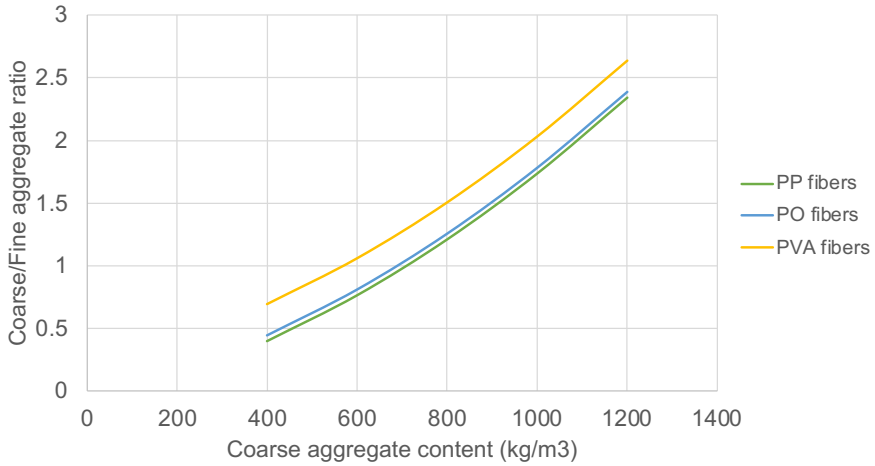

Figure 40. Estimated coarse-to-fine aggregate ratio vs coarse aggregate content (kg/m³).

However, the fact that the fiber material introduces statistically significant differences in equation (9) does not mean that *all* these differences are statistically significant. The different values obtained for the regression coefficient k given in (10) can be examined in more detail to determine which fiber materials are significantly different to others in terms of their relationship with the coarse-to-fine aggregate ratio. A direct, pairwise comparison between the different values of this coefficient is not appropriate, because, among other reasons, not all the groups being compared have the same number of data. Instead, an analysis based on Tukey's intervals for the differences between means for multiple comparisons can be performed. A graphical summary of this analysis is shown in Figure 41, where each interval represents a confidence interval for the average difference in G/S ratios between any two fiber materials, adjusted taking into account the multiple comparison context. An interval not intersecting the vertical dashed line (which corresponds to zero difference) means that the difference represented by such interval is statistically significant (that is, significantly different to zero).

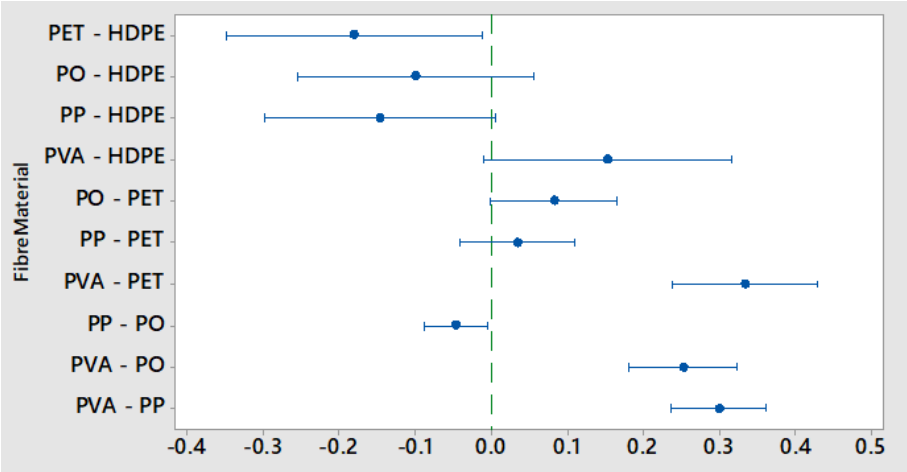

Figure 41. Tukey's intervals for the difference between means (fiber materials).

The intervals corresponding to the comparisons PVA-PO and PVA-PP do not include zero, which indicates that mixtures with PVA fibers are significantly different from mixtures with either PP or PO fibers. Also, the interval for the PP-PO comparison does not contain zero, meaning that there is a statistically significant difference between mixtures with PP fibers and mixtures with PO fibers. As a result, it can be concluded that there are three groups of mixtures in the synthetic FRC database: those with PP fibers, those with PO fibers, and those with PVA fibers, and that the differences between them are statistically significant.

Another interval indicating a significant difference is that which corresponds to the PVA-PET comparison; however, PET cases are not dissimilar from either PO or PP (as both the PO-PET and the PP-PET intervals include zero), and therefore the PVA-PET interval in Figure 41 is no different to the PVA-PO and PVA-PP intervals. However, it is important not to forget that the number of cases in the synthetic FRC database is not equally split amont all these fiber materials. If the SFRC cases are put aside, mixtures with either PP, PO, or PVA fibers represent 95% of the information in the synthetic FRC dataset.

For the reasons explained in the two preceding paragraphs, the interpretation and discussion of the equations discussed in the subsequent sections of this chapter will focus on FRC mixtures with either PP, PO, or PVA fibers and their comparative analysis.

4.3 Coarse aggregate content

4.3.1 Justification and rationale. Preliminary analyses were conducted to try and model the amounts of fine aggregate and coarse aggregate as well as the total aggregate content as a function of the other mix parameters, paying particular attention to the role of fibers. It was concluded that the most satisfactory model in terms of goodness of fit, no multicollinearity and simple specification is obtained for the coarse aggregate content. The rationale behind the analysis and modelling strategy in this section and those that follow is similar to that explained in relation to the SFRC database in chapter 2 of this report.

4.3.2 Regression analysis and fitted equation. The regression analysis yielded the following equation (R-squared = 0.61), with an error term of ±85 kg/m^3 for the estimate:

$$G = k_0 + k_1\lambda_f + 0.00171{\lambda_f}^2 + V_f(k_2 + 6.68l_f + k_3\lambda_f) + 70.3{V_f}^2 + l_f(k_4 - 0.0266\lambda_f) - 0.2456{l_f}^2 + m(0.1272\lambda_f + k_5 l_f + k_6 V_f) \pm 85 \quad (11)$$

Where m is the maximum aggregate size (mm), V_f is the fibre volume fraction (in percentage), l_f is the fibre length (mm), and λ_f is the fibre aspect ratio. The coefficients k_0, k_1, k_2, k_3, k_4, k_5, and k_6 depend on the fiber material and are given in Table 5.

Table 5. Values of the coefficients in equation (11), for different fiber materials.

Fiber material	k_0	k_1	k_2	k_3	k_4	k_5	k_6
PP	753.2	-2.95	-237.9	0.196	16.45	0.262	-17.94
PO	-370.0	4.07	-1195.0	-7.050	6.68	-0.499	97.60
PVA	1568.0	-3.95	-563.0	-0.094	-8.80	-0.440	25.90
PET	916.0	-4.21	2331.0	2.860	-51.00	5.200	-240.00
HDPE	910.0	0.00	-295.0	0.000	0.00	0.000	0.00

In comparison with with the model obtained for the coarse aggregate content of SFRC mixtures (section 2.3.2), the R-squared of the model for synthetic FRC mixtures is not so good (0.61 versus 0.76), but, interestingly, the error term is lower (85 kg/m^3 versus 129 kg/m^3). The fitted model as per equation (11) is quite complex, due to several interactions between variables being statistically significant. Furthermore, most of the coefficients in the equation vary with the fiber material. In consequence, the interpretation of equation (11) and the discussion regarding the trends that the coarse aggregate content follows with respect to the other mix design variables is challenging. This is hardly a surprise, considering the much higher variability in terms of fiber material properties and fiber shapes in the synthetic FRC database.

The following sections are concerned with the interpretation of the trends followed by the coarse aggregate content of synthetic FRC mixtures as modelled by equation (11), with respect to the maximum aggregate size and the variables related to the fiber dimensions and content. This analysis focuses on PP, PO, and PVA fibers for the following reasons: *i)* the majority of the cases in the synthetic FRC database correspond to mixtures with either PP or PO fibers; *ii)* cases with PVA fibers, though not abundant in the database, have been identified as significantly different from those with PP/PO fibers (section 4.2.4).

4.3.3 Effect of the fiber dimensions on the coarse aggregate content. Figure 42 shows the contour plots for the coarse aggregate content obtained by plotting equation (11) considering three different volume fractions of PP fibers: 0.5%, 1.0% and 1.5%. Discussing these contour plots in terms of what causes the coarse aggregate content to decrease turns out to be the most helpful way to interpret them, for the following reasons. As evidenced in Figure 39, reductions in the coarse aggregate content are generally associated with lower coarse-to-fine aggregate ratios, implying an increase in the fine aggregate content and/or a decrease in the total aggregate content, with the corresponding increase of the relative volume of paste. In other words, a reduction of the coarse aggregate content is generally associated with the need for more cohesiveness. And this, considering that fibers are present in the mixture, can be attributed to the fibers making the stability of the fresh mixture more challenging.

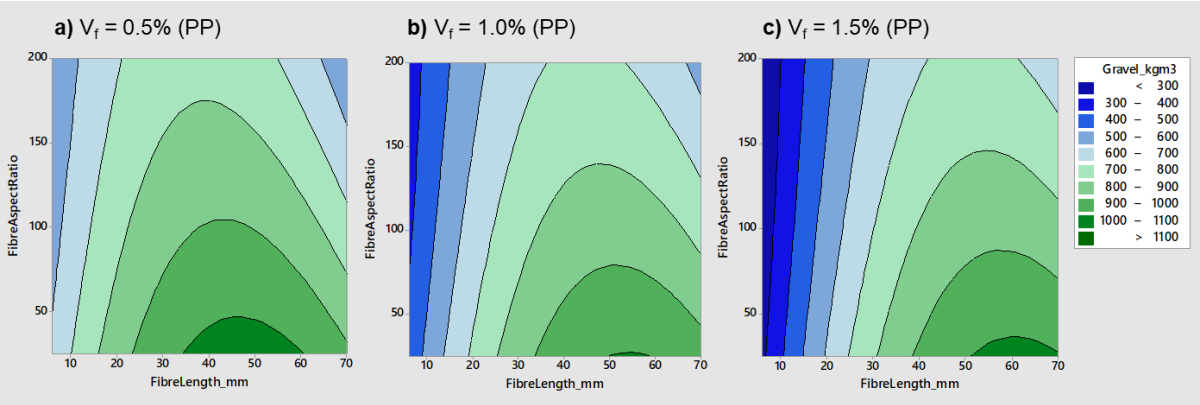

*Figure 42. Contour plots for coarse aggregate content (kg/m^3) as a function of PP fiber length and aspect ratio, assuming different PP fiber contents (*m*=16 mm).*

As the contour plots in Figure 42 show, the highest coarse aggregate contents are associated with PP fibers whose length falls within the range of approximately 45 to 60 mm. If the fiber length is assumed within that range and the fiber aspect ratio is not higher than 100, varying the fiber length or the fiber content is not associated with big variations in the coarse aggregate content. On the other hand, high to very high values of the fiber aspect ratio (100 and higher)

are generally associated with significant reductions of the coarse aggregate content. This is even more clear when shorter PP fibers (particularly 30 mm and shorter) are considered, making the coarse aggregate content more sensitive to variations in fiber length.

In summary, from Figure 42 it can be concluded that PP fibers introduce significant requirements in terms of the cohesiveness of the fresh mixture through a reduction of the coarse aggregate content. However, this becomes less critical when the fiber length is of 45-60 mm, the fiber aspect ratio is lower than 100, and the fiber volume fraction is less than 1%.

Figure 43 shows the contour plots for the coarse aggregate content obtained by plotting equation (11) and assuming PO fibers in volume fractions of 1.0% and 1.5%. The trend followed by the coarse aggregate content with respect to the fiber length and the fiber aspect ratio is not dissimilar to that observed for mixtures with PP fibers. When the PO fiber content is 1.0%, values of the fiber length between 50-65 mm are compatible with the coarse aggregate content being equal to, or close to the median (954 kg/m^3), as long as the aspect ratio is not higher than 100. In other words, PO fibers of 50-65 mm length do not seem to require significant reductions of the coarse aggregate content when dosed below 1%.

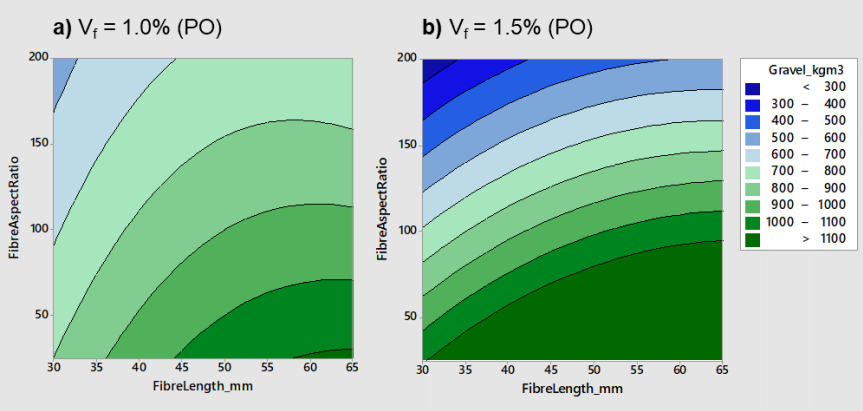

*Figure 43. Contour plots for coarse aggregate content (kg/m^3) as a function of PO fiber length and aspect ratio, assuming different PO fiber contents (*m*=16 mm).*

However, when higher volume fractions of PO fibers are considered (for example, 1.5% in Figure 43 b), the range of values of both the fiber length and aspect ratio that are compatible with coarse aggregate contents around the median becomes more limited, as is reflected by the higher proportion of the contour plot in blue.

The contour plots shown in Figure 44 assume three different volume fractions of PVA fibers: 0.5%, 1.0% and 1.5%. The dashed lines correspond to the values of the coarse aggregate content between which 50% of the cases in the synthetic FRC mixtures dataset are found: 750-1100 kg/m^3. These have been added to the contour plot in order to provide a clearer framework for comparison. It can be seen that there are no major differences between the three contour plots in Figure 44. Therefore, it can be concluded that varying the PVA fiber contents between 0.5% and 1.5% is not associated with significant changes in the relationship between the coarse aggregate content and the fiber length of aspect ratio.

To describe the association between the coarse aggregate content and the dimensions of the PVA fibers used in the mixture, it is useful to consider three reference values for the coarse aggregate content: 750, 954 (median), and 1100 kg/m^3. These define the following areas in the three contour plots (that is, regardless of the volume fraction):

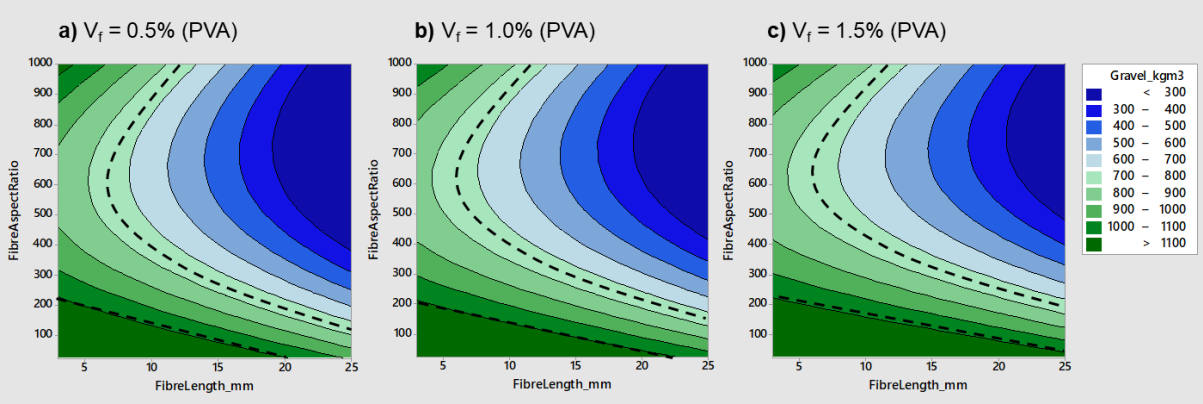

*Figure 44. Contour plots for the coarse aggregate content as a function of fibre length and aspect ratio, assuming different PVA fiber contents (*m*=16 mm).*

- Relatively short PVA fibers (length not higher than 6-7 mm) are generally compatible with median and above-median values of the coarse aggregate content, irrespective of their aspect ratio. This suggests that PVA fibers shorter than 6-7 mm do not generally require dramatic adjustments to the coarse aggregate content, not imposing particularly restrictive requirements in terms of the cohesiveness of the fresh mixture.
- PVA fibers longer than 6-7 mm are not associated with marked reductions of the coarse aggregate content either, as long as their aspect ratio is not higher than 150-200.

  For example, if the contour line corresponding to the median coarse aggregate content is considered (954 kg/m^3), a fiber length of 10 mm is associated with aspect ratios lower than 240, and a fiber length of 20 mm is associated with aspect ratios lower than 130. Hence the upper limit of 150-200 for the aspect ratio.
- Generally, reductions in coarse aggregate content (and the corresponding increase of the fine aggregate content and/or relative volume of paste) are associated with mixtures with PVA fibers that are longer than 6-7 mm and have high aspect ratios.

4.3.4 Effect of the maximum aggregate size and fiber dosage on the coarse aggregate content. The contour plots resulting from plotting equation (11) against the maximum aggregate size and the fiber volume fraction, assuming PP, PO, or PVA fibers, are shown in Figure 45. In each of these contour plots, the fiber aspect ratio and fiber length are assumed to be the median, different for each fiber material.

A common, general trend can be observed in all three cases: higher values of the maximum aggregate size are generally associated with a higher coarse aggregate content, which, in turn, means a lower fine aggregate content and/or a lower relative volume of paste. It is not surprising that mixtures with bigger aggregates tend to have a higher amount of coarse aggregate. However, this can also be interpreted as meaning that aggregates with a bigger maximum size are used in synthetic FRC mixtures when the cohesiveness of the fresh mixture is not considered a limiting factor. Or, that a higher value of the maximum aggregate size somewhat moderates the need of enhancing the cohesiveness of the mixture, indicating potentially more stable mixtures. In any case, what these contour plots show is the association between those parameters as identified in the synthetic FRC mixtures in the database, not causal relationships, and therefore the above statements should be considered with caution.

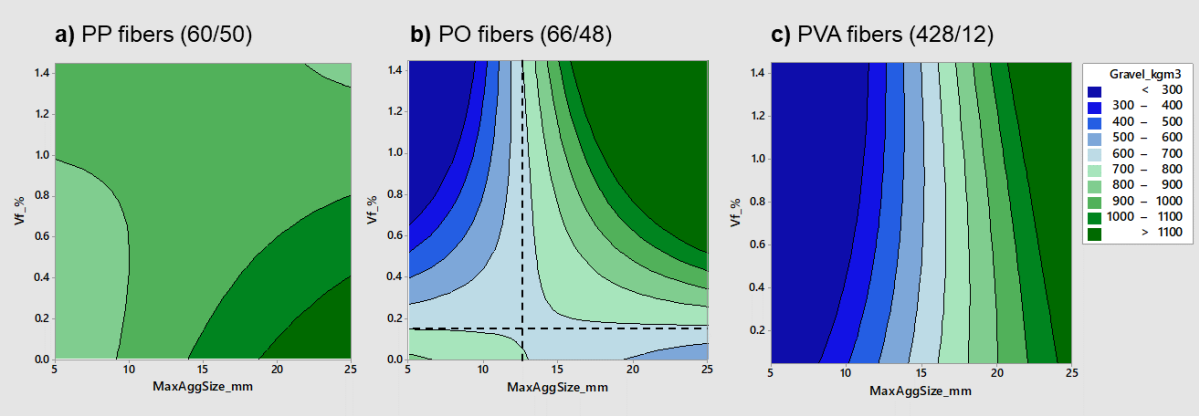

Figure 45. Coarse aggregate contents vs maximum aggregate size and fiber dosage.

4.3.4.a) PP fibers. In relation to mixtures with PP fibers, most of the contour plot shown in Figure 45a corresponds to coarse aggregate contents between 900 and 1100 kg/m^3, supporting the idea that FRC mixtures with PP fibers are not particularly sensitive to variations of the maximum aggregate size. The contour plot also shows that, for low to moderate PP fiber contents i.e. up to 0.80%, values of the maximum aggregate size equal to 15 mm or higher are associated with slightly higher-than-median values of the coarse aggregate.

4.3.4.b) PO fibers. The contour plot in Figure 45b shows that, in mixtures with PO fibers, the general trend whereby increasing values of the maximum aggregate size are associated with higher coarse aggregate contents is valid when the fiber volume fraction is higher than 0.2% (represented by a horizontal dashed line). For PO fiber contents below 0.2%, the coarse aggregate content is typically 600-700 kg/m^3 and practically insensitive to the maximum aggregate size. The coarse aggregate content is also between 600-700 kg/m^3 when the maximum aggregate size is 12-13 mm (vertical dashed line), irrespective of the PO fiber content.

When the maximum aggregate size is higher than 12-13 mm, higher PO fiber contents are associated with increasing coarse aggregate contents. On the other hand, when the maximum aggregate size is lower than 12 mm, higher amounts of PO fibers are associated with decreasing coarse aggregate contents. This can be indicative of potentially more problematic mixtures in terms of their stability, requiring their coarse aggregate content to be decreased in favor of the fine aggregate content and/or the relative amount of paste.

4.3.4.c) PVA fibers. The contour plot in Figure 45c shows that, in mixtures with PVA fibers, the coarse aggregate content is clearly determined by the maximum aggregate size rather than the fiber volume fraction. This can be partially attributed to the fact that PVA fibers are, out of the three fiber materials considered in Figure 45, the ones with the highest aspect ratio.

4.4 Total binder content

4.4.1 Justification and rationale. The rationale and methodology followed in this section are essentially the same as followed in relation to the SFRC database (section 2.4.1), with the difference that the fiber material is now incorporated to the set of variables. A multiple linear regression analysis was applied to model the total binder content as a function of the following

variables: maximum aggregate size, fine aggregate and coarse aggregate contents, fiber material, fiber length, fiber aspect ratio, and fiber volume fraction.

4.4.2 Regression analysis and fitted equation. All quadratic and pairwise interaction terms were considered in the first instance, then the model was simplified by stepwise regression. The following equation was obtained (R-squared = 0.84), with an error term of ±29 kg/m^3 for the estimate:

$$B = 2681 - 1.445\,S - 1.883\,G - c_1 10^{-6} S^2 + 0.000424\,G^2 + 0.000431\,S \times G + m\,(0.02837\,S + 0.00888\,G - c_2) \pm 29 \quad (12)$$

Where B, S, and G are the binder content, the fine aggregate, and the coarse aggregate content (kg/m^3), respectively; m is the maximum aggregate size (mm); and the regression coefficients c_1, c_2 depend on the fiber material. The values obtained for these coefficients are given in Table 6.

Table 6. Values of the coefficients in equation (12).

Fiber material	c_1	c_2
PP	8	32.21
PO	9	32.78
PVA	146	28.92
PET	361	18.35
HDPE	1237	0.00

The variables related to the fiber content and the fiber dimensions (volume fraction, fiber length and aspect ratio) were statistically non-significant in relation to the binder content, and that is the reason why they do not appear in equation (12). This can seem somewhat surprising, but the effect of the fibers does influence the coarse aggregate content and in consequence the fine aggregate content as well, via the coarse aggregate/fine aggregate ratio. In consequence, the associations between the binder content, the fiber volume fraction and the fiber dimensions are implicit in equation (12). On the other hand, differences in fiber material have a statistically significant effect on the binder content as they modify the terms representing the maximum aggregate size and the fine aggregate content. This is reflected in equation (12) through the coefficients c_1 and c_2.

4.4.3 Model diagnosis and potential outliers. The plot of the estimates of the binder content as per equation (12) versus the actual binder contents is shown in Figure 46. Actual values of the binder contents are, in 90% of the cases, between 310 and 600 kg/m^3, and equation (12) estimates those cases relatively well, although the scatter is not negligible. In 10% of the cases where the binder content takes values outside of the above range, the estimates produced by equation (12) showed a similar goodness of fit. In other words, Figure 46 shows that there is no need to discard any of the potential outliers.

4.4.4 Maximum aggregate size and binder content. The relationship between the maximum aggregate size and the binder content is represented by three terms in equation (12): the interactions between the maximum aggregate size and the fine and coarse aggregate contents, and the regression coefficient c_2, which depends on the fiber material. As Table 6 shows, the values of c_2 are very similar for mixtures with PP, PO, and PVA fibers. For this discussion, the average of the three values is adopted for coefficient c_2.

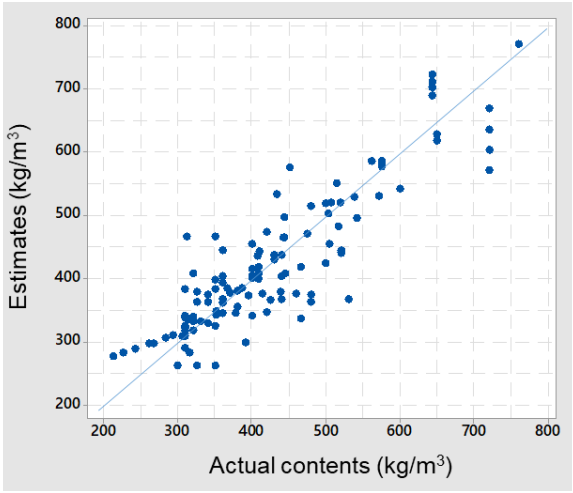

Figure 46. Binder content estimates vs actual binder contents (kg/m^3).

In order to interpret the relationship between maximum aggregate size and the binder content as represented by equation (12), it is useful to consider how the average binder content changes when the maximum aggregate size is increased, for instance, from 10 mm to 20 mm, for different contents of the fine and coarse aggregates. This is what is shown in Figure 47 as a surface plot. It can be seen that increasing the maximum aggregate size from 10 to 20 mm can be associated with either an increase or a decrease of the binder content, depending on the relative amounts of fine and coarse aggregates. If the fine and the coarse aggregate contents are assumed at their median values (849 and 954 kg/m^3, respectively), a variation of the maximum aggregate size from 10 mm to 20 mm is associated with the binder content increasing by 12.6 kg/m^3 on average, which is a small change. However, this variation is associated with the binder content decreasing by 50 kg/m^3 if the fine aggregate content is 600 kg/m^3 and the coarse aggregate content is 1000 kg/m^3.

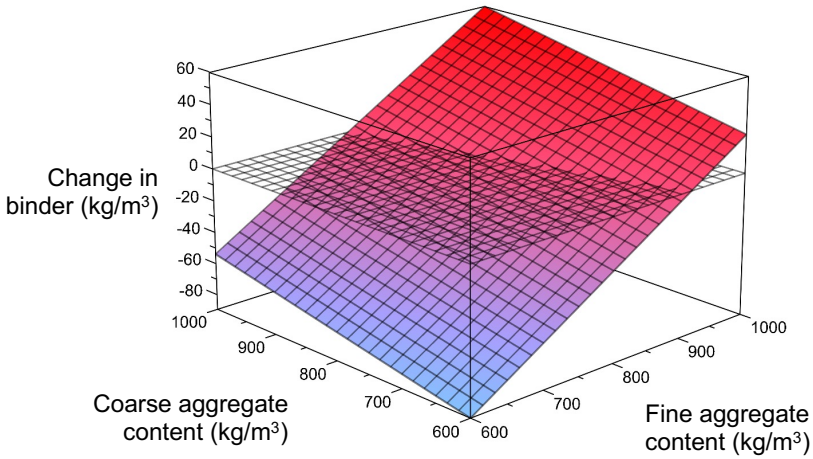

Figure 47. Change in binder content when m is increased from 10 to 20 mm.

4.4.5 Binder content vs fine aggregate and coarse aggregate contents. At the end of the previous section, it has been shown that the trend followed by the binder content with respect to a variable concerned with the aggregates can be of a different sign depending on the values of the other variables. In this section, the contour plots for the binder content as per equation (12) as a function of the fine and coarse aggregate contents, are discussed, assuming mixtures with PP, PO, or PVA fibers. For these contour plots, shown in Figure 48, the same range is

considered for the amounts of fine aggregate and coarse aggregate, based on the ranges identified as containing no potential outliers (sections 3.4.1 and 3.4.2). The maximum aggregate size has been assumed as 10 mm. Furthermore, since not all combinations of fine and coarse aggregate contents in are possible in normal density mixtures, an additional feasibility condition has been imposed, following the same reasoning described in section 2.4.5. The grayed out areas in Figure 48 correspond to such unrealistic combinations.

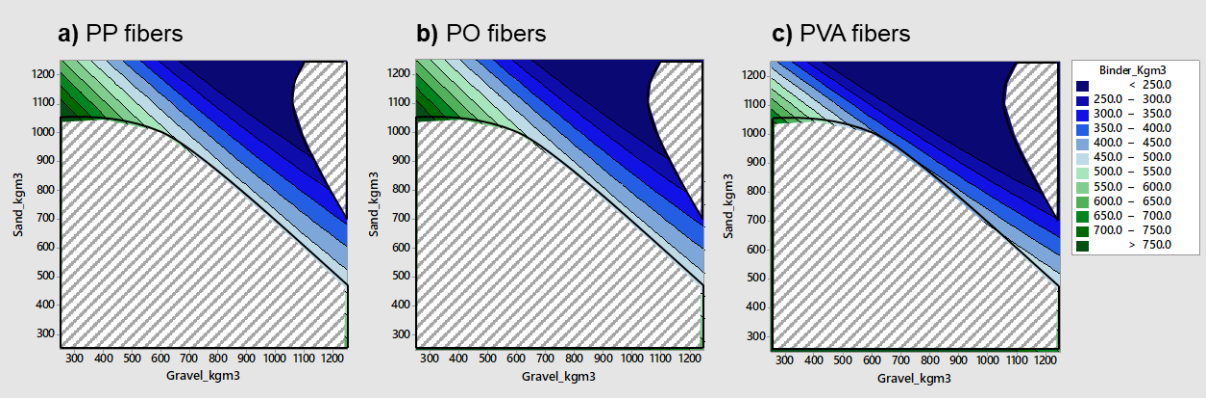

Figure 48. Contour plots of total binder vs fine aggregate and coarse aggregate contents, for two different values of the maximum aggregate size.

In all three contour plots, higher values of the binder content are associated with the coarse aggregate content being lower than the fine aggregate content. That is, the coarse-to-fine aggregate ratio decreases with the binder content. On the other hand, lower values of the binder content are associated with mixtures where the fine aggregate and the coarse aggregate contents are not too dissimilar, i.e. coarse-to-fine aggregate ratios close to unity. In this respect, the trend followed by the binder content with respect to the fine and coarse aggregate contents in synthetic FRC mixtures is not dissimilar to that observed in relation to SFRC mixtures (section 2.4.5).

5. Residual flexural strength parameters of SFRC as a function of the mix design variables

5.1 Introduction

5.1.1 Context and scope of this chapter. This chapter is concerned with the statistical modeling and analysis of the relationships between each of the residual flexural strength parameters (f_{R1}, f_{R2}, f_{R3}, and f_{R4} as per EN 14651) and the variables describing the SFRC mixtures in terms of the relative amounts of their constituents and the fundamental descriptors of such constituents.

This analysis builds on the study and modeling of the relationships between the different mix design variables of SFRC, presented in chapter 2. The multivariate analysis and the study of the variability of residual flexural strength, in chapters 6 and 8 of this report, respectively, complement this analysis.

5.1.2 Dataset of SFRC mixtures. The data used to develop the models discussed in this chapter is the database of SFRC mixtures, which has been described in detail in chapter 1.

Cases with extremely high residual flexural strength values are potentially too influential, as a result of having a disproportionate leverage with respect to other data points. Following what is generally considered good practice in data analysis, the most extreme data were excluded from the dataset prior to the multiple linear regression analysis. To identify such cases without introducing bias, the 99th percentile of the limit of proportionality (LOP) was adopted as reference: cases with a LOP > 25 MPa, a total of 24 out of 766, were excluded.

5.1.3 Methodological considerations. The approach followed for this analysis is based on the statistical technique known as multiple linear regression, which is a supervised learning method for obtaining a set of equations that relate each of the residual flexural strength parameters to the mix design variables.

The two main objectives of the multiple linear regression analysis were: the equations themselves, and the knowledge that can be extracted from their interpretation and discussion. These equations can be used as part of the mix proportioning process, e.g. to estimate the average residual flexural strength values that can be expected from a SFRC mixture. Furthermore, they can be used to generate different plots (sometimes called response surfaces) that help to visualize, describe, discuss and understand the trends that each residual flexural strength parameter follows with respect to the mix design variables. Response surfaces can be represented as three-dimensional graphs or as contour plots. In this report, contour plots are used.

In the development of the model specification (that is, the structure of the equations to be fitted to the SFRC data), considerable efforts were made to go beyond the merely predictive / estimation purpose. The accuracy of the equations in fitting the residual flexural strength values in the SFRC dataset (measured through the coefficient of determination, R^2 or R-squared) was, of course, a key aspect, but not the only one. In addition to that, the following considerations were taken into account:

- The equations to be obtained for f_{R1}, f_{R2}, f_{R3}, and f_{R4} had to follow the same generic 'format' or structure, that is: be a function of the same set of variables and products between variables (i.e. interactions), differing only in the values of the regression coefficients. This was motivated by two reasons:
    - All four residual flexural strength parameters are highly correlated and generally follow similar trends with respect to mix design variables.
    - All four residual flexural strength parameters can be regarded as alternative measurement of the same multivariate phenomenon, which is the residual flexural strength of the material.

  Because of these reasons, the modeling assumption that all four predictive equations had to be consistent was adopted. Throughout this chapter, the term 'model' is used to refer to the four predictive equations.

- The model had to be relatively simple in its specification: it had to include a relatively small number of terms. There was a balance to be sought between the goodness of fit (i.e. R-squared) and the complexity of the model. For several reasons:
    - Many alternative models can be specified and fitted to any dataset. Specifying more complex regression models (i.e. with more terms in the regression equation) generally leads to higher R-squared values. However, the widely accepted principle of parsimony in statistical modeling states that, between models that have a comparable accuracy, the simplest one is preferable. Regression models with too many terms are usually the result of over-fitting the data and are therefore less robust (this is known as the accuracy paradox[1]).
    - The equations to be obtained for f_{R1}, f_{R2}, f_{R3}, and f_{R4} had to be unnecessarily complicated so that they can be easily interpreted and manipulated mathematically. The idea was that these expressions are accessible for any concrete technologist to interpret and use them to obtain estimates or compare mixtures with a simple spreadsheet.
    - Concrete shows considerable variability in its mechanical properties, even between samples from the same batch. In particular, the values of the residual flexural strength parameters of SFRC as obtained from beam bending tests are highly scattered: high coefficients of variation are not unusual[2]. With this in mind, trying to fit models with a very high goodness of fit (R-squared values of, say, 0.90 or higher) would artificially inflate their accuracy.

  Based on the above, aiming at an R-squared value above 0.70 (70%) was considered a realistic target for the regression equations to be obtained for f_{R1}, f_{R2}, f_{R3}, and f_{R4}.

[1] The problem of over-fitting data and the accuracy paradox has been widely discussed in data analytics and machine learning literature. Two good references for the non-specialist are, for example: Lever, J. et al (2016), "Model selection and overfitting", *Nature Methods* 13(9):703-704, and Ben-David, A. (2007), "A lot of randomness is hiding in accuracy", *Engineering Applications of Artificial Intelligence* 20(7):875-885.

[2] See, for example, Cavalaro, S. and Aguado, A. (2014), "Intrinsic scatter of FRC: an alternative philosophy to estimate characteristic values", *Materials and Structures* 48():3537-3555.

5.2 Fitted model

5.2.1 Regression analysis and fitted model. Several alternative specifications were explored to find an expression relating each residual flexural strength parameter to the mix design variables. In all the attempts, quadratic terms and pairwise interactions (e.g. fiber volume fraction times fiber aspect ratio) were initially included in the model. Following an analysis of variance, those terms that were found not to have a statistically significant effect on the residual flexural strength parameters were sequentially discarded, until the fitted equations included only statistically significant terms.

The obtained model can be expressed as follows:

$$f_{Ri} = k_0 + k_1\frac{G}{S} + (a_0 + a_1 m)\, l_f + \left(b_0 + b_1 C + b_2 SP + b_3\lambda_f + b_4 l_f\right) V_f + k_2\, SCM + k_3\, SP + k_4\lambda_f + k_5 m + k_6 C + \left(c_1\, C + c_2\, SCM + c_3\frac{G}{S}\right)(G + S) \pm \varepsilon \quad (13)$$

Where:

f_{Ri} represents either f_{R1}, f_{R2}, f_{R3}, or f_{R4}, expressed in MPa.

k_0 is a regression coefficient, which is different for f_{R1}, f_{R2}, f_{R3}, and f_{R4}. It groups the intercept and the term that depends on the test/specimen configuration. Its fitted values are given in Table 7.

k_1, k_2,…, a_0, a_1,…, b_0, b_1,…, c_1, c_2, c_3 are the regression coefficients corresponding to the effect of the SFRC mixture proportioning variables. They are different for f_{R1}, f_{R2}, f_{R3}, and f_{R4}, and their fitted values are given in Table 8.

S and G are the relative amounts of fine and coarse aggregate, respectively, in kg/m^3.

m is the maximum aggregate size, in mm.

C and SCM are the relative amounts of cement and supplementary cementitious materials, respectively, in kg/m^3.

SP is the relative amount of superplasticizer, in kg/m^3.

V_f is the steel fiber volume fraction, in percentage.

l_f and λ_f are the fiber length (expressed in mm) and the fiber aspect ratio, respectively.

ε is the error term of the estimation, which is 2.5 MPa, 3.0 MPa, 3.1 MPa, and 2.9 MPa for f_{R1}, f_{R2}, f_{R3}, and f_{R4}, respectively.

Table 7. Values of the regression coefficients: k_0.

Test / specimen configuration	**Residual flexural strength parameter**			
	f_{R1}	f_{R2}	f_{R3}	f_{R4}
3-point, notched	-1.61	0.78	1.39	3.18
4-point, unnotched	-2.35	-0.19	0.13	2.15

Table 8. Values of the regression coefficients.

Coefficient	Residual flexural strength parameter			
	f_{R1}	f_{R2}	f_{R3}	f_{R4}
$\mathbf{k_1}$	0	-5.67	-7.16	-3.07
$\mathbf{k_2}$	0.07563	0.04655	0.02071	0.0186
$\mathbf{k_3}$	0.0963	0	-0.1054	-0.1088
$\mathbf{k_4}$	-0.0679	-0.077	-0.0668	-0.0322
$\mathbf{k_5}$	0.385	0.1923	0	-0.149
$\mathbf{k_6}$	-0.01117	0.0041	0.01466	0.00347
$\mathbf{a_0}$	0.1842	0.1662	0.0894	0
$\mathbf{a_1}$	-0.00807	-0.00463	0	0.003275
$\mathbf{b_0}$	-3.897	-5.969	-5.41	-6.822
$\mathbf{b_1}$	0.00558	0	-0.00376	0
$\mathbf{b_2}$	-0.0984	0.0237	0.0943	0.0937
$\mathbf{b_3}$	0.1616	0.2179	0.2077	0.1651
$\mathbf{b_4}$	-0.0708	-0.0606	-0.0433	0
$\mathbf{c_1}$	0.000005	-0.000003	-0.000006	0
$\mathbf{c_2}$	-0.000044	-0.000028	-0.000012	-0.000011
$\mathbf{c_3}$	0	0.002981	0.00377	0.001505

In equation (13), the different terms and interactions of the model have been rearranged and grouped so that the meaning of the statistically significant interactions is clearly represented in the way the model is written. The most salient observations are:

- There is only one term that depends on the test and specimen configuration, and that is the intercept, k_0. Therefore, according to the fitted model, the relative effect that varying any proportioning variable has on the residual flexural strength parameters is independent from, and not significantly affected by the test/specimen being 3PBT/notched or 4PB/unnotched. As can be seen from the k_0 values in Table 7, the residual flexural strength values obtained when testing notched specimens in 3-point bending are, on average, between 0.74 and 1.26 MPa higher than in the 4-point bending test.
- The relationship between the residual flexural strength parameters and the fiber volume fraction does depend on several other factors too, namely: the fiber length, the fiber aspect ratio, the cement content and the amount of superplasticizer.
- The effect of the fiber length, besides being dependent on the fiber volume fraction, is also influenced by the maximum aggregate size.

- There is a statistically significant relationship between the total amount of aggregates (G+S) and the residual flexural strength parameters, and this, in turn, is influenced by the cement content and the total amount of SCMs as well as the coarse-to-fine aggregate ratio.

5.2.2 Goodness of fit and cross-validation. The model consistently shows good accuracy in fitting the residual flexural strength values corresponding to the SFRC mixtures in the database. The R-squared values were 86%, 82%, 77% and 74% for f_{R1}, f_{R2}, f_{R3}, and f_{R4}, respectively. In Figure 49, the estimates calculated by the model for each of the SFRC mixtures in the database are plotted against the actual values of the residual flexural strength parameters, together with the exact equivalence lines for reference.

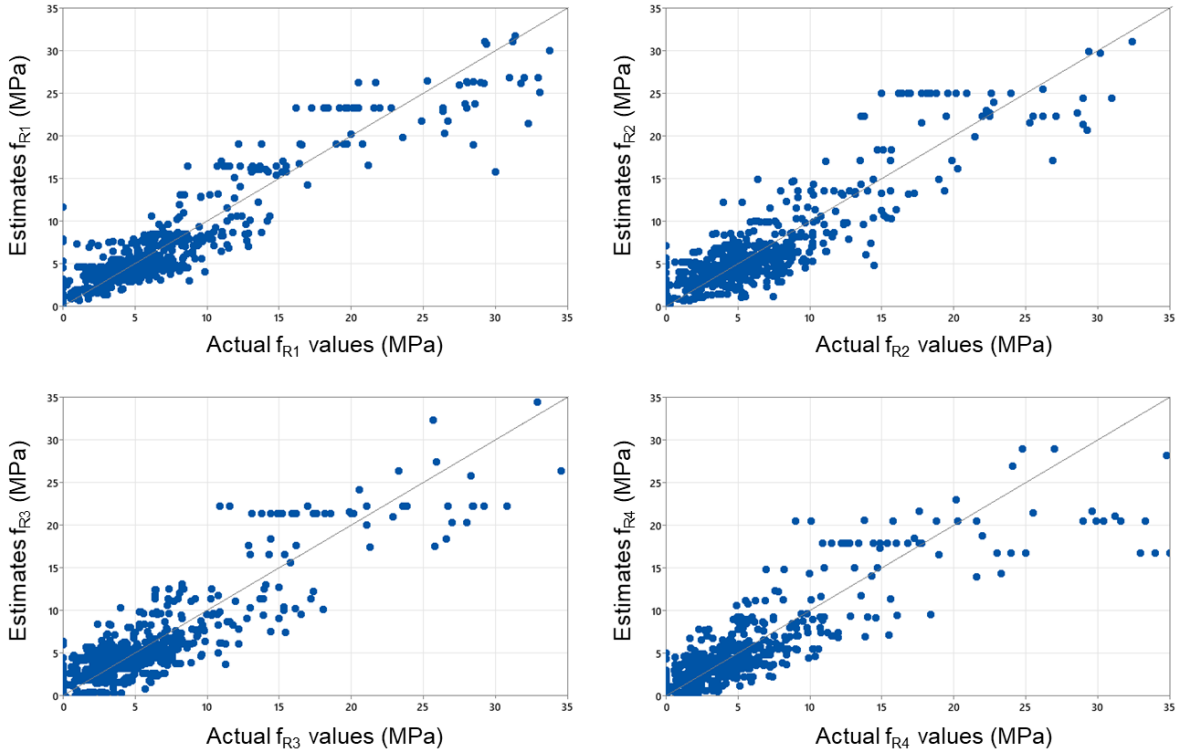

Figure 49. Fitted vs actual residual flexural strength values.

In addition to the overall R-squared values as a measure of the goodness of fit or accuracy of the model in fitting the values in the database, a k-fold cross-validation was performed for all four residual flexural strength parameters. This is a resampling procedure to assess the performance of the fitted equations in estimating new data, that is, other than those used in the regression analysis. It consists in randomly splitting the dataset into k different subsets, re-fitting the equation to the data in all subsets but one, and then measuring the goodness-of-fit in estimating the values left out. After doing this k times, an adjusted R-squared based on the prediction of data not used in fitting the equation is obtained. The cross-validation was done with k = 10, as this has been shown to work well in most cases[3]. Figure 50 shows the comparison between the original R-squared and the recalculated R-squared after the 10-fold

[3] An accessible overview can be found in chapter 5, and particularly sections 5.1.3 and 5.1.4, of James, G. (2013) *An Introduction to Statistical Learning with Applications in R*, Springer Texts in Statistics 103, DOI 10.1007/978-1-4614-7138-7_5

cross-validation. The differences between them are quite small, which shows that the model in equation (13) is robust in terms of predictive performance.

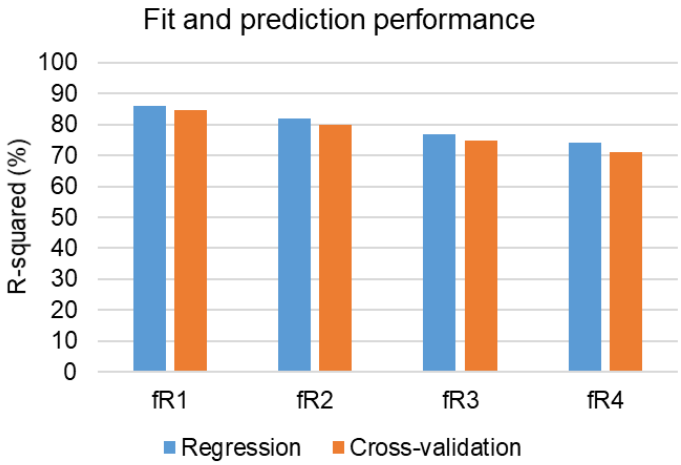

Figure 50. Assessment of predictive performance (cross-validation).

5.2.3 Interpretation and discussion of the terms in the model. The sections that follow are concerned with the interpretation of the trends followed by the residual flexural strength parameters as modelled by equation (13) with respect to the mixture proportioning variables identified as statistically significant. This will be done by means of contour plots mainly.

The modelled equation will also be used to quantify relevant magnitudes (such as optima) that arise from the analysis of the contour plots as well as to compare the relative impact of varying the different variables. Mostly, the trends with respect to mix design variables are consistent across all four residual flexural strength parameters and, to avoid repetition, the interpretation and discussion focus on one or two of them in each section.

5.3 Effect of fiber length and fiber content

5.3.1 Contour plots. Figure 51 shows the contour plots obtained by plotting the response surfaces corresponding to f_{R1} and f_{R2} as per equation (13) against the fiber length and the fiber volume fraction, assuming median values for the rest of mix design variables. The contour plots corresponding to f_{R3} and f_{R4} are very similar to the contour plot of f_{R2}. The discussion in this section focuses on f_{R1} and f_{R2}, as per the two plots in Figure 51.

5.3.2 Fiber length and f_{R1}. The fact that increasing the fiber volume fraction is associated with increasing values of f_{R1} is hardly surprising. However, the effect of the fiber volume fraction is connected to that of the fiber length and, in consequence, the effect of the fiber length on f_{R1} varies with the fiber content.

The contour plot of f_{R1} (Figure 51, left) shows that, for low or moderate fiber contents (up to ~0.8%), increasing the fiber length is associated with an increase of f_{R1} even if only slightly. This effect is more pronounced the lower the fiber volume fraction is. On the other hand, when high fiber contents are considered, the effect of the fiber length on f_{R1} is reversed, and increasing the fiber length is associated with decreasing levels of f_{R1}. The model as per equation (13) shows that, in general terms, f_{R1} is maximized when the fiber volume fraction is high and the fibers used are short (or, perhaps more appropriately put, not long).

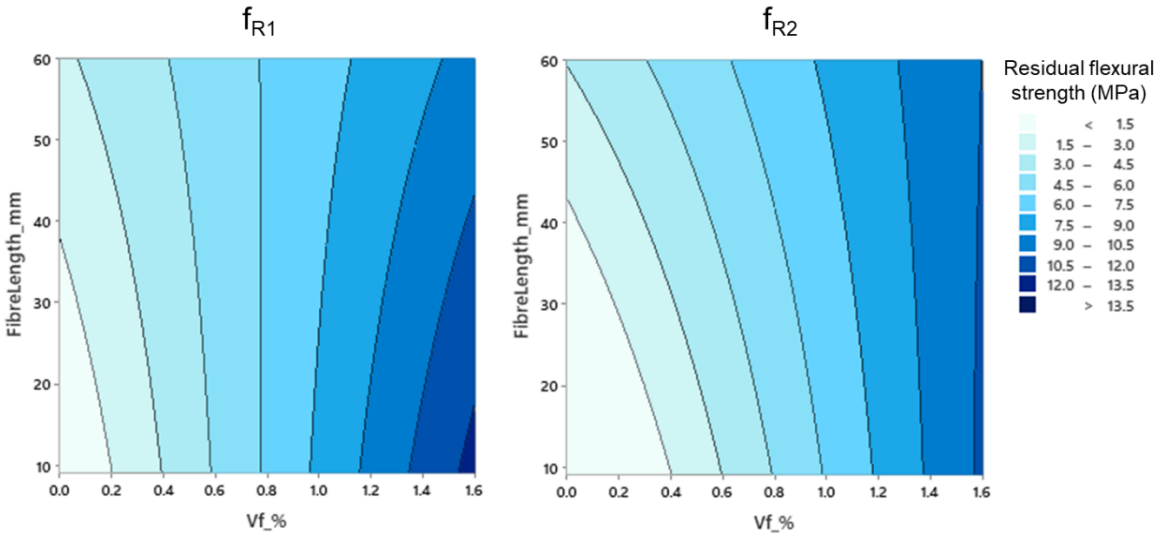

Figure 51. Contour plots of f_{R1} and f_{R2} vs fiber length and fiber volume fraction.

Interestingly, this means that there is a certain value of the fiber volume fraction which makes the effect of the fiber length on f_{R1} negligible, making the SFRC mixture insensitive to variations of the fiber length. Based on the contour plot in Figure 51 (left), this happens when the fiber volume fraction is between 0.8% and 1.0% approximately. However, it is important to question whether such 'threshold' value is valid in general, since this contour plot assumes median values for the rest of the mix design variables. The exact value can be obtained by differentiating equation (13) with respect to the fiber length and equating to zero:

$$\frac{\partial f_{R1}}{\partial l_f} = a_0 + a_1 m + b_4 V_f = 0 \tag{14}$$

After replacing the coefficients a_0, a_1, and b_4 with their values from Table 8, it follows that such 'threshold' fiber volume fraction is a function of the maximum aggregate size:

$$V_f = \frac{0.1842 - 0.00807\, m}{0.0708} = \begin{cases} 1.46\% & if\ m = 10mm \\ 0.89\% & if\ m = 15mm \\ 0.32\% & if\ m = 20mm \end{cases} \tag{15}$$

In consequence, in SFRC mixtures with fiber contents below 0.9%, increasing the fiber length has a positive effect on f_{R1} as long as the maximum aggregate size is not higher than 14-16 mm. In SFRC mixtures with bigger aggregates, increasing the fiber length can have a negative impact on f_{R1}.

5.3.3 Fiber length and f_{R2} (and f_{R3}, f_{R4}). The contour plot of f_{R2} (Figure 51, right), although similar to the plot of f_{R1}, presents a significant difference: there is no apparent change of sign in the trend with respect to the fiber length, considering values of the fiber length and the fiber volume fraction within the ranges considered in this study. Increasing the fiber length is associated with increasing f_{R2} values. However, the relative importance of the effect of fiber length on f_{R2} becomes less important when high fiber dosages are considered.

Theoretically, there is a value of the fiber volume fraction which makes f_{R2} insensitive to the fiber length. This can be determined by, again, differentiating equation (13) with respect to the

fiber length and equating to zero. After replacing coefficients a_0, a_1, and b_4 in equation (14) with the values from Table 8 corresponding to f_{R2}, it is obtained that:

$$V_f = \frac{0.1662 - 0.00463\,m}{0.0606} = \begin{cases} 1.98\% & if\ m = 10mm \\ 1.59\% & if\ m = 15mm \\ 1.21\% & if\ m = 20mm \end{cases} \quad (16)$$

What this means is that increasing the fiber length has a positive, non-negligible effect on f_{R2} when the fiber volume fraction does not exceed 1.6% as long as the maximum aggregate size is not bigger than 14-16 mm. However, steel fiber contents rarely exceed 1.6% in volume (section 1.5.1), and the maximum aggregate size of SFRC mixtures is generally not higher than 16 mm (in 75% of the cases, section 1.4.3). Therefore, in practical terms, it can be said that increasing the fiber length generally has a positive effect on f_{R2}.

In fact, the same can be said in relation to f_{R3} and f_{R4}: irrespective of the maximum aggregate size, increasing the fiber length is associated with higher values of f_{R3} and f_{R4}.

5.3.4 How 'important' is the effect of fiber length? A pertinent question that arises from the analysis of the contour plots in Figure 51 is whether the effect of the fiber length on the residual flexural strength parameters is comparable to that of the fiber volume fraction. It is not a straightforward comparison because a unit variation of the fiber length (e.g. from 45 mm to 46 mm) is not comparable to a unit variation of the fiber volume fraction (e.g. from 0.5% to 1.5%). It is more appropriate to consider, for example, a 10 mm increase of the fiber length and a 0.1% increase of the fiber content. For reference, f_{R2} can be considered.

This can be evaluated by, first, differentiating equation (13) for f_{R2} with respect to the fiber length, assuming median values for the rest of mix design variables:

$$\frac{\partial f_{R2}}{\partial l_f} = a_0 + a_1\,m + b_4\,V_f = 0.1662 - 0.00463 \times 16 - 0.0606 \times 0.5 = 0.062\ MPa/mm \quad (17)$$

Therefore, the expected variation of f_{R2} when the fiber length is increased in 10 mm is:

$$E\left(\Delta f_{R2} \middle| \Delta l_f = +10mm\right) = \frac{\partial f_{R2}}{\partial l_f} \times \Delta l_f = 0.62\ MPa \quad (18)$$

Similarly, by differentiating equation (13) for f_{R2} with respect to the fiber volume fraction, assuming median values for the rest of mix design variables, the following is obtained:

$$\frac{\partial f_{R2}}{\partial V_f} = b_0 + b_1 C + b_2 SP + b_3 \lambda_f + b_4 l_f = -5.97 + 0.024 \times 3.5 + 0.22 \times 65 - 0.061 \times 45 = 5.55\ MPa/\% \quad (19)$$

The expected variation of f_{R2} when the the fiber volume fraction is increased in 0.1% is:

$$E\left(\Delta f_{R2} | \Delta V_f = +0.1\%\right) = \frac{\partial f_{R2}}{\partial V_f} \times \Delta V_f = 0.55\ MPa \quad (20)$$

The values obtained in equations (18) and (20) can now be compared. Since 0.62 MPa and 0.55 MPa are similar, it can be concluded that gains in f_{R2} (and f_{R3} and f_{R4}, for that matter) associated with increasing the fiber length in 10 mm are comparable to the effect that increasing the fiber volume fraction in 0.1% has on those parameters.

5.3.5 Summary. The most salient conclusions from this section can be summarized as follows:

- Longer fibers are generally associated with higher values of f_{R2}, f_{R3} and f_{R4}: the positive effect that increasing the fiber length has on these parameters is not negligible.
- As long as the fiber dosage is not high (V_f below 0.9%) and the maximum aggregate is not higher than 16 mm, longer fibers are also associated with increasing f_{R1} values. However, in SFRC mixtures with higher fiber contents or bigger aggregates (cases with a relatively low prevalence, ~25%, in the dataset compiled in this study), increasing the fiber length can have a negative impact on f_{R1}.
- In terms of f_{R2}, f_{R3} and f_{R4}, the improvement associated with a 10 mm increase of the fiber length is similar to the improvement that increasing the fiber dosage in 0.1% yields on average. Therefore, the fiber length is as important a variable as the fiber volume fraction in terms of maximizing residual flexural strength.

5.4 Effect of fiber aspect ratio and fiber content

5.4.1 Contour plots. Figure 52 shows the contour plots of the response surfaces corresponding to f_{R1} and f_{R2} as per equation (13) against the fiber aspect ratio and the fiber volume fraction, assuming median values for the rest of mix design variables. The plots corresponding to f_{R3} and f_{R4} are not shown because they are very similar.

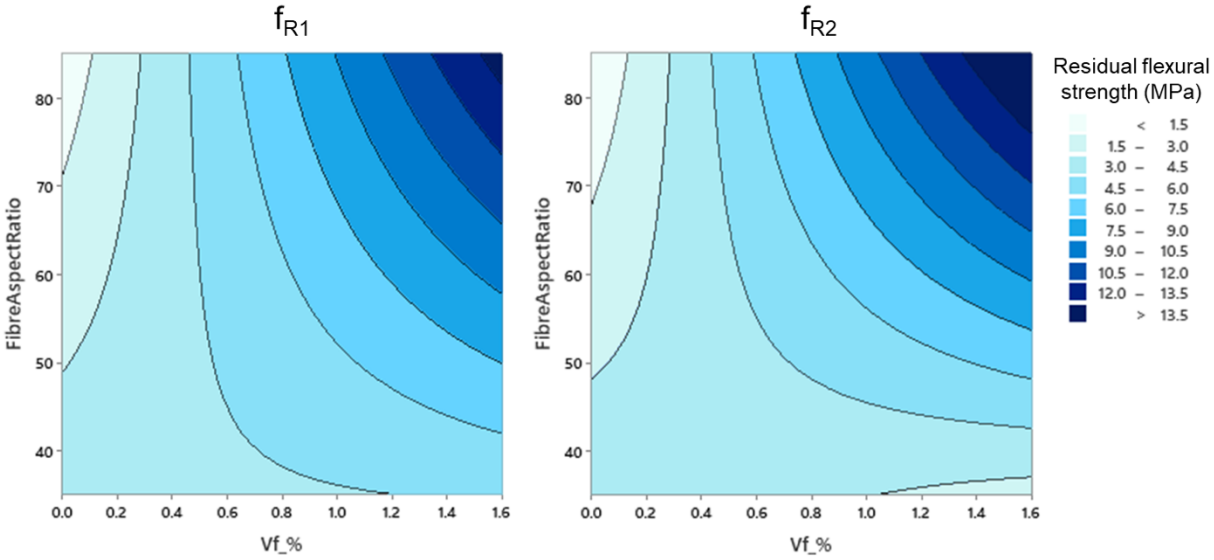

Figure 52. Contour plots of f_{R1} and f_{R2} vs fiber aspect ratio and volume fraction.

5.4.2 Interaction between the fiber aspect ratio and the fiber content. The contour plots in Figure 52 show that the effect of the fiber aspect ratio depends on the fiber volume fraction. When moderate to high fiber contents are considered, increasing the aspect ratio has a clear, positive impact on the residual flexural strength parameters. For relatively low values of the fiber volume fraction, on the other hand, increasing the fiber aspect ratio can have a negative impact. There is, therefore, a value of the fiber volume fraction at which the trend followed by residual flexural strength parameters with respect to the aspect ratio is reversed. Such value can

be determined by differentiating equation (13) with respect to the fiber aspect ratio and equating to zero. If f_{R1} is considered, the following is obtained:

$$\frac{\partial f_{R1}}{\partial \lambda_f} = b_3 V_f + k_4 = 0 \quad \rightarrow \quad V_f = \frac{-k_4}{b_3} \tag{21}$$

After replacing coefficients b_3 and k_4 with their corresponding values from Table 8, it follows that such 'threshold' value of the fiber volume fraction is 0.42%. It is important to note that the expression in equation (21) does not depend on any other variables and, therefore, this value does not depend on the relative amount of any other constituent of the SFRC mixture: it is an invariant. If the same calculation is done considering f_{R2}, f_{R3}, or f_{R4}, the 'threshold' values of the fiber volume fraction are 0.35%, 0.32%, and 0.20%, respectively –not too dissimilar.

Based on the above, it can be said that, when the fiber content is higher than 0.4% in volume, increasing the fiber aspect ratio is clearly associated with increasing values of the residual flexural strength parameters. Also, as can be observed in Figure 52, the positive impact of aspect ratio becomes more pronounced the higher the fiber content is. On the other hand, when the fiber volume fraction is less than 0.3%, increasing the fiber aspect ratio can have a negative impact on the residual flexural strength parameters. In SFRC mixtures with a fiber content between 0.3% and 0.4% in volume (or between 0.2% and 0.5%, considering margin of error), f_{R1}, f_{R2}, f_{R3}, and f_{R4} are practically insensitive to the fiber aspect ratio.

5.4.3 Better-than-average residual flexural strength. Even more information can be extracted from the contour plots in Figure 52 if they are interpreted bearing in mind representative values for f_{R1} and f_{R2}. Based on the SFRC dataset compiled in this study, the median of f_{R1} is 5.33 MPa, and the median of f_{R2} is 5.04 MPa. They can be considered as representative of the residual flexural strength values to be expected in an 'average' SFRC mixture. In Figure 53, these values are represented by the dashed lines in red.

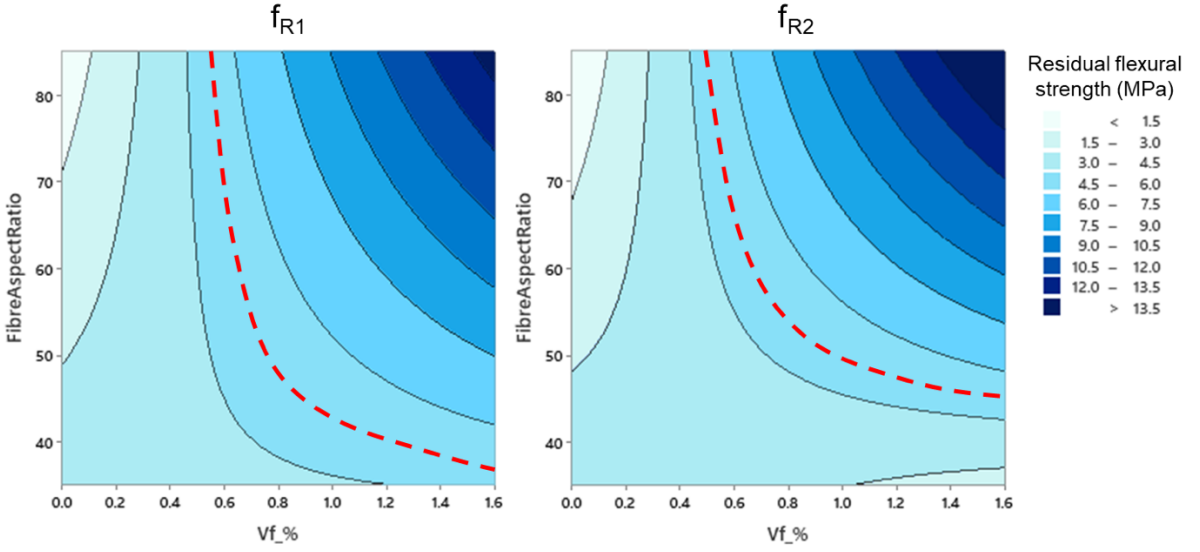

Figure 53. Contour plots of f_{R1} and f_{R2}, with median lines.

A simple visual examination of the contour plots in Figure 53 allows the identification of the pairs of values (fiber volume fraction, fiber aspect ratio) that are associated with higher-than-average values of f_{R1} and/or f_{R2}, that is, to the right of the red dashed line. For instance: in relation to f_{R1} (Figure 53, left), it is observed that, when fibers with an aspect ratio between 60

and 80 are considered, the f_{R1} value associated with a fiber volume fraction of 0.7% is higher than average. The same observation can be made with respect to f_{R2} (Figure 53, right). What this means is that, for a SFRC mixture to present better-than-average residual flexural strength parameters, it is not necessary to consider very high fiber contents. This is a step towards optimization and shows that the model given in equation (13) and Tables 7-8 is more than a merely predictive tool.

Equation (13) can be used to obtain the mathematical expression defining the region to the right of the red dashed lines rather than relying on a contour plot. For a given value of the fiber aspect ratio, the question is: what is, on average, the minimum fiber volume fraction that is associated with an average or a higher-than-average f_{R1} (or f_{R2}) value? By imposing the conditions f_{R1} = 5.33 MPa and f_{R2} = 5.04 MPa to equation (13), and using the appropriate coefficient values from Tables 7-8, assuming median values for the rest of mix design variables and rearranging terms, the following inequalities are obtained:

$$f_{R1} \geq 5.33\ MPa \rightarrow \quad V_f(\%) \geq \frac{-1.087 + 0.0679\ \lambda_f}{0.1616\ \lambda_f - 5.1954} \tag{22}$$

$$f_{R2} \geq 5.04\ MPa \rightarrow \quad V_f(\%) \geq \frac{-1.538 + 0.077\ \lambda_f}{0.2179\ \lambda_f - 8.613} \tag{23}$$

These two inequalities can be plotted in the aspect ratio – volume fraction plane to determine the minimum fiber volume fraction needed to have higher-than-average f_{R1} and f_{R2} values when the fiber aspect ratio is, for example, 45, 60, or 80. This is illustrated in Figure 54, where it can be observed that the fiber volume fraction requirement is 0.69% (or 0.56%) for a fiber aspect ratio of 60 (or 80). A significant improvement from the fiber content requirement of 1.61% associated with a fiber aspect ratio of 45, thus highlighting the importance of approaching the optimization of residual flexural strength *globally*, and not just through increasing the fiber content.

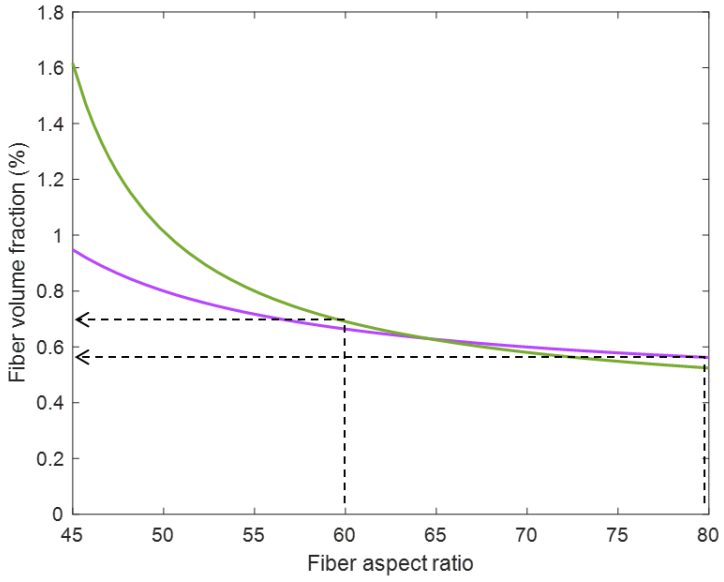

Figure 54. Fiber content requirement for better-than-average f_{R1} and f_{R2}.

5.4.4 How 'important' is the effect of the fiber aspect ratio? To put things into perspective, it is useful to compare the magnitude of the effect that the fiber aspect ratio has on residual flexural strength to that of the fiber content. Following the same rationale as in section 5.3.4, the question is whether the effect of varying the aspect ratio in 10 is comparable to that of increasing the fiber volume fraction in 0.1%. For reference, f_{R2} can be considered.

The gradient of f_{R2} with respect to the fiber aspect ratio can be evaluated by differentiating equation (13) for f_{R2} with respect to this variable, and considering the median fiber volume fraction of 0.51%:

$$\frac{\partial f_{R2}}{\partial \lambda_f} = b_3 V_f + k_4 = 0.2179 \times 0.51 - 0.077 = 0.032\ MPa/mm \tag{24}$$

Therefore, the expected variation of f_{R2} when the fiber aspect ratio is increased in 10 is:

$$E\left(\Delta f_{R2} \middle| \Delta \lambda_f = +10\right) = \frac{\partial f_{R2}}{\partial \lambda_f} \times \Delta \lambda_f = 0.32\ MPa \tag{25}$$

If this figure is compared to the expected variation of f_{R2} associated with an increase of 0.1% in the fiber volume fraction, which is 0.55 MPa as determined in equations (19) and (20), it follows that they are not dissimilar in terms of order of magnitude. In consequence, the effect of the fiber aspect ratio on f_{R2} is as important as that of the fiber volume fraction.

If the calculations above are repeated for f_{R1}, f_{R3} and f_{R4}, their expected variations are 0.15 MPa, 0.39 MPa, and 0.52 MPa, respectively. In general terms, the conclusion is the same for all four residual flexural strength parameters, albeit the effect on f_{R1} is less relevant. However, it is important to bear in mind that the values above assume V_f = 0.51%, but the effect of the fiber aspect ratio (particularly on f_{R1}) becomes more pronounced for higher fiber contents (as discussed in 5.4.2). If the V_f value is assumed, for example, as 0.8%, the expected variations of f_{R1}, f_{R2}, f_{R3} and f_{R4} are 0.61 MPa, 0.97 MPa, 0.99 MPa, and 0.99 MPa, respectively.

5.4.5 Summary. The most salient conclusions from this section can be summarized as follows:

- Increasing the fiber aspect ratio is clearly associated with increasing values of the residual flexural strength parameters when the fiber volume fraction is 0.4% or higher.
- When low fiber contents are considered (less than 0.3%), increasing the fiber aspect ratio can have a negative impact on residual flexural strength. On average, f_{R1}, f_{R2}, f_{R3}, and f_{R4} are practically insensitive to the fiber aspect ratio in mixtures with fiber contents between 0.3% and 0.4%.
- If fibers with an aspect ratio of 60-80 are considered, mixtures with higher-than-average residual flexural strength values can be obtained with volume fractions not higher than 0.7%-0.8%. In most cases, it can be argued, steel fiber contents of 1% or higher are hardly justified.
- For all residual flexural strength parameters, increasing the fiber aspect ratio has a positive effect that is comparable to that resulting from increasing the fiber content in 0.1%. Therefore, on average, the fiber aspect ratio is as important a variable as the fiber volume fraction in terms of maximizing residual flexural strength.

5.5 Interaction between the fiber length and the maximum aggregate size

5.5.1 Preliminary observations. As equation (13) shows, the variables corresponding to the fiber length and the maximum aggregate size influence each other in terms of their impact on the residual flexural strength parameters. However, as per Table 8, the interaction between the variables does not have a statistically significant effect on f_{R3} (coefficient $a_1 = 0$). This section focuses on the analysis of the relationship between f_{R1}, the fiber length and the maximum aggregate size.

Since the fiber length also interacts with the fiber content (section 5.3), it is relevant to the discussion to consider this variable as well. The contour plots discussed in this section are shown for three different values of the fiber volume fraction: 0.5%, 1.0%, and 1.5%.

It is also relevant to comment on the bivariate distribution of the values of fiber length and maximum aggregate size in the SFRC database, as it affects the region where the model can be interpreted correctly. Figure 55 shows the scatterplot of the cases in the database with respect to these two variables. The green dashed line defines the region where actual data have informed the model. The interpretation of the model in relation to the interaction between the fiber length and the maximum aggregate size must therefore be limited to this region, as extrapolations outside of it would not be supported by evidence. This is not the case in relation to the pairs of variables analyzed and discussed in the preceding sections, as can be seen in Figure 56.

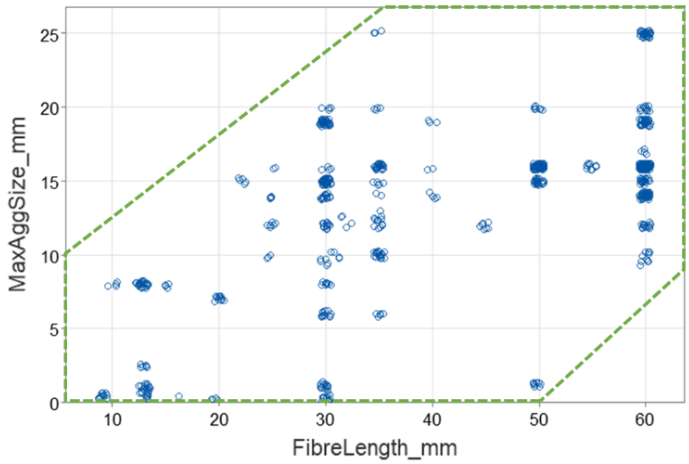

Figure 55. Scatterplot of fiber length – maximum aggregate size in dataset.

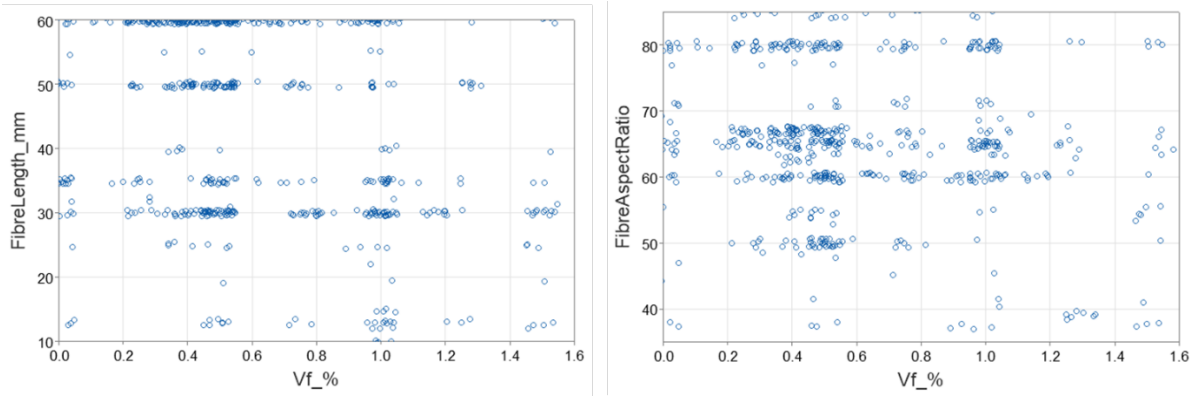

Figure 56. Scatterplots of fiber length and aspect ratio vs volume fraction in dataset.

5.5.2 Sensitivity to the maximum aggregate size. Figure 57 shows the contour plots of f_{R1} as modelled by equation (13) against the fiber length and the maximum aggregate size, considering three different fiber contents, and assuming median values for the rest of mix design variables. Combinations of short fibers and low values of the maximum aggregate size are associated with lower f_{R1} values, particularly for low and moderate fiber contents (V_f = 0.5%).

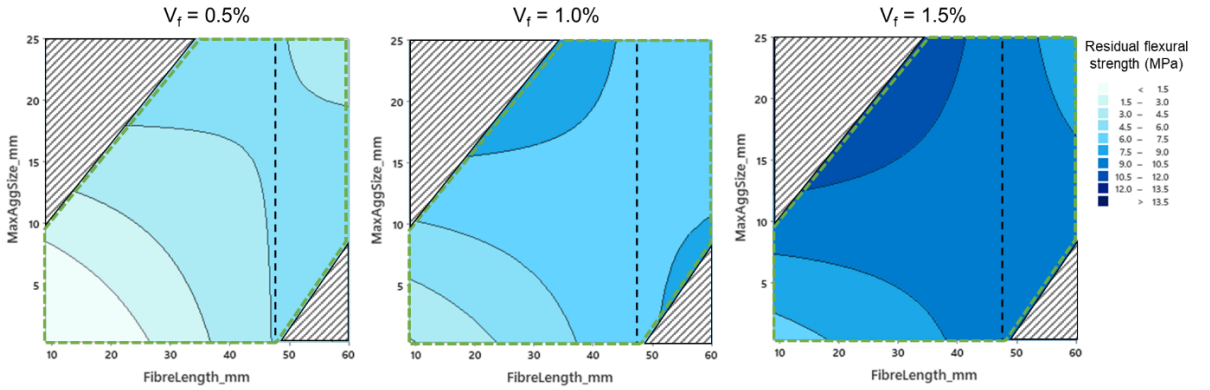

Figure 57. Contour plots of f_{R1} vs fiber length and maximum aggregate size.

The dashed lines in the contour plots represent the fiber length that makes f_{R1} practically insensitive to variations in the maximum aggregate size. This value can be determined by differentiating equation (13) with respect to the maximum aggregate size and equating to zero:

$$\frac{\partial f_{R1}}{\partial m} = a_1\, l_f + k_5 = 0 \quad \rightarrow \quad l_f = \frac{-k_5}{a_1} \tag{26}$$

After replacing a_1 and k_5 with the appropriate values from Table 8, a fiber length of 47.7 mm is obtained. This value does not depend on any other mix design parameter. If the same calculation is done in relation to f_{R2} and f_{R4}, fiber lengths of 41.5 mm and 45 mm, respectively, are obtained. The three values are invariant and are, in fact, very similar. Since fibers with a length of 45 mm are quite standard in practice, it can be concluded that using steel fibers of such a length makes the residual flexural strength practically insensitive to the maximum aggregate size.

5.5.3 Additional comments regarding fiber length. In these contour plots, values of the maximum aggregate size that make f_{R1} practically insensitive to the fiber length can also be observed. They correspond to the horizontal dashed lines in Figure 58.

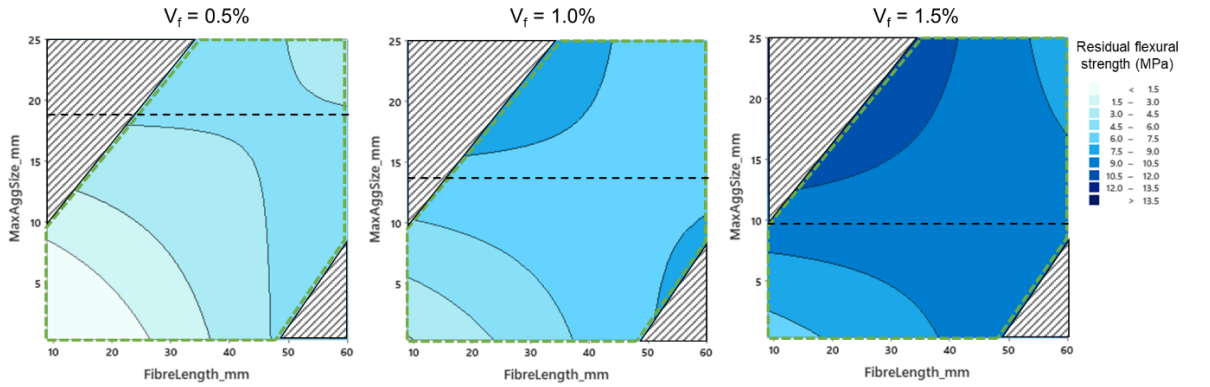

Figure 58. Contour plots of f_{R1} vs fiber length and maximum aggregate size (2).

This value of the maximum aggregate size does change with the fiber volume fraction, as can be seen in Figure 58. What has emerged from the analysis of these contour plots is exactly the same that has been observed in relation to equation (16): the interrelationship between fiber content, maximum aggregate size, and fiber length. This has been discussed already in section 5.3.3.

5.6 Effect of the superplasticizer content

5.6.1 Contour plots. The model developed for f_{R1}, f_{R2}, f_{R3} and f_{R4} as per equation (13) and Tables 7 and 8 includes one term that represents the effect of the amount of superplasticizer and another term that reproduces the interaction between this variable and the fiber volume fraction. Both terms are in the model because they were found to have a statistically significant effect on the residual flexural strength parameters. However, the fact that these are statistically significant does not necessarily imply that their effect is important in magnitude. As the contour plots in Figure 59 show, this is exactly the case with the superplasticizer content.

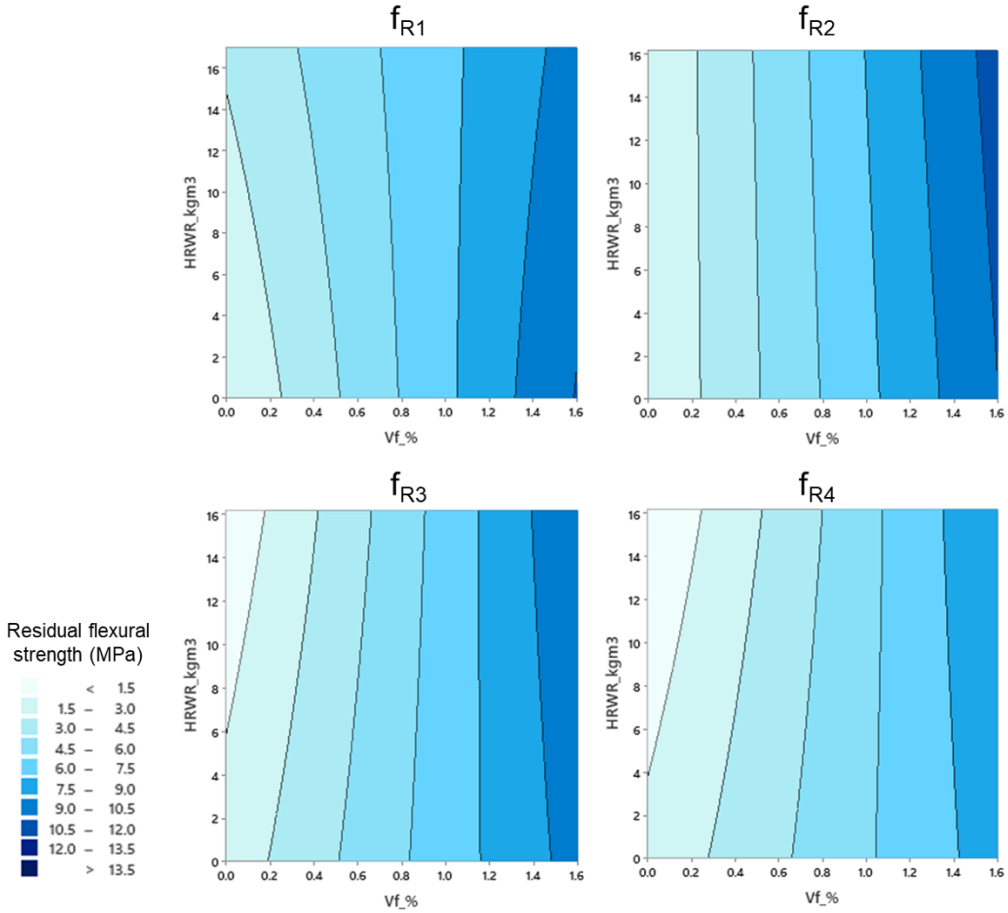

Figure 59. Contour plots of f_{R1}, f_{R2}, f_{R3} and f_{R4} vs amount of superplasticizer and fiber content.

In all four contour plots, the gradient of the residual flexural strength parameters has a very small component in the superplasticizer axis. Although there are, of course, some small variations, in general it is clear that the trend followed by the residual flexural strength

parameters is mostly explained by the fiber volume fraction and not the superplasticizer content.

5.6.2 How 'important' is the effect of superplasticizer? Some calculations can be done to put some numbers to the abovementioned statement. The median superplasticizer content in SFRC mixtures, based on the dataset compiled for this study, is 3.5 kg/m^3 (section 1.3.7): half of the mixtures contain this amount of superplasticizer or more. With that in mind, varying the superplasticizer content in +3.5 kg/m^3 is a considerable increase.

The expected variation of any of the four residual parameters (noted as f_{Ri}) resulting from an increase of the superplasticizer amount ΔSP can be determined based on the partial derivative of equation (13) with respect to the superplasticizer amount, that is:

$$E(\Delta f_{Ri}|\Delta SP) = \frac{\partial f_{Ri}}{\partial SP} \times \Delta SP = \left(b_2\, V_f + k_3\right) \times \Delta SP \tag{27}$$

If an increase of the superplasticizer amount $\Delta SP = 3.5$ kg/m^3 is considered, the expected variation is:

$$E(\Delta f_{Ri}|\Delta SP = +3.5 kg/m^3) = \left(b_2\, V_f + k_3\right) \times 3.5 \tag{28}$$

Taking the values of coefficients b_2 and k_3 from Table 8, and considering three reference values of 0.5%, 1.0% and 1.5% for the fiber volume fraction V_f, the largest variations are: an increase of 0.16 MPa in f_{R1}, and a decrease of 0.22 MPa in f_{R4}.

These expected variations are indeed of minor importance. The average increase of f_{R2} when the fiber volume fraction is increased in 0.1% is 0.55 MPa (equation (20), section 5.3.4). That is more than twice the expected variations associated to an increase in the superplasticizer content of 3.5 kg/m^3. In fact, if an increase in the superplasticizer content of 1 kg/m^3 is considered, which is a less extreme value than 3.5 kg/m^3, the expected variations of the residual flexural strength parameters are between –0.062 MPa and +0.047 MPa, which are minimal in comparison to the 0.55 MPa variation associated with the fiber volume fraction being increased by 0.1%.

In summary, the impact that the amount of superplasticizer has on the residual flexural strength parameters is not comparable in magnitude to the effect of the fiber content, or that of the fiber length or aspect ratio. Of course, the dosage of superplasticizer is key to the workability of the mixtures but, as long as they are adequately vibrated/compacted, the amount of superplasticizer does not have a substantial, *direct* effect on the residual flexural strength.

5.7 Interaction between the cement content and the fiber content

5.7.1 Contour plots. As equation (13) and Tables 7 and 8 show, the model developed for the residual flexural strength parameters includes one term representing the effect of the cement content and another term representing the interaction between this and the fiber volume fraction. This interaction is not statistically significant in relation to f_{R2} and f_{R4} (as $b_1 = 0$), but it is in relation to both f_{R1} and f_{R3}. What this means is that the effect that the fiber content has on f_{R1} and f_{R3} is influenced by the cement content. Figure 60 shows the contour plots of these

two residual flexural strength parameters as per equation (13) against the cement content and the fiber volume fraction, assuming median values for the rest of mix design variables.

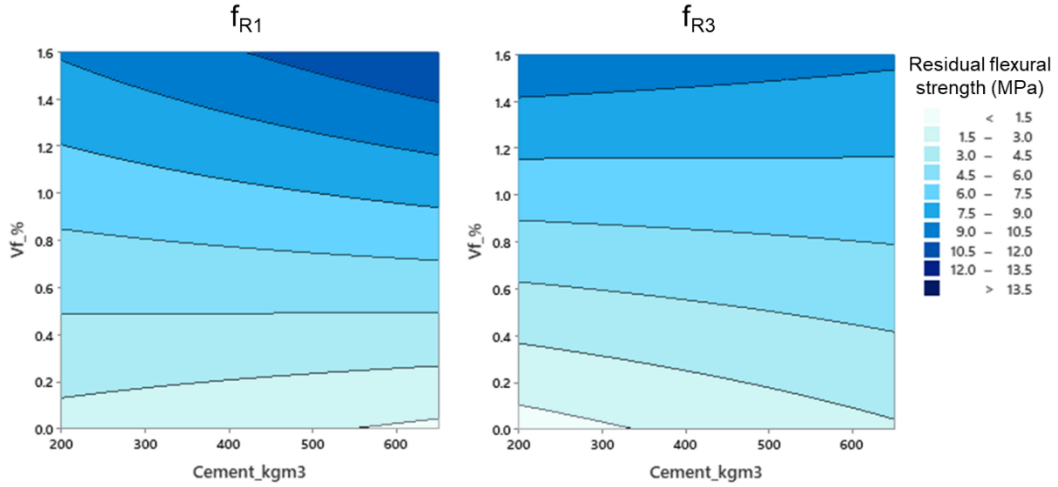

Figure 60. Contour plots of f_{R1} and f_{R3} vs cement content and fiber content.

5.7.2 Cement content and f_{R1}. Generally, higher cement contents are associated with higher f_{R1} values when the fiber volume fraction is relatively high (Figure 60, left). This is not the case when low to moderate fiber contents are considered. There is a certain value of the fiber content that, on average, makes f_{R1} insensitive to the cement content, which can be determined by differentiating equation (13) with respect to the cement content and equating to zero:

$$\frac{\partial f_{Ri}}{\partial C} = b_1 V_f + k_6 + c_1(G+S) = 0 \tag{29}$$

After replacing the coefficients b_1, k_6 and c_1 with the values corresponding to f_{R1} as per Table 8, such value of the fiber volume fraction is a function of the total aggregate content:

$$V_f = \frac{-k_6 - c_1(G+S)}{b_1} = 2 - 0.000896 \times (G+S) \tag{30}$$

Bearing in mind that the median fine aggregate and coarse aggregate contents in the SFRC database compiled in this study are 862 kg/m^3 and 882 kg/m^3, respectively (i.e. a total aggregate content of 1744 kg/m^3, sections 1.4.1 and 1.4.2), the result of equation (30) is a fiber volume fraction of 0.44%. Therefore, increasing the cement content is associated with an improvement of the effect of steel fibers on f_{R1} when the fiber volume fraction is higher than 0.44% when the total aggregate content is not lower than 1744 kg/m^3. The model developed for f_{R1} adequately captures that, in SFRC mixtures with high fiber contents and typical aggregate contents, increasing the amount of cement in the mixture tends to maximize the effect of fibers on f_{R1}. However, the contour plot in Figure 60 (left) also shows that such a positive effect only becomes noticeable at high fiber contents.

5.7.3 Cement content and f_{R3}. In general terms, the same can be said in relation to f_{R1} and f_{R3}: higher cement contents are associated with higher f_{R3} values. There is, again, a certain value of the fiber volume fraction that makes f_{R3} insensitive to variations in the cement content, but in this case such change in the trend occurs at the higher end of the range of V_f values, as can be seen in Figure 60 (right). After replacing the coefficients b_1, k_6 and c_1 in equation (29) with the

values corresponding to f_{R3} as per Table 8, such value of the fiber volume fraction is a function of the total aggregate content:

$$V_f = \frac{-k_6 - c_1(G+S)}{b_1} = 3.9 - 0.001596 \times (G+S) \quad (31)$$

This corresponds to a fiber volume fraction of 1.12% if the median fine and coarse aggregate contents in the database are assumed (i.e. a total aggregate content of 1744 kg/m^3). As the contour plot in Figure 60 (right) shows, increasing the cement content is associated with an improvement of the effect of steel fibers on f_{R3} when the fiber volume fraction is *lower* than 1.12%. And this positive effect of the interaction between the cement content and the fiber volume fraction is only noticeable for low to moderately high fiber contents.

5.7.4 Cement content, f_{R1} and f_{R3}. Based on the discussion in the preceding subsections, it follows that increasing the cement content contributes to enhance the effect of steel fibers on both f_{R1} and f_{R3}, for fiber contents between 0.44% and 1.12% in volume, and particularly in the central part of that range. However, the contour plots in Figure 60 suggest that the effect of this interaction is relatively minor.

5.7.5 How 'important' is the effect of cement content on f_{R1} and f_{R3}? An important question at this point is whether the effect that the cement content has on f_{R1} and f_{R3} is comparable to that of the fiber volume fraction. That is: is the interaction between these two variables really important in magnitude? For comparison, the expected variations of f_{R1} and f_{R3} associated with an increase of 100 kg/m^3 in the cement content can be evaluated.

This can be done by differentiating equation (13) with respect to the cement content and assuming median aggregate contents and a fiber volume fraction of 0.78% (which is the average of the 0.44% to 1.12% range):

$$\frac{\partial f_{R1}}{\partial C} = b_1 V_f + k_6 + c_1(G+S) = 0.00192 \frac{MPa}{kg/m^3} \quad (32)$$

$$\frac{\partial f_{R3}}{\partial C} = b_1 V_f + k_6 + c_1(G+S) = 0.00126 \frac{MPa}{kg/m^3} \quad (33)$$

The expected variations of f_{R1} and f_{R3} if the cement content is increased in 100 kg/m^3 are:

$$E(\Delta f_{R1} | \Delta C = +100\ kg/m^3) = \frac{\partial f_{R1}}{\partial C} \times \Delta C = 0.19\ MPa \quad (34)$$

$$E(\Delta f_{R3} | \Delta C = +100\ kg/m^3) = \frac{\partial f_{R3}}{\partial C} \times \Delta C = 0.13\ MPa \quad (35)$$

Similarly, by differentiating equation (13) with respect to the fiber volume fraction, and assuming median values for the rest of mix design variables:

$$\frac{\partial f_{R1}}{\partial V_f} = b_0 + b_1 C + b_2 SP + b_3 \lambda_f + b_4 l_f = 5.31\ MPa/\% \quad (36)$$

$$\frac{\partial f_{R3}}{\partial V_f} = b_0 + b_1 C + b_2 SP + b_3 \lambda_f + b_4 l_f = 4.97\ MPa/\% \quad (37)$$

And the expected variations of f_{R1} and f_{R3} when the fiber content is increased in 0.1% are:

$$E\left(\Delta f_{R1} | \Delta V_f = +0.1\%\right) = \frac{\partial f_{R1}}{\partial V_f} \times \Delta V_f = 0.53\ MPa \tag{38}$$

$$E\left(\Delta f_{R3} | \Delta V_f = +0.1\%\right) = \frac{\partial f_{R3}}{\partial V_f} \times \Delta V_f = 0.50\ MPa \tag{39}$$

Comparing the values obtained in equations (34)-(35) to those obtained in equations (38)-(39), it is evident that the impact of even a considerable increase in cement content on f_{R1} and f_{R3} is relatively minor when compared to the effect that an increase of 0.1% in the fiber content has on the two parameters. In conclusion, higher cement contents can *slightly* enhance the effect that a certain fiber content has on the residual flexural strength parameters.

5.8 Interaction between total aggregate content and amount of SCMs

5.8.1 Contour plots. The contour plots representing the response surfaces of f_{R1} and f_{R2} as per equation (13) against the total amount of SCMs and the total aggregate content are shown in Figure 61. The plots of f_{R3} and f_{R4} are very similar to these in terms of their trends with respect to these two variables: the actual values are of course different, but the shape of the response surfaces, and therefore their interpretation in relation to the the total aggregate content and the SCMs content, are very similar. This section initially focuses on f_{R1} and f_{R2}, and the findings and conclusions in relation to f_{R3} and f_{R4} are also outlined.

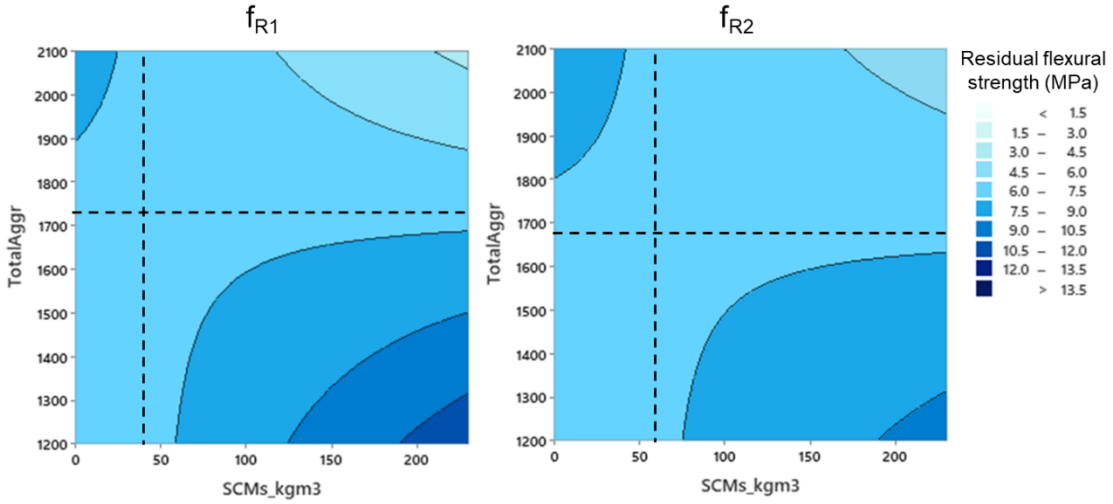

Figure 61. Contour plots of f_{R1} and f_{R2} vs the total aggregate and SCMs contents.

Another important aspect to note is that these trends do not vary with the fiber volume fraction, because the interactions between this variable and the contents of aggregates and SCMs were found to be statistically non-significant. In equation (13), the term that describes the effect of the fiber volume fraction does not depend on the total aggregate content or the SCMs content. The baseline of these contour plots changes with the fiber volume fraction, but the trends with respect to the aggregate content and the amount of SCMs do not. The contour plots in Figure 61 assume V_f = 1.0% and median values for the rest of mix design parameters. If a different

fiber content is assumed, the interpretation of the relative effects of the total aggregate content and SCMs content discussed in this section are still valid.

The contour plots in Figure 61 show that higher values of the residual flexural strength parameters are associated with either a total aggregate content higher than ~1700 kg/m^3 and an amount of SCMs below ~50 kg/m^3, or a total SCMs content higher than ~50 kg/m^3 if the aggregate content is lower than ~1700 kg/m^3. These approximate values are represented by the dashed lines defining four quadrants in Figure 61.

5.8.2 Restricting the analysis to possible cases only. Not all combinations of the aggregate content and the SCMs content values in these contour plots are possible in normal weight SFRC mixtures. This has already been discussed in section 2.4.5 and the paper published in the journal *Materials*[4]. The following inequalities are applicable:

$$2096.5 \leq C + SCM + (G + S) \leq 2396.5 \tag{40}$$

Since the representative range of cement contents in the SFRC dataset in this study is between 325 kg/m^3 and 678 kg/m^3, the above can be rewritten as:

$$1418 \leq SCM + (G + S) \leq 2071.5 \tag{41}$$

These inequalities define the region of possible combinations of total aggregate and SCMs content values that are realistic in terms of SFRC mixture proportions. The greyed-out areas in Figure 62 correspond to those combinations that do not satisfy equation (41) and are therefore outside of the ranges where these contour plots can be interpreted and discussed.

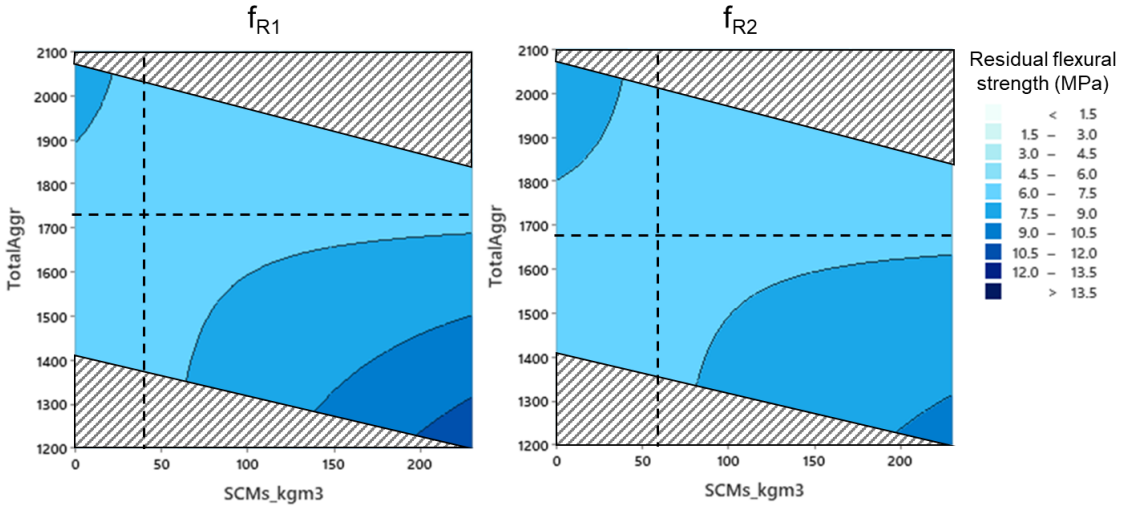

Figure 62. Contour plots of f_{R1} and f_{R2} vs the total aggregate and SCMs contents, excluding combinations that do not satisfy equation (41).

5.8.3 Sensitivity to changes in SCMs content. These contour plots show that there is a value of the total aggregate content (horizontal dashed line in Figure 62) that makes f_{R1} and f_{R2}

[4] Garcia-Taengua, E.; Bakhshi, M.; Ferrara, L. "Meta-Analysis of Steel Fiber-Reinforced Concrete Mixtures Leads to Practical Mix Design Methodology", *Materials* 2021, 14, 3900. https://doi.org/10.3390/ma14143900

insensitive to the SCMs content. Such value can be determined by differentiating equation (13) with respect to the SCMs content and equating to zero:

$$\frac{\partial f_{Ri}}{\partial SCM} = k_2 + c_2\,(G+S) = 0 \quad \rightarrow \quad (G+S) = \frac{-k_2}{c_2} \tag{42}$$

By replacing the coefficients k_2 and c_2 with the corresponding values from Table 8, the total aggregate content obtained is 1719 kg/m^3 and 1663 kg/m^3, for f_{R1} and f_{R2}, respectively. The same applies to f_{R3} and f_{R4}, leading to total aggregate contents of 1726 kg/m^3, and 1691 kg/m^3, respectively. The four values are remarkably similar, their average being 1700 kg/m^3, and interestingly very close to the median aggregate content in the SFRC database. Therefore, the total aggregate content that makes the residual flexural strength insensitive to the SCMs content can be taken as 1700 kg/m^3. It is also noteworthy that this value is an invariant as it does not depend on any other mix design variables, as per equation (42).

5.8.4 Sensitivity to changes in aggregate content. There is also a value of the SCMs content that makes f_{R1} and f_{R2} insensitive to the aggregate content. However, this is not an invariant but a function of the cement content and the coarse-to-fine aggregate ratio, as the following equation shows:

$$\frac{\partial f_{Ri}}{\partial (G+S)} = c_1 C + c_2 SCM + c_3 \frac{G}{S} = 0 \quad \rightarrow \quad SCM = \frac{-c_1}{c_2} C + \frac{-c_3}{c_2} \frac{G}{S} \tag{43}$$

The values of such SCMs content are not as stable across the board as the aggregate content obtained from equation (42). In addition to it being a function of the cement content and the coarse-to-fine aggregate ratio, it differs substantially depending on the residual flexural strength parameter considered. This is shown in Figure 63 (left), where the SCMs content as per equation (43) is plotted against these two variables for f_{R1}, f_{R2}, f_{R3}, and f_{R4}.

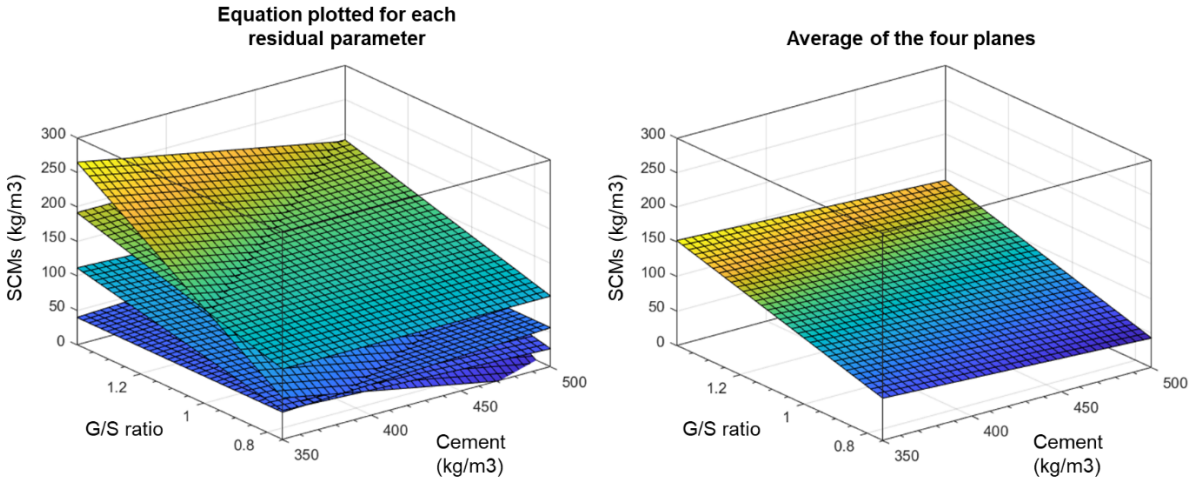

Figure 63. SCMs amounts that make residual flexural strength insensitive to changes in the total aggregate content.

Some values can be obtained for illustration purposes. If the cement content and coarse-to-fine aggregate ratio are assumed as 400 kg/m^3 and 1.0, the SCMs content as per equation (43) is: 45 kg/m^3, 64 kg/m^3, 114 kg/m^3, and 137 kg/m^3, for f_{R1}, f_{R2}, f_{R3}, and f_{R4}, respectively. The surfaces represented in Figure 63 (left) clearly show that the dominant variable is the coarse-to-fine aggregate ratio. This becomes even clearer in Figure 63 (right), which shows the

average of all four surfaces, thus providing a more 'unified' view on all residual flexural parameters.

There are two main aspects that can be concluded from Figure 63:

- The residual flexural strength of SFRC mixtures can be practically insensitive to variations in the total aggregate content if a certain amount of SCMs present in the mixture.
- When the coarse-to-fine aggregate ratio is lower than 1, such amount is approximately between 50-100 kg/m^3. However, when the coarse aggregate content is higher than the fine aggregate content, the amount of SCMs required for the SFRC mixture to be insensitive to the total aggregate content increases considerably.

The two above considerations reinforce the idea that the relationship between the proportioning of coarse and fine aggregates and the amount of SCMs, which is closely related to the cohesiveness of the fresh SFRC mixture, has a strong connection with the values of the residual flexural strength parameters. This is a recurrent message emerging on different occasions throughout this report, which comes up again in the next section.

5.9 Effect of the aggregate content and G/S ratio

5.9.1 Contour plots. The interaction between the total aggregate content and the coarse-to-fine aggregate ratio (*G/S*) was found to have a statistically significant on f_{R2}, f_{R3}, and f_{R4}, but its effect on f_{R1} was not statistically significant ($c_3 = 0$ in Table 8). The contour plots of f_{R2} and f_{R3} as described by equation (13) against these two variables are shown in Figure 64. The plot for f_{R4} is very similar in terms of the trends with respect to these two variables.

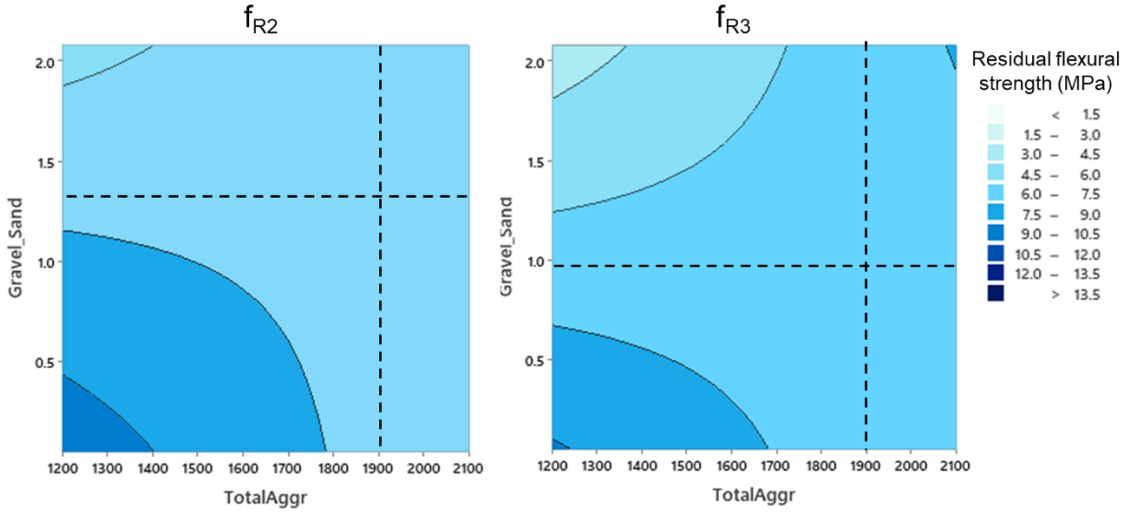

Figure 64. Contour plots of f_{R2} and f_{R3} vs the total aggregate content and G/S ratio.

These trends are not dependent on the fiber volume fraction, as their interactions with this variable were found to be statistically non-significant. The 'baseline' of these contour plots does change with the fiber volume fraction, but the trends with respect to the aggregate content and the *G/S* ratio do not. For the contour plots in this section, a fiber volume fraction of 1.0% and median values for the rest of mix design parameters have been assumed.

The contour plots in Figure 64 show that higher values of f_{R2} and f_{R3} are associated with values of the total aggregate content lower than ~1900 kg/m^3 when the *G/S* ratio is lower than a certain value. These threshold values of both variables are represented by dashed lines in Figure 64 and discussed below.

5.9.2 Sensitivity to the G/S ratio. The total aggregate content that makes the residual flexural strength parameters insensitive to changes in the *G/S* ratio (represented by vertical dashed lines in Figure 64) can be determined by differentiating equation (13) with respect to the *G/S* ratio and equating to zero:

$$\frac{\partial f_{Ri}}{\partial (G/S)} = k_1 + c_3\,(G+S) = 0 \quad \rightarrow \quad (G+S) = \frac{-k_1}{c_3} \tag{44}$$

By replacing the coefficients k_1 and c_3 with the appropriate values from Table 8, the total aggregate content obtained is 1902 kg/m^3, 1899 kg/m^3, and 2040 kg/m^3 for f_{R2}, f_{R3} and f_{R4}, respectively. Since these three values are remarkably similar, their average of 1947 kg/m^3 can be taken as representative. Therefore, it can be concluded that a total aggregate content of 1947 kg/m^3 makes the residual flexural strength insensitive to the *G/S* ratio, this value being a general result as it does not depend on any other mix design variables, as per equation (44).

5.9.3 Effect of the aggregate content. The result from the previous subsection, together with the contour plots in Figure 64, indicates that higher values of the residual flexural strength parameters are associated with aggregate contents lower than 1947 kg/m^3, as long as the *G/S* ratio is kept below a certain limit (determined and discussed below). This is compatible with the findings from section 5.8.3, i.e. that higher residual flexural strength values are associated with aggregate contents not higher than 1700 kg/m^3 as long as a certain amount of SCMs is incorporated to the SFRC mixture.

Both results, taken together, confirm an association between the total aggregate content and higher values of the residual flexural strength parameters and demonstrate the extent to which equation (13) –a relatively straightforward, uncomplicated model– reproduces the complex relationships that underpin the proportioning of SFRC mixtures. This is a good opportunity to explain an element of the terminology used throughout this report. The fact that aggregate contents below a certain value are associated with higher values of the residual flexural strength does not imply that this is due to a *direct* effect of the aggregates. When the aggregate content of a SFRC mixture is reduced, it is generally because the cement content and/or the total amount of SCMs are increased. That is probably the root cause of the residual flexural strength improving, rather than the amount of aggregates, which is hardly a surprise: the model has not unveiled an unknown effect of aggregates. This is the reason why terminology referring to *association* is preferred to phrases implying *causality* throughout this report.

5.9.4 Sensitivity to the total aggregate content. The horizontal dashed lines in Figure 64 correspond to values of the *G/S* ratio that make the residual flexural strength parameters insensitive to variations of the aggregate content. Such value can be obtained by differentiating equation (13) with respect to the total aggregate content and equating to zero. What is obtained is a function of the cement content and the total amount of SCMs:

$$\frac{\partial f_{Ri}}{\partial (G+S)} = c_1 C + c_2 SCM + c_3 \frac{G}{S} = 0 \quad \rightarrow \quad \frac{G}{S} = \frac{-c_1}{c_3}\,C + \frac{-c_2}{c_3}\,SCM \tag{45}$$

Conceptually, equation (45) makes perfect sense. The *G/S* ratio, the cement content and the amount of SCMs are at interplay in terms of the cohesiveness of the fresh mixture, and this, together with the total aggregate content, has an impact on the residual flexural strength that a SFRC mixture with a given fiber content can develop. The *G/S* values obtained from equation (45) vary considerably with the cement content and the amount of SCMs and it is therefore difficult to derive a specific reference value from it. This is seen in Figure 65, which presents the three surfaces obtained by replacing the coefficients c_1, c_2 and c_3 with the appropriate values from Table 8 for f_{R2}, f_{R3}, and f_{R4}.

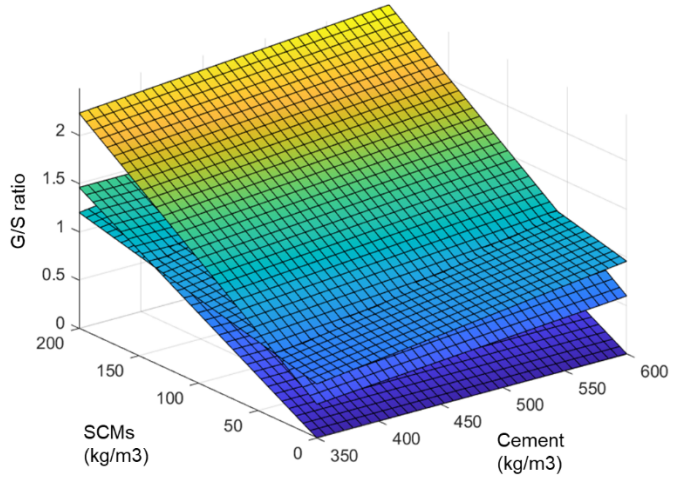

Figure 65. G/S ratio as per equation (45) against cement and SCMs content.

5.9.5 How 'important' is the effect of G/S ratio? To have an idea of the relative importance of *G/S* ratio in terms of its effect on f_{R2}, f_{R3} and f_{R4}, the expected variation of each of these parameters associated with a representative change of the *G/S* ratio can be determined and compared to that corresponding to a representative change in the fiber volume fraction. Assuming a change of –0.5 for the *G/S* ratio (e.g. a reduction from *G/S*=1.5 to *G/S*=1.0), the expected variation of the residual flexural strength parameters can be evaluated as follows:

$$\Delta f_{Ri} = \frac{\partial f_{Ri}}{\partial (G/S)} \times \Delta(G/S) = \left(k_1 + c_3(G+S)\right) \times \Delta(G/S) = \left(k_1 + c_3(G+S)\right) \times (-0.5) \qquad (46)$$

By replacing coefficients k_1 and c_3 with the corresponding values from Table 8, the expected variations of f_{R2}, f_{R3} and f_{R4} are 0.28 MPa, 0.35 MPa, and 0.25 MPa, respectively. If compared to the expected variation due to 0.1% increase in fiber volume fraction (0.50-0.55 MPa, from equations 20, 39), these values are of the same order of magnitude, although a bit lower. Therefore, although the effect of the *G/S* ratio on the residual flexural strength parameters is not as important as that of the fiber content, it is not at all negligible.

6. Reduction of the SFRC residual flexural strength to a single parameter

6.1 Introduction

6.1.1 Context and scope of this chapter. This part of the report is concerned with:

- The dimensionality reduction of the residual flexural strength parameters and the limit of proportionality (f_L, f_{R1}, f_{R2}, f_{R3}, and f_{R4} as per EN 14651) in order to compress the information of these five parameters into one single variable (called factor) which describes the flexural strength of SFRC mixtures; and
- The statistical modeling and analysis of the relationships between the abovementioned factor and the variables describing the steel fiber-reinforced concrete (SFRC) mixtures in terms of the relative amounts of their constituents and the fundamental descriptors of such constituents (i.e. the mix design variables).

By adopting a multivariate perspective, in which f_L, f_{R1}, f_{R2}, f_{R3}, and f_{R4} are considered as different representations or 'measurements' of the same phenomenon, this chapter complements the analysis in section 5, where each of the residual flexural strength parameters was described by a separate equation.

6.1.2 Dataset of SFRC mixtures. The data used for the analysis and the development of the model discussed in this chapter is the database of SFRC mixtures, described in chapter 1.

As explained in 5.1.2, cases with a limit of proportionality higher than 25 MPa were discarded. Also, cases where the values of the residual flexural strength parameters were missing and could not be remedied by multiple imputation were also discarded. As a result, a dataset of 733 cases was used for the study presented in this chapter.

6.1.3 Methodological considerations. The approach followed in this analysis is based on the statistical techniques known as factor extraction by principal component analysis (PCA) and multiple linear regression.

PCA is one of the most versatile tools among the machine learning techniques to reduce the dimensionality of a set of data. In this study, it is used to transform the original set of five, highly correlated parameters (f_L, f_{R1}, f_{R2}, f_{R3}, and f_{R4}) into a set of new, completely uncorrelated (i.e. orthogonal) variables known as principal components. Since PCA is based on the diagonalization of the correlation matrix, the first principal component is always aligned with the highest variance in the original data and therefore condenses most of the original information. The factor extraction consists in the selection of some of the principal components as factors, ideally just one.

A simplified illustration of how PCA can be used to compress the information contained by several, highly correlated variables in just one new variable is shown in Figure 66. It represents a simplified scenario where only three variables are considered, for illustration. PCA rotates the original variables so that the first of the new ones (i.e. the first principal component) captures as much of the original information as possible. As a result, this can be retained and

used to describe the data instead of the original three. This technique compresses the information into a smaller number of variables and makes a more coherent, holistic analysis possible.

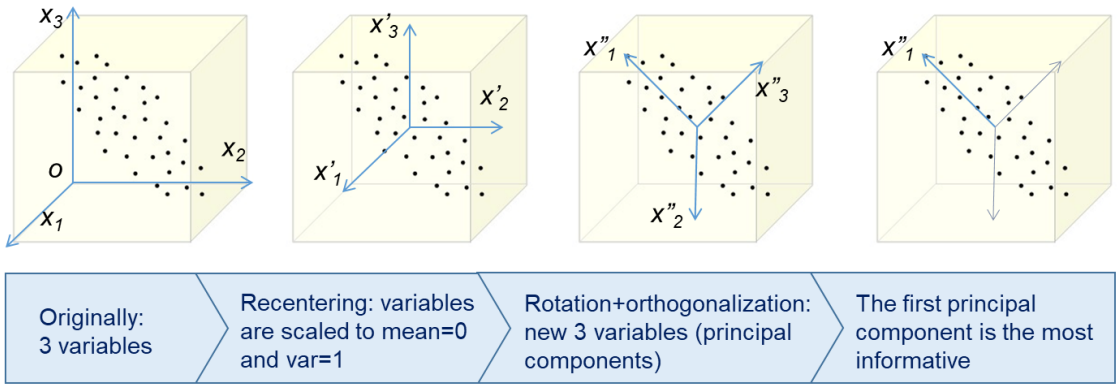

Figure 66. An example of PCA to reduce the dimensionality of a dataset.

Multiple linear regression is then applied to obtain an equation that relates this new variable, the first principal component or factor, to the mix design variables. The most relevant methodological aspects concerning multiple linear regression as applied to the analysis in this chapter have already been described (section 5.1.3). For consistency, the same model specification is adopted for the new factor. That is, the equation to be obtained will have the same generic 'format' or structure as that obtained for f_{R1}, f_{R2}, f_{R3}, and f_{R4}. It will be the same regression model described by equation (13) in section 5.2.1 but differing in the fitted values of the regression coefficients.

6.2 Principal Component Analysis and factor extraction

6.2.1 Factor analysis by PCA. A factor analysis has been applied to the set of data consisting of the parameters f_L, f_{R1}, f_{R2}, f_{R3}, and f_{R4}, where the different rows contain the values corresponding to the different SFRC mixtures and follow the same order as in the SFRC mixtures database. This factor analysis is carried out by means of PCA and extracts all five principal components. Table 9 shows the so-called factor loadings corresponding to each of the original variables, as well as the eigenvalues associated with each principal component.

Table 9. PCA: factor loadings, eigenvalues, and explained variance.

Variables	**Principal components**				
	F1	***F2***	***F3***	***F4***	***F5***
f_L	0.843	0.511	-0.166	0.016	0
f_{R1}	0.952	0.179	0.235	-0.076	0.008
f_{R2}	0.984	-0.099	0.099	0.104	-0.03
f_{R3}	0.968	-0.237	-0.049	0.038	0.045
f_{R4}	0.942	-0.29	-0.142	-0.085	-0.023
Eigenv.	**4.4123**	**0.4432**	**0.1153**	**0.0257**	**0.0035**

% of variance	**88.2%**	**8.9%**	**2.3%**	**0.5%**	**0.1%**

The percentage of variance associated with each of the principal components represents the proportion of the information contained by the original 5 variables that the principal component explains. The percentage of variance explained by each principal component is directly related to the eigenvalue associated with it. As both Table 9 and the eigenvalue plot in Figure 67 show, the first principal component was the only one with an eigenvalue higher than unity, and it explains 88.2% of the total variance in the data as described by the original 5 variables. In consequence, the first principal component is the only factor which is worthwhile to retain. From now on, this factor is referred to as *Z*.

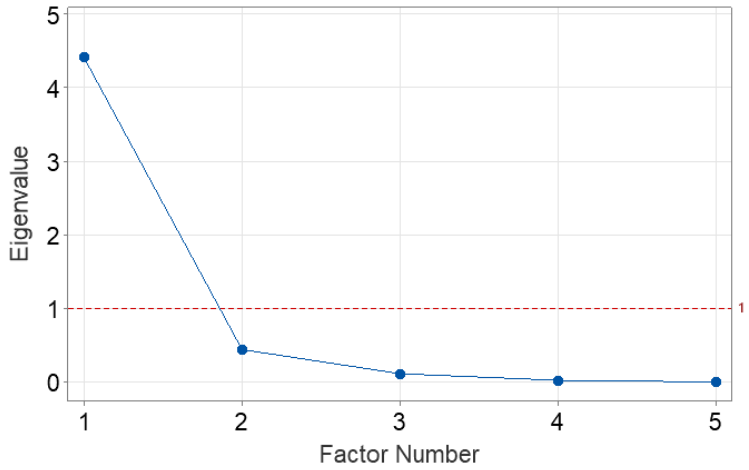

Figure 67. Screeplot after the PCA.

6.2.2 Descriptive analysis of Z. *Z* is a linear combination of the original variables (f_L, f_{R1}, f_{R2}, f_{R3}, and f_{R4}) after centering them to a mean of zero and scaling them to unit variance. For each of the SFRC mixtures in the dataset, the value of *Z* can be calculated as follows:

$$Z = 0.191\, Z_{fL} + 0.216\, Z_{fR1} + 0.223\, Z_{fR2} + 0.219\, Z_{fR3} + 0.214\, Z_{fR4} \tag{47}$$

where Z_{fL}, Z_{fR1}, Z_{fR2}, Z_{fR3}, and Z_{fR4} are the standardized values of f_L, f_{R1}, f_{R2}, f_{R3}, and f_{R4}, after centering them to mean zero and unit variance, as follows:

$$Z_{fL} = \frac{f_L - 6.063}{3.684} \tag{48}$$

$$Z_{fR1} = \frac{f_{R1} - 6.965}{6.523} \tag{49}$$

$$Z_{fR2} = \frac{f_{R2} - 6.751}{6.873} \tag{50}$$

$$Z_{fR3} = \frac{f_{R3} - 5.839}{6.210} \tag{51}$$

$$Z_{fR4} = \frac{f_{R4} - 5.030}{5.406} \tag{52}$$

It is important to note that *Z* is a non-dimensional factor, because of the standardization as per equations (48)–(52): the means are subtracted from each residual flexural strength parameter,

and the denominators are their respective, univariate standard deviations. The histogram of the Z values corresponding to all the SFRC mixtures in the database is shown in Figure 68.

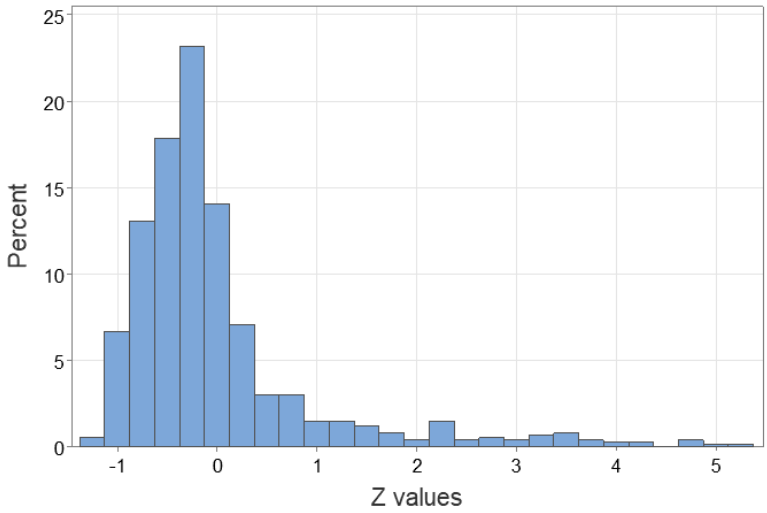

Figure 68. Histogram of Z values for the SFRC mixtures in the dataset.

The histogram in Figure 68 shows a skewed distribution, very similar in shape to the histograms observed for any of the original parameters f_L, f_{R1}, f_{R2}, f_{R3}, or f_{R4}. This is not surprising, because Z is a linear combination of these variables and all of them are weighed approximately the same (i.e. all the coefficients in equation 47 are similar). It is good practice, however, to discard the 5% most extreme cases prior to modeling. This meant discarding cases with $Z < -1$ (the 2.5% percentile) as well as cases with $Z > 3.36$ (the 97.5% percentile). The recalculated histogram is shown in Figure 69.

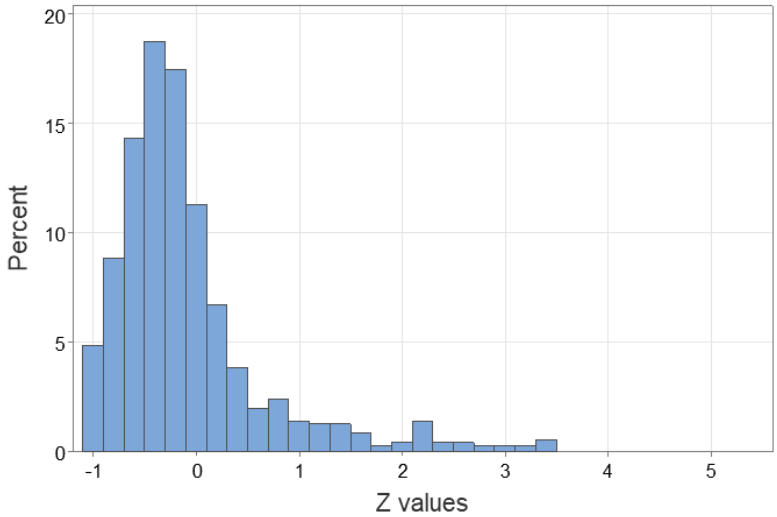

Figure 69. Histogram of Z values for the SFRC mixtures in the dataset, extremes excluded.

Some more meaningful information can be obtained from the empirical cumulative distribution plot, which is shown in Figure 70. The median of Z (i.e. the 50% percentile) is –0.2714 and is represented by a black dashed line. Therefore, it follows that SFRC mixtures with $Z > –0.2714$ are better than the 'median' mixture in the dataset, or better-than-average, in terms of flexural strength. There are two other relevant, useful values in addition to the median: $Z < –0.5$ for 30% of the SFRC mixtures (dashed blue lines), and $Z > 0$ for another 30% of them (dashed red lines). These two values, together with the median, can be used to classify any of the SFRC

mixtures in terms of how good its residual flexural strength is in terms of the characterization test results. For example:

- If $Z > 0$, the mixture is in the 30% of cases that show the best performance.
- If $Z < -0.5$, the mixture is in the 30% of cases that show the worst performance.
- If $-0.5 < Z < -0.2714$, the mixture is adequate, but its performance is worse than average.
- If $-0.2714 < Z < 0$, the mixture is adequate, and its performance is better than average.

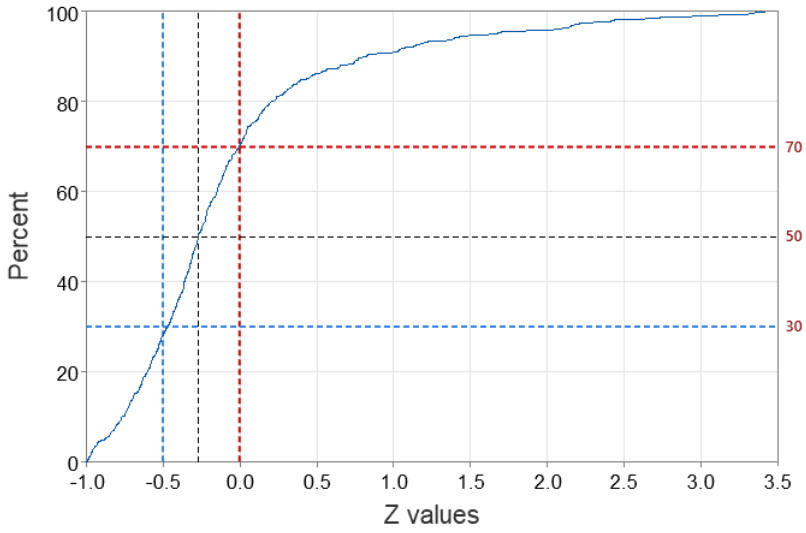

Figure 70. Empirical cumulative distribution function of Z.

6.2.3 Using Z as an indicative classifier of SFRC mixtures. *Z* and the rules summarized in the bullet points above constitute what in machine learning is called a *classifier*. These rules provide the basis for the global assessment of the flexural strength performance of SFRC mixtures based on one single parameter. Used in conjunction with the model described in the following pages, which is concerned with the estimation of *Z* as a direct function of the mix design variables, this classifier can be a useful tool to estimate the level of residual flexural strength that can be expected from any SFRC mixture. Such functionality can be easily implemented as a color bar or as a formatting rule that updates depending on the mixture proportions and the length and aspect ratio of the fibers, as illustrated in Figure 71.

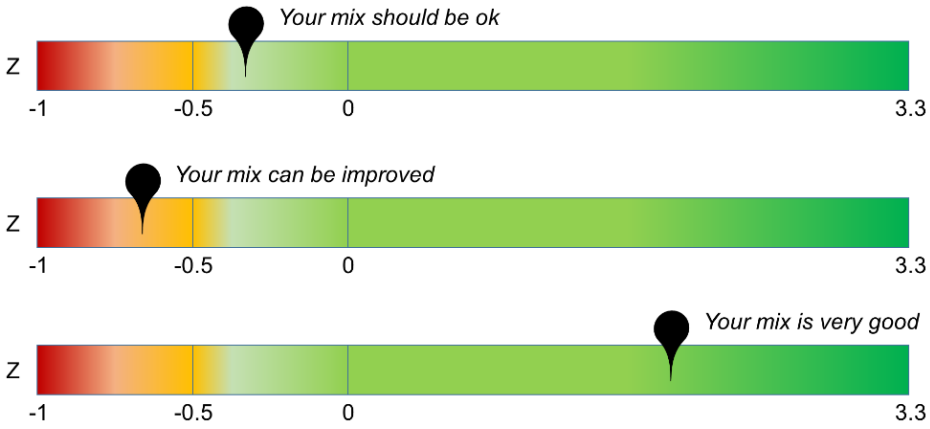

Figure 71. An example of the Z-based classifier for SFRC mixtures.

A tool like the one proposed in Figure 71 can be very helpful in guiding the proportioning of new SFRC mixtures and their optimization, based on the global assessment of the flexural strength and not just focusing on the individual residual flexural strength parameters.

6.3 Modeling *Z* as a function of mixture proportions

6.3.1 Regression analysis and fitted model. A multiple linear regression analysis was carried out to relate Z to the mix design variables of SFRC. The rationale and considerations made in relation to the modeling of f_{R1}, f_{R2}, f_{R3}, and f_{R4} (section 5.2.1) are applicable to this analysis.

The model obtained is essentially the same as that presented in equation (13), the only difference being the fitted values of the regression coefficients. The model specification as per equation (13) was satisfactory for the residual flexural strength parameters independently. Z is a linear combination of those, and Z and f_{R1}, f_{R2}, f_{R3}, and f_{R4} are but different representations of the same phenomenon. In consequence, it made sense for the specification of all these models to be consistent. The fitted model obtained for Z can be expressed as follows:

$$Z = k_0 + k_1\frac{G}{S} + (a_0 + a_1 m)\, l_f + \left(b_0 + b_1 C + b_2 SP + b_3\lambda_f + b_4 l_f\right) V_f + k_2\, SCM + k_3\, SP + k_4\lambda_f + k_5 m + k_6 C + \left(c_1\, C + c_2\, SCM + c_3\frac{G}{S}\right)(G + S) \pm \varepsilon \quad (53)$$

Where:

k_0 is a regression coefficient that includes the intercept and the term that depends on the test and specimen configuration.

k_1, k_2,…, a_0, a_1,…, b_0, b_1,…, c_1, c_2, c_3 are the regression coefficients representing the effect of the SFRC mixture proportioning variables.

S and G are the relative amounts of fine and coarse aggregate, respectively, expressed in kg/m^3, and m is the maximum aggregate size, expressed in mm.

C and SCM are the relative amounts of cement and supplementary cementitious materials, respectively, in kg/m^3.

SP is the relative amount of superplasticizer, in kg/m^3.

V_f is the steel fiber volume fraction, in percentage.

l_f and λ_f are the fiber length (expressed in mm) and the fiber aspect ratio, respectively.

ε is the error term of the estimation, which is 0.33 (non-dimensional).

The values of the fitted coefficients k_0, k_1, k_2,…, a_0, a_1,…, b_0, b_1,…, c_1, c_2, c_3 are given in Table 10. It must be noted that the fitted value of the coefficient k_3, which multiplies the amount of superplasticizer in equation (53), is zero. This is because the term corresponding to the amount of superplasticizer alone is not statistically significant. The term $k_3\, SP$ has only been maintained in equation (53) for consistency across the report. However, this does not mean that the amount of superplasticizer does not have a statistically significant effect on Z: its interaction with the fiber volume fraction is statistically significant (i.e. the coefficient b_3 is not zero).

6.3.2 Goodness of fit and cross-validation. The model is considerably accurate in fitting the Z values corresponding to the SFRC mixtures in the database, the R-squared value being 83%.

The Z values as estimated by the model in equation (53) and Table 10 are plotted against the actual Z values (i.e. obtained by the PCA-based factor analysis, sections 6.2.1 and 6.2.2) in Figure 72, together with the exact equivalence line, for reference.

Table 10. Fitted coefficient values.

Coefficient	3-point, notched	4-point, unnotched
$\mathbf{k_0}$	–1.363	–1.512
$\mathbf{k_1}$	–1.21	
$\mathbf{k_2}$	0.00331	
$\mathbf{k_3}$	0	
$\mathbf{k_4}$	–0.00547	
$\mathbf{k_5}$	0.0286	
$\mathbf{k_6}$	0.001973	
$\mathbf{a_0}$	0.01719	
$\mathbf{a_1}$	–0.000601	
$\mathbf{b_0}$	–0.485	
$\mathbf{b_1}$	–0.000319	
$\mathbf{b_2}$	0.00348	
$\mathbf{b_3}$	0.02384	
$\mathbf{b_4}$	–0.00389	
$\mathbf{c_1}$	-7×10^{-7}	
$\mathbf{c_2}$	-1.4×10^{-6}	
$\mathbf{c_3}$	0.000641	

Figure 72. Fitted vs actual Z values.

In addition to the R-squared as an indicator of the accuracy of the model in fitting the Z values for the different mixtures in the dataset, a k-fold cross-validation was also done (details as in 5.2.2). After the 10-fold cross-validation, the R-squared was estimated as 81%. As this value is very close to the overall R-squared of 83%, it can be concluded that the model in equation (53) is sufficiently robust in terms of its expected predictive performance.

6.3.3 How much information does this model describe? In machine learning and multivariate data analytics, the amount of information in a set of values is quantified by their variance.

As explained in 6.2.1, the extraction of the first principal component led to the Z factor, which contains 88.2% of the variance of the set of $\{ f_L, f_{R1}, f_{R2}, f_{R3}, f_{R4} \}$ values for all the SFRC mixtures in the dataset. That is, by considering only Z instead of the five original variables, only 11.8% of the information is lost.

On the other hand, the R-squared of the model fitted to Z values as per equation (53) and Table 10 is 83%, which means that it explains 83% of the variance in the set of Z values corresponding to the SFRC mixtures in the database.

Considering the abovementioned aspects together, it follows that the model represented by equation (53) describes 83% of 88.2% of the original information in the set of $\{ f_L, f_{R1}, f_{R2}, f_{R3}, f_{R4} \}$ values, that is: 0.83 x 0.882 = 73.2%. This is illustrated in Figure 73. Despite the intrinsic scatter of the residual flexural strength parameters, and after the original parameters have been compressed into one single factor, the values of Z as estimated by equation (53) reproduce the original information with an accuracy of 73%. This level of performance is not dissimilar to that of the individual equations obtained for $f_{R1}, f_{R2}, f_{R3}, f_{R4}$ separately (section 5.2.2).

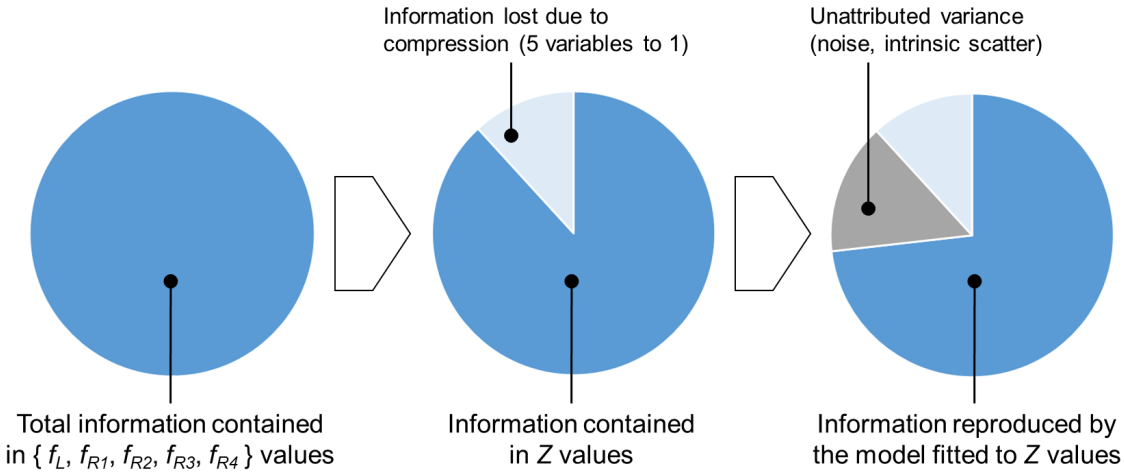

Figure 73. Information explained by the model after dimension reduction and regression.

6.3.4 Relative importance of the different terms in the model. Each of the terms in equation (53) represent the contribution of different mix design variables to the residual flexural strength of SFRC mixtures, since the Z factor is an aggregated view of all the residual flexural strength parameters. The relative importance of each of these terms can be quantified through their contribution to the total variance of Z, that is, the ratio of the variance explained by each term to the total variance of Z. In multiple linear regression, variance is directly related to the so-called sums of squares, and therefore the relative importance of each term in the model can be evaluated as the ratio of the sum of squares associated with that term to the total sum of squares. Such values are given in Table 11. It has been assumed that the variance explained by any

pairwise interaction is equally split between the two variables in the interaction. With this simplification, it is possible to obtain a quite useful, visual representation of the relative importance of the main variables in the model, as shown in Figure 74.

Table 11. Share of the total sum of squares per mix design variables.

Source of variation	Sums of squares	Percentage
Fiber volume fraction	120.2	30.5%
Fiber aspect ratio	32.8	8.3%
Fiber length	8.5	2.2%
SCMs content	51.7	13.1%
Cement content	7.6	1.9%
Coarse-to-fine aggr. ratio	83.3	21.1%
Total aggregate content	3.6	0.9%
Max. aggregate size	1.2	0.3%
Superplasticizer content	3.2	0.8%
Test configuration	14.5	4.0%
Unattributed variation (noise)	68.0	17.2%

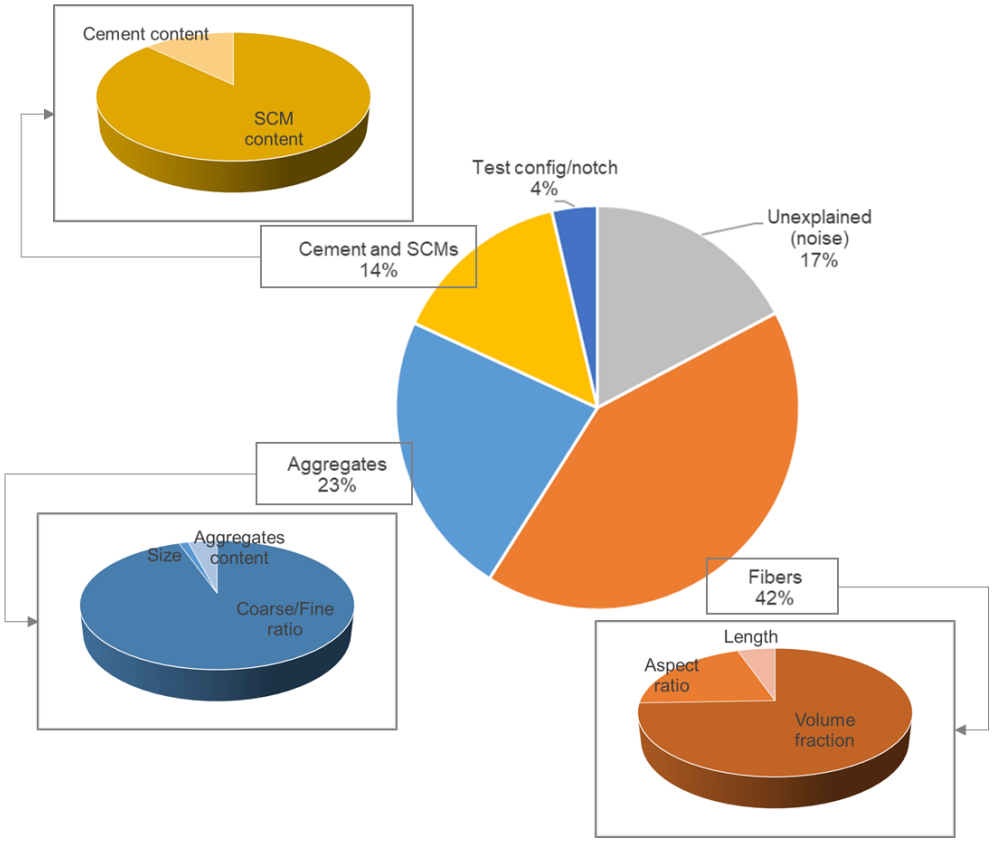

Figure 74. Relative importance of the different terms in the model.

The slices of the main pie chart in Figure 74 represent the relative importance of the mix design variables grouped in the 'main' categories of fibers, aggregates, cement and SCMs, and test/specimen configuration, in addition to the 17% of variability which the model does not attribute to any specific variables (i.e. noise in the data). The secondary pie charts show the relative weight of the different variables within each of these categories. Fibers are the most important category contributing to the residual flexural strength and, in terms of the fibers, the most determining variable is the volume fraction, followed by the fiber aspect ratio and the fiber length. None of this is a surprise. However, it is important to note that the relative contribution of other variables is as important as that of the fibers. The three variables representing the effect of the fibers account for 42% of the total variance. If the 17% unattributed variance or noise is put aside, they account for 50.6% of the 'explained' variance, which means that almost 49.4% of it is attributable to the other mix design variables. The split is almost 50-50. In other words, this analysis proves that the residual flexural strength of SFRC is influenced equally by the fibers and the rest of the constituents of the mixture.

The aggregates are the second most important category, and the most relevant variable is not the aggregate content but the coarse-to-fine aggregate ratio. Furthermore, in terms of the binder composition, the total amount of SCMs is more relevant than the amount of cement in the mixture. The marked prominence of the coarse-to-fine aggregate ratio and the amount of SCMs in the mixture substantiates, once again, the conclusion that the cohesiveness of the mixture can have a significant impact on the residual flexural strength of the SFRC mixtures by enhancing the effect of the fibers.

6.4 Effect of the fiber length and the fiber content

6.4.1 Contour plot. The contour plot of Z against the fiber length and the fiber volume fraction shown in Figure 75 corresponds to the response surface as per equation (53) and the fitted coefficients in Table 10, assuming median values for the other mix design variables. The contour colors in this and other contour plots in the sections that follow have been chosen so that they change from blue to green at $Z = -0.25$, very close to the median of Z. Therefore, areas in blue correspond to worse-than-average cases, whilst areas in green correspond to cases that are better than average in terms of their residual flexural performance.

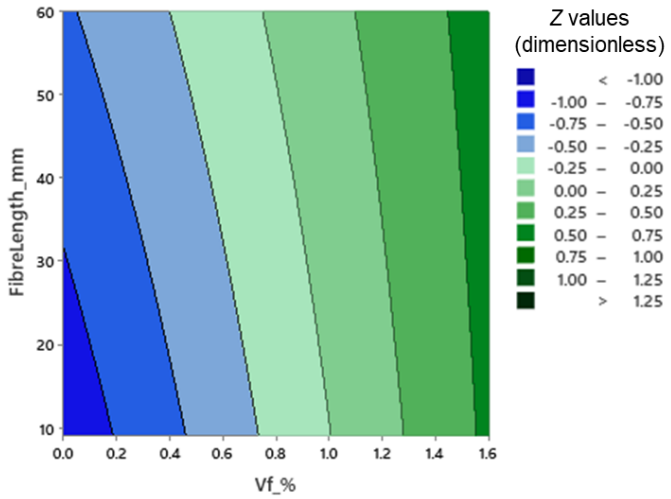

Figure 75. Contour plot of Z against fiber length and fiber volume fraction.

6.4.2 Interaction between fiber length and fiber content. The contour plot of *Z* is similar to the contour plots discussed in section 5.3, and the general trends are very similar to the contour plots for f_{R2}, f_{R3} and f_{R4}. Higher values of *Z* are strongly associated with increasing fiber contents, as expected. There is also a positive association between the fiber length and *Z*, but the importance of this variable changes with the fiber volume fraction.

In fact, the effect of the fiber length on *Z* becomes less and less important when higher fiber contents are considered, so much so that there is a theoretical value of the fiber volume fraction that makes the effect of fiber length on *Z* null. Looking at Figure 75, this seems higher than 1.6% and therefore out of the range within which the models in this study are based upon (see section 1.5.1). Such value can be determined by differentiating equation (53) with respect to the fiber length and equating to zero:

$$\frac{\partial Z}{\partial l_f} = a_0 + a_1 m + b_4 V_f = 0 \tag{54}$$

And, after replacing coefficients a_0, a_1, and b_4 with their fitted values from Table 10, it is obtained that such fiber volume fraction is a function of the maximum aggregate size:

$$V_f = \frac{0.01719 - 0.000601\, m}{0.00389} = \begin{cases} 2.87\% & if\ m = 10mm \\ 2.10\% & if\ m = 15mm \\ 1.33\% & if\ m = 20mm \end{cases} \tag{55}$$

Therefore, as long as the maximum aggregate size is not higher than 15-16 mm (which, in most of the cases, it is not: see section 1.4.3), the fiber content at which the effect of the fiber length on *Z* becomes null is only theoretical and has no practical implications. That is: in general, increasing the fiber length is associated with increasing *Z* values, i.e. improved residual flexural performance. This result is consistent with the considerations emerging from the analysis of the residual flexural strength parameters in section 5.3.

6.4.3 How 'important' is the effect of fiber length? As explained in section 5.3.4, the expected variation of *Z* corresponding to a 10 mm increase of the fiber length can be compared to the expected variation associated with a 0.1% increase of the fiber content.

By differentiating equation (53) with respect to the fiber length, and assuming median values for the rest of mix design variables, the expected variation of *Z* when the fiber length is increased in 10 mm can be obtained:

$$E\left(\Delta Z \middle| \Delta l_f = +10mm\right) = \frac{\partial Z}{\partial l_f} \times \Delta l_f = (a_0 + a_1\, m + b_4\, V_f) \times \Delta l_f = 0.0559 \tag{56}$$

On the other hand, the expected variation of *Z* when the fiber content is increased in 0.1% can be obtained by differentiating equation (53) with respect to the fiber volume fraction, and assuming median values for the other mix design variables:

$$E\left(\Delta Z \middle| \Delta V_f = +0.1\%\right) = \frac{\partial Z}{\partial V_f} \times \Delta V_f = (b_0 + b_1 C + b_2 SP + b_3 \lambda_f + b_4 l_f) \times \Delta V_f = 0.0776 \tag{57}$$

These expected variations, 0.0559 and 0.0776 (both dimensionless), are comparable in magnitude. In consequence, it can be said that the positive effect that increasing the fiber length has on *Z* is, in general, as important as that of the fiber content. This is also consistent with the

observations made in relation to the individual residual flexural strength parameters (section 5.3.4).

6.5 Effect of fiber aspect ratio and fiber content

6.5.1 Contour plot. Figure 76 shows the contour plot of Z as a function of the fiber content and the fiber aspect ratio, as modelled by equation (53), assuming median values for the other mix design variables. This response surface is highly consistent with those that were obtained from the analysis of f_{R1}, f_{R2}, f_{R3} and f_{R4} (section 5.4), and the general trends are very similar.

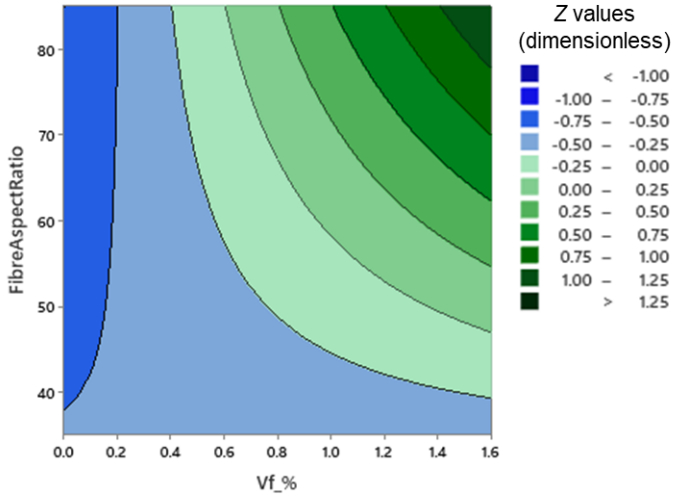

Figure 76. Contour plot of Z against fiber aspect ratio and fiber volume fraction.

6.5.2 Interaction between the fiber aspect ratio and fiber content. The effect of the fiber aspect ratio on Z changes depending on the fiber content. As Figure 76 shows, when moderate or high fiber contents are considered, increasing the fiber aspect ratio is associated with higher Z values and, therefore, better residual flexural strength. The higher the fiber content is, the more important the impact of the fiber aspect ratio on Z is.

It is also observed in Figure 76 that, for the fiber aspect ratio to have a noticeable, positive effect on Z, the fiber volume fraction must be higher than a certain value. This threshold corresponds to the fiber content that makes Z insensitive to the fiber aspect ratio. It can be determined by differentiating equation (53) with respect to the fiber aspect ratio and equating to zero:

$$\frac{\partial Z}{\partial \lambda_f} = b_3 V_f + k_4 = 0 \tag{58}$$

After replacing the coefficients b_3 and k_4 in equation (58) with their values from Table 10, the threshold fiber volume fraction obtained is 0.23%. This value does not depend on any other variables and is consistent with the threshold values that resulted from the analysis of the residual flexural strength parameters one by one (which ranged between 0.2%-0.4%).

In consequence, when the fiber content is low (i.e. around V_f = 0.23%), Z values are practically insensitive to the fiber aspect ratio, and increasing (or decreasing) the fiber aspect ratio does not have a determining impact on residual flexural strength. On the other hand, when the fiber volume fraction is higher than 0.23%, higher values of the fiber aspect ratio are associated with

higher values of Z, this meaning a better residual flexural strength. At this point it is important to recall that, based on the data compiled in this study, SFRC mixtures with a fiber volume fraction lower than 0.23% are very rare. The 5th to 95th percentile range is 0.25% to 2.0% (see section 1.5), which means that the prevalence of mixtures with a fiber content not higher than 0.23% is less than 5%. Therefore, the conclusion is that, in the vast majority of cases, increasing the fiber aspect ratio is associated with higher values of the Z factor and therefore better levels of residual flexural strength.

6.5.3 Better-than-average flexural strength. In Figure 76, the region of the contour plot that is colored in shades of green corresponds to values of the Z factor higher than its median (section 6.4.1). It is possible to obtain the mathematical expression that defines such region by imposing the condition $Z \geq -0.27$ on equation (53). If median values are assumed for the other mix design values, the result is the following:

$$V_f(\%) \geq \frac{0.0535 + 0.0547\,\lambda_f}{0.238\,\lambda_f - 7.73} \tag{59}$$

The above inequality can be plotted in the aspect ratio – volume fraction plane and it gives the minimum fiber content required to have a value of the Z factor that is better than the average mixture in the SFRC database. This is shown in Figure 77. If fibers with an aspect ratio of 60 are assumed, the minimum fiber volume fraction required to have better-than-average residual flexural strength is 0.51%. If a fiber aspect ratio of 80 is assumed, the minimum fiber content is 0.40%, which is a significant improvement from the V_f = 0.84% required if fibers with an aspect ratio of 45 are considered instead.

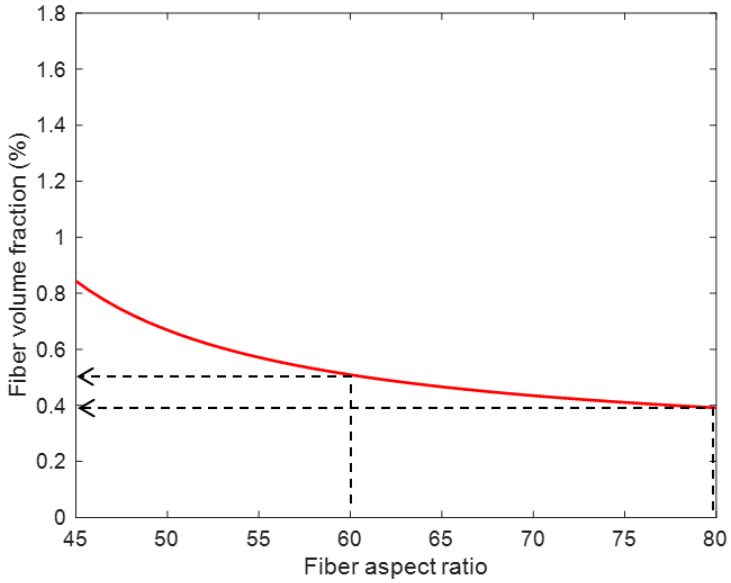

Figure 77. Fiber content requirement for better-than-average Z factor.

6.5.4 How 'important' is the effect of the fiber aspect ratio? Although the contour plot in Figure 76 clearly shows that the effect of the fiber aspect ratio on Z is considerable and seems comparable in importance to that of fiber content, it is interesting to try and put some numbers into the comparison. With practical applications in mind, it is useful to compare the effect of varying the aspect ratio in +10 to the effect that a 0.1% increase of the fiber content has on Z. The expected variation of Z if the fiber aspect ratio is increased in 10 (from 50 to 60, for example) can be determined by differentiating equation (53) and multiplying by 10:

$$E\left(\Delta Z\middle|\Delta\lambda_f = +10\right) = \frac{\partial Z}{\partial \lambda_f} \times \Delta\lambda_f = \left(b_3\, V_f + k_4\right) \times \Delta\lambda_f \tag{60}$$

After replacing the coefficients b_3 and k_4 with their fitted values from Table 10, the expected variation $E\left(\Delta Z\middle|\Delta\lambda_f = +10\right)$ is a function of the fiber volume fraction:

$$E\left(\Delta Z\middle|\Delta\lambda_f = +10\right) = 0.2384 V_f - 0.0547 \tag{61}$$

Therefore, if the median fiber volume fraction of 0.51% is assumed for reference, the expected variation of Z when the fiber aspect ratio is increased in 10 is 0.0645. On the other hand, the expected variation of Z corresponding to a 0.1% increase of the fiber volume fraction is 0.0776 (equation (57)). As the two values are comparable in magnitude, it can be concluded that the effect of the fiber aspect ratio on Z is no less important than that of the fiber volume fraction.

Although the above are sufficiently representative values and the overall conclusion is clear, strictly speaking $E\left(\Delta Z\middle|\Delta\lambda_f = +10\right)$ is a function of V_f and $E\left(\Delta Z\middle|\Delta V_f = +0.1\%\right)$ is a function of λ_f. Their comparative analysis provides even more information if no particular values are assumed for either V_f or λ_f. This can be done through the ratio between the two as given in equations (57) and (61), assuming median values for the rest of mix design variables:

$$\frac{E\left(\Delta Z\middle|\Delta\lambda_f = +10\right)}{E\left(\Delta Z\middle|\Delta V_f = +0.1\%\right)} = \frac{0.2384 V_f - 0.0547}{0.002384\lambda_f - 0.07737} \tag{62}$$

This ratio is an indirect measure of the relative importance of λ_f compared to V_f. When the ratio is higher than 1, the expected variation of Z associated with $\Delta\lambda_f = +10$ is higher than that associated with $\Delta V_f = +0.1\%$, and the effect of increasing the fiber aspect ratio is even more important than that of increasing the fiber content. When the ratio is lower than 1, the conclusion is the opposite. Figure 78 shows the plot of the ratio in equation (62) against the two variables, and the plane corresponding to the ratio being equal to 1 is included as reference. It can be seen that there is a wide range of combinations of values of the fiber aspect ratio and the fiber content that are associated with the effect of the former being more important.

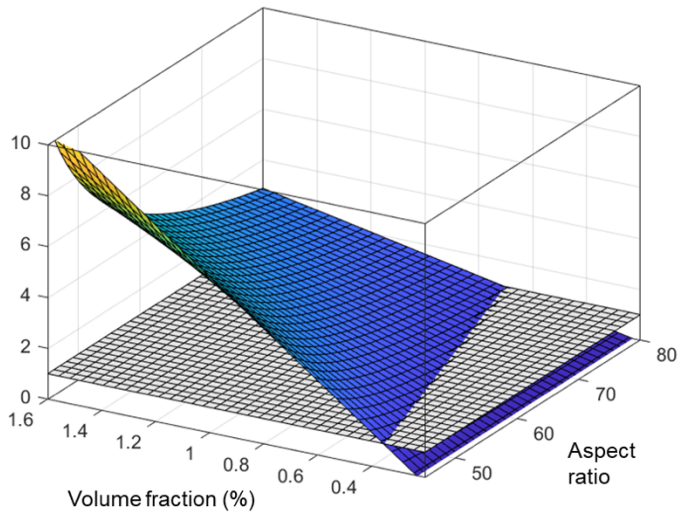

Figure 78. Relative effect of fiber aspect ratio on Z compared to that of fiber content.

If the intersection between the surface plot and the unity plane in Figure 78 is projected unto the fiber aspect ratio – fiber content plane, the line separating both regions is obtained, as shown in Figure 79. This can be a useful tool when trying to optimize SFRC mixtures. For example, if fibers with an aspect ratio of 45 are being considered for a mixture with a fiber volume fraction of 0.6%, increasing the fiber aspect ratio to 55 can be more advantageous in terms of overall flexural performance than increasing the fiber content to 0.7%. The plot in Figure 79 shows that, for moderate to high fiber contents, increasing the fiber content any further is, generally speaking, not as advantageous as increasing the fiber aspect ratio.

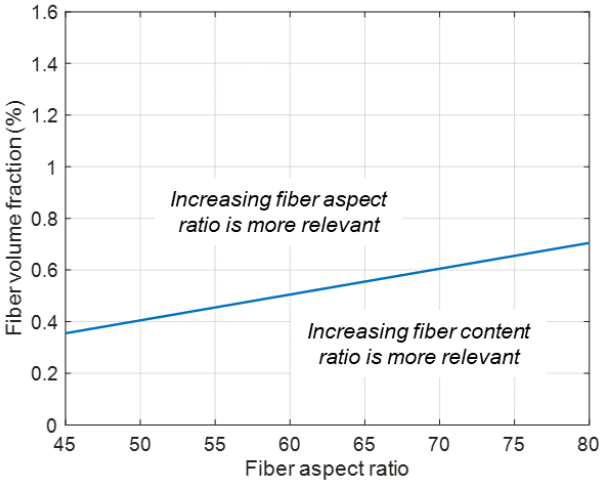

Figure 79. Importance of fiber aspect ratio compared to fiber content.

6.6 Interaction between fiber length and maximum aggregate size

6.6.1 Contour plots. Three contour plots of the *Z* factor against the fiber length and the maximum aggregate size are shown in Figure 80. As explained in 5.5.1, three different values of the fiber volume fraction are assumed, and the interpretation of the contour plots is limited to the region defined by the orange dashed line. The grayed-out areas correspond to cases where there is not sufficient evidence to support what the model predicts.

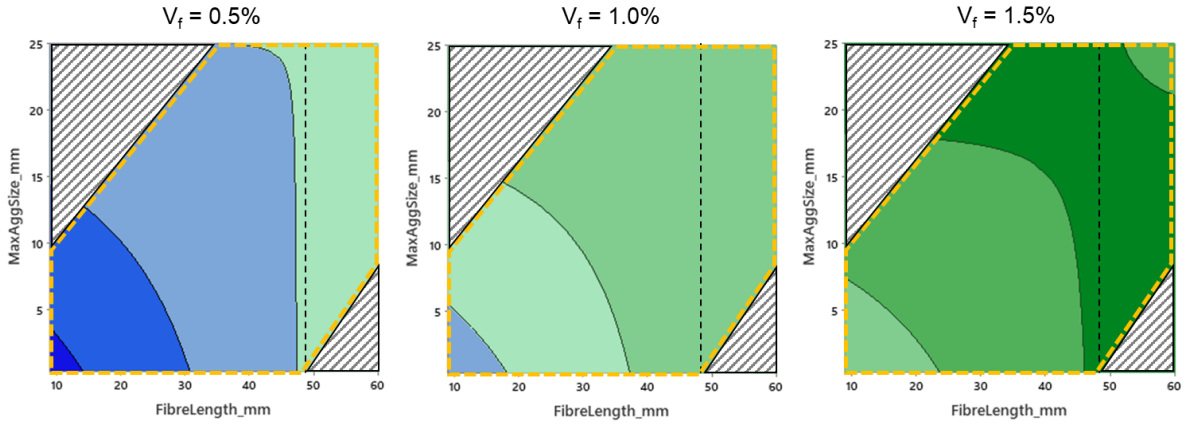

Figure 80. Contour plots of Z vs fiber length and maximum aggregate size.

6.6.2 Sensitivity to the maximum aggregate size. As can be seen in the contour plots in Figure 80, the combination of short fibers and small values of the maximum aggregate size are associated with the lowest values of *Z*, particularly when the fiber content is low or moderate

(i.e. plot for V_f = 0.5%). When higher fiber contents are considered (i.e. plots for V_f = 1.0% and 1.5%), this is also true, but the contour plots do not show much change in terms of *Z* values when the maximum aggregate size and the fiber length are varied. These observations are consistent with the trends in relation to these two variables observed in the models for each of the residual flexural strength parameters separately (see 5.5.2). It can be concluded that, although the interaction between these two variables is statistically significant, it is not associated with large variations of the residual flexural strength. Furthermore, the maximum aggregate size is the variable with the least relative importance in the fitted model, as established in section 6.3.4 and shown in Figure 74, so it is not surprising that its interaction with the fiber length is of limited practical relevance.

There is, however, a certain value of the fiber length that makes *Z* insensitive to changes in the maximum aggregate size, represented by the vertical dashed lines in Figure 80. This can be determined by differentiating equation (53) with respect to the maximum aggregate size and equating to zero:

$$\frac{\partial Z}{\partial m} = a_1\, l_f + k_5 = 0 \quad \rightarrow \quad l_f = \frac{-k_5}{a_1} \tag{63}$$

Using the a_1 and k_5 values from Table 10, the fiber length obtained from equation (63) is 47.6 mm and does not depend on any other mix design variable. It is strikingly similar to the fiber length values obtained when the same calculation was made in relation to the models for each of the residual flexural strength parameters separately (47.7 mm, 41 mm, 45 mm, section 5.5.2).

6.7 Effect of the superplasticizer content

6.7.1 Contour plot and interpretation. The contour plot of *Z* as per equation (53) against the fiber volume fraction and the superplasticizer content, assuming median values for the other mix design variables, is shown in Figure 81. It is very consistent with the equivalent contour plots that resulted from the models obtained for each of the residual flexural strength parameters (section 5.6.1). The term in the model that represents the simple effect of the superplasticizer on *Z* is not statistically significant (k_3 = 0 in equation (53), Table 10): the superplasticizer content only influences *Z* through its interaction with the fiber content (b_2 in equation (53), Table 10), by modifying the effect of this variable. Even so, its relevance is limited, as Figure 81 shows: increasing the superplasticizer content is associated with some improvement of *Z*, but very minor in comparison with the effect of the fiber content.

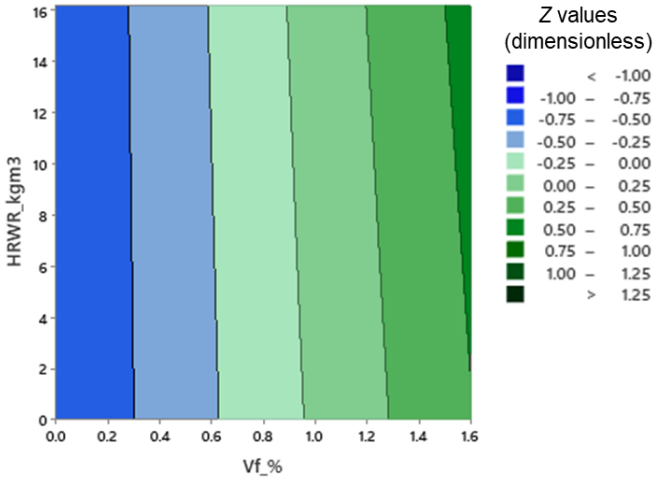

Figure 81. Contour plot of Z vs superplasticizer content and fiber volume fraction.

6.7.2 How 'important' is the effect of superplasticizer? As explained in 5.6.2, an increase of the superplasticizer content equal to +3.5 kg/m^3 is a considerable increase. The expected variation of Z associated with such substantial increase can be compared to the variation to be expected as a result of a 0.1% increase of the fiber content.

An indicative value of the expected variation of Z corresponding to $\Delta SP = +3.5$ kg/m^3 can be obtained based on the partial derivative of equation (53) with respect to the superplasticizer content, and assuming the median fiber content of 0.51%:

$$E(\Delta Z|\Delta SP) = \frac{\partial Z}{\partial SP} \times \Delta SP = \left(b_2\, V_f + k_3\right) \times 3.5 = 0.01218\, V_f = 0.00621 \tag{64}$$

On the other hand, the expected variation of Z given $\Delta V_f = +0.1\%$, assuming median values for the mix design variables, is 0.0776 (calculated in equation (57)).

Comparing the two expected variations, it is clear that the effect of the superplasticizer content on Z is much less important than that of the fiber content. In fact, even when a substantial increase such as +3.5 kg/m^3 is assumed for the superplasticizer content, the effect of an increase of 0.1% in the fiber content is, on average, 0.0776/0.00621 = 12.5 times more important in magnitude.

6.8 Effect of cement content and fiber content

6.8.1 Contour plot and interpretation. The contour plot of Z against the cement content and the fiber volume fraction is shown in Figure 82 and corresponds to the response surface obtained by plotting equation (53) as a function of these two variables, assuming median values for the rest of the mix design variables. The model as per equation (53) includes an interaction term between the fiber volume fraction and the cement content. Since the cement content not only influences Z directly but also modifies the effect of the fiber content, it is appropriate to discuss the effect of the two variables together.

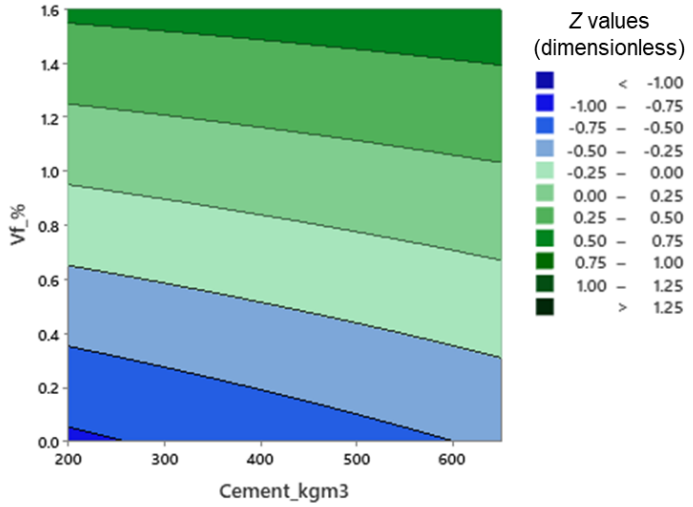

Figure 82. Contour plot of Z vs cement content and fiber volume fraction.

The contour plot in Figure 82 shows that the effect of the cement content on *Z* is, in principle, not negligible (particularly at low to moderate fiber contents), although it becomes less important when higher fiber contents are considered. In fact, if the average variation of *Z* is plotted against the fiber volume fraction for three different cement contents between 300 kg/m^3 and 600 kg/m^3, the trend with respect to the fiber volume fraction does not change dramatically, as can be seen in Figure 83([5]). The cement content is, on average, associated with a slight improvement of the residual flexural performance.

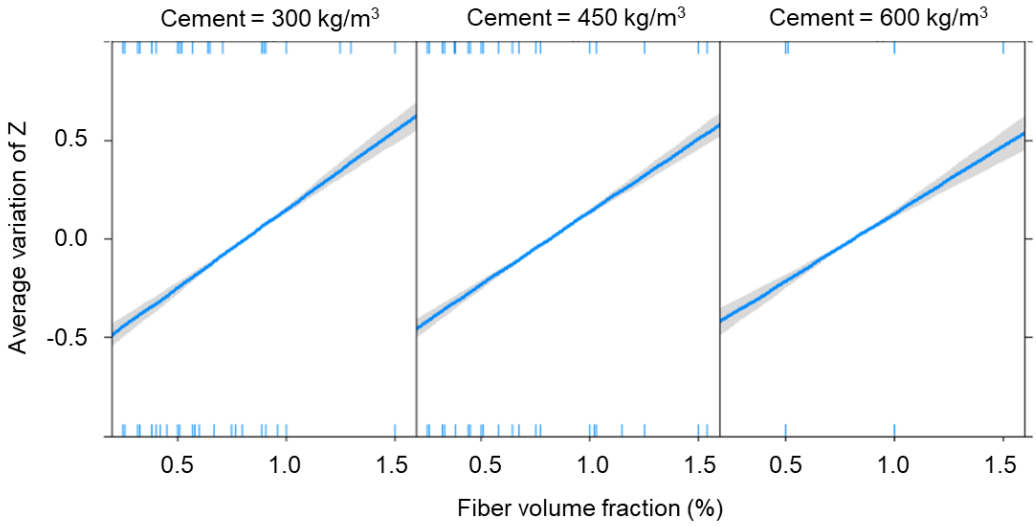

Figure 83. Average change of Z with cement content and fiber volume fraction.

It is interesting to note, however, that the trend observed for *Z* with respect to the cement content is somewhat different to the observations made in relation to the models for each of the residual flexural strength parameters separately. In section 5.7, it was pointed out that the cement content and its interaction with the fiber volume fraction did not have a statistically

[5] These are sometimes called 'contrast' plots and are based on partial residuals. They can be useful in visualizing effects in multiple regression models with interactions, as they do not assume a particular set of values for the variables not in the plot. What is plotted in the vertical axis is not *Z* but the *change* of *Z* when the variable in the horizontal axis (fiber volume fraction in this case) is increased or decreased with respect to its average. For more information on contrast plots, see: Breheny, P., and Burchett, W. (2017), "Visualization of regression models using visreg." The R Journal 9(2): 56-71.

significant effect on f_{R2} and f_{R4}, and the sign of the relationship between the cement content and f_{R1} was not the same as that between the cement content and f_{R3}. At this point it is useful to bear in mind that Z also accounts for the limit of proportionality in addition to all the residual flexural strength parameters, providing a more global description of the residual flexural strength. Having said that, the effect of the cement content on f_{R1} and f_{R3} was less important in magnitude than that of the fiber content (section 5.7.5), and that is not completely inconsistent with what the plots in Figure 83 (and the calculations in the next paragraph) show.

6.8.2 How 'important' is the effect of cement content? It is useful to compare the effect of the cement content to that of the fiber content on Z through the expected variations of this parameter when comparable changes in each of these two variables are considered. It seems reasonable to compare an increase of 100 kg/m^3 cement content with a 0.1% increase of the fiber volume fraction. As shown in equation (57), the expected variation of Z given $\Delta V_f = +0.1\%$, and assuming median values for the rest of mix design variables, is 0.0776.

The expected variation of Z corresponding to $\Delta C = +100$ kg/m^3 can be determined by multiplying this increment times the partial derivative of equation (53) with respect to the superplasticizer content, assuming median values for the other variables and taking the values of coefficients b_1, k_6 and c_1 from Table 10:

$$E(\Delta Z|\Delta C = 100) = \frac{\partial Z}{\partial C} \times \Delta C = \Big(b_1 V_f + k_6 + c_1(G+S)\Big) \times 100 = 0.061 \qquad (65)$$

Although both expected variations are of the same order of magnitude, 0.061 is lower than 0.0776, and therefore the change of Z to be expected when the cement content is increased in 100 kg/m^3 is smaller than that associated with a 0.1% increase in the fiber content. In other words: not even 100 kg/m^3 more cement is sufficient to match the effect of adding just 0.1% more fibers. The effect of the cement content on Z, in practice, is less important than the effect of the fiber content, although comparable.

6.9 Interaction between total aggregate content and amount of SCMs

6.9.1 Contour plot (limited to possible cases only). The contour plot of Z against the total amount of SCMs and the total aggregate content, as modeled by equation (53) and assuming median values for the other mix design variables, is shown in Figure 84.

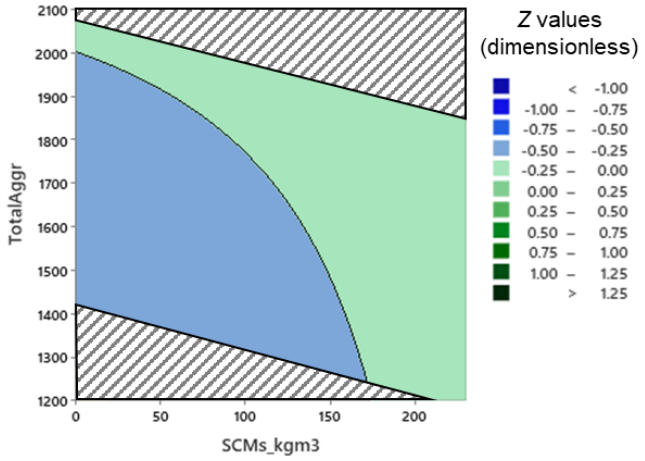

Figure 84. Contour plot of Z vs the total aggregate and SCMs contents.

The grayed-out areas in the plot correspond to combinations of values of the aggregate content and the SCMs content that are not possible in the context of the data this model is based upon. As explained in section 5.8.2, given that the model has been developed for SFRC mixtures with normal density, the grayed-out areas in the plot correspond to combinations that do not satisfy the following inequalities:

$$1418.5 \leq SCM + (G + S) \leq 2071.5 \tag{66}$$

6.9.2 How relevant is this interaction? What the interaction between the total aggregate content and the total amount of SCMs represents in the model as per equation (53) is that the effect of any of these two variables on Z depends on the value of the other. The multiple regression analysis showed that this term was statistically significant. However, as can be observed in Figure 84, there is not much variation when these two variables are varied together, which means that the interaction between them does not have a major impact on Z values. In other words: although the effect of their interaction is statistically significant, it is not so important in magnitude.

This is perhaps more evident if the average variation of Z is plotted as a function of the total aggregate content for different amounts of SCMs. The contrast plots in Figure 85 show this variation for three different contents of SCMs: 0 kg/m^3, 75 kg/m^3, and 150 kg/m^3. Varying the SCMs content does not dramatically change the trend with respect to the total aggregate content, although some slight differences can be seen.

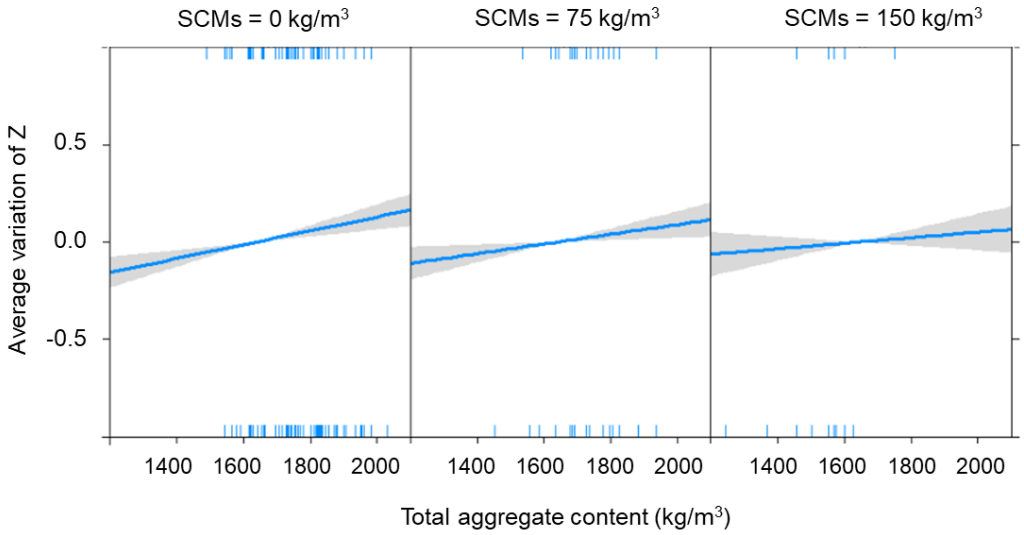

Figure 85. Average change of Z with total aggregate content and SCMs content.

The in-depth discussion of this interaction as described by the regression models fitted to f_{R1}, f_{R2}, f_{R3} and f_{R4} separately (see section 5.8) revealed more complex effects and provided some more detailed information than the analysis from a multivariate perspective presented above. This can be due to the model obtained for Z not describing the effect of the amount of SCMs as accurately. It is important to bear in mind that Z condenses five parameters into one, with some loss of granularity in the information reproduced to be expected (see 6.3.3).

6.10 Interaction between total aggregate content and cement content

6.10.1 Contour plots (limited to possible cases only). Figure 86 shows the contour plots of Z against the total aggregate content and the amount of cement, as per equation (53), assuming median values for the other mix design variables. Since the model includes a statistically significant term corresponding to the interaction between the cement content and the fiber content, three contour plots are shown, for fiber contents of 0.5%, 1.0%, and 1.5% in volume.

As in the previous section, unrealistic combinations of aggregate content and cement content are grayed out of these plots. The interpretation and discussion of the model obtained for Z is limited to values that satisfy the following inequalities (section 5.8.2):

$$2096.5 \leq C + SCM + (G + S) \leq 2396.5 \tag{67}$$

Since the representative range of the total amount of SCMs in the SFRC database in this study is between 20 kg/m^3 and 198 kg/m^3 (5th and 95th percentile, respectively), the above can be rewritten as follows:

$$1898.5 \leq C + (G + S) \leq 2376.5 \tag{68}$$

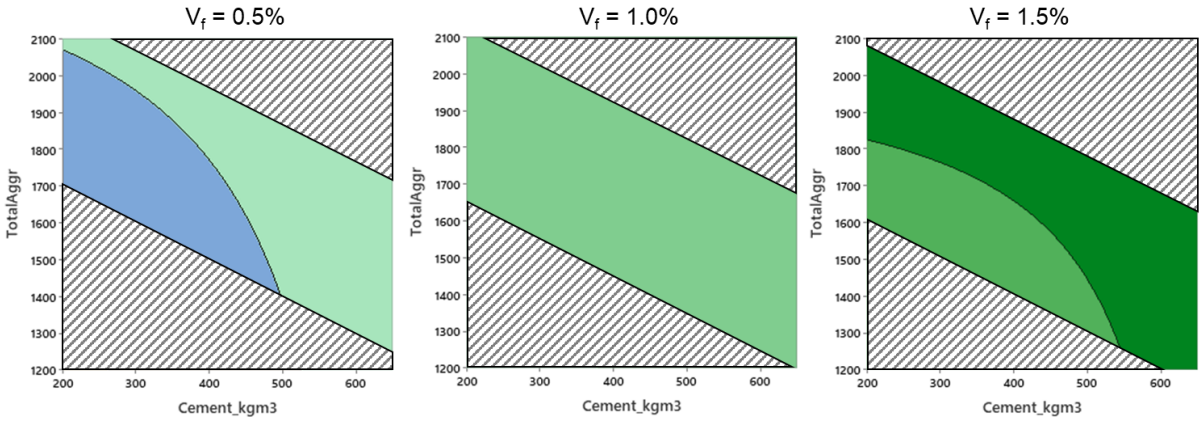

Figure 86. Contour plots of Z vs cement and aggregate contents, for three different fiber volume fractions.

6.10.2 How relevant is this interaction? The contour plots in Figure 86 show that there is not much variation in the Z factor when the cement content and the total aggregate content are varied together. In this respect, the comments made in the previous section in relation to the interaction between SCMs and the total aggregate content are applicable here. Although the interaction between the amount of cement and the total aggregate content is statistically significant, in practical terms its impact on Z values is not so relevant. The contrast plots in Figure 87 show that the relationship between the variation of Z and the total aggregate content is not substantially affected by the cement content.

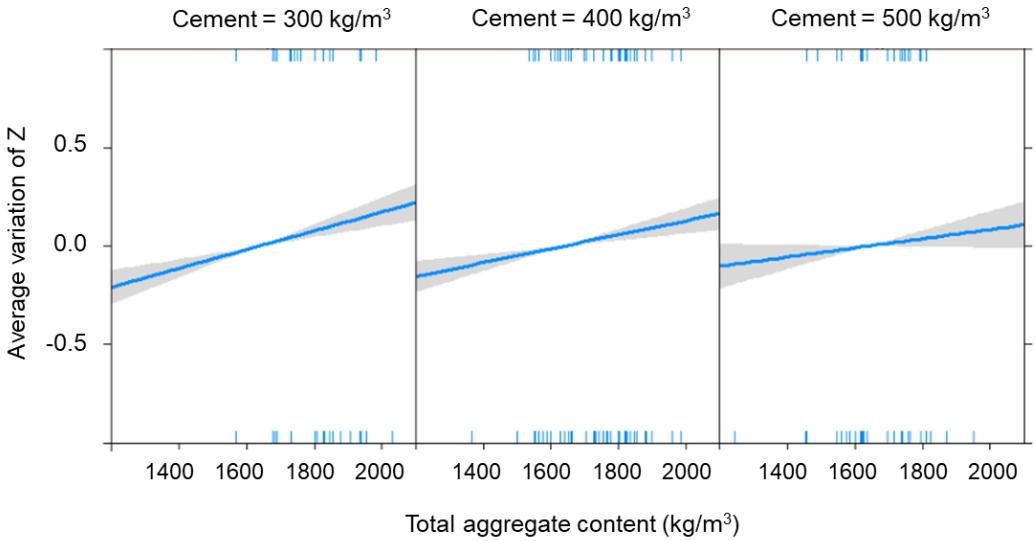

Figure 87. Average change of Z with total aggregate and cement contents.

6.11 Effect of the coarse-to-fine aggregate ratio

6.11.1 The relevance of the G/S ratio, in context. In the model developed for Z, given by equation (53) and the coefficients in Table 10, there are three terms that represent the effect of the total aggregate content (coarse plus fine aggregate, G+S) on the residual flexural strength of SFRC mixtures. The interactions between these variables have a statistically significant effect on Z and this is factored in the model through the coefficients c_1, c_2, and c_3. In equation (53), these three terms are grouped together as follows:

$$\left(c_1\, C + c_2\, SCM + c_3 \frac{G}{S}\right)(G + S) \tag{69}$$

Written as above, grouped in one single term, the joint interpretation of these interactions becomes clear: the total amount of aggregates in the mixture has an effect on the residual flexural strength, which is, in turn, influenced by the cement content, the total amount of SCMs, and the coarse-to-fine aggregate ratio.

The interaction between the cement content and the amount of aggregates has been discussed in section 6.10, and that between the SCMs content and the amount of aggregates has been discussed in section 6.9. In both cases, a similar conclusion was reached: that the effect of the total amount of aggregates is not markedly modified by either the cement or the SCMs content. However, the analysis presented in 6.3.3 showed that the variables related to the aggregates explain 23% of the total variance of the Z factor and therefore their influence on the residual flexural strength should be substantial. Since the first two summands multiplying G+S in equation (69) have but a minor importance, it follows that the G/S ratio and its interaction with the total aggregate content must have a substantial effect on Z.

This is very clearly observed in the contrast plots shown in Figure 88: the relationships between the average variation of Z and the total aggregate content are clearly sensitive to the coarse-to-fine aggregate ratio. When this ratio is low (as in Figure 88, left), Z is much less sensitive to the total aggregate content than when this ratio is high (as in Figure 88, right). Z values are more dependent on the total amount of aggregates if there is substantially more coarse

aggregate than fine aggregate in the mixture. On the other hand, if the mixture is proportioned with considerably more fine aggregate than coarse aggregate, *Z* values are less sensitive to the amount of aggregate.

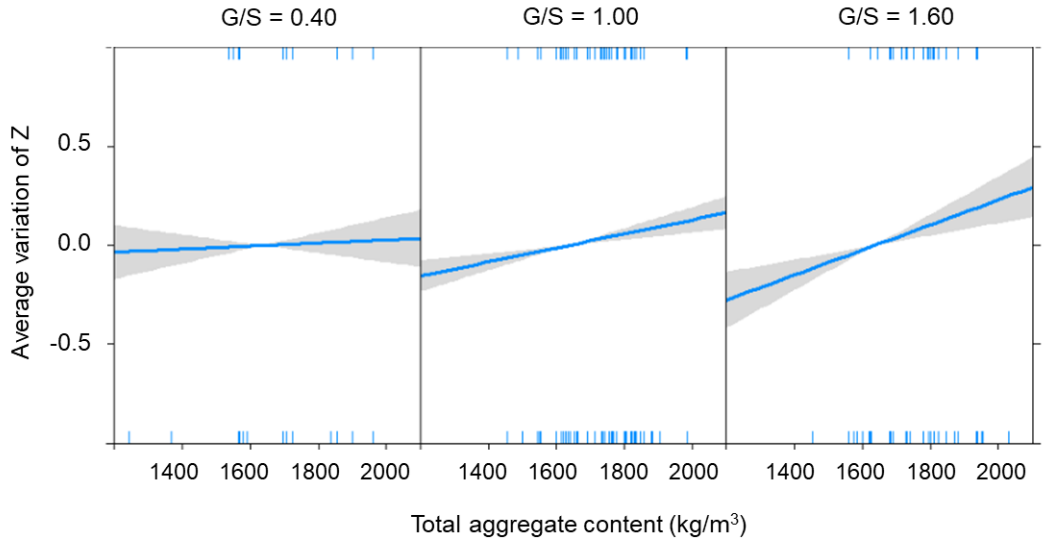

Figure 88. Average change of Z with total aggregates and the G/S ratio.

Two things are, therefore, clear: *i)* there is an important connection between the cohesiveness of the mixture from the proportioning point of view and the flexural performance it can deliver, and *ii)* the model developed in this study does reproduce such connection.

6.11.2 Contour plots. The contour plots of *Z* against the total amount of aggregates and the coarse-to-fine aggregate ratio, for three different fiber volume fractions and assuming median values for the rest of mix design variables, are shown in Figure 89. It can be seen that the combinations of high *G/S* ratios and low amounts of aggregates are associated with the lowest values of the *Z* factor.

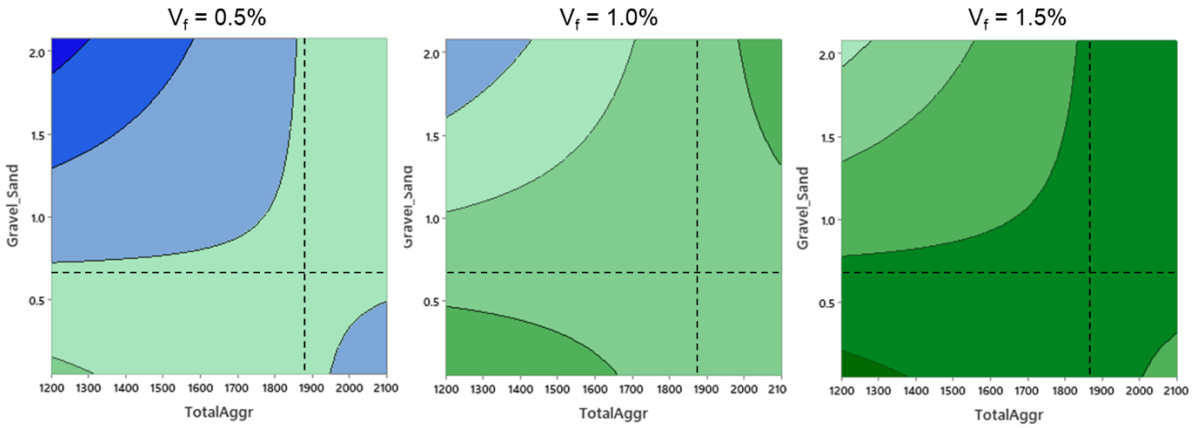

Figure 89. Contour plots of Z vs the total aggregate content and the G/S ratio.

6.11.3 Sensitivity to the G/S ratio. The vertical dashed lines in Figure 89 correspond to the value of the total aggregate content that makes *Z* practically insensitive to variations of the coarse-to-fine aggregate ratio. This value can be obtained by differentiating equation (53) with respect to the *G/S* ratio and equating to zero:

$$\frac{\partial Z}{\partial (G/S)} = k_1 + c_3\,(G+S) = 0 \quad \rightarrow \quad (G+S) = \frac{-k_1}{c_3} \tag{70}$$

Considering the values of the coefficients k_1, c_3 from Table 10, the amount of aggregates from equation (70) is 1888 kg/m^3, and it does not depend on any other mix design variable. This is very close to the values obtained from the equivalent analysis in relation to the residual flexural strength parameters (section 5.9.2), which averaged 1947 kg/m^3.

6.11.4 Sensitivity to the total aggregate content. The horizontal dashed lines in the contour plots in Figure 89 correspond to the value of the *G/S* ratio that make *Z* insensitive to variations of the total aggregate content. This can be determined by differentiating equation (53) with respect to the total aggregate content and equating to zero:

$$\frac{\partial Z}{\partial (G+S)} = c_1 C + c_2 SCM + c_3 \frac{G}{S} = 0 \quad \rightarrow \quad \frac{G}{S} = \frac{-c_1}{c_3}\,C + \frac{-c_2}{c_3}\,SCM \tag{71}$$

Replacing the coefficients c_1, c_2, and c_3 in equation (71) with their corresponding values from Table 10, the following relationship is obtained:

$$\frac{G}{S} = (1.092\,C + 2.18\,SCM) \times 10^{-3} \tag{72}$$

Therefore, the *G/S* ratio that makes *Z* insensitive to variations of the total amount of aggregates is not an invariant but a function of the cement and SCMs contents. The plot of equation (72) is shown in Figure 90.

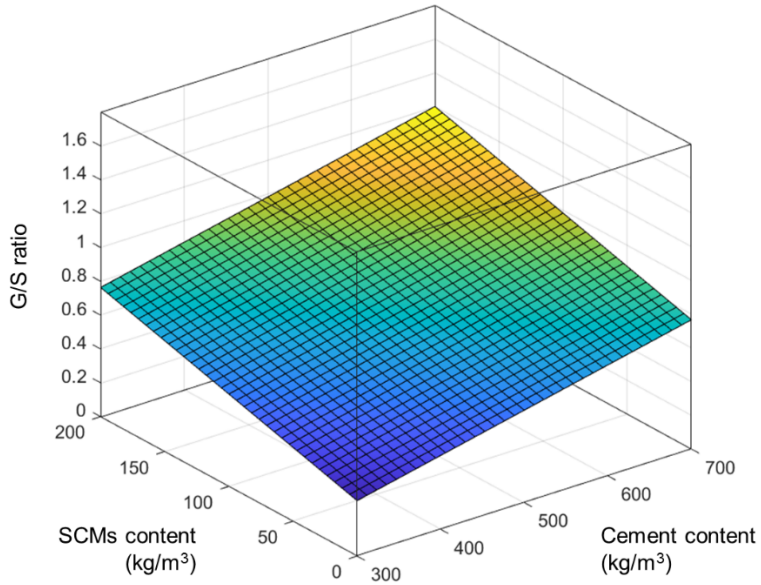

Figure 90. G/S ratio as per equation (72) vs cement content and amount of SCMs.

This is, once again, consistent with the observations made when discussing the effect of these variables in relation to each of the residual flexural strength parameters separately (section 5.9.4). It is yet another indication that the relationship between the amount of aggregates and the residual flexural capacity (represented by the *Z* factor) depends on the interplay of the three main contributors to the cohesiveness of the mixture.

6.11.5 Maximum G/S ratios to optimize flexural performance. Based on the contour plots in Figure 89 and the calculations in the previous two subsections, the values of the total aggregate content and of the *G/S* ratio associated with high values of *Z* can be taken as indicative of the direction in which the *G/S* ratio can be adjusted to optimize the residual flexural capacity of SFRC mixtures.

Mixtures with a total aggregate content not higher than 1888 kg/m^3 represent 92.6% of the cases in the database of SFRC mixtures compiled in this study: the vast majority of cases. In the contour plots in Figure 89, this corresponds to the region to the left of the vertical dashed line, where *Z* values increase when the G/S ratio is reduced. More specifically, when the *G/S* ratio is lower than the value given by equation (72), which is 0.67 if median amounts of cement and SCMs are considered. Therefore, as a general reference, it can be said that *Z* values can be maximized when the amount of coarse aggregate is not higher than 40% of the total aggregate content.

7. Residual flexural strength parameters of Synthetic FRC mixtures and mix design variables

7.1 Introduction

7.1.1 Context and scope of this chapter. This part of the report is concerned with the modeling of the relationships between the residual flexural strength parameters (f_{R1}, f_{R2}, f_{R3}, and f_{R4} as per EN 14651) and the variables describing the synthetic FRC mixtures, including the fiber material. This builds on the analysis and modeling of the relationships between the mix design variables presented in chapter 4.

7.1.2 Dataset of Synthetic FRC mixtures. The data used for the models and analysis discussed in this chapter is the database of Synthetic FRC mixtures, which is described in chapter 3.

7.1.3 Methodological considerations. The approach followed for this analysis is based on multiple linear regression, and the same methodological considerations presented in 5.1.3 are applicable. The two main objectives of the multiple linear regression analysis were to obtain equations that relate each of the residual flexural strength parameters to the mix design variables, and to analyze and discuss these equations to describe general trends and extract knowledge from them.

The fiber material was considered as an additional categorical variable. For consistency, it was decided to adopt the same model specification as in the case of SFRC database, so that the equations to be obtained for the synthetic FRC mixtures has the same structure and differs only in the fitted values of the regression coefficients. Since different synthetic fibers can be expected to interact differently with the mixture constituents, it was assumed that all the coefficients, at least in principle, could vary with the fiber material. To allow for this possibility, the model specification was modified to include the interactions of all variables with the categorical variable representing the fiber material. All were initially included as terms of the model, and only removed when found not to be statistically significant.

As justified in section 5.1.3, the model had to be simple in its specification, and a compromise between its complexity and its accuracy or goodness of fit (R-squared) was sought. This proved more challenging with synthetic FRC mixtures than with SFRC data. The variability of f_{R1}, f_{R2}, f_{R3}, and f_{R4} is exacerbated when fibers of different materials (often different in terms of geometry and surface textures too) are considered. In consequence, it was not realistic to expect the equations for synthetic FRC to be as accurate as those obtained for SFRC mixtures and discussed in chapters 5 and 6.

7.1.4 Discussion focused on PP and PO fibers. Although the model (equations and coefficient values presented in the following section) was fitted to the data consisting of all the cases in the synthetic FRC mixtures database, the discussion and interpretation is limited to FRC mixtures with either polypropylene (PP) or polyolefin (PO) fibers. This is because the model can only be interpreted with some confidence in relation to these two types of fibers, given the information it is based upon. As explained in section 3.1.3 and illustrated in Figure 24, the synthetic FRC dataset included 514 cases of mixtures with PP fibers and 119 cases of mixtures with PO fibers. The regression analysis in this chapter considers 12 variables (including the

categorical variables representing the test/specimen configuration and the fiber material). Since it is generally accepted that the number of cases in a dataset needs to be, at least, 10 times the number of predictive variables in the model[6], the number of data points concerning PVA and other fiber materials was too small for any conclusions to be drawn with confidence.

7.2 Fitted model

7.2.1 Regression analysis and fitted model. A multiple regression analysis was performed on each of the residual flexural strength parameters to relate them to the mix design variables of synthetic FRC. Those terms that were found to have a statistically non-significant effect were removed, until the fitted equations included only statistically significant terms.

The obtained model can be expressed as follows:

$$f_{Ri} = k_0 + k_1\frac{G}{S} + (a_0 + a_1 m)\, l_f + \left(b_0 + b_1 C + b_2 SP + b_3 \lambda_f + b_4 l_f\right) V_f + k_2\, SCM + k_3\, SP + k_6 C + \left(c_1\, C + c_2\, SCM + c_3\frac{G}{S}\right)(G + S) \pm \varepsilon \quad (73)$$

Where:

f_{Ri} represents either f_{R1}, f_{R2}, f_{R3}, or f_{R4}, expressed in MPa.

k_0 is a regression coefficient, which is different for f_{R1}, f_{R2}, f_{R3}, and f_{R4} and groups the intercept and the term that depends on the test/specimen configuration. Its fitted values, given in Table 12, do not depend on the fiber material. This is because the interactions between the fiber material and the test/specimen configuration were not statistically significant.

k_1, k_2,…, a_0, a_1,…, b_0, b_1,…, c_1, c_2, c_3 are the regression coefficients corresponding to the effect of the FRC mix design variables, and are different for f_{R1}, f_{R2}, f_{R3}, and f_{R4}. The values of k_1, a_0, b_0 and b_3 vary with the fiber material, whilst all others do not. Their fitted values are given in Table 13 (PP fibers) and Table 14 (PO fibers).

S and G are the relative amounts of fine and coarse aggregate, respectively, in kg/m^3.

m is the maximum aggregate size, expressed in mm.

C and SCM are the relative amounts of cement and supplementary cementitious materials, respectively, in kg/m^3.

SP is the relative amount of superplasticizer, in kg/m^3.

V_f is the fiber volume fraction, in percentage.

l_f and λ_f are the fiber length (expressed in mm) and the fiber aspect ratio, respectively.

[6] This is known as the 'rule of 10': the volume of data necessary to train a well performing model should be at least 10 times the number of parameters in the model. For more details, see:
Harrel F. et al. (1996) "Multivariable Prognostic Models: Issues in Developing Models, Evaluating Assumptions and Adequacy, and Measuring and Reducing Errors" Statistics in Medicine 15():361-387, https://doi.org/10.1002/(SICI)1097-0258(19960229)15:4%3C361::AID-SIM168%3E3.0.CO;2-4

ε is the error term of the estimation, which is 1.2, 1.3, 1.4, and 1.4 MPa for f_{R1}, f_{R2}, f_{R3}, and f_{R4}, respectively.

Table 12. Fitted coefficient values (PP or PO fibers): k_0.

Test / specimen configuration	**Residual flexural strength parameter**			
	f_{R1}	f_{R2}	f_{R3}	f_{R4}
3-point, notched	0.463	-0.313	0.137	0.249
4-point, unnotched	-0.033	-0.905	-0.257	-0.209

Table 13. Fitted coefficient values (PP fibers).

Coefficient	**Residual flexural strength parameter**			
	f_{R1}	f_{R2}	f_{R3}	f_{R4}
$\mathbf{k_1}$	-2.272	-2.763	-3.322	-3.253
$\mathbf{k_2}$	0.03685	0.03105	0.02346	0.01901
$\mathbf{k_3}$	0.0245	0.0857	0	0
$\mathbf{k_6}$	0.00422	0.00372	0.00535	0.00468
$\mathbf{a_0}$	0.00929	0.0309	0.04459	0.04678
$\mathbf{a_1}$	0.000588	0.000979	0	0
$\mathbf{b_0}$	-0.078	-0.825	-0.425	-0.748
$\mathbf{b_1}$	0.00414	0.01070	0.00954	0.01005
$\mathbf{b_2}$	0	-0.0997	0	0
$\mathbf{b_3}$	0.001263	0.000801	-0.00011	-0.00083
$\mathbf{b_4}$	-0.0161	-0.03726	-0.0398	-0.038
$\mathbf{c_1}$	-0.000004	-0.000004	-0.000005	-0.000005
$\mathbf{c_2}$	-0.000022	-0.000017	-0.000012	-0.00001
$\mathbf{c_3}$	0.001706	0.001603	0.001921	0.001812

In equation (73), the different terms and interactions have been rearranged and grouped together so that the interpretation of the statistically significant interactions is clearly reflected in the way the model is written. Its structure is similar to that of the model developed for SFRC, the main difference being that it does not include the terms $k_4\lambda_f$ and $k_5 m$ because they are not statistically significant. This does not mean that the fiber aspect ratio and the maximum aggregate size are not relevant, because their interactions with the fiber volume fraction and the fiber length have a statistically significant effect on the residual flexural parameters: $a_1 m\, l_f$ and $b_3\lambda_f\, V_f$.

The coefficient corresponding to the intercept, k_0 is the only one term that depends on the test/specimen configuration. Therefore, according to the fitted model, the relative effect that

any of the mix design variables has on the residual flexural strength parameters is independent from, and not significantly affected by the test being 3PBT or 4PBT or by the specimen being notched or unnotched. Interestingly, the interaction between the test/specimen configuration and the fiber material was not statistically significant, and as a result the value of k_0 does not change with the fiber material. As can be seen from the k_0 values in Table 12, the values of the residual flexural strength parameters obtained when testing notched specimens in 3-point bending are, on average, between 0.4 MPa and 0.6 MPa higher than with unnotched specimens in the 4-point bending test.

Table 14. Fitted coefficient values (PO fibers).

Coefficient	Residual flexural strength parameter			
	f_{R1}	f_{R2}	f_{R3}	f_{R4}
$\mathbf{k_1}$	-1.861	-1.367	-1.867	-1.826
$\mathbf{k_2}$	0.03685	0.03105	0.02346	0.01901
$\mathbf{k_3}$	0.0245	0.0857	0	0
$\mathbf{k_6}$	0.00422	0.00372	0.00535	0.00468
$\mathbf{a_0}$	-0.0048	0.0016	0.0195	0.0235
$\mathbf{a_1}$	0.000588	0.000979	0	0
$\mathbf{b_0}$	-1.397	-1.89	-1.04	-1.03
$\mathbf{b_1}$	0.00414	0.01070	0.00954	0.01005
$\mathbf{b_2}$	0	-0.0997	0	0
$\mathbf{b_3}$	0.02216	0.01935	0.00818	0.00363
$\mathbf{b_4}$	-0.0161	-0.03726	-0.0398	-0.038
$\mathbf{c_1}$	-0.000004	-0.000004	-0.000005	-0.000005
$\mathbf{c_2}$	-0.000022	-0.000017	-0.000012	-0.00001
$\mathbf{c_3}$	0.001706	0.001603	0.001921	0.001812

Another interesting observation is that only four of the regression coefficients vary significantly with the fiber material: k_1, a_0, b_0 and b_3, whilst all other coefficients have the same values irrespective of the fibers being PP or PO. Looking at the structure of equation (73), this means that some of the terms are not modified by the fiber material: $k_2\ SCM$, $k_3\ SP$, $k_6 C$, and $(c_1\ C + c_2\ SCM + c_3 G/S)(G + S)$**.** However, this does not imply that different fiber materials do not require adjustments in terms of these variables. The model describes associations, which do not necessarily imply causality. For example, the fact that the effect of the amount of aggregates is not significantly modified by the fiber material could simply be due to the nature of the studies from which the data was compiled. Researchers often devise their experimental programs starting with a mixture that they use as reference to define mixtures with different types of fibers at different dosages making only slight adjustments, keeping the aggregate contents generally unchanged. Furthermore, the variables in the abovementioned terms of equation (73) are not isolated terms in the model, which makes inferential caution even more

important. For instance: the cement content modifies the effect of the fiber volume fraction ($b_1 C\, V_f$), which is in turn influenced by the fiber material ($b_0 V_f$, with b_0 depending on fiber material). With that in mind, it would be incorrect to claim that the fiber material does not modify the effect of the cement content on the residual flexural strength, even though $k_6 C$ does not change with the fiber material.

To summarize: the main conclusion from the above observations is that no conclusions should be rushed in relation to the interactions between the fiber material and the mix design variables.

7.2.2 Goodness of fit. The model shows good accuracy in fitting the values of the residual flexural strength parameters corresponding to the mixtures in the synthetic FRC database. The R-squared values were 84%, 84%, 80% and 76% for f_{R1}, f_{R2}, f_{R3}, and f_{R4}, respectively. In Figure 91, the values estimated by the model for each of the mixtures in the database are plotted against the actual residual flexural strength values, together with the exact equivalence lines for reference.

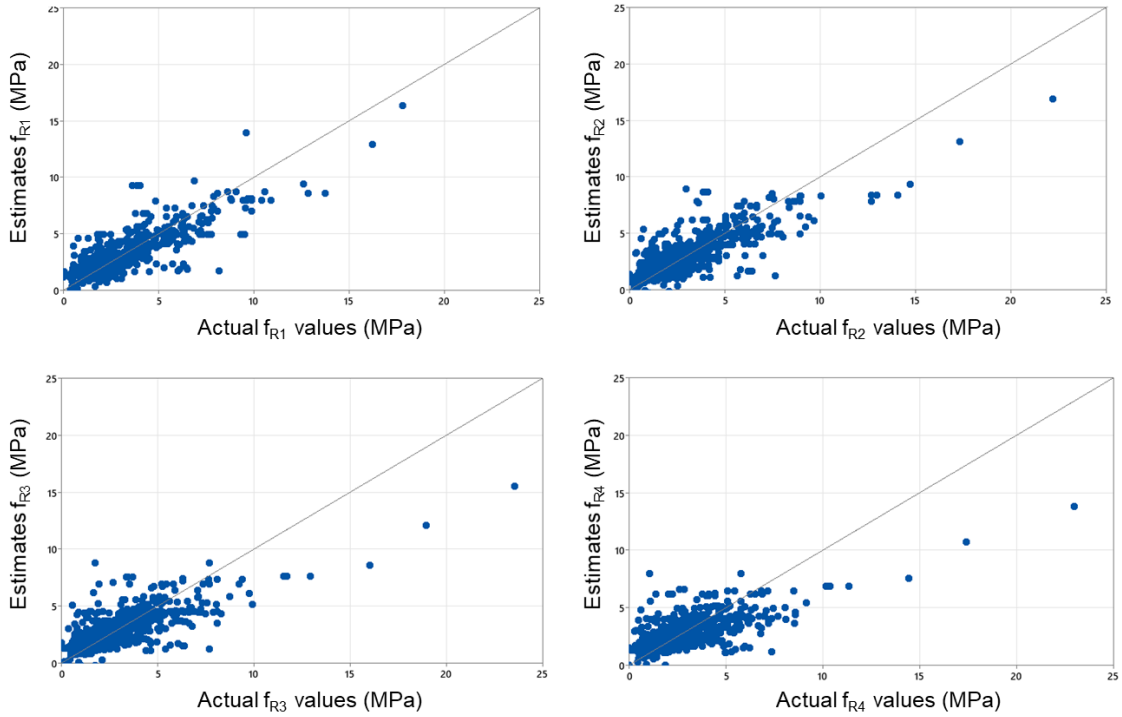

Figure 91. Fitted vs actual residual flexural strength values.

Further scrutiny of the model's performance after segmenting the database by fiber type reveals that the R-squared values and the plots in Figure 91 overstate its accuracy and can be a misleading representation of its predictive capacity. The fact that these R-squared values are remarkably similar to their counterparts for SFRC (section 5.2.2) seems to imply that the accuracy of the model in estimating the residual flexural strength parameters of synthetic FRC mixtures is similar to that of the model developed for SFRC. However, this is not true: the predictive performance of the model for synthetic FRC mixtures is worse than that of its counterpart for SFRC mixtures, as explained in the next subsection.

7.2.3 A note on error and variability. The plots in Figure 91 as well as the R-squared values reported above consider all the mixtures in the synthetic FRC dataset, including also the reference SFRC mixtures (section 3.1). If only the information corresponding to FRC mixtures

with synthetic fibers is considered, the plots of estimates vs actual values in Figure 92 are obtained (note that the scale is different to that of the plots in Figure 91). These plots show that there is significantly more scatter than in the case of SFRC database (section 5.2.2). The model does not perform so well on synthetic FRC mixtures as the R-squared values seem to imply.

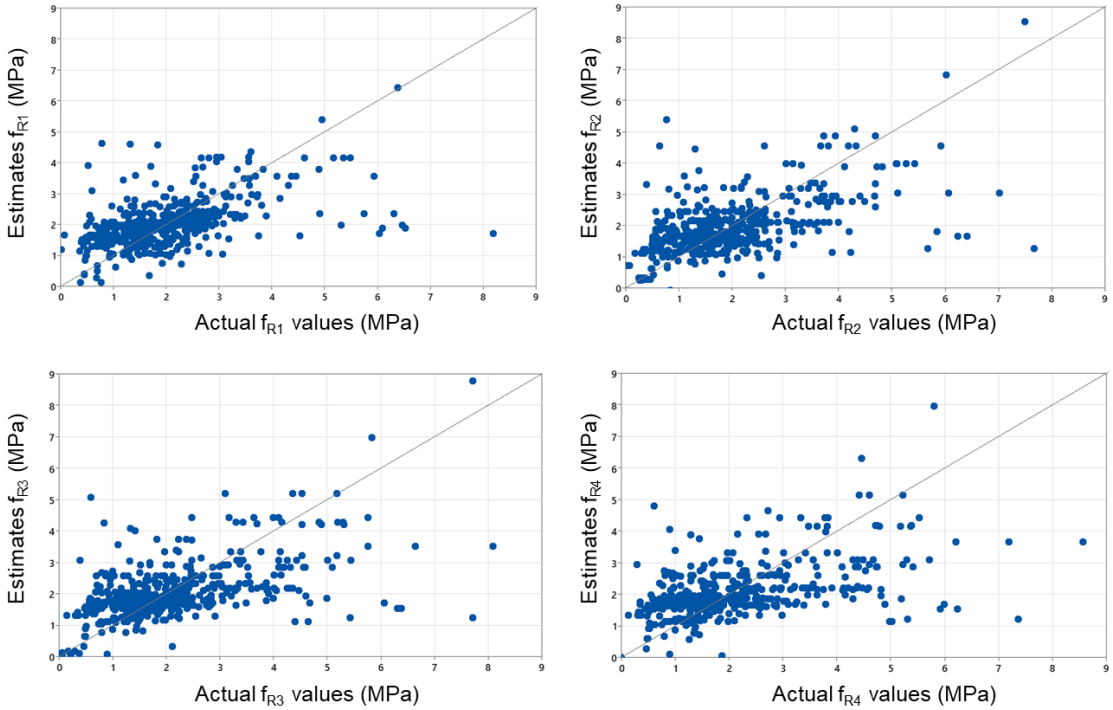

Figure 92. Fitted vs actual residual flexural strength values (only synthetic FRC cases).

A more representative assessment of the model's goodness of fit, considering only the FRC mixtures with synthetic fibers, can be obtained by calculating the root of the mean squared error (RMSE) and the mean absolute error (MAE). Both RMSE and MAE are measurements of the average difference between actual values and their estimates, but there is growing consensus in favor of the MAE over the RMSE[7]. These values are shown in Table 15.

Table 15. Representative measures of prediction errors.

	Residual flexural strength parameter			
	fR1	***fR2***	***fR3***	***fR4***
Median (MPa)	1.94	1.68	1.68	1.64
RMSE (MPa)	0.92	0.98	1.06	1.11
RMSE/median	47.6%	58.4%	62.8%	67.7%
MAE (MPa)	0.63	0.67	0.73	0.77
MAE/median	32.6%	40.1%	43.3%	47.1%

The ratios between either the RMSE or the MAE to the median of the corresponding residual flexural strength parameter, expressed in percentage, are particularly illustrative as they are

[7] For a succinct and accessible overview of the differences between both parameters, see:
Willmott, C. and Matsuura, K. (2005), "Advantages of the Mean Absolute Error (MAE) over the Root Mean Square Error (RMSE) in assessing average model performance", Climate Research, 30, 79–82.

analogous to the coefficient of variation, so commonly referred to in concrete technology. The values in Table 15 clearly show that there is considerable variability in the differences between the estimates as per equation (73) and the actual values of the residual flexural strength parameters. Efforts were made to improve the goodness of fit by considering alternative specifications of the model, but no significantly better alternatives were found.

This does not mean that the model is not valid: it is, but any estimate is essentially an average or mathematical expectation, and the variability or error associated with an estimate is what it is. This section is an honest effort to try and very clearly expose the limitations of the model as a note of caution. It is a valuable tool to describe and interpret the trends followed by the residual flexural strength parameters with respect to the variables describing synthetic FRC mixtures, and to gain knowledge about the material. However, even though it can be used to obtain preliminary estimates, these need to be considered within a wide margin of error and cannot be used as predictions.

7.2.4 Interpretation and discussion of the terms in the model. The sections that follow are concerned with the interpretation of the trends followed by the residual flexural strength parameters as modelled by equation (73) with respect to the mix design variables identified as statistically significant. This is done mostly through contour plots, focusing on mixtures with either PP or PO fibers.

7.3 Effect of fiber length and fiber content

7.3.1 Contour plots (PP fibers). Figure 93 shows the contour plots obtained by plotting the response surfaces corresponding to f_{R1}, f_{R2}, f_{R3} and f_{R4} as per equation (73) against the fiber length and the fiber volume fraction, assuming median values for the rest of mix design variables. In general, increasing the fiber length is associated with higher values of the residual flexural strength parameters. The relative effect of the fiber length on the residual flexural strength parameters is more important the lower the fiber content is.

7.3.2 Sensitivity to fiber length (PP fibers). In mixtures with high dosages of PP fibers, the relative influence of the fiber length becomes less important, up to a certain volume fraction that makes the residual flexural strength parameters insensitive to the fiber length. This value of the fiber volume fraction is represented by dashed lines in Figure 93, and can be determined by differentiating equation (73) with respect to the fiber length and equating to zero:

$$\frac{\partial f_{Ri}}{\partial l_f} = a_0 + a_1 m + b_4 V_f = 0 \quad \rightarrow \quad V_f = \frac{-a_0 - a_1 m}{b_4} \tag{74}$$

By replacing the coefficients a_0, a_1, and b_4 with their corresponding values from Table 13, and assuming the median value of the maximum aggregate size, the fiber contents obtained from equation (74) are 1.16%, 1.25%, 1.12%, and 1.23% in relation to f_{R1}, f_{R2}, f_{R3} and f_{R4}, respectively. The first two values do not vary much with the maximum aggregate size (1.02%-1.31% and 1.14%-1.36% if m is varied between 12 mm and 20 mm), and the last two values are invariant, since a_1=0 for f_{R3} and f_{R4}. All these values are therefore quite similar and 1.2% can be taken as representative of them all, and it can be concluded that the residual flexural strength parameters are insensitive to the fiber length when the volume fraction of PP fibers is 1.2%. This is, however, a very high volume fraction for this fiber material: the median is 0.5%

and, in 95% of the PP FRC mixtures in the database, the fiber volume fraction is lower than 1.35%. In most of the cases, therefore, FRC mixtures with PP fibers are situated to the left of the dashed lines in Figure 93, and the conclusion is that, in most of the cases, increasing the fiber length is associated with an overall improvement of the residual flexural strength parameters.

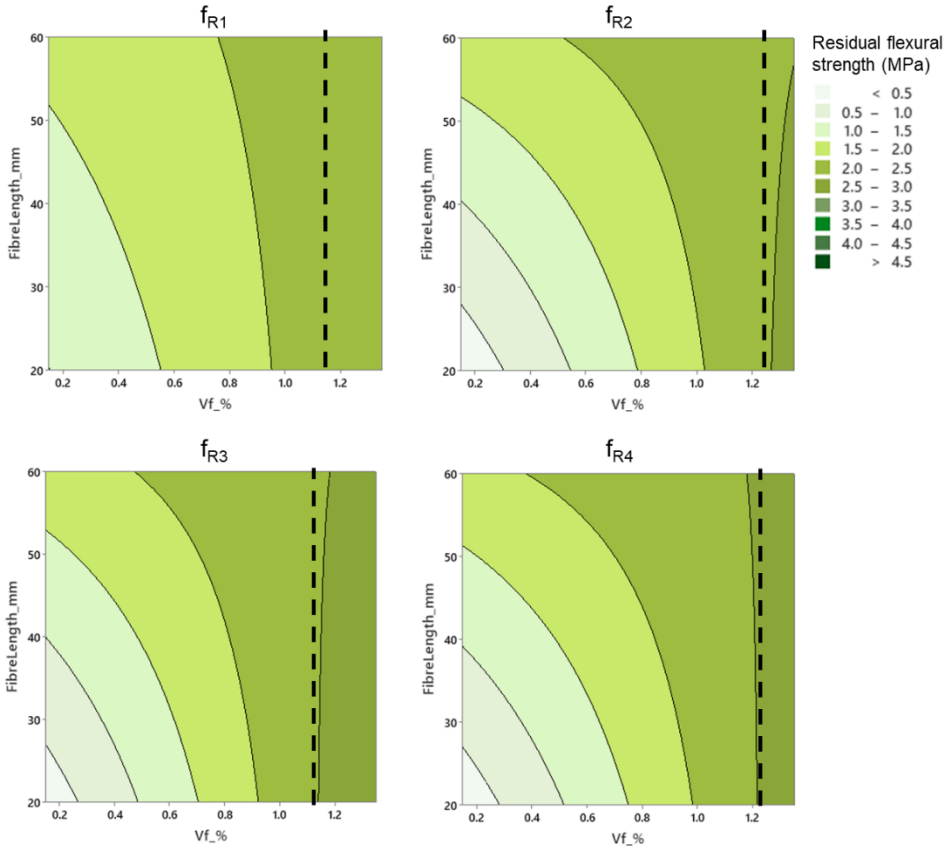

Figure 93. Residual flexural strength against fiber length and fiber content (PP fibers).

7.3.3 How important is the length of PP fibers? The contour plots in Figure 93 show that, particularly in the case of f_{R2}, f_{R3} and f_{R4}, the positive effect of the fiber length is quite relevant when low and moderate fiber contents are considered. The relative effect of the fiber length can be evaluated in comparison with the effect of fiber content by using some representative values. To this effect, the expected variation of the residual flexural strength parameters associated with a 10-mm increase of the fiber length can be compared to the expected variations associated with $\Delta V_f = +0.1\%$.

The expected variation of any of the residual flexural strength parameters resulting from a 0.1% increase of the fiber volume fraction can be determined as follows:

$$E\left(\Delta f_{Ri} | \Delta V_f = +0.1\%\right) = \frac{\partial f_{Ri}}{\partial V_f} \times \Delta V_f = \left(b_0 + b_1 C + b_2 SP + b_3 \lambda_f + b_4 l_f\right) \times 0.1 \qquad (75)$$

Assuming median values for the cement and superplasticizer contents, the aspect ratio and length of PP fibers, and replacing the coefficients b_0, b_1, b_2, b_3, and b_4 in equation (75) with the corresponding values from Table 13, the expected variations obtained are 0.07 MPa, 0.11 MPa, 0.11 MPa, and 0.10 MPa for f_{R1}, f_{R2}, f_{R3} and f_{R4}, respectively. The average of these four values, 0.10 MPa, can be retained as representative for comparative purposes.

The expected variations resulting from a 10 mm increase of the fiber length, on the other hand, can be determined as follows:

$$E\left(\Delta f_{Ri} | \Delta l_f = +10mm\right) = \frac{\partial f_{Ri}}{\partial l_f} \times \Delta l_f = \left(a_0 + a_1 m + b_4 V_f\right) \times 10 \tag{76}$$

Assuming median values for the maximum aggregate size and the fiber volume fraction, and replacing the coefficients a_0, a_1, and b_4 in equation (76) with their values from Table 13, the expected variations obtained are 0.11 MPa, 0.28 MPa, 0.25 MPa, and 0.28 MPa for f_{R1}, f_{R2}, f_{R3} and f_{R4}, respectively. Their average is 0.23 MPa.

Based on the above calculations, the expected variation of the residual flexural strength parameters when the fiber length is increased in 10 mm is not only comparable to, but higher than that which corresponds to the fiber volume fraction being increased in 0.1%. In conclusion, in FRC mixtures with PP fibers, the positive effect of the fiber length on the residual flexural strength is as important as the effect of the fiber content.

7.3.4 Contour plots (PO fibers). When FRC mixtures with PO fibers are considered, the trends followed by the residual flexural strength parameters with respect to the fiber length are different from those observed for mixtures with PP fibers. The contour plots obtained by plotting the response surfaces corresponding to f_{R1}, f_{R2}, f_{R3} and f_{R4} as per equation (73) against the fiber length and the fiber volume fraction are shown in Figure 94.

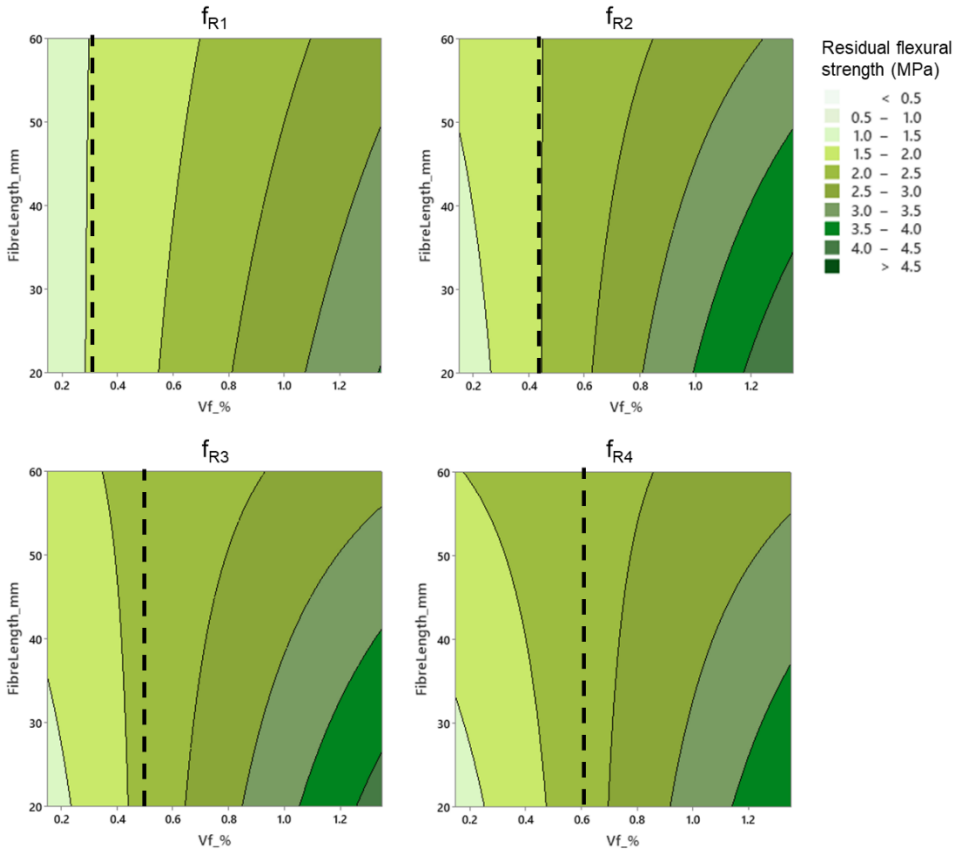

Figure 94. Residual flexural strength against fiber length and fiber content (PO fibers).

When interpreting the trends in Figure 94, it is important to bear in mind that the median fiber volume fraction of all the synthetic FRC mixtures is 0.5%, and 0.62% if only FRC mixtures with PO fibers are considered (see section 3.5). The contour plots show that, when PO fibers

are used in relatively low dosages, increasing the fiber length is associated with slight improvements of the residual flexural strength. On the other hand, if PO fibers are used in moderate to high dosages, shorter fiber lengths are associated with higher values of the residual flexural strength parameters.

7.3.5 Sensitivity to fiber length (PO fibers). What the phrases 'relatively low' or 'moderate to high' dosages actually mean can be calculated. FRC mixtures with contents of PO fibers around a certain value (approx. 0.3-0.6% according to Figure 94) are practically insensitive to variations in the fiber length, as far as the residual flexural strength values are concerned. Such threshold V_f value can be estimated by replacing the coefficients a_0, a_1, and b_4 in equation (74) with their corresponding values from Table 14. Assuming the median of the maximum aggregate size, the values obtained are 0.28%, 0.46%, 0.49%, and 0.62% in the case of f_{R1}, f_{R2}, f_{R3} and f_{R4}, respectively. These are represented with vertical dashed lines in Figure 94. The first two values vary with the maximum aggregate size (0.14%-0.43% and 0.36%-0.57% if m is varied between 12 mm and 20 mm), while the last two are invariant, since a_1=0 for f_{R3} and f_{R4}. Their average (i.e., 0.46%), or even the median fiber dosage (i.e., 0.62%), seem like an adequate representative 'threshold' value in relation to all the different residual flexural strength parameters.

In consequence, it can be said that the residual flexural strength parameters of FRC mixtures with PO fibers are insensitive to the fiber length when the fiber dosage is in the region of 0.5% in volume. This is markedly lower than the corresponding value obtained for mixtures with PP fibers (i.e., 1.2%, section 7.3.2). In fact, bearing in mind that 75% of the mixtures with PO fibers in the dataset have PO fiber contents between 0.41% and 0.75% (section 3.5.1), the conclusion is that, in general, the residual flexural strength parameters are only slightly sensitive to the length of PO fibers. It turns out that, when put in context, the trends shown in Figures 93 and 94 are not so different after all.

7.3.6 How important is the length of PO fibers? The same rationale followed in section 7.3.3 can be applied to assess how the effect of the length of PO fibers on f_{R1}, f_{R2}, f_{R3} and f_{R4} compares to that of the fiber content.

The expected variations of f_{R1}, f_{R2}, f_{R3} and f_{R4} resulting from a 0.1% increase of the fiber volume fraction, considering FRC mixtures with PO fibers, can be determined by replacing the coefficients b_0, b_1, b_2, b_3, and b_4 in equation (75) with the corresponding values from Table 14, and assuming median values for the cement and superplasticizer contents. The expected variations obtained are: 0.08 MPa, 0.12 MPa, 0.10 MPa, and 0.10 MPa for f_{R1}, f_{R2}, f_{R3} and f_{R4}, respectively. Their average, 0.10 MPa, can be taken as representative for comparative purposes.

On the other hand, the expected variations resulting from increasing the length of PO fibers by 10 mm can be determined by replacing the coefficients a_0, a_1, and b_4 in equation (76) with their values from Table 14, and assuming median values for the maximum aggregate size and the fiber volume fraction. The values obtained for the expected variations are 0.034 MPa, 0.014 MPa, 0.004 MPa, and -0.045 MPa, for f_{R1}, f_{R2}, f_{R3} and f_{R4}, respectively. For comparison purposes, their average can be considered: 0.0017 MPa.

The above calculations show that, in FRC mixtures with PO fibers, increasing the fiber volume fraction in 0.1% leads to an average increase of the residual flexural strength parameters that is almost 60 times higher than that resulting from the fiber length being increased in 10 mm.

That is to say, the effect of fiber length on f_{R1}, f_{R2}, f_{R3} and f_{R4} in FRC mixtures with PO fibers is clearly less important in magnitude than the effect of the fiber content. This conclusion is not in contradiction with what the contour plots in Figure 94 show, but rather, it results from their contextualized interpretation.

7.3.7 Comparison between PP and PO fibers. In FRC mixtures with either PP or PO fibers, higher fiber contents are associated with higher values of the residual flexural strength parameters. In average, an increase of $\Delta V_f = +0.1\%$ is associated with a similar increase in residual flexural strength for both fiber materials ($\Delta f_{Ri} \cong +0.10$ MPa). The relative effect of the fiber length on the residual flexural strength parameters, on the other hand, depends on the fiber content and is not the same for PP and PO fibers. When the usual ranges of fiber dosages are considered, longer PP fibers are clearly associated with better residual flexural strength, whilst the fiber length has a very minor effect in FRC mixtures with PO fibers.

7.4 Effect of fiber aspect ratio and fiber content

7.4.1 Comparison between PP and PO fibers. One of the main conclusions of the previous section is that the effect of the fiber length on the residual flexural strength parameters is relatively important in FRC mixtures with PP fibers but not in FRC mixtures with PO fibers. It turns out that, when it comes to the aspect ratio, it is the other way around.

There is only one term in the model as defined by equation (73) that includes the fiber aspect ratio, and that is: $b_3 \lambda_f V_f$. Therefore, a very quick comparison between the effect of the aspect ratio in mixtures with PP fibers and in mixtures with PO fibers can be made by comparing the values of coefficient b_3 from Tables 13 and 14: they have a different order of magnitude, the values of b_3 in Table 13 (PP fibers) are much smaller than those in Table 14 (PO fibers).

7.4.2 Contour plots (PP fibers). Figure 95 shows the contour plots corresponding to f_{R1}, f_{R2}, f_{R3} and f_{R4} as per equation (73) against the aspect ratio and volume fraction of fibers, assuming median values for the other mix design variables. Consistently with the observations made above, the variations of the residual flexural strength parameters observed in these contour plots are mostly associated to variations in the fiber content, whilst the fiber aspect ratio has a very minor effect: the gradient is almost parallel to the V_f axis.

7.4.3 How important is the aspect ratio of PP fibers? As explained in the previous paragraph in relation to the contour plots in Figure 95, the effect of the fiber aspect ratio on the residual flexural strength parameters when FRC mixtures with PP fibers are considered is almost negligible. It is so obvious from the contour plots that it is not necessary to quantify the magnitude of such effect and/or compare it to that of the fiber volume fraction.

7.4.4 Contour plots (PO fibers). The contour plots corresponding to f_{R1}, f_{R2}, f_{R3} and f_{R4} as modelled by equation (73) against the fiber aspect ratio and content of PO fibers are shown in Figure 96, where the rest of mix design parameters have been assumed at their median values. With PO fibers, increasing the fiber aspect ratio is markedly associated with higher values of f_{R1} and f_{R2}, and the effect of this variable seems comparable in magnitude to that of the fiber content. In relation to f_{R3} and f_{R4}, the same trend is observed but the relative importance of the fiber aspect ratio is more modest, particularly when f_{R4} is considered.

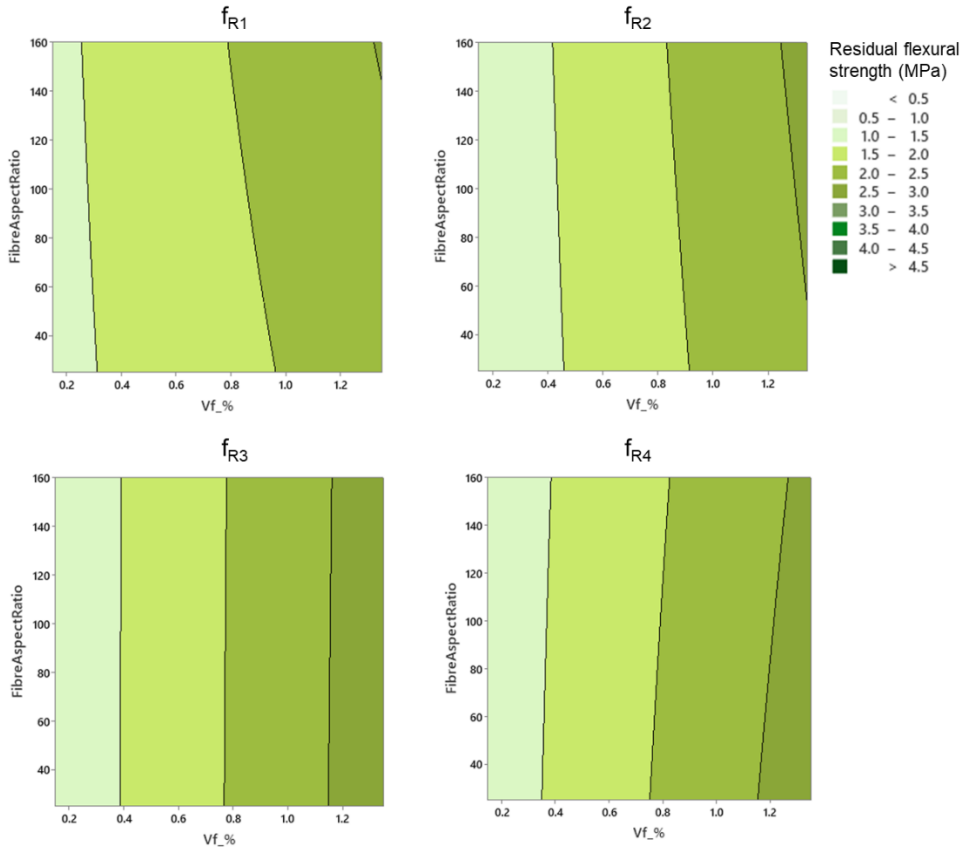

Figure 95. Residual flexural strength against fiber aspect ratio and fiber content (PP fibers).

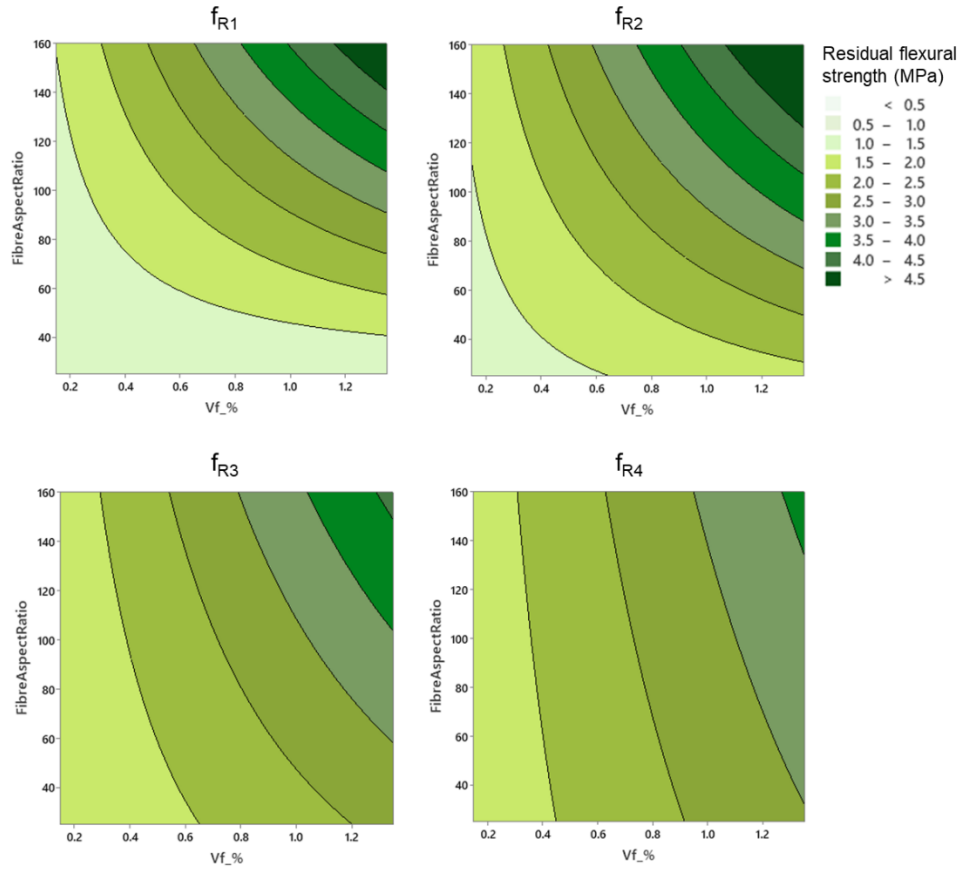

Figure 96. Residual flexural strength against fiber aspect ratio and fiber content (PO fibers).

7.4.5 How 'important' is the aspect ratio of PO fibers? An assessment of the relative importance of the effect of the fiber aspect ratio on f_{R1}, f_{R2}, f_{R3} and f_{R4} in FRC mixtures with PO fibers can be made by comparing it to the effect of increasing the fiber volume fraction in 0.1%. As per section 7.3.6, the expected variation of any of the residual flexural strength parameters when the fiber volume fraction is increased in 0.1% is, on average, 0.10 MPa.

The expected variations resulting from increasing the fiber aspect ratio in 10 units can be determined as follows:

$$E\left(\Delta f_{Ri} | \Delta\lambda_f = +10\right) = \frac{\partial f_{Ri}}{\partial \lambda_f} \times \Delta\lambda_f = \left(b_3 V_f\right) \times 10 \tag{77}$$

Assuming the median value for the fiber volume fraction when PO fibers are used (V_f = 0.62%) and replacing the coefficient b_3 in equation (77) with the corresponding values from Table 14, the expected variations obtained are 0.14 MPa, 0.12 MPa, 0.05 MPa, and 0.03 MPa for f_{R1}, f_{R2}, f_{R3} and f_{R4}, respectively. The expected variations of f_{R1} and f_{R2} are therefore quite similar, their average being 0.13 MPa, but the expected variations of f_{R3} and f_{R4} are considerably lower, their average being 0.04 MPa. When these values are compared to the expected variation of +0.10 MPa associated with an $\Delta V_f = +0.1\%$, it can be concluded that the effect that increasing the aspect ratio has on f_{R1} and f_{R2} is comparable, in terms of magnitude, to that of increasing the fiber content. It is, however, less important as far as f_{R3} and f_{R4} are concerned.

7.5 Interaction between fiber length and maximum aggregate size

In the model developed for the residual flexural strength parameters of synthetic FRC mixtures with PP or PO fibers (equation 73), the variable that represents the maximum aggregate size only appears in the term that describes its interaction with the fiber length: $a_1 m\, l_f$. This means that the maximum aggregate size influences the residual flexural strength parameters by modifying the effect of the fiber length. And that is only true in relation to f_{R1} and f_{R2}, as this interaction does not have a statistically significant effect on f_{R3} and f_{R4} (a_1 is zero for f_{R3} and f_{R4} in Tables 13-14).

Figures 97 and 98 show the contour plots f_{R1} and f_{R2}, considering PP and PO fibers, respectively. These plots, however, can be easily misinterpreted.

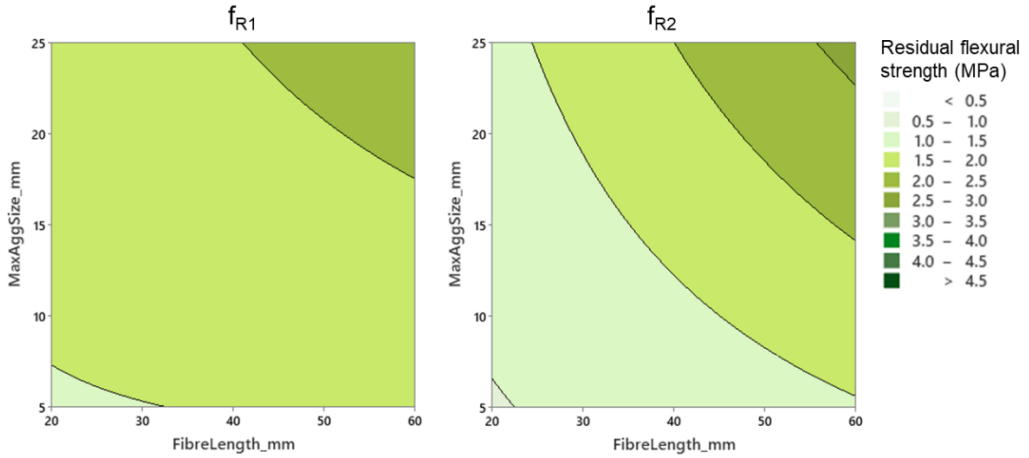

Figure 97. Contour plots for f_{R1}, f_{R2} vs fiber length and maximum aggregate size (PP fibers).

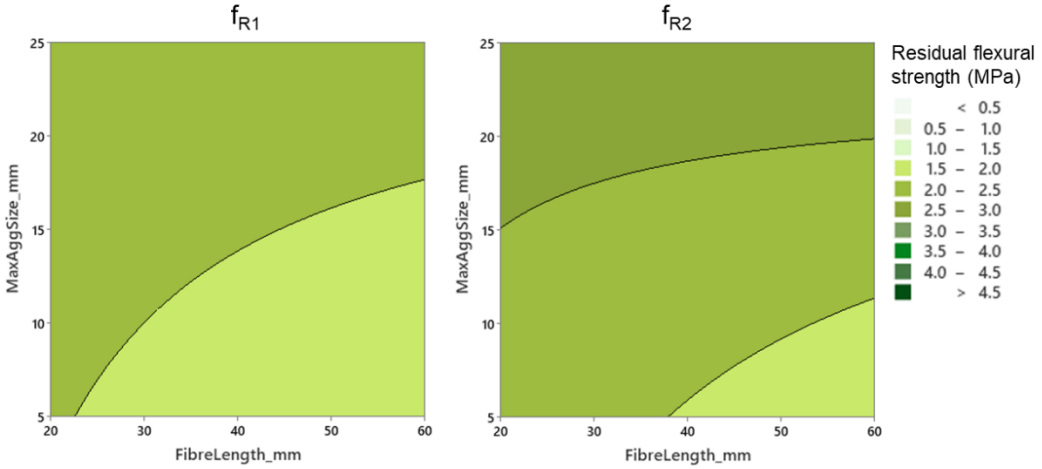

Figure 98. Contour plots for f_{R1}, f_{R2} vs fiber length and maximum aggregate size (PO fibers).

The fact that the contour plots in Figure 97 (PP fibers) look different to those shown in Figure 98 (PO fibers) does not mean that the interaction between the maximum aggregate size and the fiber length changes with the fiber material. In fact, the values of the coefficient in equation (73) associated to this interaction, a_1, is the same irrespective of the fiber material (Tables 13-14). The reason why Figures 97 and 98 look different is the fact that the relationships between the fiber length and the residual flexural strength parameters do change with the fiber material: the value of the coefficient a_0 in equation (73) is different for PP and PO fibers. In synthetic FRC mixtures with either PP or PO fibers, the maximum aggregate size only has an effect on f_{R1} and f_{R2}, which is codependent with the fiber length but not the fiber material.

7.6 Effect of the superplasticizer content

According to the model fitted to the data in the synthetic FRC mixtures database compiled for this study, given in equation (73), the effect of the superplasticizer content on the residual flexural strength parameters is described by the terms $b_2 SP\ V_f + k_3 SP$.

The values of coefficients b_2 and k_3 are the same in Tables 13 and 14 because the interactions between these terms and the fiber material were statistically non-significant. What this means is that the effect of the superplasticizer content on the residual flexural strength parameters is not influenced by the fibers being PP or PO. In previous sections, trends have been discussed in relation to contour plots which were different depending on the fiber material, but this is not applicable in relation to the superplasticizer content.

Furthermore, both b_2 and k_3 are zero when the residual flexural parameter considered is f_{R3} or f_{R4}. This means that changes in the superplasticizer content are not associated with variations in either f_{R3} or f_{R4}. In consequence, only f_{R1} and f_{R2} are sensitive to changes of the superplasticizer content. However, the interaction between the superplasticizer content and the fiber volume fraction described by the term $b_2 SP\ V_f$ is only significant in relation to f_{R2}, because b_2 is zero for f_{R1}, f_{R3}, and f_{R4}.

Therefore:

- In relation to f_{R1}, the effect of the superplasticizer content is statistically significant but not influenced by the fiber volume fraction or any other variable.

- In relation to f_{R2}, the effect of the superplasticizer is co-dependent on the fiber content.
- The superplasticizer content does not have a statistically significant effect on f_{R3} or f_{R4}.

Figure 99 shows the expected variation of f_{R1} as a function of the superplasticizer content as described by the term $k_3 SP$ in equation (73). Higher superplasticizer contents are associated with higher f_{R1} values, and the dosage of 10 kg/m^3 of superplasticizer is associated with f_{R1} increasing by 0.25 MPa on average. However, bearing in mind that the median superplasticizer content in the synthetic FRC database is 2.4 kg/m^3, and that almost 40% of those mixtures do not incorporate superplasticizer, considering a smaller amount of superplasticizer (the median, for example) would be more representative. The expected variation of f_{R1} associated with the addition of 2.4 kg/m^3 of superplasticizer is 0.06 MPa. This is comparable to the expected variation of f_{R1} associated with the fiber volume fraction being increased by 0.1%, which is, on average, 0.07-0.08 MPa if the values calculated in previous sections for PP and PO fibers are considered.

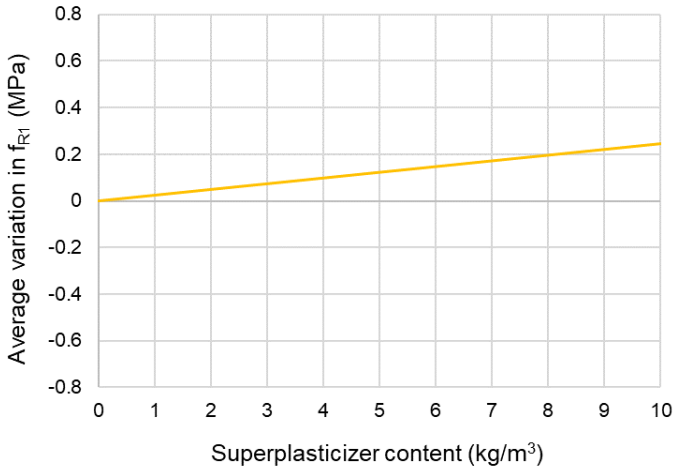

Figure 99. Average effect of the superplasticizer content on f_{R1}.

The plot in Figure 100 shows the expected variation of f_{R2} against the superplasticizer content as given by the terms $b_2 SP\ V_f + k_3 SP$ in equation (73). Three different fiber contents (0.2%, 0.6% and 1.0%) have been assumed, the range being wide enough to be representative of FRC mixtures with either PP or PO fibers.

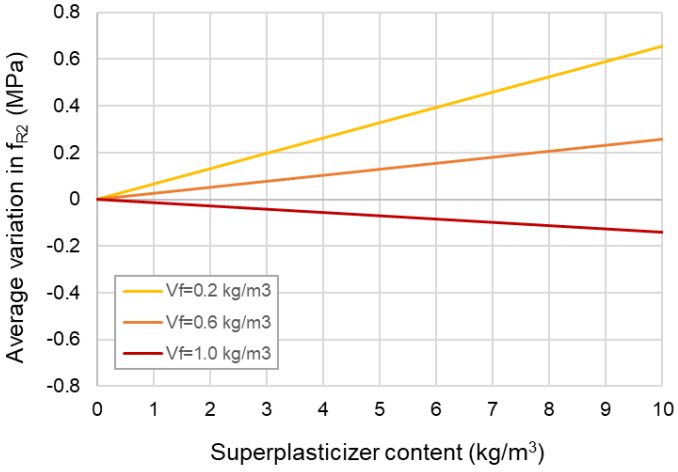

Figure 100. Effect of the superplasticizer content on f_{R2} for different fiber contents.

The effect of the superplasticizer content on f_{R2} becomes more important when low values are assumed for the amount of PP or PO fibers. Bearing in mind that the median fiber volume fraction is 0.5% or 0.62%, for PP or PO fibers respectively, the line corresponding V_f = 0.6% in the plot can be taken as representative of the average trend. The expected variation of f_{R2} associated with adding 2.4 kg/m^3 of superplasticizer to a synthetic FRC mixture with 0.6% of fibers is 0.062 MPa, which is similar to the representative value obtained in relation to f_{R1} in the previous paragraph. Therefore, it can be said that, on average, the effect that incorporating 2.4 kg/m^3 of superplasticizer has on f_{R1} and f_{R2} is not minor, as it is comparable to the effect of increasing the fiber volume fraction by 0.1%.

However, Figure 100 shows that high superplasticizer contents can be associated with a slight reduction of f_{R2} when the volume fraction of PP or PO fibers is higher than a certain value. This can be estimated by differentiating equation (73) with respect to the fiber volume fraction and equating to zero:

$$\frac{\partial f_{R2}}{\partial SP} = k_3 + b_2 V_f = 0 \quad \rightarrow \quad V_f = \frac{-k_3}{b_2} \tag{78}$$

Replacing the coefficients b_2 and k_3 in the equation above with their values from Tables 13-14 yields a fiber volume fraction of 0.86%. This can be interpreted as meaning that increasing the superplasticizer content is not necessarily advantageous when mixtures with relatively high contents of PP or PO fibers are considered. This is likely to be related to the difficulties of achieving homogeneity in the dispersion of PP or PO fibers in those cases.

7.7 Interaction between cement content and fiber content

7.7.1 Fiber material and interactions. The effect of the cement content on the residual flexural strength parameters in equation (73) is described by the following terms: $b_1 C\, V_f + k_6 C + c_1 C\, (G + S)$. All the coefficients in these terms (b_1, k_6 and c_1) have the same values in Tables 13 and 14 because the interactions between these terms and the variable 'fiber material' were found to be statistically non-significant. Therefore, the relationships between the cement content in synthetic FRC mixtures with PP or PO fibers and their residual flexural strength parameters are not affected by the fiber material. This is the reason why only the plots corresponding to mixtures with PP fibers are presented and discussed in this section (analogous trends are observed if PO fibers are considered instead).

It is important to note that the terms describing the effect of the cement content in equation (73) include the interaction between this variable and the fiber volume fraction: $b_1 C\, V_f$. What this means is that the effect of the cement content on f_{R1}, f_{R2}, f_{R3}, and f_{R4} depends on the fiber volume fraction. This section is concerned with understanding the effect of the cement content through its interaction with the amount of fibers.

7.7.2 Contour plots (PP fibers). The contour plots representing the response surfaces corresponding to f_{R1}, f_{R2}, f_{R3} and f_{R4} against the cement content and the fiber volume fraction, according to the model given by equation (73), are shown in Figure 101. These contour plots assume the median for the other mix design variables. The residual flexural strength parameters are mostly insensitive to the cement content when the fiber content is not high (i.e., not higher than approximately 0.4%, reading from the plots). This is particularly clear in relation to f_{R2},

f_{R3} and f_{R4}. However, in mixtures with fiber contents on the higher end of the range, increasing the cement content does have a positive effect on the residual flexural strength parameters. It is apparent that, when the cement content and the fiber content are both higher than certain values, high cement contents are associated with increasing values of the residual flexural strength parameters.

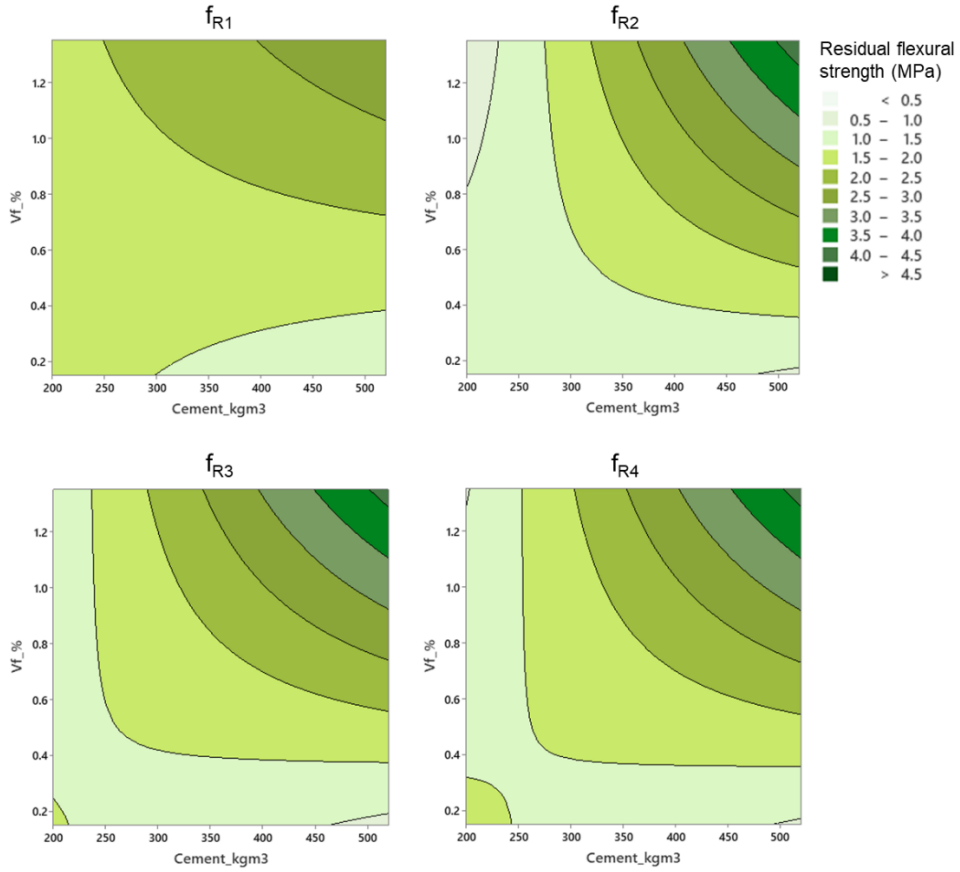

Figure 101. Residual flexural strength vs cement content and fiber volume fraction.

7.7.3 Sensitivity to the cement content. The volume fraction of PP or PO fibers that makes the residual flexural strength parameters of synthetic FRC mixtures insensitive to variations of the cement content can be determined by differentiating equation (73) with respect to the cement content and equating to zero:

$$\frac{\partial f_{Ri}}{\partial C} = b_1 V_f + k_6 + c_1(G+S) = 0 \quad \rightarrow \quad V_f = \frac{-k_6}{b_1} + \frac{-c_1}{b_1}(G+S) \tag{79}$$

If the median of the total aggregate content is assumed (G+S = 1721 kg/m^3) and the coefficients b_1, c_1, and k_6 in equation (79) are replaced with their values from Tables 13-14, the fiber volume fraction obtained is 0.64%, 0.29%, 0.34%, and 0.39%, in relation to f_{R1}, f_{R2}, f_{R3} and f_{R4}, respectively. The V_f values obtained in relation to f_{R2}, f_{R3} and f_{R4} are quite similar, and their average, 0.34%, can be considered as representative of the three. The V_f value obtained in relation to f_{R1} is, however, higher. It can be concluded that, if the fiber volume fraction is 0.34%, f_{R1} can vary slightly depending on the cement content, but f_{R2}, f_{R3} and f_{R4} are unaffected. If the fiber volume fraction is 0.64%, increasing the cement content does not affect f_{R1} but is associated with higher values of f_{R2}, f_{R3} and f_{R4}.

Although the 'threshold' V_f value obtained in relation to f_{R1} is higher than the other three, the average of the four values (0.42%) can still be taken as representative to produce a general statement that is applicable to all four residual flexural strength parameters. The conclusion would then be that the cement content does not significantly influence the residual flexural strength when the volume fraction of PP or PO fibers is 0.42%.

7.7.4 Sensitivity to the fiber content. The contour plots in Figure 101 also show that there is a certain value of the cement content that makes the residual flexural strength parameters, particularly f_{R2}, f_{R3} and f_{R4}, insensitive to the fiber content. This can be obtained by differentiating equation (73) with respect to V_f:

$$\frac{\partial f_{Ri}}{\partial V_f} = b_0 + b_1 C + b_2 SP + b_3 \lambda_f + b_4 l_f = 0 \quad \rightarrow \quad C = \frac{-b_0}{b_1} + \frac{-b_2}{b_1} SP + \frac{-b_3}{b_1} \lambda_f + \frac{-b_4}{b_1} l_f \qquad (80)$$

Such value of the cement content can be calculated by replacing the coefficients b_0, b_1, b_2, b_3 and b_4 in equation (80) with their corresponding values from Table 13 (or 14) and assuming the median values for the superplasticizer content, fiber aspect ratio and fiber length (which are different depending on the fibers being PP or PO). The values obtained are: 262 kg/m^3 (247 kg/m^3), 246 kg/m^3 (252 kg/m^3), and 261 kg/m^3 (260 kg/m^3) in relation to f_{R2}, f_{R3}, and f_{R4} respectively (values between brackets assume PO fibers). All these values are in fact remarkably similar, their average being 255 kg/m^3. If the calculation is made in relation to f_{R1}, the cement content obtained is 185 kg/m^3 (171 kg/m^3), which is of no practical value because it is out of range (the cement content ranges from 200 to 452 kg/m^3 in synthetic FRC mixtures, section 3.3.3).

In conclusion, it can be said that the residual flexural strength parameters of synthetic FRC mixtures with PP or PO fibers are sensitive to the fiber dosage only if the cement content is 255 kg/m^3. If the cement content is lower than that, f_{R1} is sensitive to the fiber dosage, but not the other residual flexural strength parameters.

7.7.5 How 'important' is the effect of cement content? The above findings in relation to the cement content that makes the residual flexural strength parameters insensitive to the fiber content, and vice versa, are relevant because they define the conditions in which increasing the cement content is associated with better performance, represented by the rectangles superimposed to the contour plots in Figure 102. That is: if the fiber content is not less than 0.42% and the cement content is not less than 255 kg/m^3, higher cement contents are associated with higher f_{R1}, f_{R2}, f_{R3} and f_{R4} values.

It is, therefore, only in the context defined by these rectangles that it is pertinent to assess the relative impact of the cement content (through its interaction with the fiber content) on the residual flexural strength. This can be done by calculating the expected variations of f_{R1} and f_{R3} associated with an increase of 50 kg/m^3 in the cement content, and then comparing them to the expected variations corresponding to an increase of 0.1% in the fiber volume fraction. For these calculations, a fiber volume fraction of 0.75% can be considered, which corresponds to the 75th percentile of V_f values in the synthetic FRC mixtures dataset.

Following the calculations already reported in previous sections, the expected variations of f_{R1} and f_{R3} associated with an $\Delta V_f = +0.1\%$ are 0.07 MPa, 0.11 MPa, 0.08 MPa, and 0.10 MPa (assuming PP and PO fibers respectively). Since these values are all similar, their average, 0.09 MPa, can be taken for comparison purposes.

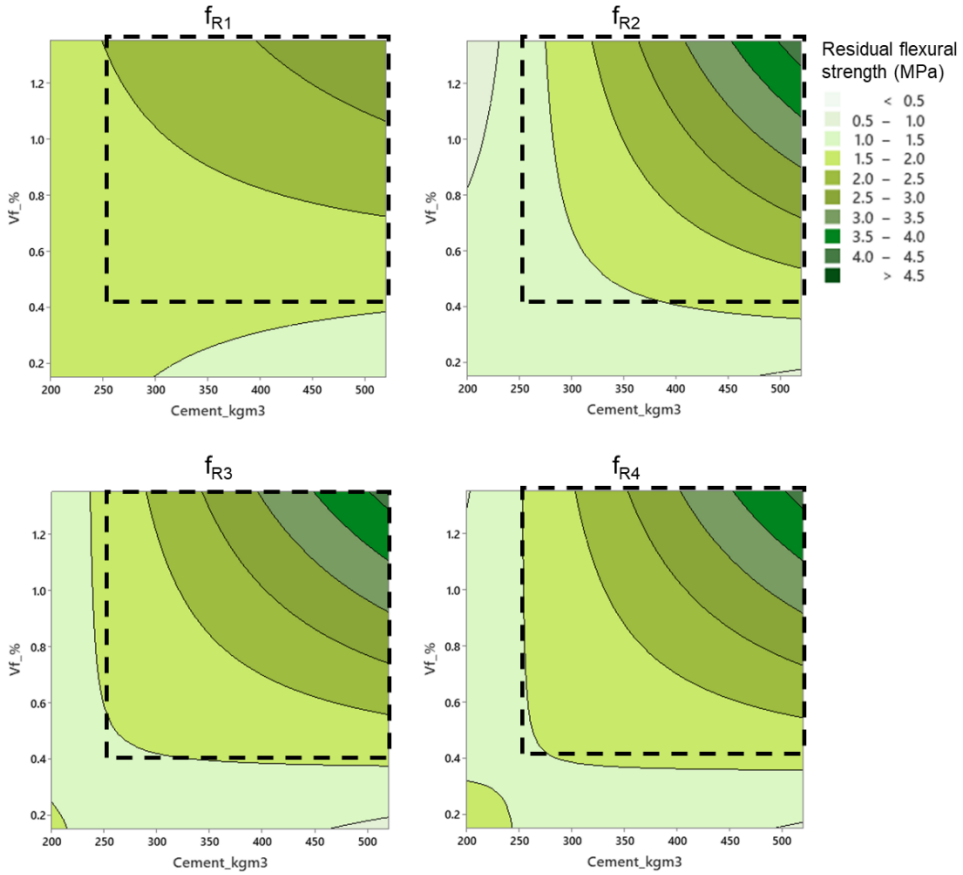

Figure 102. Residual flexural strength vs cement content and fiber volume fraction.

The expected variations of f_{R1} and f_{R3} resulting from an $\Delta C = +50$ kg/m^3 can be calculated by means of the following expression:

$$E\left(\Delta f_{Ri} | \Delta C = +50 \frac{kg}{m^3}\right) = \frac{\partial f_{Ri}}{\partial C} \times \Delta C = \left(b_1 V_f + k_6 + c_1(G+S)\right) \times 50 \tag{81}$$

By replacing the coefficients b_1, k_6, and c_1 in equation (81) with their values from Table 13 or 14, and assuming the total aggregate content at its median and V_f = 0.75%, the expected variations of f_{R1} and f_{R3} are 0.022 MPa and 0.20 MPa, respectively. Comparing these two values to the expected variation of 0.10 MPa associated with $\Delta V_f = +0.1\%$, it is clear that the effect of increasing the cement content on f_{R1} is minor, but quite important on f_{R3} (as well as f_{R2} and f_{R4}).

Therefore, it can be concluded that the effect of the cement content on f_{R1} is minor, but its effect on f_{R2}, f_{R3} and f_{R4} is important and comparable in magnitude to that of the fiber content.

7.8 Effect of SCMs and its interactions with variables related to aggregates

7.8.1 Fiber material and interactions. The terms that represent, in equation (73), the contributions of the total amount of SCMs and the total aggregate content to the residual flexural strength are: $k_2 SCM + (c_1 C + c_2 SCM + c_3 G/S)(G+S)$. None of these terms are affected by the fiber material since their interactions with this variable were found to be statistically non-significant. As a result, the coefficients k_2, c_1, c_2, and c_3 have the same values

irrespective of the fibers being PP or PO (Tables 13 and 14), and the relationships between the amount of SCMs, the total aggregate content, and f_{R1}, f_{R2}, f_{R3} and f_{R4} follow the same trends independently of the fiber material. The discussion presented in this section is based on the plots obtained assuming PP fibers, but the same conclusions apply to mixtures with PO fibers.

The amount of SCMs and the total aggregate content are jointly discussed because the effect of the interaction between these two variables, in relation to the residual flexural strength parameters, was found to be very relevant, as demonstrated in this section. The effect of the SCMs amount on f_{R1}, f_{R2}, f_{R3} and f_{R4} varies with the total aggregate content to such an extent that it cannot be interpreted without considering the latter.

7.8.2 Contour plots (PP fibers). The contour plots corresponding to f_{R1}, f_{R2}, f_{R3} and f_{R4} as described by equation (73) are shown in Figure 103 as a function of the total amount of SCMs and the total aggregate content, assuming median values for the other mix design variables.

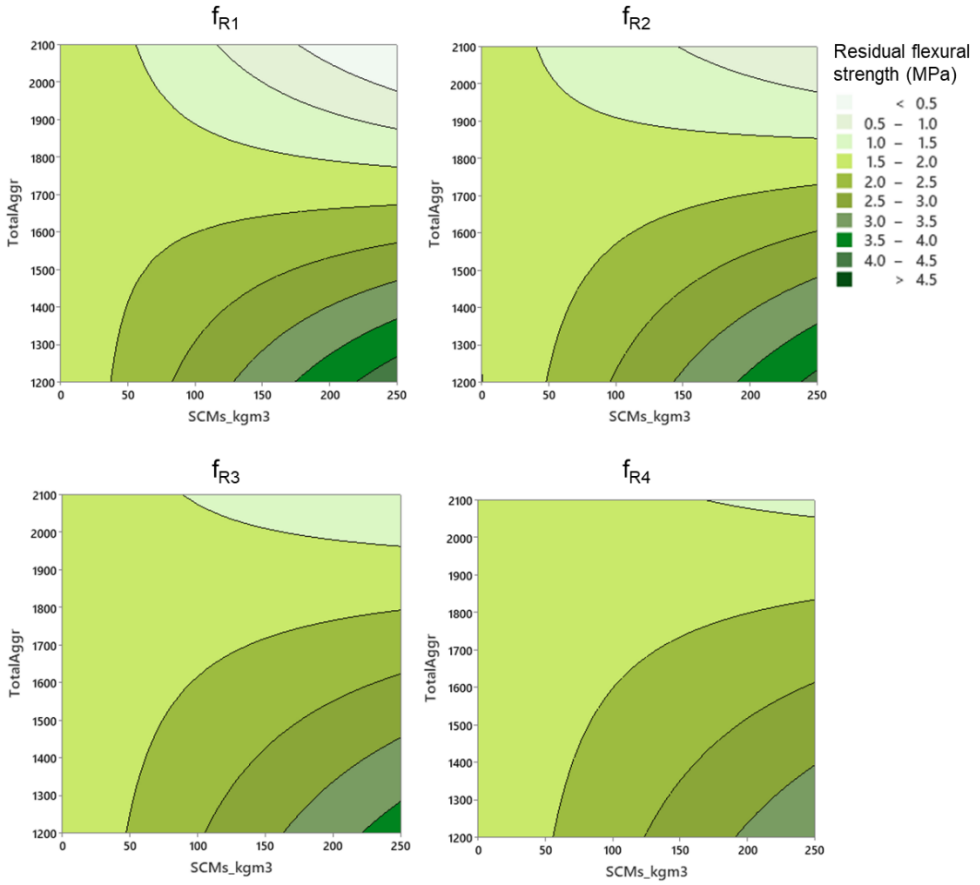

Figure 103. Residual flexural strength vs SCMs and total aggregate contents.

All four plots show that, if the total aggregate content does not exceed a certain value, higher amounts of SCMs are associated with higher values of the residual flexural strength parameters. This can be attributed to the improved cohesiveness of the mixture caused by the SCMs, which can have a positive effect on workability and the dispersion of fibers, indirectly enhancing the hardened state properties of the mixture, including the residual flexural strength.

On the other hand, the contour plots also show that high SCMs contents can be associated with lower levels of residual flexural strength if the FRC mixture has a high aggregate content. At this point, it is important to note that these observations are intentionally expressed in terms of

association and should not be taken as necessarily implying a cause-effect relationship. When the relative volume of aggregates in a mixture is high, the relative volume of binder is low, and so is the cement content if the amount of SCMs is high. The contour plots in Figure 103 can therefore be misleading: the negative effect that high amounts of SCMs seem to have (on f_{R1}, in particular) when the aggregate content is also high is not attributable to the SCMs but, rather, a consequence of the cement content being low in such cases.

7.8.3 Sensitivity to SCMs contents. The total aggregate content below which the amount of SCMs is associated with higher residual flexural strength is also the total aggregate content that makes the residual flexural strength parameters insensitive to the SCMs content. This can be calculated by differentiating equation (73) with respect to the SCMs content and equating to zero:

$$\frac{\partial f_{Ri}}{\partial SCM} = k_2 + c_2(G+S) = 0 \quad \rightarrow \quad (G+S) = \frac{-k_2}{c_2} \tag{82}$$

By replacing the coefficients k_2 and c_2 with their values from Table 13 (or 14), the total aggregate content values obtained are: 1675 kg/m^3, 1826 kg/m^3, 1955 kg/m^3, and 1901 kg/m^3, in relation to f_{R1}, f_{R2}, f_{R3} and f_{R4}, respectively. Their average, 1839 kg/m^3, can be taken as representative, and is slightly higher than the value obtained in relation to SFRC mixes (1700 kg/m^3, section 5.8.3). It can be concluded that the residual flexural strength of synthetic FRC mixtures with a total aggregate content of 1839 kg/m^3 (or, around 1800 kg/m^3) is not sensitive to the amount of SCMs. For lower aggregate contents, higher SCMs contents have a positive effect on the residual flexural strength parameters.

7.8.4 Sensitivity to the total aggregates content. Similarly, the contour plots in Figure 103 show that there is a certain value of the total amount of SCMs that makes f_{R1}, f_{R2}, f_{R3} and f_{R4} insensitive to the total aggregates content. This can be calculated as follows:

$$\frac{\partial f_{Ri}}{\partial (G+S)} = c_1 C + c_2 SCM + \frac{c_3 G}{S} = 0 \quad \rightarrow \quad SCM = \frac{-c_1}{c_2} C + \frac{-c_3}{c_2} G/S \tag{83}$$

When coefficients c_1, c_2, and c_3 in equation (83) are replaced with their values from Table 13 or 14, the amount of SCMs obtained is a function of the cement content and the coarse-to-fine aggregate ratio. If the cement content and the coarse-to-fine aggregate ratio are taken at their median values in the synthetic FRC mixtures dataset (360 kg/m^3 and 1.09, respectively), the amounts of SCMs obtained are: 19 kg/m^3, 18 kg/m^3, 24 kg/m^3, and 18 kg/m^3, in relation to f_{R1}, f_{R2}, f_{R3} and f_{R4}, respectively. These are small figures and consistent with the contour plots in Figure 103, where it can be seen that, if the total amount of SCMs is ~20 kg/m^3, the residual flexural strength parameters do not significantly change with the total aggregate content.

However, it is important not to forget that the contour plots in Figure 103 assume median values for the mix design variables other than the amounts of SCMs and aggregates. As per equation (83), the SCMs amount that makes f_{R1}, f_{R2}, f_{R3} and f_{R4} insensitive to changes in the total aggregate content is a function of the cement content and the coarse-to-fine aggregate ratio. When this equation is plotted for f_{R1}, f_{R2}, f_{R3} and f_{R4}, the four planes shown in Figure 104 are obtained. It becomes clear that the amount of SCMs that makes the residual flexural strength parameters insensitive to the amount of aggregates is not always low: it can be of the order of 100 kg/m^3 when the coarse-to-fine aggregate ratio is high and the cement content is low. This, once again, is related to the cohesiveness of the mixture, and evidences that the model described

by equation (73) and Tables 13 and 14 captures even the connections between the mix design, cohesiveness, and the residual flexural strength parameters.

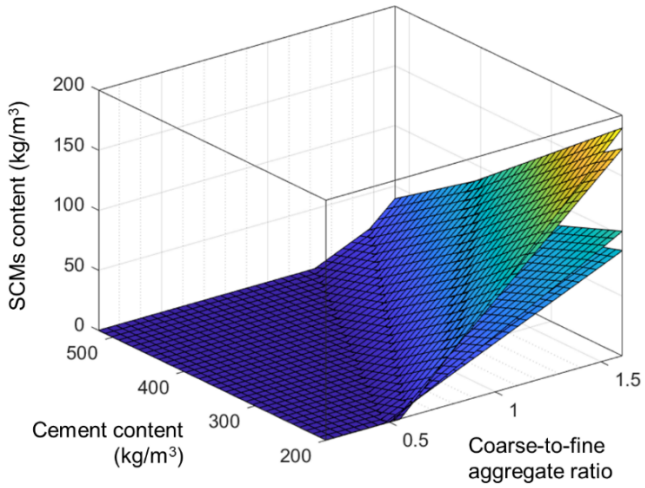

Figure 104. SCMs content as per equation (83) vs cement content and G/S ratio.

7.8.5 Coarse-to-fine aggregate ratio and SCMs requirements. It can be argued that equation (83) establishes the balance between the amounts of cement, SCMs, coarse and fine aggregates necessary for synthetic FRC mixtures to have a level of cohesiveness which makes them relatively robust in terms of the residual flexural strength parameters. This relationship can be used to determine what is the maximum coarse-to-fine aggregate ratio that makes SCMs unnecessary or, in other words, makes the mixture cohesive enough without SCMs:

$$SCM = \frac{-c_1}{c_2} C + \frac{-c_3}{c_2} \frac{G}{S} \leq 0 \quad \rightarrow \quad \frac{G}{S} \leq \frac{-c_1}{c_3} C \tag{84}$$

After replacing the coefficients c_1 and c_3 in equation (84) with their values from Table 13 or 14, the four lines represented in Figure 105 are obtained, each of them related to one of the four residual flexural strength parameters. The region of the plot where equation (84) is satisfied in relation to all of them is colored in green and includes all possible combinations of cement content and *G/S* ratio for which the mixture would be cohesive enough without SCMs.

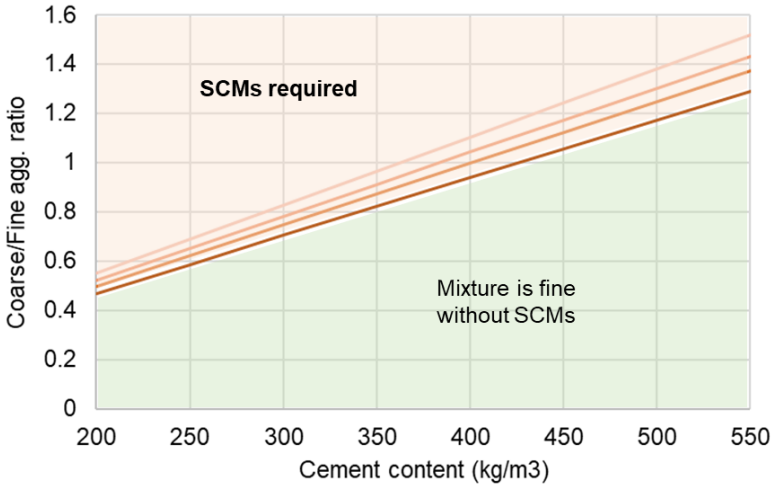

Figure 105. Maximum G/S ratios as a function of cement content, as per equation (84).

It is worth commenting on some representative values from Figure 105 which can be useful in practice. A synthetic FRC mixture with a cement content equal to the median (360 kg/m^3, section 3.3.3) can be sufficiently cohesive without SCMs as long as the coarse-to-fine aggregate ratio is not higher than 0.84. Taking into account that 50% of the synthetic FRC mixtures in the database compiled for this study have a cement content between 309 kg/m^3 and 400 kg/m^3, such maximum coarse-to-fine aggregate ratio ranges from 0.72 to 0.94. With these figures in mind, the conclusion is that, in general, it seems like good practice to proportion synthetic FRC mixtures keeping the coarse-to-fine aggregate ratio lower than 0.72.

It would be a misinterpretation of the above to conclude that the introduction of SCMs can be dismissed as 'unnecessary' as long as the coarse-to-fine aggregate ratio is lower than 0.72. A more appropriate reading is that, in those conditions, the incorporation of SCMs does not merely adjust or 'correct' the mixture in terms of cohesiveness: it enhances it. At this point it is important to recall that, as the contour plots in Figure 103 show, increasing the amount of SCMs is associated with higher values of f_{R1}, f_{R2}, f_{R3} and f_{R4}, particularly when the total aggregate content is lower than 1800 kg/m^3 (section 7.8.3).

7.8.6 How 'important' is the effect of the SCMs content? The values of the total aggregate content and SCMs content obtained in 7.8.3 and 7.8.4 define the region within which the residual flexural strength parameters are positively influenced by increasing the amount of SCMs, represented by the rectangles over the contour plots in Figure 106.

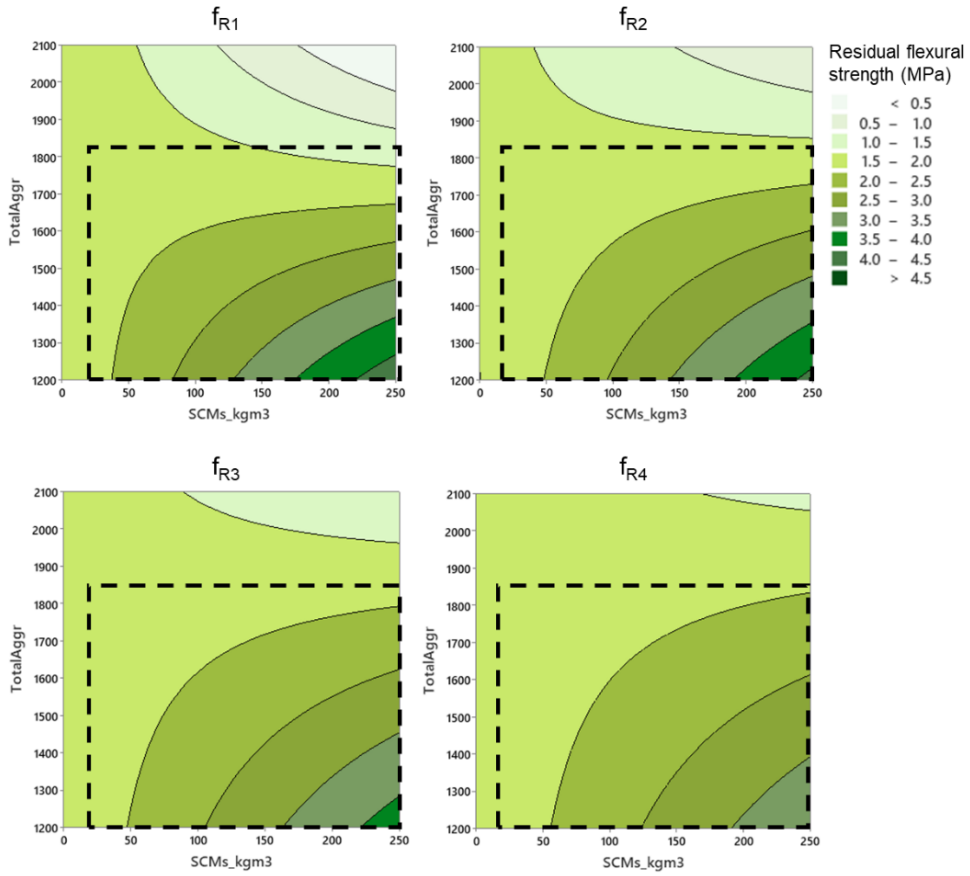

Figure 106. Residual flexural strength vs SCMs and total aggregate contents.

The relative influence of SCMs on the residual flexural strength parameters is best assessed if the effect of a representative variation of the amount of SCMs is quantified and compared to

that of a representative variation of the fiber volume fraction. A value of $\Delta SCM = +50$ kg/m^3 seems reasonable for the purpose of comparison. As in previous sections, the expected variation of f_{R1}, f_{R2}, f_{R3} and f_{R4} associated with $\Delta SCM = +50$ kg/m^3 can be compared to that associated with an $\Delta V_f = +0.1\%$, which is 0.10 MPa on average.

The expected variation of the residual flexural strength parameters corresponding to $\Delta SCM = +50$ kg/m^3 can be determined as follows:

$$E\left(\Delta f_{Ri} | \Delta SCM = +50 \frac{kg}{m^3}\right) = \frac{\partial f_{Ri}}{\partial SCM} \times \Delta SCM = \left(k_2 + c_2(G+S)\right) \times 50 \quad (85)$$

By replacing the coefficients in equation (85) with their values from Tables 13-14, and assuming the first quartile of the total aggregate content (1651 kg/m^3), the values of the expected variation are: 0.03 MPa, 0.15 MPa, 0.18 MPa, and 0.13 MPa for f_{R1}, f_{R2}, f_{R3} and f_{R4}, respectively. The expected variation of f_{R1} is smaller than the values obtained for f_{R2}, f_{R3} and f_{R4}, but they are all of the same order of magnitude. Their average is 0.13 MPa, which is comparable to 0.10 in order of magnitude.

In short, it can be concluded that, in synthetic FRC mixtures with a total aggregate content of less than 1839 kg/m^3, increasing the amount of SCMs can have a positive effect on the residual flexural strength parameters that is comparable to that of increasing the fiber volume fraction.

7.9 Interaction between the G/S ratio and the fiber material

7.9.1 Comparison between PP and PO fibers. Mix design variables related to the aggregates have already been discussed in the preceding section, because of their synergies with the amount of SCMs. However, there is one additional term that partially describes the links between aggregates and the residual flexural strength in equation (73) which is unrelated to the SCMs content but whose effect varies with the fiber material: $k_1 G/S$.

The interaction between the coarse-to-fine aggregate ratio and the fiber material was found to be statistically significant and, therefore, the values of the coefficient k_1 for PP and PO fibers are different (Tables 13 and 14). The terms that represent the contribution of the coarse-to-fine aggregate ratio to the residual flexural strength parameters in equation (73) can be rewritten together as: $\left(k_1 + c_3(G+S)\right) G/S$. That is, the coarse-to-fine aggregate ratio has an impact on the residual flexural strength, and this effect is affected not only by the total aggregate content but also by the fiber material being PP or PO.

7.9.2 Contour plots (PP fibers). Figure 107 shows the contour plots corresponding to f_{R1}, f_{R2}, f_{R3} and f_{R4} against the coarse-to-fine aggregate ratio and the total aggregate content, assuming PP fibers and median values for the rest of mix design parameters. The response surfaces obtained for f_{R2}, f_{R3} and f_{R4} are all very similar, where the higher values of these parameters are associated with coarse-to-fine aggregate ratios below 1.5 and total aggregate contents lower than ~1700 kg/m^3. Although the response surface corresponding to f_{R1} is a bit different, it is still consistent with the observations made in relation to f_{R2}, f_{R3} and f_{R4} insofar as reductions in the total aggregate content and the coarse-to-fine aggregate ratio are associated with increasing values of f_{R1}.

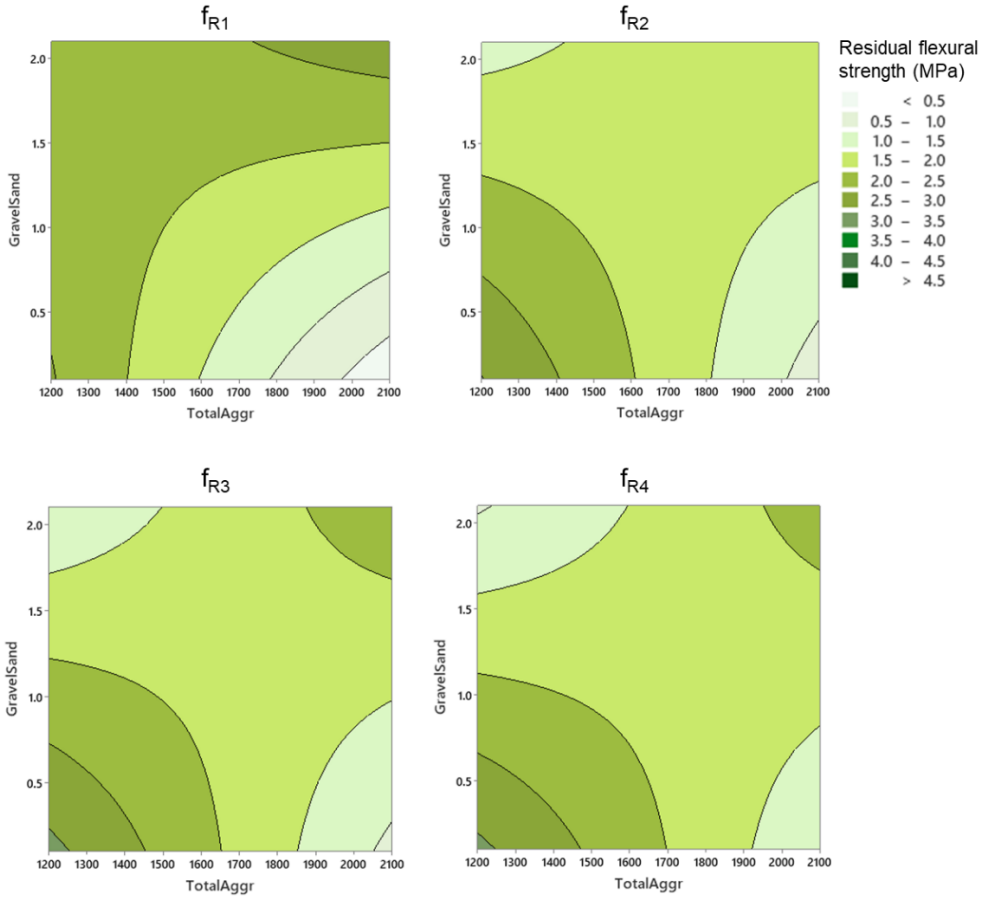

Figure 107. Residual flexural strength vs aggregate content and G/S ratio (PP fibers).

7.9.3 Sensitivity to the total aggregate content (PP fibers). This has already been discussed in sections 7.8.4 and 7.8.5.

7.9.4 Sensitivity to the G/S ratio (PP fibers). The contour plots in Figure 107 show that there is a certain value of the total aggregate content which makes the residual flexural strength parameters insensitive to the coarse-to-fine aggregate ratio. This can be obtained by differentiating equation (73) with respect to the *G/S* ratio and equating to zero:

$$\frac{\partial f_{Ri}}{\partial (G/S)} = k_1 + c_3(G+S) = 0 \quad \rightarrow \quad (G+S) = \frac{-k_1}{c_3} \tag{86}$$

After replacing the coefficients in equation (86) with their values from Table 13, the total aggregate contents that make f_{R1}, f_{R2}, f_{R3} and f_{R4} insensitive to the coarse-to-fine aggregate ratio are: 1331 kg/m^3, 1723 kg/m^3, 1729 kg/m^3, and 1795 kg/m^3, in relation to f_{R1}, f_{R2}, f_{R3} and f_{R4}, respectively. The first value (obtained in relation to f_{R1}) is merely theoretical and has no practical relevance: 95% of the synthetic FRC mixtures in the dataset used in this study have a total aggregate content higher than 1381 kg/m^3. The other three values are very similar, their average being 1749 kg/m^3. It is noteworthy that these values are invariant as they are not a function of any variables apart from the fiber material.

In consequence, it can be said that a total aggregate content of 1749 kg/m^3 makes f_{R2}, f_{R3} and f_{R4} of FRC mixtures with PP fibers practically insensitive to the coarse-to-fine aggregate ratio. Values of the total aggregate content below 1749 kg/m^3 are associated with increasing values of the residual flexural strength.

7.9.5 Contour plots (PO fibers). The contour plots of f_{R1}, f_{R2}, f_{R3} and f_{R4} against the coarse-to-fine aggregate ratio and the total aggregate content assuming PO fibers and median values for the rest of mix design parameters are shown in Figure 108. All these response surfaces are very similar, with higher values of the residual flexural strength associated with coarse-to-fine aggregate ratios above 1.5 as well as a significant content of SCMs, as discussed in 7.8.5. It is also apparent that, in contrast with PP fibers, the effect of the coarse-to-fine aggregate ratio is more important in mixtures with PO fibers.

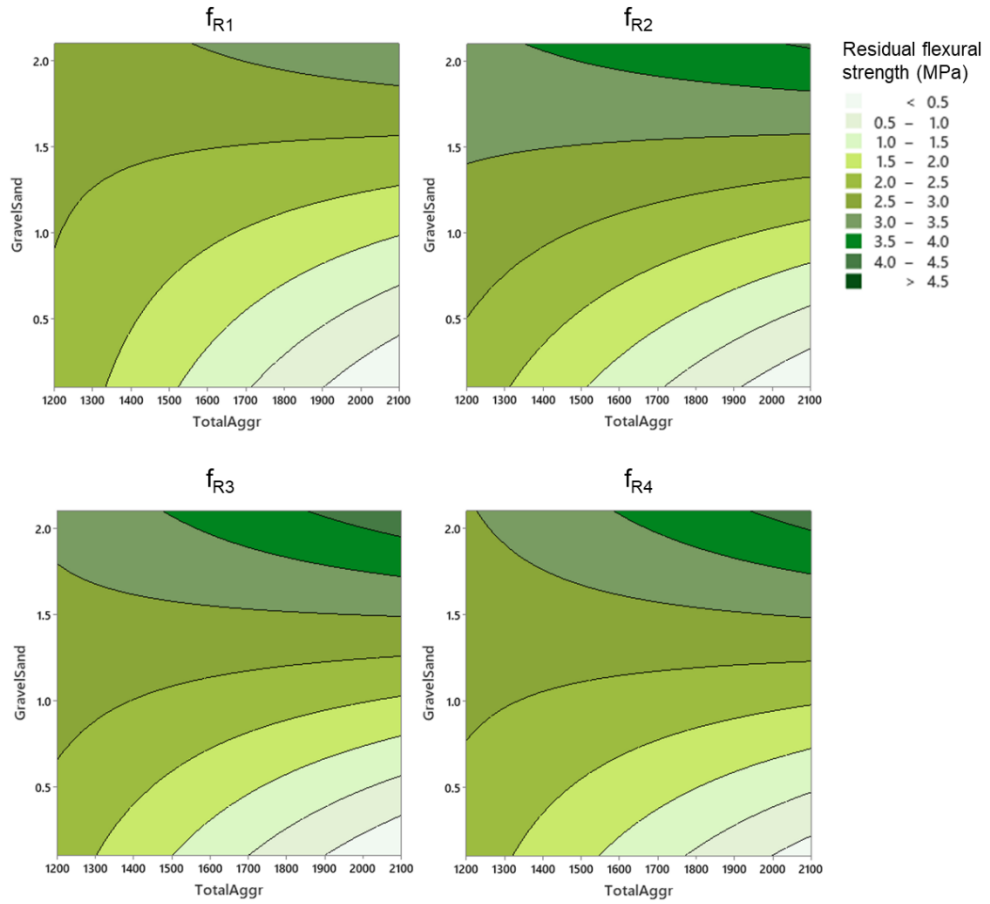

Figure 108. Residual flexural strength vs aggregate content and G/S ratio (PO fibers).

7.9.6 Sensitivity to the G/S ratio (PO fibers). Based on the contour plots in Figure 106, there does not seem to be a value of the total aggregate content that nullifies the impact of the coarse-to-fine aggregate ratio on the residual flexural strength parameters. In fact, if equation (86) is used with the coefficient values from Table 14, the total aggregate content values obtained are: 1091 kg/m^3, 853 kg/m^3, 972 kg/m^3, and 1008 kg/m^3, in relation to f_{R1}, f_{R2}, f_{R3} and f_{R4}, respectively. Again, these values are not relevant, bearing in mind that the total aggregate content is higher than 1190 kg/m^3 in 99% of the synthetic FRC mixtures in the dataset.

Therefore, it can be concluded that the residual flexural strength parameters of FRC mixtures with PO fibers are generally influenced by the coarse-to-fine aggregate ratio, irrespective of the total aggregate content.

8. Variability of the residual flexural strength of SFRC mixtures

8.1 Introduction

8.1.1 Context and scope of this chapter. This chapter presents the analysis of the variability of the residual flexural strength parameters (f_{R1}, f_{R2}, f_{R3}, and f_{R4} as per EN 14651) and of the multivariate factor Z as a function of the variables that describe SFRC mixtures in terms of the relative amounts of their constituents and the fundamental descriptors of such constituents.

8.1.2 Data used in the analysis. The values used in the analysis of SFRC variability reported in this chapter are the differences between the actual values of the residual flexural strength parameters in the dataset of SFRC mixtures and their estimates as per the model given by equation (13) and Tables 7 and 8 (chapter 5, section 5.2). These differences are known as *residuals* and quantify the regression error or deviation of data points from their estimated values, hence being directly connected to their variability. Four new variables are therefore calculated and incorporated to the information corresponding to each mixture in the SFRC database: e_1, e_2, e_3, and e_4, being the residuals of f_{R1}, f_{R2}, f_{R3}, and f_{R4}. The same applies to the factor Z as calculated based on f_{R1}, f_{R2}, f_{R3}, and f_{R4} and its estimates as per the model given by equation (53) and Table 10.

8.1.3 Methodological considerations. In concrete technology, the measures of variability most commonly used are the standard deviation (σ) and the coefficient of variation, whilst variance, which is the square of the standard deviation (σ^2, also noted as *Var*), is used less often. However, variance is a more convenient measure of dispersion or variability in the context of statistical modeling due to its mathematical properties[8]. One reason is that the squares of the residuals obtained after fitting a regression model to a set of data are estimators of the variance of the parameter being analyzed. In the context of this study, this means that the analysis of ${e_1}^2$, ${e_2}^2$, ${e_3}^2$, and ${e_4}^2$ and their correlations with the mix design variables makes it possible to estimate the variances of f_{R1}, f_{R2}, f_{R3}, and f_{R4} and their sensitivity to the proportioning of the SFRC mixture.

The models developed in this chapter are therefore concerned with the variances of the residual flexural strength parameters, noted as $\sigma^2(f_{R1})$, $\sigma^2(f_{R2})$, $\sigma^2(f_{R3})$, and $\sigma^2(f_{R4})$. The interpretation and discussion of these models in relation to the mix design variables is made in terms of both variance as well as standard deviation values, as is customary amongst concrete practitioners.

The residuals analyzed in this study derive from the analysis of a dataset that is not the result of a structured, predefined experimental program where all the cases are reproduced a certain number of times. In other words, differences between replicates of the same SFRC mixture cannot be determined, quite simply because there are no replicates in some cases and, when there are, the number of replicates are inconsistent. Yet it is still possible to investigate the variability of such a set of data because there are methods for the estimation of variance in the

[8] In fact, mean and variance are the statistics that 'naturally' emerge when the moments of probability distributions are calculated. The standard deviation is useful simply because it is expressed in the same units as the variable it describes, but variance has better mathematical properties and is therefore preferred.

absence of replicates. The methodology followed in this study is based on what has been called the modified two-step estimator[9]. Let us consider f_{R1} to outline the procedure of analysis:

- After having fitted the multiple linear regression model for f_{R1} as a function of the variables describing the SFRC mixture, the equation obtained (equation 13, section 5.2) can be used to produce an estimate or expected value of f_{R1} for each of the cases in the database. The squares of the differences between the actual values of f_{R1} and the estimates are calculated for all cases: these are the squares of residuals, ${e_1}^2$.

- Another multiple linear regression analysis is performed, this time to correlate the natural logarithm of the squares of the residuals to the variables describing the SFRC mixtures. If these variables are collectively noted as x_j, and the regression coefficients are noted as m_j, the specification of this regression model can be written as:

$$\ln({e_1}^2) = m_0 + \sum m_j \, x_j \tag{87}$$

  In a first iteration, all mix design variables are included in the model. Terms that are not statistically significant are sequentially removed until the fitted equation contains only statistically significant terms.

- The equation fitted to the squares of residuals is then corrected by adding +1.27 to the right-hand side[10] of equation (87). The resulting equation estimates the natural logarithm of the variance of f_{R1}:

$$E[\ln \sigma^2(f_{R1})] \cong 1.27 + m_0 + \sum m_j \, x_j \tag{88}$$

- By exponentiating both sides of the above equation, what is obtained is the equation that can be used to estimate the variance of f_{R1} (or, more appropriately put, the mathematical expectation of the variance of f_{R1}):

$$E[\sigma^2(f_{R1})] \cong \exp\left(1.27 + m_0 + \sum m_j \, x_j\right) \tag{89}$$

The same procedure has been applied to the square residuals corresponding to f_{R1}, f_{R2}, f_{R3}, and f_{R4} as well as the factor Z obtained from the multivariate analysis in chapter 6. The expressions obtained for these five parameters, which follow the model specification shown in equation (89), are discussed with the help of line plots. Goodness-of-fit measures are not given because they have no real meaning (the residuals are not observations and therefore their regression analysis is not based on actual data for which predictions can be calculated). As the values of f_{R1}, f_{R2}, f_{R3}, and f_{R4} are expressed in MPa in the database, variance estimates are expressed in MPa^2, and the standard deviation values in MPa. Variance and standard deviation estimates for the factor Z have no units as this parameter is non-dimensional.

[9] The original paper is: Harvey, A.C. (1976), "Estimating regression models with multiplicative heteroscedasticity". *Econometrica: Journal of the Econometric Society* (): 461-465.
A more recent (and perhaps clearer for non-mathematicians) account can be found in: Ferrer, A. (2002), "Estudio de efectos de dispersión en ausencia de replicaciones: revisión del estado del arte y perspectivas de futuro". *Estadística española* 44.151 (): 365-392 [in Spanish].

[10] This is a chi-square correction, and its justification can be found in the papers cited in the previous footnote.

8.2 Variability of f_{R1}

8.2.1 Fitted model. The following equation was obtained for the estimator of the variance of f_{R1} as a function of the mix design variables:

$$E[\sigma^2(f_{R1})] \cong \exp\Big(0.12 + 0.00475\,SCM + 0.589\,V_f - 0.01643\,l_f - 0.0886\,m + 0.000828\,(G+S) + 0.795\,\frac{G}{S}\Big) \quad (90)$$

Where: SCM is the amount of supplementary cementitious materials in kg/m^3, V_f is the fiber volume fraction as a percentage, l_f is the fiber length in mm, m is the maximum aggregate size in mm, and S and G are the amounts of fine and coarse aggregates, respectively, in kg/m^3.

Equation (90) contains only those terms that have a statistically significant effect on the squared residuals of f_{R1} and, in consequence, on its variance. It is worth noting that the variables representing the test setup and configuration (3-point vs 4-point test, notched vs unnotched specimen) were not found to have a statistically significant effect on the variance of f_{R1}. This is in contrast with the findings in relation to the variances of f_{R2}, f_{R3}, f_{R4}, and Z, which were all found to be significantly different depending on the test setup and configuration, as will be discussed in subsequent sections.

8.2.2 A general estimate of the variability of f_{R1}. An average value of the variance of f_{R1}, representative of the variability of this parameter in SFRC, can be estimated by replacing the variables in equation (90) with their median values as obtained from the SFRC database compiled as part of this study. These values are: 60 kg/m^3 of SCMs, V_f = 0.51%, l_f = 45 mm, a maximum aggregate size of 15 mm, G/S = 1.0, and a total aggregate content of 1715 kg/m^3. With these values, the expected variance is $\sigma^2(f_{R1})$ = 2.6 MPa^2, which corresponds to a standard deviation of $\sigma(f_{R1}) = 1.6$ MPa. Bearing in mind that the median value of f_{R1} in the SFRC dataset is 5.33 MPa, it follows that a representative value for the coefficient of variation of f_{R1} is, on average, 30%.

8.2.3 Sensitivity of the variance of f_{R1} to the mix design. As the variance estimators reported in this chapter, and that in equation (90) in particular, include no pairwise interactions between mix design variables, simple line plots suffice to illustrate the effect of these variables on the expected variance of f_{R1}.

In the two graphs shown in Figure 109, the expected variance of f_{R1} as per equation (90) is plotted against the fiber volume fraction and the fiber length, assuming median values for the rest of the mix design variables in the equation. Higher amounts of fibers are associated with higher variance of f_{R1} values to be expected, whilst increasing the fiber length is associated with a variance reduction. This suggests that the changes in the variability of f_{R1} that are directly related to the fibers can in fact be attributed to changes in the number of fibers per unit volume of concrete, rather than the fiber length or the fiber volume fraction separately.

Some useful values of the variance and standard deviation of f_{R1} can be obtained if the 25th and 75th percentiles of the fiber volume fraction and the fiber length are considered. In 50% of the SFRC mixtures in the dataset, the fiber volume fraction ranges from 0.4% to 1.0% and the fiber length is between 30 and 60 mm. The expected variance of f_{R1} if V_f is assumed to be 0.4% and the rest of variables in equation (90) are set to their median is 2.4 MPa^2, which corresponds to a standard deviation of 1.6 MPa. If the V_f is increased to 1.0%, the expected standard deviation

is 1.9 MPa. If the fiber length is considered between 30 mm and 60 mm, the expected standard deviation of f_{R1} changes from 1.8 MPa to 1.4 MPa.

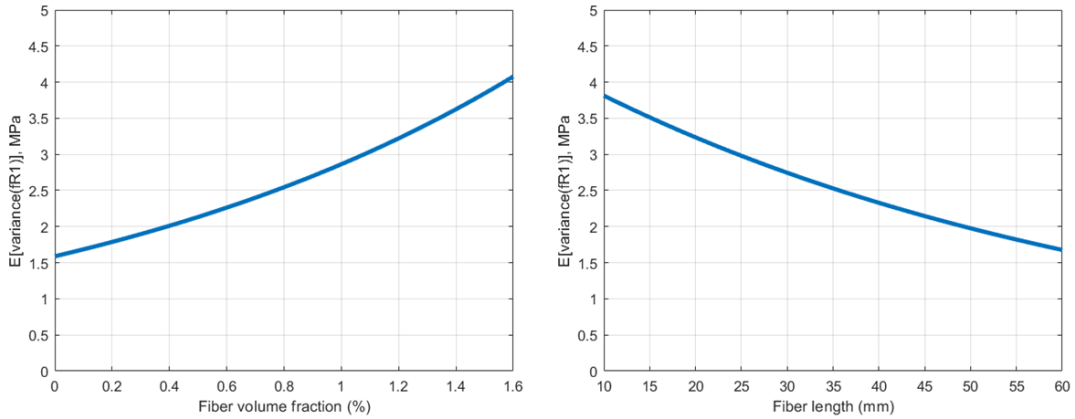

Figure 109. Expected variance of f_{R1} related to fiber content and fiber length.

Figure 110 shows the expected variance of f_{R1} against the total amount of SCMs, the coarse-to-fine aggregate ratio, the total aggregate content, and the maximum aggregate size, assuming in each case median values for the variables other than that represented by the horizontal axis.

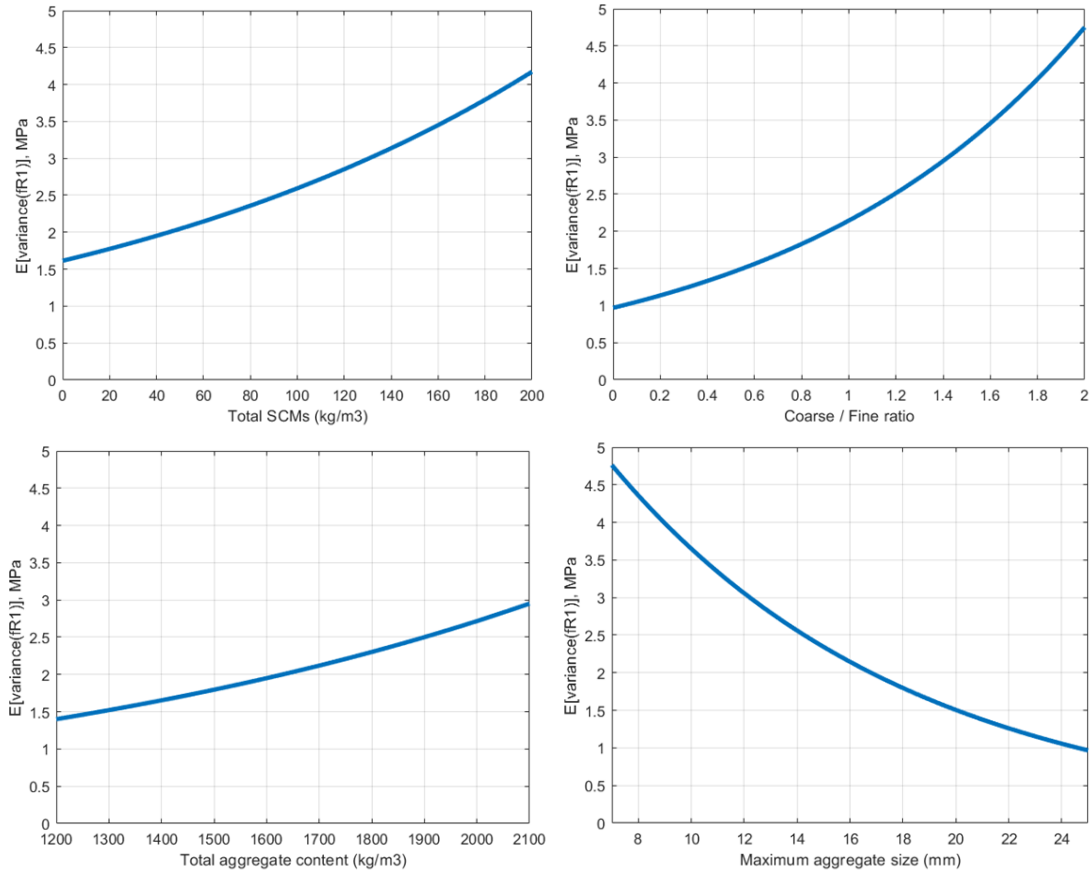

Figure 110. Expected variance of f_{R1} related to the SCMs and total aggregate content, the G/S ratio and maximum aggregate size.

The graphs in Figure 110 show that the expected variance of f_{R1} increases with the amount of SCMs, the aggregate content, and with the coarse-to-fine aggregate ratio, whilst higher values of the maximum aggregate size are associated with lower variance values. It must be noted that

the relationships between these variables and the variance of f_{R1} should not be interpreted in isolation, at least not when some conclusion in terms of causation is sought. As proven by the findings in chapter 2, these variables are all interdependent in terms of the proportioning of SFRC mixtures. It would be misleading, for example, to conclude from the graphs in Figure 110 that increasing the SCMs 'causes' the variance of f_{R1} to increase. As higher amounts of SCMs are often found in mixtures with a higher coarse-to-fine aggregate ratio to improve their cohesiveness, the attribution of differences in variance to a single variable is difficult to justify. The model described by equation (90) and throughout this chapter make it possible to estimate the relative contribution of each of these variables to the variability of the residual flexural strength parameters, but definite conclusions about causation are not implied.

The first graph in Figure 110 shows that the expected variance of f_{R1} is higher in SFRC mixtures with SCMs than in mixtures without SCMs (which does not imply that the addition of SCMs increases the variance, as explained above). The median SCMs content in SFRC mixtures that do have SCMs is 100 kg/m^3, and in that case the expected variance of f_{R1} is, on average, 3.1 MPa^2, the standard deviation being 1.8 MPa. The expected standard deviation of f_{R1} in mixtures with no SCMs decreases to 1.4 MPa.

Reducing the coarse-to-fine aggregate ratio is associated with a reduction in variability, consistently with the generally positive effect that reductions of this ratio have been shown to have on residual flexural strength throughout this report. This is possibly linked to the cohesiveness of the mixture. Typically, the coarse-to-fine aggregate ratio ranges from 0.6 to 1.4 in the SFRC dataset. If G/S = 0.6, the average value of the expected variance of f_{R1} is 1.9 MPa^2, the standard deviation being 1.4 MPa. If G/S = 1.4, the standard deviation is 1.9 MPa. That is, reducing the coarse-to-fine aggregate ratio from 1.4 to 0.6 is associated with an average reduction of the standard deviation of f_{R1} from 1.9 MPa to 1.4 MPa.

Higher values of the total aggregate content and the maximum aggregate size are both associated with a higher variance of f_{R1}. The typical ranges of variation for these two variables in the SFRC dataset are 1575-1800 kg/m^3 and 10-16 mm, respectively. If the aggregate content is increased from 1570 kg/m^3 to 1800 kg/m^3, the expected variance of f_{R1} changes from 2.1 MPa^2 to 2.5 MPa^2 (i.e. the standard deviation changes from 1.5 to 1.6 MPa). If the maximum aggregate size is varied from 10 mm to 16 mm, the expected variance of of f_{R1} changes from 3.7 MPa^2 to 2.1 MPa^2 (i.e. the standard deviation changes from 1.9 to 1.5 MPa).

8.2.4 Concluding remarks. The variability of f_{R1} is sensitive to changes in the SFRC mixture design as the correlations between the variables in equation (90) and the variance of f_{R1} are statistically significant. However, as the values discussed above show, such sensitivity does not necessarily imply big changes of the standard deviation of f_{R1} when the values of the SFRC mix design variables are considered within their typical ranges.

Figure 111 presents a summary of the expected standard deviation of f_{R1} against the different mix design variables in equation (90), where the 25th and 75th percentiles for each variable have been labelled as low and high, respectively. The biggest changes are observed with respect to the coarse-to-fine aggregate ratio and the maximum aggregate size. This shows that, in order to control variability of SFRC, a holistic approach to the proportioning of the mixtures is necessary, not just focused on the fiber content and fiber dimensions but all the mix design variables.

In the case of f_{R1} in particular, all estimates of the standard deviation shown in Figure 111 are within the range of 1.3 and 1.9 MPa. Bearing in mind the representative value of the standard deviation of f_{R1} determined in 8.2.2, it can be concluded that $E\left(\sigma(f_{R1})\right) = 1.6 \pm 0.3$ MPa for the majority of SFRC mixtures.

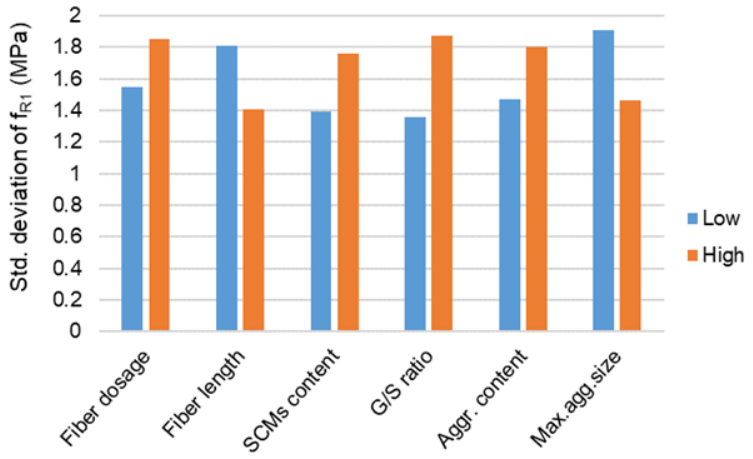

Figure 111. Expected standard deviation of f_{R1}: a summary.

8.3 Variability of f_{R2}

8.3.1 Fitted model. The equation obtained for the estimator of the variance of f_{R2} as a function of the mix design variables is the following:

$$E[\sigma^2(f_{R2})] \cong \exp\left(t + 0.00361\, SCM + 0.811\, V_f - 0.01035\, l_f + 0.01135\, \lambda_f\right) \quad (91)$$

Where: t is a coefficient that depends on the test and specimen configuration, SCM is the amount of supplementary cementitious materials in kg/m^3, V_f is the fiber volume fraction as a percentage, l_f is the fiber length in mm, and λ_f is the fiber aspect ratio.

Only the terms that are present in equation (91) were found to have a statistically significant correlation with the variance of f_{R2}. Contrary to what was concluded in relation to f_{R1}, the test/specimen configuration was found to significantly influence the expected variance of f_{R2}. This is represented by the coefficient t in equation (91). The fitted values for this coefficient are: 0.831 when notched specimens are tested in the 3-point bending configuration (3PBT hereafter) and 0.033 when unnotched specimens are tested in the 4-point bending configuration (4PBT hereafter). Equation (91) can be rewritten as two separate equations, one for each test/specimen configuration, if exp(t) is taken out of the exponential:

$$E[\sigma^2(f_{R2})|\, 3PBT] \cong 2.296 \exp\left(0.00361\, SCM + 0.811\, V_f - 0.01035\, l_f + 0.01135\, \lambda_f\right) \quad (92)$$

$$E[\sigma^2(f_{R2})|\, 4PBT] \cong 1.034 \exp\left(0.00361\, SCM + 0.811\, V_f - 0.01035\, l_f + 0.01135\, \lambda_f\right) \quad (93)$$

8.3.2 Effect of the test configuration. From equations (92) and (93), it follows that the expected variance of f_{R2} when tested in 3PBT conditions is, on average, 2.296/1.034 = 2.22 times higher than the variance when measured in the 4PBT configuration. The ratio of the expected standard deviation is 1.49, as shown in equation (94). This means that, for the same SFRC mixture, the

3-point bending test yields f_{R2} values with a standard deviation that is, on average, 49% higher than in the 4-point bending test.

$$\frac{E[\sigma(f_{R2})|3PBT]}{E[\sigma(f_{R2})|4PBT]} = \sqrt{\frac{E\left[\sigma^2\left(f_{R2}\right)|3PBT\right]}{E\left[\sigma^2\left(f_{R2}\right)|4PBT\right]}} = \sqrt{\frac{2.296}{1.034}} = 1.49 \quad (94)$$

The abovementioned findings provide a quantification of the differences between the 3-point and 4-point bending tests but also provide some more information. The coefficient multiplying the fiber content in equations (92) and (93) does not depend on the testing configuration, and the same can be said of the other terms. As a result, it is possible to analyze and quantify the effect of the fiber content, the fiber length and aspect ratio, and the amount of SCMs on the variability of f_{R2} irrespective of the test setup. The model specification adopted in this methodology effectively decouples the sources of variation attributable to the SFRC mixture from the source of variation that can be attributed to the test being either 3PBT or 4PBT.

8.3.3 A general picture of the variability of f_{R2}. Equations (92) and (93) can be used to obtain a representative value of the variance of f_{R2} by setting each of the mix design variables to its median, as calculated from the SFRC dataset used in this study: 60 kg/m^3 of SCMs, V_f = 0.51%, l_f = 45 mm, and λ_f = 65. In the case of 3PBT, the expected variance of f_{R2} is 5.7 MPa^2, which corresponds to a standard deviation of 2.4 MPa. Assuming a 4PBT setup, the expected variance of f_{R2} is 2.5 MPa^2 and the standard deviation is 1.6 MPa.

The abovementioned standard deviation figures cannot be directly compared to those obtained for f_{R1} in the previous section. To compare f_{R1} and f_{R2} in terms of their variability, it is more appropriate to consider the coefficient of variation. In order to calculate an indicative value of the coefficient of variation, an estimate of the expected variance of f_{R2} irrespective of the test setup can be calculated as the weighted average of 5.7 MPa^2 and 2.5 MPa^2. Taking into account that the number of 3PBT cases in the SFRC dataset is 2.2 times the number of 4PBT cases, the recalculated variance estimate is 4.7 MPa^2, which corresponds to a standard deviation of 2.2 MPa. Since the median of f_{R2} in the SFRC dataset is 5.04 MPa, an overall estimate for the coefficient of variation of f_{R2} is 44%, which is substantially bigger than the 30% obtained in relation to f_{R1}.

8.3.4 Sensitivity to the mix design variables. The plots showing the trends of the expected variance of f_{R2} as described by (92) and (93) are shown in Figures 112 and 113, where the mix design variables other than those in the horizontal axes have been assumed at their median values in the SFRC dataset. The lines in red correspond to 3PBT conditions, whilst the lines in blue correspond to the 4PBT configuration. Since the differences introduced by the test setup have already been discussed (section 8.3.2), the values mentioned in the following paragraphs refer to the 3PBT case unless otherwise stated.

The first graph in Figure 112 shows that the expected variance of f_{R2} increases with the total amount of SCMs in the SFRC mixture. In the absence of SCMs, the expected variance of f_{R2} is 4.6 MPa^2, which corresponds to a standard deviation of 2.1 MPa. If a total of 100 kg/m^3 of SCMs is assumed (which is the median SCMs content in the SFRC database), the expected variance is 6.5 MPa^2 and the standard deviation is 2.6 MPa. That is: the incorporation of 100 kg/m^3 of SCMs into the SFRC mixture is associated, on average, with the expected standard deviation of f_{R2} increasing from 2.1 MPa to 2.6 MPa.

The second graph in Figure 112 shows the effect of the fiber volume fraction. In 50% of the SFRC mixtures in the database, the fiber volume fraction is between 0.4% and 1.0%. If a fiber content of 0.4% is assumed, the expected variance of f_{R2} is 5.2 MPa^2 and the standard deviation is 2.3 MPa. When the fiber content is 1.0%, the expected variance and standard deviation of f_{R2} increase to 8.4 MPa^2 and 2.9 MPa, respectively.

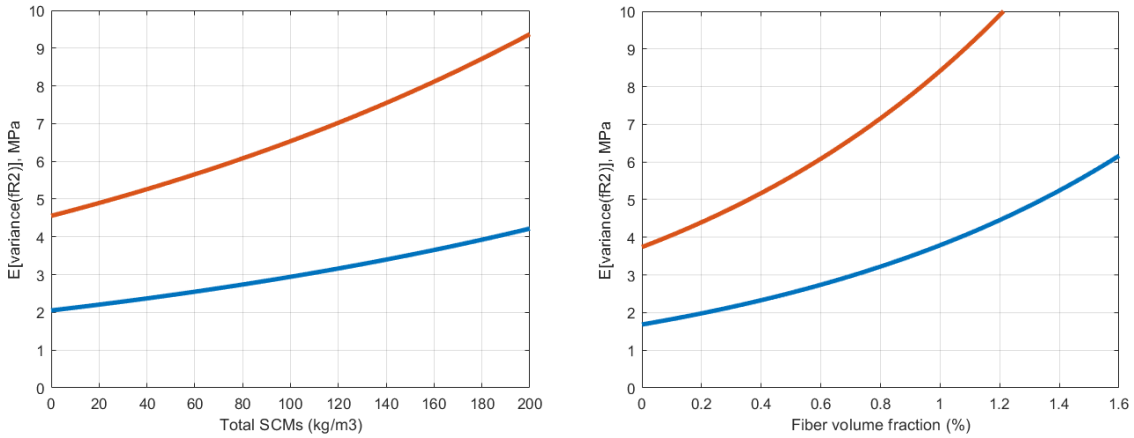

Figure 112. Expected variance of f_{R2} vs fiber dosage and total amount of SCMs.

The part of the variability of f_{R2} that is attributable to the fibers does not only depend on the fiber content but also the fiber length and aspect ratio, as can be seen in equations (92) to (93). Figure 113 shows the expected variance of f_{R2} against the fiber length and the fiber aspect ratio. Similarly to f_{R1}, higher values of the fiber length are associated with a higher variance of f_{R2}. However, when the four graphs in Figures 112 and 113 are compared, it is clear that the fiber volume fraction has the most influence on the variability of f_{R2}.

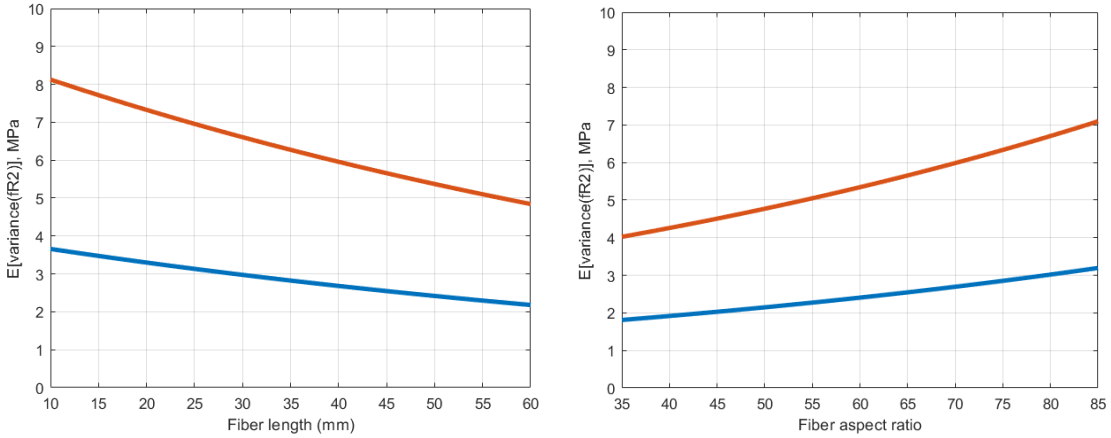

Figure 113. Expected variance of f_{R2} against the fiber length and fiber aspect ratio.

In relation to the fiber length, it is useful to quantify the difference in the variability of f_{R2} between 30 mm and 60 mm, as these are the 25th and 75th percentiles and describe the most typical range in the SFRC database. If the fiber length is 30 mm, the expected variance of f_{R2} is 6.6 MPa^2, corresponding to a standard deviation of 2.6 MPa. If the fiber length is 60 mm, the variance and standard deviation decrease to 4.8 MPa^2 and 2.2 MPa, respectively.

The effect of the fiber aspect ratio on the expected variance of f_{R2}, although statistically significant, becomes of minor importance when it is considered within the typical range as defined by the 25th and 75th percentiles of the SFRC database, which are 60 and 70. If the aspect

ratio is assumed as 60, the expected variance and standard deviation of f_{R2} are 5.3 MPa^2 and 2.3 MPa, respectively. If the aspect ratio is increased from 60 to 70, the expected value of the standard deviation of f_{R2} changes from 2.3 MPa to 2.4 MPa.

8.3.5 Concluding remarks. This analysis has identified that the following factors have a statistically significant effect on the variability of f_{R2}: the test setup being 3PBT or 4PBT, the total amount of SCMs, the fiber volume fraction, the fiber length, and the fiber aspect ratio. A summary of the relative importance of these variables in terms of their contribution to the variability of f_{R2} is provided in Figure 114. The expected values of standard deviation are shown for the 25th and 75th percentiles of each of the abovementioned variables, which correspond to the lower and upper limits of their typical ranges of variation as per the SFRC database.

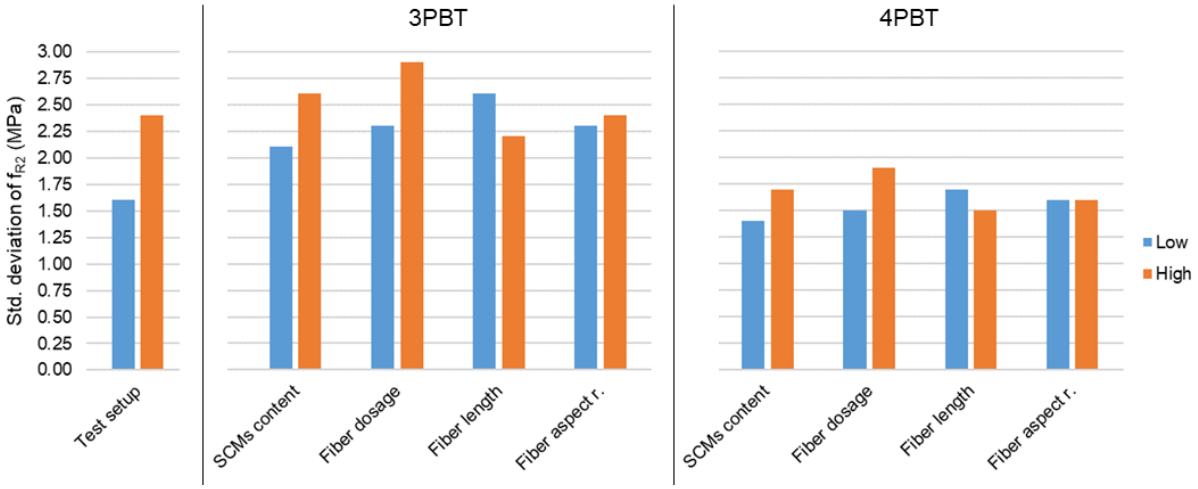

Figure 114. Expected standard deviation of f_{R2}: a summary.

The test being 3PBT or 4PBT, the amount of SCMs in the mixture, and the fiber volume fraction are the variables associated with the biggest changes of the expected standard deviation of f_{R2}. The fact that the variability of f_{R2} depends not only on the variables related to the fibers but also on the amount of SCMs in the SFRC mixture stresses, once again, the importance of considering all the mix design variables when proportioning SFRC mixtures. The effect of varying the fiber aspect ratio when considered within its typical range of values is almost negligible, and the effect of the fiber length is moderate.

The estimates of the standard deviation of f_{R2} shown in Figure 114 are within the range of 2.1 to 2.9 MPa (3PBT) or 1.4 to 1.9 MPa (4PBT). It can therefore be concluded that, for he majority of SFRC mixtures (i.e. when the mix design variables have values within their typical ranges of variation), $E(\sigma(f_{R2})|3PBT) = 2.5 \pm 0.4$ MPa and $E(\sigma(f_{R2})|4PBT) = 1.6 \pm 0.3$ MPa.

8.4 Variability of f_{R3}

8.4.1 Fitted model. The following equation was obtained for the estimator of the variance of f_{R3} in relation to the variables describing the SFRC mixture:

$$E[\sigma^2(f_{R3})] \cong \exp\big(t + 0.00283\,SCM + 0.00129\,C - 0.0172\,SP + 0.323\,G/S + 1.053\,V_f - 0.016\,l_f + 0.0312\,\lambda_f\big) \quad (95)$$

Where: t is a coefficient that depends on the test/specimen configuration, SCM is the total amount of supplementary cementitious materials in kg/m^3, C is the cement content in kg/m^3, SP is the amount of superplasticizer in kg/m^3, G/S is the coarse-to-fine aggregate ratio, V_f is the fiber volume fraction, l_f is the fiber length in mm, and λ_f is the fiber aspect ratio.

As with f_{R2}, the test/specimen configuration was found to have a statistically significant effect on the expected variance of f_{R3}. The coefficient t in equation (95) is: -1.102 when notched specimens are tested in the 3-point bending configuration (3PBT) and -1.735 when unnotched specimens are tested in the 4-point bending configuration (4PBT). Equation (95) can be rewritten as the following two equations, one for each test/specimen configuration:

$$E[\sigma^2(f_{R3})|\,3PBT] \cong 0.3322 \exp\big(0.00283\,SCM + 0.00129\,C - 0.0172\,SP + 0.323\,G/S + 1.053\,V_f - 0.016\,l_f + 0.0312\,\lambda_f\big) \quad (96)$$

$$E[\sigma^2(f_{R3})|\,4PBT] \cong 0.1764 \exp\big(0.00283\,SCM + 0.00129\,C - 0.0172\,SP + 0.323\,G/S + 1.053\,V_f - 0.016\,l_f + 0.0312\,\lambda_f\big) \quad (97)$$

8.4.2 Effect of the test configuration. Based on equations (96) and (97), the expected variance of f_{R3} when obtained from 3PBT tests is, on average, 0.3322/0.1764 = 1.88 times the variance of f_{R3} when determined in a 4PBT setup. In terms of standard deviation, the ratio is 1.37. This means that 3-point bending tests yield f_{R3} results with a standard deviation that is, on average, 37% higher than in the case of 4-point bending tests.

8.4.3 A general picture of the variability of f_{R3}. Using equations (96) and (97) and setting the mix design values to their median based on the SFRC database, a representative value of the variance of f_{R3} can be obtained. The median values are: SCM = 60 kg/m^3, C = 400 kg/m^3, SP = 4 kg/m^3, G/S = 1.0, V_f = 0.51%, l_f = 45 mm, and λ_f= 65. The expected variance of f_{R3} when obtained from 3PBT is 5.4 MPa^2, and the standard deviation is 2.3 MPa. In the case of 4PBT, the expected values of variance and standard deviation are 2.9 MPa^2 and 1.7 MPa, respectively.

A general estimate of the coefficient of variation of f_{R3} can be obtained assuming the median of f_{R3} for the mixtures in the SFRC database (4.3 MPa) and an estimate of the expected variance of this parameter. Bearing in mind that the ratio of the number of 3PBT cases to the number of 4PBT cases in the SFRC dataset is 2.2, the weighted average of the two variance values mentioned in the previous paragraph is 4.62 MPa^2, the standard deviation being 2.15 MPa. As a result, a representative value of the expected coefficient of variation of f_{R3} is 50%.

8.4.4 Sensitivity to the mix design variables. In Figures 115 and 116, the expected variance of f_{R3} as modelled by equations (96) and (97) is shown against the different mix design variables. The curves in red correspond to the 3PBT case, while the curves corresponding to 4PBT values are shown in blue. Unless stated otherwise, all the variance and standard deviation values referred to in the following paragraphs correspond to the 3PBT case.

Higher values of the fiber content and of the fiber aspect ratio are associated with higher values of the expected variance of f_{R3}. The trend followed by the expected variance of f_{R3} with respect to the fiber volume fraction is similar to that observed for the expected variance of f_{R2}. When the test is 3PBT, the variance estimates are in fact very close to those obtained for f_{R2}.

If a value of 0.4% is assumed for the fiber volume fraction, the expected variance and standard deviation of f_{R3} are 4.8 MPa^2 and 2.2 MPa, respectively. If a fiber volume fraction of 1.0% is

assumed, then the expected variance and standard deviation of f_{R3} increase to 9.0 MPa^2 and 3.0 MPa, respectively.

The effect of the fiber aspect ratio on the variance of f_{R3} is more prominent than its effect on the variance of f_{R2} or f_{R1}. Based on the plot in Figure 115, it is as important as the effect of the fiber content. In 50% of the SFRC mixtures in the database, the fiber aspect ratio ranges from 60 to 70. The expected variance and standard deviation of f_{R3} are 4.6 MPa^2 and 2.1 MPa when the fiber aspect ratio is assumed to be 60, and increase to 6.3 MPa^2 and 2.5 MPa if the fiber aspect ratio is 70.

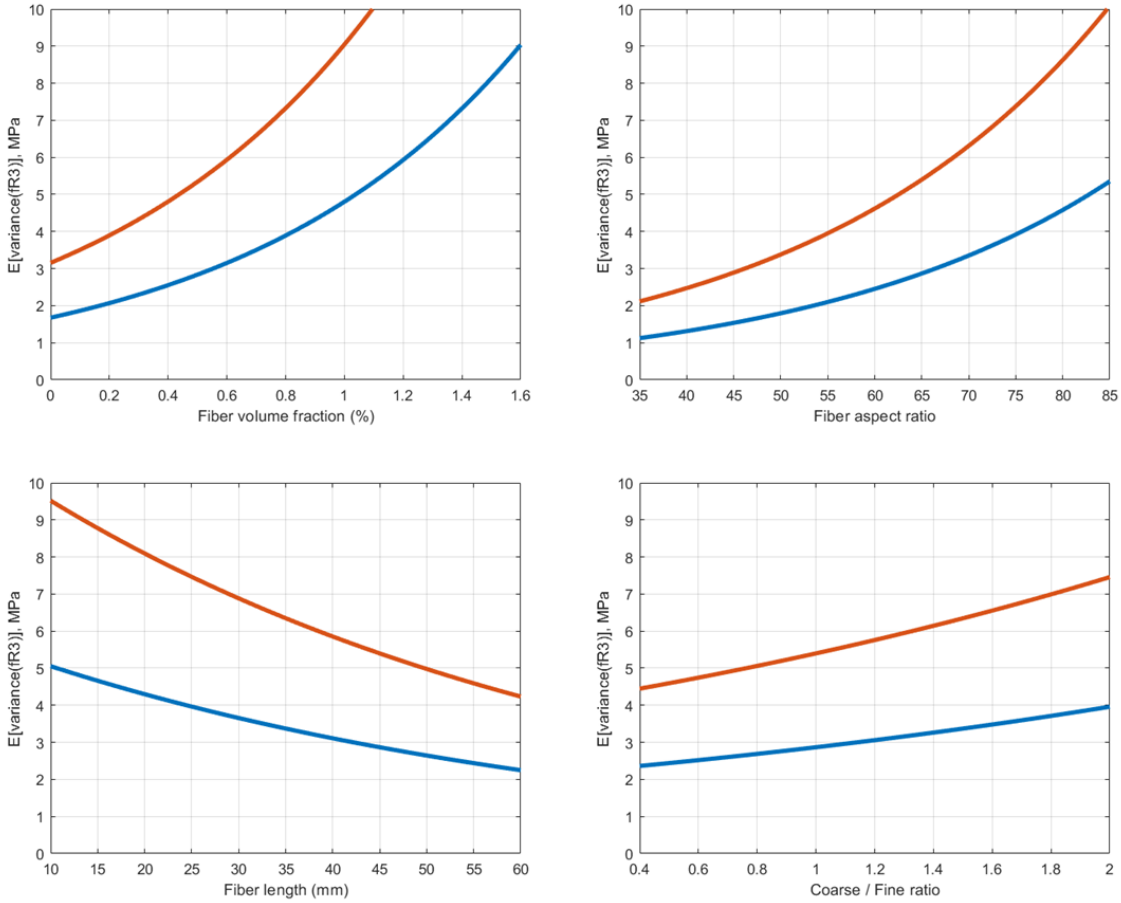

Figure 115. Expected variance of f_{R3} against the fiber volume fraction, fiber length, fiber aspect ratio, and the coarse-to-fine aggregate ratio.

Higher values of the fiber length are associated with decreasing values of the variance of f_{R3}, following a trend that is very similar to those observed in relation to f_{R1} and f_{R2}. The expected variance and standard deviation of f_{R3} are 6.9 MPa^2 and 2.6 MPa when a fiber length of 30 mm is assumed. These values drop to 3.6 MPa^2 and 1.9 MPa if the fiber length is 70 mm.

The effect of the coarse-to-fine aggregate ratio on the variability of f_{R3}, although statistically significant, is relatively minor, as can be seen in Figure 115. This is also the case in relation to the cement content, the total amount of SCMs, and the superplasticizer content, as the graphs in Figure 116 show. Higher values of the coarse-to-fine aggregate ratio, the cement content and the amount of SCMs are associated with a higher variance and standard deviation of f_{R3}, whilst increasing the superplasticizer content decreases them, albeit very slightly.

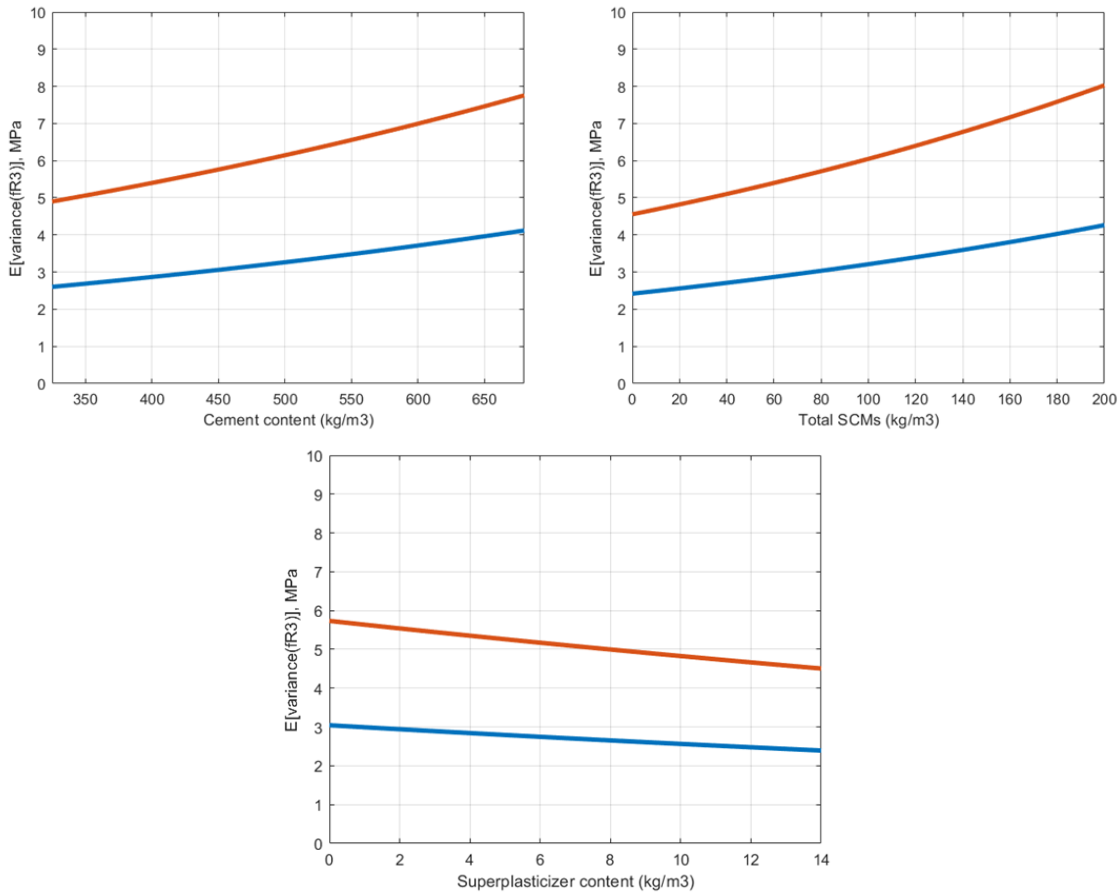

Figure 116. Expected variance of f_{R3} vs. the cement, SCMs, and superplasticizer contents.

8.4.5 Concluding remarks. Several variables have been identified as having a statistically significant effect on the variability of f_{R3}. The relative importance of each of them in terms of their contribution to the standard deviation of f_{R3} is summarized in Figure 117, where the 25th and 75th percentiles of each variable have been considered as representative of their typical ranges of variation in the SFRC database. These percentiles have been labelled as 'low' and 'high'. The bars in solid colors correspond to 3PBT conditions, whilst the patterned bars assume a 4PBT configuration.

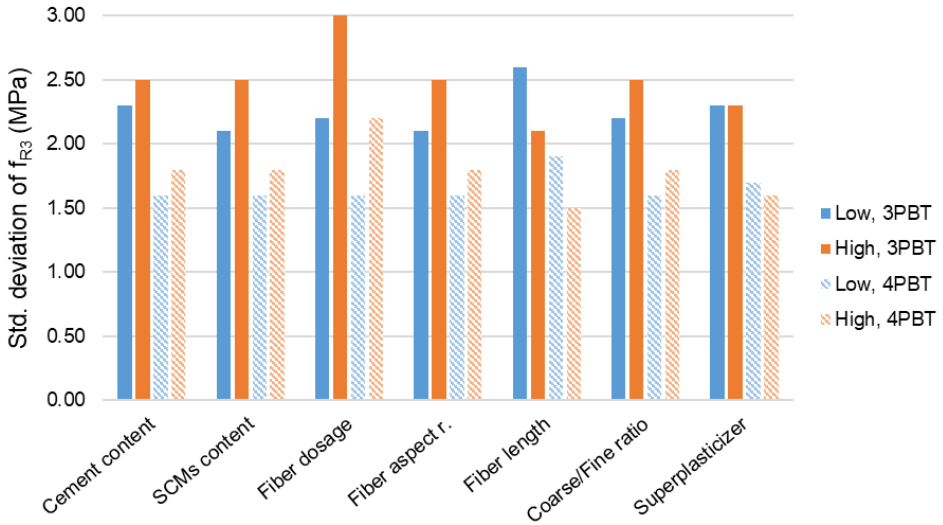

Figure 117. Expected standard deviation of f_{R3}: a summary.

The variables that, when varied within their typical ranges, have the most salient effect on the standard deviation of f_{R3} are: the test configuration (3PBT or 4PBT), the fiber volume fraction, the fiber length, and the fiber aspect ratio. The variability of f_{R3} is also moderately affected by the total amount of SCMs in the mixture and the coarse-to-fine aggregate ratio. On the other hand, variations of the amount of cement or the superplasticizer content within their typical ranges have an almost negligible impact on variability.

As per Figure 117, the expected values of the standard deviation of f_{R3} are typically within the following ranges: 2.1 to 3.0 MPa (3PBT), and 1.5 to 2.2 MPa (4PBT). In consequence, for typical SFRC mixtures, the following estimates can be retained as representative: $E(\sigma(f_{R3})|3PBT) = 2.5 \pm 0.4$ MPa and $E(\sigma(f_{R3})|4PBT) = 1.8 \pm 0.3$ MPa.

8.5 Variability of f_{R4}

8.5.1 Fitted model. The equation obtained for the estimator of the variance of f_{R4} is:

$$E[\sigma^2(f_{R4})] \cong \exp\Big(t + 0.00253\,SCM + 0.00325\,C - 0.019\,SP + 0.925\,V_f + 0.0313\,\lambda_f + 0.000828(G+S)\Big) \quad (98)$$

Where: the coefficient t depends on the test and specimen configuration, SCM is the amount of supplementary cementitious materials in kg/m^3, C is the cement content in kg/m^3, SP is the amount of superplasticizer in kg/m^3, V_f is the fiber volume fraction, λ_f is the fiber aspect ratio, and S and G are the amounts of fine and coarse aggregates, respectively, in kg/m^3.

Since the coefficient t in equation (98) is -3.88 (3PBT) or -4.26 (4PBT), equation (98) can be rewritten as the following two equations, one for each test/specimen configuration:

$$E[\sigma^2(f_{R4})|\,3PBT] \cong 0.02065 \exp\Big(0.00253\,SCM + 0.00325\,C - 0.019\,SP + 0.925\,V_f + 0.0313\,\lambda_f + 0.000828(G+S)\Big) \quad (99)$$

$$E[\sigma^2(f_{R4})|\,4PBT] \cong 0.01412 \exp\Big(0.00253\,SCM + 0.00325\,C - 0.019\,SP + 0.925\,V_f + 0.0313\,\lambda_f + 0.000828(G+S)\Big) \quad (100)$$

8.5.2 Effect of the test configuration. The ratio between equations (99) and (100), all mix design parameters being constant, is 0.02065/0.01412 = 1.46. That is, the expected variance of f_{R4} when measured in 3PBT conditions is, on average, 1.46 times the variance of f_{R4} if measured in 4PBT conditions. The square root of 1.46 is 1.21, which means that 3-point bending tests produce f_{R4} results with a standard deviation that is, on average, 21% higher than in the case of 4-point bending tests.

8.5.3 A general picture of the variability of f_{R4}. By setting the values of the variables in equations (99) and (100) to their median from the SFRC database, a representative value of the variance of f_{R4} can be obtained. If the test setup considered is 3PBT, the expected variance of f_{R4} is 4.2 MPa^2, which corresponds to a standard deviation of 2.0 MPa. If 4PBT conditions are assumed, the expected values of variance and standard deviation are 2.9 MPa^2 and 1.7 MPa, respectively.

Since the of the number of 3PBT vs 4PBT cases is 2.2, the weighed average of the two variance values mentioned above is 1.93 MPa. Considering that the median of f_{R4} for the mixtures in the SFRC dataset is 3.65 MPa, a representative value of the coefficient of variation of f_{R4} is 53%.

8.5.4 Sensitivity to the mix design variables. The expected variance of f_{R4} as modelled by equations (99) and (100) is shown against the different mix design variables in Figure 118. The curves in red correspond to the 3PBT case, while the curves corresponding to 4PBT conditions are shown in blue.

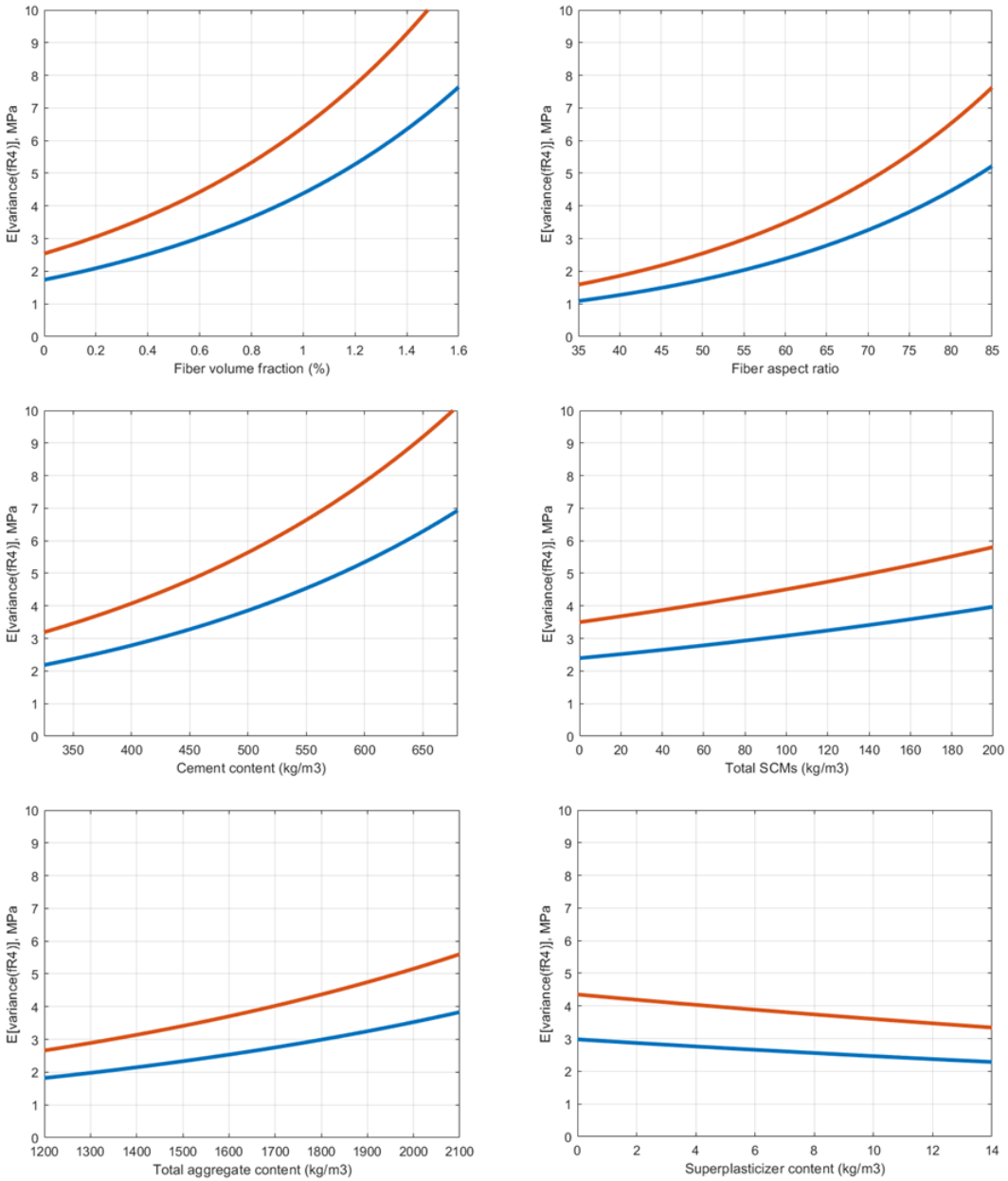

Figure 118. Expected variance of f_{R4} against different SFRC mix design variables.

Since the trends followed by the expected variance of f_{R4} with respect to the mix design variables are, as shown in Figure 118, largely consistent with those observed in relation to the variance of f_{R1}, f_{R2}, and f_{R3}, a detailed discussion is not repeated here. Figure 119 shows the estimates of the standard deviation of f_{R4} for the typical 'low' and 'high' values of each of the

variables (as per their 25th and 75th percentiles in the SFRC database) for both the 3PBT and 4PBT configurations.

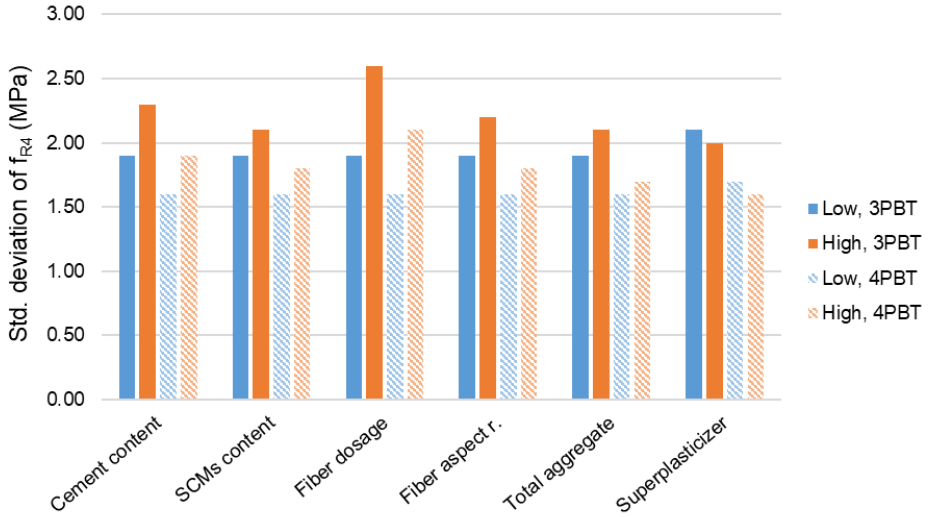

Figure 119. Expected standard deviation of f_{R4}: a summary.

The most relevant variables in terms of their influence on the variability of f_{R4} are: the test/specimen configuration, the fiber content, and the cement content. The fiber aspect ratio and the total amount of SCMs have a moderate importance. The total aggregate content and the amount of superplasticizer have only a relatively minor effect. When the values of the different mix design variables are within their typical range of variation, the standard deviation of f_{R4} can be expected to range from 1.9 to 2.6 MPa (3PBT), and from 1.6 to 2.1 MPa (4PBT). The following estimates can be regarded as representative in most cases: $E(\sigma(f_{R4})|3PBT) = 2.3 \pm 0.3$ MPa and $E(\sigma(f_{R4})|4PBT) = 1.8 \pm 0.3$ MPa.

8.6 Multivariate analysis: variability of *Z*

8.6.1 Fitted model. *Z* is the non-dimensional factor that compresses the information of all four residual flexural strength parameters, f_{R1}, f_{R2}, f_{R3}, and f_{R4}, and the limit of proportionality (see section 6.2). The equation obtained for the estimator of the variance of *Z* as a function of the SFRC mix design variables is the following:

$$E[\sigma^2(Z)] \cong \exp\Big(t + 0.00177\,SCM + 0.00206\,C + 0.921\,V_f + 0.0179\,\lambda_f + 0.00101(G+S)\Big) \quad (101)$$

Where: the coefficient *t* depends on the test and specimen configuration, *SCM* is the amount of supplementary cementitious materials in kg/m^3, *C* is the cement content in kg/m^3, V_f is the fiber volume fraction in percentage, λ_f is the fiber aspect ratio, and *S* and *G* are the amounts of fine and coarse aggregates, respectively, in kg/m^3.

Since the fitted values for the coefficient *t* in equation (101) are -6.92 and -7.33, for 3PBT and 4PBT conditions respectively, equation (101) can be rewritten as two separate equations, one for each test/specimen configuration:

$$E[\sigma^2(Z)|\,3PBT] \cong 0.000988 \exp\left(0.00177\,SCM + 0.00206\,C + 0.921\,V_f + 0.0179\,\lambda_f + 0.00101(G+S)\right) \quad (102)$$

$$E[\sigma^2(Z)|\,4PBT] \cong 0.000656 \exp\left(0.00177\,SCM + 0.00206\,C + 0.921\,V_f + 0.0179\,\lambda_f + 0.00101(G+S)\right) \quad (103)$$

8.6.2 General considerations. Some indicative values of the expected variance of *Z* can be obtained by assuming the median of the mix design variables in equations (102) and (103). If *Z* is calculated based on 3PBT results, the expected variance is, on average, 0.08. If *Z* is calculated from 4PBT results, it can be expected to have an average variance of 0.05. These values, however, provide little context. The variability of *Z* cannot be discussed in the same way as the variability of the individual residual flexural strength parameters has been dealt with in the preceding sections. There are three fundamental differences: by definition, *Z* is non-dimensional (i.e. it has no units), its average is zero, and it takes positive and negative values (in fact, the median for the SFRC mixes in the dataset compiled in this study is -0.27). As a result, the standard deviation and the variance of *Z* are not dimensionally different (both are nondimensional) and the coefficient of variation as a representative measure, so common in concrete technology, is not applicable because it would be a division by zero.

The interest of having fitted equation (101) is, therefore, not that it can be used to estimate the variance or standard deviation of a directly measurable parameter, because it cannot. Rather, its significance resides on the fact that it makes it possible to optimize SFRC mix designs so that the 'global' variability of the residual flexural strength can be minimized, and that this can be done using one explicit equation.

8.6.3 Effect of the test configuration. All the mix design variables being constant, the ratio between equations (102) and (103) above is 0.000988/0.000656 = 1.51. This means that the expected variance of *Z* when calculated based on specimens tested in 3PBT conditions is, on average, 51% higher than when calculated based on data obtained in 4PBT conditions. Since the square root of 1.51 is 1.23, the expected standard deviation of *Z* when calculated from 3PBT results is 23% higher than when obtained from 4PBT results. This quantification of the effect of 3PBT/4PBT conditions on the variability of *Z* is highly consistent with the findings presented in the previous sections in relation to the individual residual flexural strength parameters.

8.6.4 Sensitivity to the mix design variables. Figure 120 shows the graphs where the expected variance of *Z* is shown against the mix design variables that appear in equations (102) and (103). The colors red and blue correspond to 3PBT and 4PBT, respectively.

It can be seen that all the mix design variables that have a statistically significant effect on the expected variance of *Z* introduce trends in the same direction: when the value of any of these variables increases, so does the expected variance of *Z*.

None of the variables that are inversely correlated with the expected variance of some of the residual flexural strength parameters (the superplasticizer content, the fiber length, and the maximum aggregate size) have a statistically significant effect on the expected variance of *Z*. This is probably because, when all the residual flexural strength parameters are aggregated in one single factor, the influence of those variables becomes not significantly different to the noise or unattributable variation.

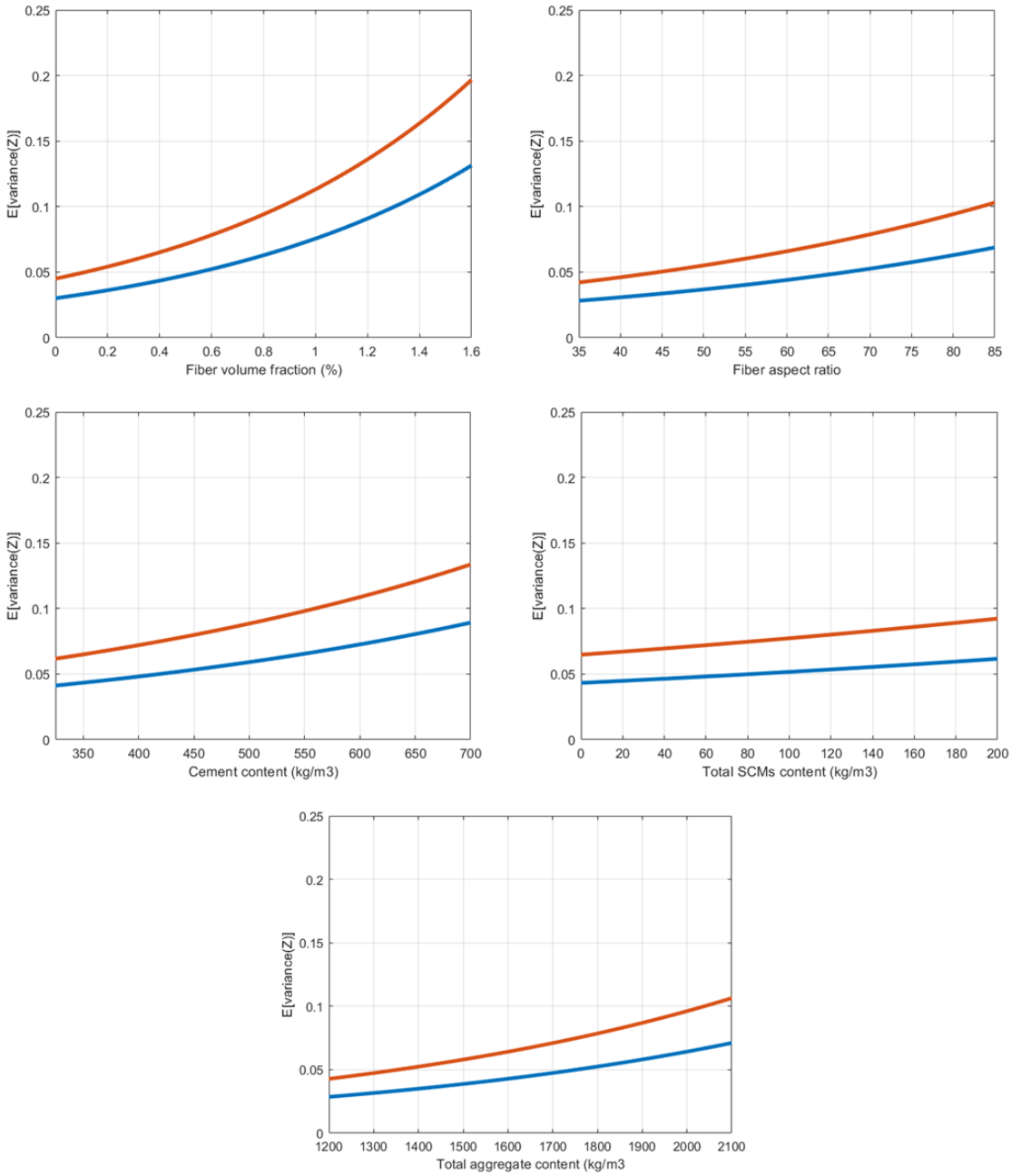

Figure 120. Expected variance of Z against different SFRC mix design variables.

The plots in Figure 120 show that the variables with a most prominent effect on the expected variance of Z are the fiber volume fraction and the cement content, together with the test/specimen configuration. The total aggregate content and the fiber aspect ratio have a moderate influence on the variability of Z, whilst the effect of the total amount of SCMs is relatively minor.

The trends followed by the variance of Z with respect to each of these variables are all consistent with the trends observed in relation to the variance of each of the residual flexural strength parameters, separately, in the preceding sections of this chapter.

The values of the different mix design variables can be set to their 25th and 75th percentiles as representative of their typical range of variation in the SFRC database. These are labelled as 'low' and 'high', respectively, in Figure 121, where the expected variance of Z is shown

assuming either 3PBT or 4PBT conditions. Figure 121 shows that increasing the fiber volume fraction from 'low' to 'high' (i.e. from 0.4% to 1.0%) is associated with the expected variance of *Z* going up by 71%, that is, the standard deviation increasing by 31% on average. If any of the other mix design variables is increased from 'low' to 'high', the expected variance of *Z* never goes up by more than 32%, the standard deviation by 15%.

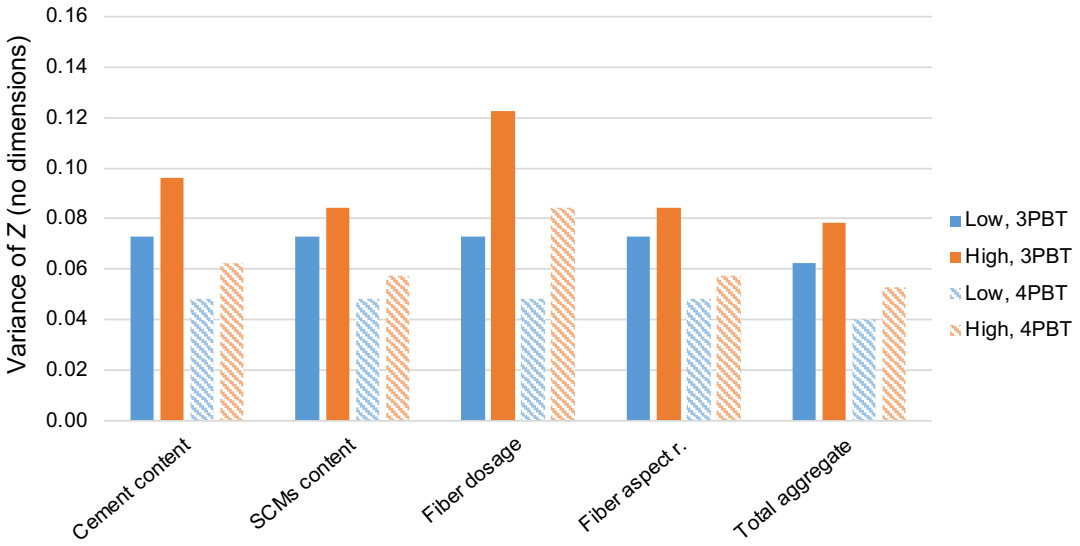

Figure 121. Expected variance of Z: a summary.

9. Summary and conclusions

- A database of SFRC mixtures and a database of synthetic FRC mixtures have been compiled from papers published over the last two decades and used as the basis for this study. The information compiled on SFRC mixtures constitutes a coherent set of data where the main sources of variability are clear, providing the basis for the development of robust models and conclusions. This has proven more challenging in relation to synthetic FRC mixtures.
- A detailed statistical analysis of hundreds of FRC mixtures has made it possible to define indicative averages, truly representative minimum and maximum values, and typical ranges of values for each of the different mix design variables, including the fiber length and the fiber aspect ratio, which describe current practice.
- The semi-empirical analysis of the database of SFRC mixtures reveals that the relationships between the relative amounts of the mixture constituents are adequately described by a set of four equations. These can be used as a first approximation to the proportioning of SFRC mixtures based on the following inputs: the fiber content, length and aspect ratio; the maximum aggregate size, and the water-to-cement ratio.
- A unified model has been obtained which relates the residual flexural capacity of FRC to the mixture proportions, the maximum aggregate size, the fiber length and the fiber aspect ratio. The same equation can be used to estimate any of the residual flexural strength parameters of SFRC or synthetic FRC (with PP or PO fibers) in 3PBT or 4PBT conditions, considering notched or unnotched specimens, by simply changing the values of the coefficients in the equation. The model is robust, parsimonious and sufficiently accurate (R-squared between 74% and 86%).
- On average, the values of the residual flexural strength parameters obtained by testing notched specimens in 3PBT conditions are between 0.74-1.26 MPa higher than by testing unnotched specimens in 4PBT conditions.
- The effect of the fiber length and the fiber aspect ratio on the residual flexural capacity is comparable in magnitude to that of the fiber volume fraction. It is possible to obtain better-than-average levels of performance by varying the fiber length and/or the fiber aspect ratio without requiring high dosages of fibers. For example, in SFRC, increasing the fiber volume fraction beyond 0.7%-0.8% is hardly justified.
- One key aspect that repeatedly emerges from the different analyses reported in this document is that there is a clear connection between the cohesiveness of the fresh FRC mixture and its residual flexural capacity. The interplay between the coarse-to-fine aggregate ratio, the amount of SCMs and the cement content is key to maximizing the efficiency of fibers. Simple equations and plots have been developed to illustrate in what cases a certain amount of SCMs is necessary.
- The multivariate analysis of the residual flexural strength parameters has led to the definition of a unique, non-dimensional parameter (Z) that can be used to predict whether

the residual flexural capacity of a SFRC mixture is good, optimal, or sub-optimal, based on the mixture proportions.

- It has been demonstrated that the mix design variables representing the binder composition and the aggregates content and combined grading explain 49% of the differences in residual flexural strength parameters, as opposed to the 51% explained by the variables directly related to the fibers. This proves that the residual flexural capacity of FRC is heavily influenced by variables other than the fibers and supports the idea that proportioning FRC mixtures mainly by modifying the fiber content is not a good approach.
- The variability of the residual flexural strength parameters has also been studied, and equations have been obtained to estimate their standard deviation as a function of the mixture proportions, the fiber dimensions, and the test/specimen configuration (3PBT or 4PBT).
- The mixture proportions and the dimensions of the fibers have a significant effect on the intrinsic variability of the residual flexural strength parameters. The equations obtained, jointly with the model for the residual flexural strength parameters, makes it possible to maximize their value and minimize their variability at the same time.
- The standard deviation of the residual flexural strength results obtained from testing notched specimens in 3PBT conditions can be up to 49% higher than that of results obtained from unnotched specimens in 4PBT conditions. Generally speaking, the coefficient of variation of the residual flexural strength parameters can typically range from 30% to 50%.

Appendix A

Abdallah, Sadoon, Mizi Fan, Xiangming Zhou, and Simon Le Geyt. "Anchorage effects of various steel fibre architectures for concrete reinforcement." International Journal of Concrete Structures and Materials 10, no. 3 (2016): 325-335.

Altun, Fatih, and Bekir Aktaş. "Investigation of reinforced concrete beams behavior of steel fiber added lightweight concrete." Construction and Building Materials 38 (2013): 575-581.

Amirineni, Krishna C. "Fracture properties of fiber reinforced concrete." (2009).

Aoude, Hassan, and Michael Cohen. "Shear response of SFRC beams constructed with SCC and Steel Fibers." Electron. J. Struct. Eng 14 (2014): 71-83.

Barros, Joaquim AO, and J. A. B. Antunes. "Experimental characterization of the flexural behaviour of steel fibre reinforced concrete according to RILEM TC 162-TDF recommendations." RILEM TC 162 (2003): 77-89.

Barros, Joaquim AO, and José Sena-Cruz. "Fracture energy of steel fibre reinforced concrete." Journal of Mechanics of Composite Materials and Structures 8, no. 1 (2001): 29-45.

Bencardino, Francesco, Lidia Rizzuti, Giuseppe Spadea, and Ramnath Narayan Swamy. "Implications of test methodology on post-cracking and fracture behaviour of steel fibre reinforced concrete." Composites Part B: Engineering 46 (2013): 31-38.

Bhosale, Aniket, M. Abdur Rasheed, S. Suriya Prakash, and Gangadharan Raju. "A study on the efficiency of steel vs. synthetic vs. hybrid fibers on fracture behavior of concrete in flexure using acoustic emission." Construction and Building Materials 199 (2019): 256-268.

Bosman, Tiaan, and Elsabe P. Kearsley. "The influence of fibre spatial characteristics on the flexural performance of SFRC." Materials and Structures 52, no. 3 (2019): 51.

Boulekbache, Bensaid, Mostefa Hamrat, Mohamed Chemrouk, and Sofiane Amziane. "Flowability of fibre-reinforced concrete and its effect on the mechanical properties of the material." Construction and Building Materials 24, no. 9 (2010): 1664-1671.

Casas Tuneu, Joan. "Assessment of fibre distribution and orientation within SFRC precast segments." Bachelor's thesis, Universitat Politècnica de Catalunya, 2015.

Cho, Hyun-Woo, Jae-Heum Moon, and Jang-Hwa Lee. "The Effects of Aggregate Sizes and Fiber Volume Fraction on Bending Toughness and Direct Tension of Steel Fiber Reinforced Concrete." World Academy of Science, Engineering and Technology, International Journal of Civil, Environmental, Structural, Construction and Architectural Engineering 6, no. 10 (2012): 816-820.

Choi, O. C., and C. Lee. "Flexural performance of ring-type steel fiber-reinforced concrete." Cement and concrete research 33, no. 6 (2003): 841-849.

Choi, Won-Chang, Kwon-Young Jung, Seok-Joon Jang, and Hyun-Do Yun. "The Influence of Steel Fiber Tensile Strengths and Aspect Ratios on the Fracture Properties of High-Strength Concrete." Materials 12, no. 13 (2019): 2105.

Concrete, Ultra High Performance, M. Schmidt, E. Fehling, and C. Geisenhansluke. "Ultra High Performance Concrete (UHPC)." (2004).

de Montaignac, Renaud, Bruno Massicotte, Jean-Philippe Charron, and Ali Nour. "Design of SFRC structural elements: post-cracking tensile strength measurement." Materials and Structures 45, no. 4 (2012): 609-622.

De Smedt, Maure, Kristof De Wilder, Lucie Vandewalle, and Els Verstrynge. "Acoustic Emission-based analysis of damage mechanisms in steel fibre reinforced concrete under monotonic and cyclic loading." In Proceedings of the 10th International Conference on Fracture Mechanics of Concrete and Concrete Structures, pp. 1-11. IA-FraMCoS, 2019.

Di Prisco, Marco, Matteo Colombo, and Ali Pourzarabi. "Biaxial bending of SFRC slabs: Is conventional reinforcement necessary?" Materials and Structures 52, no. 1 (2019): 1.

Ding, Yining. "Investigations into the relationship between deflection and crack mouth opening displacement of SFRC beam." Construction and Building Materials 25, no. 5 (2011): 2432-2440.

Domski, Jacek. "A blurred border between ordinary concrete and SFRC." Construction and Building Materials 112 (2016): 247-252.

Facconi, Luca, Fausto Minelli, and Giovanni Plizzari. "Steel fiber reinforced self-compacting concrete thin slabs–Experimental study and verification against Model Code 2010 provisions." Engineering Structures 122 (2016): 226-237.

García-Taengua, Emilio, José R. Martí-Vargas, and Pedro Serna-Ros. "Statistical approach to effect of factors involved in bond performance of steel fiber-reinforced concrete." ACI Structural Journal 108, no. 4 (2011): 461-468.

Germano, Federica, and Giovanni A. Plizzari. "Fatigue behavior of SFRC under bending." In Proceedings of the Eighth RILEM Intnl. Symp. on Fibre Reinforced Concrete: challenges and opportunities, (BEFIB 2012), pp. 19-21. 2012.

Giaccio, G., J. M. Tobes, and Raul Zerbino. "Use of small beams to obtain design parameters of fibre reinforced concrete." Cement and Concrete Composites 30, no. 4 (2008): 297-306.

Gouveia, Nuno D., Nelson AG Fernandes, Duarte MV Faria, António MP Ramos, and Válter JG Lúcio. "SFRC flat slabs punching behaviour–Experimental research." Composites Part B: Engineering 63 (2014): 161-171.

Holschemacher, K., T. Mueller, and Y. Ribakov. "Effect of steel fibres on mechanical properties of high-strength concrete." Materials & Design (1980-2015) 31, no. 5 (2010): 2604-2615.

Holschemacher, Klaus, and Torsten Müller. "Influence of fibre type on hardened properties of steel fibre reinforced concrete." Leipzig University of Applied Sciences (HTWK Leipzig), Departament of civil Enginieering (2007).

Iqbal, Shahid, Ahsan Ali, Klaus Holschemacher, and Thomas A. Bier. "Mechanical properties of steel fiber reinforced high strength lightweight self-compacting concrete (SHLSCC)." Construction and Building Materials 98 (2015): 325-333.

Jones, Peter A., Simon A. Austin, and Peter J. Robins. "Predicting the flexural load–deflection response of steel fibre reinforced concrete from strain, crack-width, fibre pull-out and distribution data." Materials and Structures 41, no. 3 (2008): 449-463.

Kaïkea, Adel, Djamel Achoura, François Duplan, and Lidia Rizzuti. "Effect of mineral admixtures and steel fiber volume contents on the behavior of high performance fiber reinforced concrete." Materials & Design 63 (2014): 493-499.

Kang, Su-Tae, and Jin-Keun Kim. "Investigation on the flexural behavior of UHPCC considering the effect of fiber orientation distribution." Construction and Building Materials 28, no. 1 (2012): 57-65.

Kelpša, Šarūnas, Mindaugas Augonis, Mindaugas Daukšys, and Algirdas Augonis. "Analysis of crack width calculation of steel fibre and ordinary reinforced concrete flexural members." Journal of Sustainable Architecture and Civil Engineering 6, no. 1 (2014): 50-57.

Kim, Wha-Jung, M. S. Kwak, and J. C. Lee. "Fracture properties of high-strength steel fiber concrete." In Proceedings of the Korea Concrete Institute Conference. Korea Concrete Institute, 2010.

Köksal, Fuat, Fatih Altun, İlhami Yiğit, and Yuşa Şahin. "Combined effect of silica fume and steel fiber on the mechanical properties of high strength concretes." Construction and building materials 22, no. 8 (2008): 1874-1880.

Komarkova, T., J. Lanik, L. Topolar, J. Stoller, and P. Stonis. "Experimental assessment of steel fibre reinforced concretes with different concentrations of fibres." In IOP Conference Series: Materials Science and Engineering, vol. 385, no. 1, p. 012028. IOP Publishing, 2018.

Kurihara, Norihiko, Minoru Kunieda, Toshiro Kamada, Yuichi Uchida, and Keitetsu Rokugo. "Tension softening diagrams and evaluation of properties of steel fiber reinforced concrete." Engineering Fracture Mechanics 65, no. 2-3 (2000): 235-245.

Lee, Jong-Han, Baiksoon Cho, and Eunsoo Choi. "Flexural capacity of fiber reinforced concrete with a consideration of concrete strength and fiber content." Construction and Building Materials 138 (2017): 222-231.

Lee, Jong-Han. "Influence of concrete strength combined with fiber content in the residual flexural strengths of fiber reinforced concrete." Composite Structures 168 (2017): 216-225.

Lee, M. K., and B. I. G. Barr. "A four-exponential model to describe the behaviour of fibre reinforced concrete." Materials and structures 37, no. 7 (2004): 464-471.

Lim, Sopokhem, Ramiz Ahmed Raju, Mitsuhiro Matsuda, Takehiro Okamoto, and Mitsuyoshi Akiyama. "Structural behavior prediction of SFRC beams by a novel integrated approach of X-ray imaging and finite element method." Construction and Building Materials 170 (2018): 347-365.

Mahmud, Goran H., Zhenjun Yang, and Aram MT Hassan. "Experimental and numerical studies of size effects of Ultra High Performance Steel Fibre Reinforced Concrete (UHPFRC) beams." Construction and Building Materials 48 (2013): 1027-1034.

Michels, Julien, Rouven Christen, and Danièle Waldmann. "Experimental and numerical investigation on postcracking behavior of steel fiber reinforced concrete." Engineering Fracture Mechanics 98 (2013): 326-349.

Mínguez, Jesús, Dorys C. González, and Miguel A. Vicente. "Fiber geometrical parameters of fiber-reinforced high strength concrete and their influence on the residual post-peak flexural tensile strength." Construction and Building Materials 168 (2018): 906-922.

Paegle, Ieva, Fausto Minelli, and Gregor Fischer. "Cracking and load-deformation behavior of fiber reinforced concrete: Influence of testing method." Cement and Concrete Composites 73 (2016): 147-163.

Pająk, M., and T. Ponikiewski. "Flexural behavior of self-compacting concrete reinforced with different types of steel fibers." Construction and Building materials 47 (2013): 397-408.

Pająk, Małgorzata, and Tomasz Ponikiewski. "Investigation on concrete reinforced with two types of hooked fibers under flexure." Procedia Engineering 193 (2017): 128-135.

Papachristoforou, Michail, and Ioanna Papayianni. "Radiation shielding and mechanical properties of steel fiber reinforced concrete (SFRC) produced with EAF slag aggregates." Radiation Physics and Chemistry 149 (2018): 26-32.

Parmentier, Benoit, Petra Van Itterbeeck, and Audrey Skowron. "The flexural behaviour of SFRC flat slabs: the Limelette full-scale experiments for supporting design model codes." In Proceedings of FRC. 2014.

Pereira, E. N. B., Joaquim AO Barros, Alberto F. Ribeiro, and Aires Camões. "Post-cracking behaviour of selfcompacting steel fibre reinforced concrete." (2004).

Pereira, E. N. B., Joaquim AO Barros, Vitor MCF Cunha, and S. P. F. Santos. "Compression and bending behavior of steel fiber reinforced self-compacting concrete." (2005).

Poveda, Elisa, Gonzalo Ruiz, Hector Cifuentes, C. Yu Rena, and Xiaoxin Zhang. "Influence of the fiber content on the compressive low-cycle fatigue behavior of self-compacting SFRC." International Journal of Fatigue 101 (2017): 9-17.

Randl, N., and F. Däuber. "Material properties of fibre reinforced UHPC." In 8th RILEM international symposium on fibre reinforced concrete: challenges and opportunities. PRO, vol. 88. 2012.

Rizzuti, Lidia, and Francesco Bencardino. "Effects of fibre volume fraction on the compressive and flexural experimental behaviour of SFRC." Contemporary Engineering Sciences 7, no. 8 (2014): 379-390.

Şahin, Yuşa, and Fuat Köksal. "The influences of matrix and steel fibre tensile strengths on the fracture energy of high-strength concrete." Construction and Building Materials 25, no. 4 (2011): 1801-1806.

Salehian, Hamidreza, and Joaquim AO Barros. "Assessment of the performance of steel fibre reinforced self-compacting concrete in elevated slabs." Cement and Concrete Composites 55 (2015): 268-280.

Sarmiento, E. V., G. Zirgulis, S. Fine aggregatebakk, M. R. Geiker, and T. Kanstad. "Influence of concrete flow on fibre distribution, orientation and mechanical properties of fibre reinforced concrete." In BEFIB2012—8th RILEM international symposium of fibre reinforced concrete, Guimaraes, Portugal, pp. 1-12. 2012.

Sharma, Satish, V. V. Arora, Suresh Kumar, Y. N. Daniel, and Ankit Sharma. "Durability Study of High-Strength Steel Fiber-Reinforced Concrete." ACI Materials Journal 115, no. 2 (2018): 219-225.

Soetens, Tim, and Stijn Matthys. "Different methods to model the post-cracking behaviour of hooked-end steel fibre reinforced concrete." Construction and Building Materials 73 (2014): 458-471.

Soulioti, D. V., N. M. Barkoula, A. Paipetis, and T. E. Matikas. "Effects of fibre geometry and volume fraction on the flexural behaviour of steel-fibre reinforced concrete." Strain 47 (2011): e535-e541.

Soulioti, D., N. M. Barkoula, A. Paipetis, T. E. Matikas, T. Shiotani, and D. G. Aggelis. "Acoustic emission behavior of steel fibre reinforced concrete under bending." Construction and Building Materials 23, no. 12 (2009): 3532-3536.

Stähli, Patrick, Rocco Custer, and Jan GM van Mier. "On flow properties, fibre distribution, fibre orientation and flexural behaviour of FRC." Materials and Structures 41, no. 1 (2008): 189-196.

Tadepalli, Padmanabha Rao, Y. L. Mo, and Thomas TC Hsu. "Mechanical properties of steel fibre concrete." Magazine of Concrete Research 65, no. 8 (2013): 462-474.

Vandewalle, Lucie, Gert Heirman, and Filip Van Rickstal. "Fibre orientation in self-compacting fibre reinforced concrete." In Proc. of the 7th Int. RILEM Symp. on Fibre Reinforced Concrete: Design and Applications (BEFIB2008), pp. 719-728. RILEM Publications SARL; Bagneux, 2008.

Venkateshwaran, Akshay, Kiang Hwee Tan, and Yi Li. "Residual flexural strengths of steel fiber reinforced concrete with multiple hooked-end fibers." Structural Concrete 19, no. 2 (2018): 352-365.

Wu, Zemei, Caijun Shi, Wen He, and Linmei Wu. "Effects of steel fiber content and shape on mechanical properties of ultra high performance concrete." Construction and building materials 103 (2016): 8-14.

Xie, Jian-he, Yong-chang Guo, Li-sha Liu, and Zhi-hong Xie. "Compressive and flexural behaviours of a new steel-fibre-reinforced recycled aggregate concrete with crumb rubber." Construction and Building materials 79 (2015): 263-272.

Yoo, Doo-Yeol, Soonho Kim, Gi-Joon Park, Jung-Jun Park, and Sung-Wook Kim. "Effects of fiber shape, aspect ratio, and volume fraction on flexural behavior of ultra-high-

performance fiber-reinforced cement composites." Composite Structures 174 (2017): 375-388.

Yoo, Doo-Yeol, Su-Tea Kang, and Young-Soo Yoon. "Effect of fiber length and placement method on flexural behavior, tension-softening curve, and fiber distribution characteristics of UHPFRC." Construction and Building materials 64 (2014): 67-81.

Yoo, Doo-Yeol, Su-Tea Kang, Joo-Ha Lee, and Young-Soo Yoon. "Effect of shrinkage reducing admixture on tensile and flexural behaviors of UHPFRC considering fiber distribution characteristics." Cement and concrete research 54 (2013): 180-190.

Yoo, Doo-Yeol, Young-Soo Yoon, and Nemkumar Banthia. "Predicting the post-cracking behavior of normal-and high-strength steel-fiber-reinforced concrete beams." Construction and Building Materials 93 (2015): 477-485.

Zerbino, Raúl L., and Bryan E. Barragán. "Long-Term Behavior of Cracked Steel Fiber-Reinforced Concrete Beams under Sustained Loading." ACI Materials Journal 109, no. 2 (2012).

Zhang, Jun, and Victor C. Li. "Simulation of crack propagation in fiber-reinforced concrete by fracture mechanics." Cement and Concrete Research 34, no. 2 (2004): 333-339.

Zhang, Shengli, Changsuo Zhang, and Lin Liao. "Investigation on the relationship between the steel fibre distribution and the post-cracking behaviour of SFRC." Construction and Building Materials 200 (2019): 539-550.

Zhang, Shengli, Lin Liao, Shuizhou Song, and Changsuo Zhang. "Experimental and analytical study of the fibre distribution in SFRC: A comparison between image processing and the inductive test." Composite Structures 188 (2018): 78-88.

Appendix B

Abaeian, Reza, Hamid Pesaran Behbahani, and Shahram Jalali Moslem. "Effects of high temperatures on mechanical behavior of high strength concrete reinforced with high performance synthetic macro polypropylene (HPP) fibres." Construction and Building Materials 165 (2018): 631-638.

Afroughsabet, Vahid, and Togay Ozbakkaloglu. "Mechanical and durability properties of high-strength concrete containing steel and polypropylene fibers." Construction and building materials 94 (2015): 73-82.

Alani, Amir M., and Derrick Beckett. "Mechanical properties of a large scale synthetic fibre reinforced concrete ground slab." Construction and Building Materials 41 (2013): 335-344.

Alani, Amir, and Morteza Aboutalebi. "Mechanical properties of fibre reinforced concrete-a comparative experimental study." International Journal of Civil, Environmental, Structural, Construction and Architectural Engineering 7, no. 9 (2013): 646-651.

Alani, Amir, Morteza Aboutalebi, and Martin J. King. "Influence of fibre content on crack propagation rate in fibre-reinforced concrete beams." International Journal of Civil, Environmental, Structural, Construction and Architectural Engineering 7, no. 9 (2013): 1-7.

Alberti, M. G., A. Enfedaque, and J. C. Gálvez. "Comparison between polyolefin fibre reinforced vibrated conventional concrete and self-compacting concrete." Construction and Building Materials 85 (2015): 182-194.

Alberti, M. G., A. Enfedaque, and J. C. Gálvez. "Fracture mechanics of polyolefin fibre reinforced concrete: Study of the influence of the concrete properties, casting procedures, the fibre length and specimen size." Engineering Fracture Mechanics 154 (2016): 225-244.

Alberti, M. G., A. Enfedaque, and J. C. Gálvez. "On the mechanical properties and fracture behavior of polyolefin fiber-reinforced self-compacting concrete." Construction and building materials 55 (2014): 274-288.

Alberti, M. G., A. Enfedaque, J. C. Gálvez, and A. Cortez. "Optimisation of fibre reinforcement with a combination strategy and through the use of self-compacting concrete." Construction and Building Materials 235 (2020): 117289.

Alberti, M. G., A. Enfedaque, J. C. Gálvez, and V. Agrawal. "Reliability of polyolefin fibre reinforced concrete beyond laboratory sizes and construction procedures." Composite Structures 140 (2016): 506-524.

Alberti, Marcos G., Alejandro Enfedaque, Jaime C. Gálvez, and Carlos Álvarez. "Using Polyolefin Fibers with Moderate-Strength Concrete Matrix to Improve Ductility." Journal of Materials in Civil Engineering 31, no. 9 (2019): 04019170.

Alberti, Marcos G., Alejandro Enfedaque, Jaime C. Gálvez, and Luis Pinillos. "Structural Cast-in-Place Application of Polyolefin Fiber–Reinforced Concrete in a Water Pipeline

Supporting Elements." Journal of Pipeline Systems Engineering and Practice 8, no. 4 (2017): 05017002.

Amin, Ali, Stephen J. Foster, R. Ian Gilbert, and Walter Kaufmann. "Material characterisation of macro synthetic fibre reinforced concrete." Cement and Concrete Composites 84 (2017): 124-133.

Aslani, Farhad, and Morteza Bastami. "Relationship between deflection and crack mouth opening displacement of self-compacting concrete beams with and without fibers." Mechanics of Advanced Materials and Structures 22, no. 11 (2015): 956-967.

Babafemi, Adewumi John, and William Peter Boshoff. "Testing and modelling the creep of cracked macro-synthetic fibre reinforced concrete (MSFRC) under flexural loading." Materials and Structures 49, no. 10 (2016): 4389-4400.

Babafemi, Adewumi John. "Tensile creep of cracked macro synthetic fibre reinforced concrete." PhD diss., Stellenbosch: Stellenbosch University, 2015.

Badogiannis, E. G., K. I. Christidis, and G. E. Tzanetatos. "Evaluation of the mechanical behavior of pumice lightweight concrete reinforced with steel and polypropylene fibers." Construction and Building Materials 196 (2019): 443-456.

Bendjillali, K., M. Chemrouk, and B. Boulekbache. "Recycled synthetic waste fibres for the reinforcement of concrete." In WASTES–Solutions, Treatments and Opportunities II, pp. 9-15. CRC Press, 2017.

Bester, Hermanus Lambertus. "Generic model for predicting the performance of macro-synthetic fibre reinforced concrete for industrial flooring applications." PhD diss., Stellenbosch: Stellenbosch University, 2017.

Bhosale, Aniket, M. Abdur Rasheed, S. Suriya Prakash, and Gangadharan Raju. "A study on the efficiency of steel vs. synthetic vs. hybrid fibers on fracture behavior of concrete in flexure using acoustic emission." Construction and Building Materials 199 (2019): 256-268.

Borg, Ruben Paul, Owen Baldacchino, and Liberato Ferrara. "Early age performance and mechanical characteristics of recycled PET fibre reinforced concrete." Construction and Building Materials 108 (2016): 29-47.

Boulekbache, Bensaid, Mostefa Hamrat, Mohamed Chemrouk, and Sofiane Amziane. "Flowability of fibre-reinforced concrete and its effect on the mechanical properties of the material." Construction and Building Materials 24, no. 9 (2010): 1664-1671.

Buratti, N., and C. Mazzotti. "Experimental tests on the effect of temperature on the long-term behaviour of macrosynthetic Fibre Reinforced Concretes." Construction and Building Materials 95 (2015): 133-142.

Buratti, N., C. Mazzotti, and M. Savoia. "Experimental study on the flexural behaviour of fibre reinforced concretes strengthened with steel and macro-synthetic fibres." Fracture Mechanics of Concrete and Concrete Structures-Assessment, Proceedings of FraMCoS-7, May (2010): 23-28.

Buratti, Nicola, Claudio Mazzotti, and Marco Savoia. "Identification of Constitutive Relationships for Fibre Reinforced Concretes by Inverse Analysis."

Buratti, Nicola, Claudio Mazzotti, and Marco Savoia. "Post-cracking behaviour of steel and macro-synthetic fibre-reinforced concretes." Construction and Building Materials 25, no. 5 (2011): 2713-2722.

Çelik, Zinnur, and Ahmet Ferhat Bingöl. "Effect of basalt, polypropylene and macro-synthetic fibres on workability and mechanical properties of self-compacting concrete." CHALLENGE 5, no. 2 (2019): 35-41.

Chiranjeevi Reddy, Kamasani, and Kolluru VL Subramaniam. "Experimental investigation of crack propagation and post-cracking behaviour in macrosynthetic fibre reinforced concrete." Magazine of Concrete Research 69, no. 9 (2017): 467-478.

Choumanidis, D., E. Badogiannis, P. Nomikos, and A. Sofianos. "The effect of different fibres on the flexural behaviour of concrete exposed to normal and elevated temperatures." Construction and Building Materials 129 (2016): 266-277.

Conforti, A., G. A. Plizzari, and R. Zerbino. "Vibrated and self-compacting fibre reinforced concrete: experimental investigation on the fibre orientation." In IOP Conference Series: Materials Science and Engineering, vol. 246, no. 1, p. 012019. IOP Publishing, 2017.

Conforti, Antonio, Fausto Minelli, and Giovanni A. Plizzari. "Shear behaviour of prestressed double tees in self-compacting polypropylene fibre reinforced concrete." Engineering Structures 146 (2017): 93-104.

Conforti, Antonio, Fausto Minelli, Andrea Tinini, and Giovanni A. Plizzari. "Influence of polypropylene fibre reinforcement and width-to-effective depth ratio in wide-shallow beams." Engineering Structures 88 (2015): 12-21.

Conforti, Antonio, Fausto Minelli, Giovanni A. Plizzari, and Giuseppe Tiberti. "Comparing test methods for the mechanical characterization of fiber reinforced concrete." Structural Concrete 19, no. 3 (2018): 656-669.

Conforti, Antonio, Giuseppe Tiberti, and Giovanni A. Plizzari. "Combined effect of high concentrated loads exerted by TBM hydraulic jacks." Magazine of Concrete Research 68, no. 21 (2016): 1122-1132.

Conforti, Antonio, Giuseppe Tiberti, Giovanni A. Plizzari, Angelo Caratelli, and Alberto Meda. "Precast tunnel segments reinforced by macro-synthetic fibers." Tunnelling and Underground Space Technology 63 (2017): 1-11.

Conforti, Antonio, Raúl Zerbino, and Giovanni A. Plizzari. "Influence of steel, glass and polymer fibers on the cracking behavior of reinforced concrete beams under flexure." Structural Concrete 20, no. 1 (2019): 133-143.

Daneshfar, M., A. Hassani, M. R. M. Aliha, and F. Berto. "Evaluating Mechanical Properties of Macro-Synthetic Fiber-Reinforced Concrete with Various Types and Contents." Strength of Materials 49, no. 5 (2017): 618-626.

Dawood, Eethar Thanon, and Mahyuddin Ramli. "High strength characteristics of cement mortar reinforced with hybrid fibres." Construction and building materials 25, no. 5 (2011): 2240-2247.

De Alencar Monteiro, Vitor Moreira, and Flávio de Andrade Silva. "Mechanical behaviour of polypropylene and steel fiber self-consolidating concrete." 4th Brazilian Conference on Composite Materials, Rio de Janeiro, 2018.

De la Fuente, Albert, Renata C. Escariz, Antonio D. de Figueiredo, and Antonio Aguado. "Design of macro-synthetic fibre reinforced concrete pipes." Construction and Building Materials 43 (2013): 523-532.

De Rivaz, B., and Y. Ding. "Relevant Perform ance Characterisation Test for Fibre Reinforced Sprayed Concrete."

de Rivaz, Benoit. "Fibre reinforced spray concrete for compliance with site safety requirement." Concreto y cemento. Investigación y desarrollo 2, no. 2 (2011): 48-58.

De Souza Castoldi, Raylane, Lourdes Maria Silva de Souza, and Flávio de Andrade Silva. "Comparative study on the mechanical behavior and durability of polypropylene and sisal fiber reinforced concretes." Construction and Building Materials 211 (2019): 617-628.

Denneman, Erik, Rongzong Wu, Elsabe P. Kearsley, and Alex T. Visser. "Discrete fracture in high performance fibre reinforced concrete materials." Engineering Fracture Mechanics 78, no. 10 (2011): 2235-2245.

Di Maida, Pietro, Corrado Sciancalepore, Enrico Radi, and Federica Bondioli. "Effects of nano-silica treatment on the flexural post cracking behaviour of polypropylene macro-synthetic fibre reinforced concrete." Mechanics Research Communications 88 (2018): 12-18.

Domski, Jacek, and Jacek Katzer. "Load-deflection characteristic of fibre concrete based on waste ceramic aggregate." Annual Set The Environment Protection 15 (2013): 213-230.

Dopko, Michael, Meysam Najimi, Behrouz Shafei, Xuhao Wang, Peter Taylor, and Brent M. Phares. "Flexural performance evaluation of fiber-reinforced concrete incorporating multiple macro-synthetic fibers." Transportation Research Record 2672, no. 27 (2018): 1-12.

Enfedaque, A., M. G. Alberti, J. A. Paredes, and J. C. Gálvez. "Interface properties of polyolefin fibres embedded in self-compacting concrete with a bond improver admixture." Theoretical and Applied Fracture Mechanics 90 (2017): 287-293.

Erdem, Savaş, Andrew Robert Dawson, and Nicholas Howard Thom. "Microstructure-linked strength properties and impact response of conventional and recycled concrete reinforced with steel and synthetic macro fibres." Construction and Building Materials 25, no. 10 (2011): 4025-4036.

Sandbakk, Sindre. "Fibre Reinforced Concrete: Evaluation of test methods and material development." (2011). PhD thesis, Norwegian University of Science and Technology NTNU.

Galeote, Eduardo, Ana Blanco, Sergio HP Cavalaro, and Albert De la Fuente. "Correlation between the Barcelona test and the bending test in fibre reinforced concrete." Construction and Building Materials 152 (2017): 529-538.

Gali, Sahith, and Kolluru VL Subramaniam. "Multi-linear stress-crack separation relationship for steel fiber reinforced concrete: Analytical framework and experimental evaluation." Theoretical and Applied Fracture Mechanics 93 (2018): 33-43.

Garcez, Estela O., Muhammad I. Kabir, Mahbube Subhani, Alastair MacLeod, Andras Fehervari, Mitchell Hall, and Patrick Moulton. "Development of high strength self-compacting fibre reinforced concrete for prefabricated concrete industry." In MATEC Web of Conferences, vol. 275, p. 02011. EDP Sciences, 2019.

Ghaffar, Abdul, Amit S. Chavhan, and Dr RS Tatwawadi. "Steel Fibre reinforced concrete." International Journal of Engineering Trends and Technology (IJETT) 9, no. 15 (2014): 791-797.

Giaccio, G., M. E. Bossio, M. C. Torrijos, and R. Zerbino. "Contribution of fiber reinforcement in concrete affected by alkali–silica reaction." Cement and Concrete Research 67 (2015): 310-317.

Hardy, Nell, Stephen Foster, Ron Cox, Hamid Vali Pour Goudarzi, and Ali Amin. "Investigation into the use of macro synthetic fibre reinforced concrete for breakwater armour units." Coastal Engineering 140 (2018): 60-71.

Hesami, Saeid, Iman Salehi Hikouei, and Seyed Amir Ali Emadi. "Mechanical behavior of self-compacting concrete pavements incorporating recycled tire rubber crumb and reinforced with polypropylene fiber." Journal of cleaner production 133 (2016): 228-234.

Hu, Hang, Panos Papastergiou, Harris Angelakopoulos, Maurizio Guadagnini, and Kypros Pilakoutas. "Mechanical properties of SFRC using blended manufactured and recycled tyre steel fibres." Construction and Building Materials 163 (2018): 376-389.

Ige, Olubisi, S. J. Barnett, Ayman Nassif, and J. B. Williams. "Distribution and orientation of steel fibres in steel fibre reinforced concrete." In 4th International Conference on Advances in Civil, Structural and Construction Engineering, pp. 43-47. IRED, 2016.

Isla, F., B. Luccioni, G. Ruano, M. C. Torrijos, F. Morea, G. Giaccio, and R. Zerbino. "Mechanical response of fiber reinforced concrete overlays over asphalt concrete substrate: experimental results and numerical simulation." Construction and Building Materials 93 (2015): 1022-1033.

Jose, Sujatha, S. J. Stephan, and Ravindra Gettu. "Study of the post-cracking behavior of steel and polymer fibre reinforced concretes." 2nd RN Raikar Memorial Biennial International Conferences & 'Banthia–Basheer International Symposium. Mumbai, India, 2015.

Juhász, K. P., P. Schaul, and L. Nagy. "Effect of the loading rate on fibre reinforced concrete beams." In IOP Conference Series: Materials Science and Engineering, vol. 246, no. 1, p. 012040. IOP Publishing, 2017.

Juhász, Károly Péter, and Péter Schaul. "The effect of age and testing method on the added fracture energy of fibre reinforced concrete." Concrete Structures 20 (2019): 20-24.

Kamasani, Chiranjeevi Reddy, and Kolluru VL Subramaniam. "Experimental evaluation of flexural response and postcracking behavior in macro-synthetic fiber reinforced concrete." (2016): 64-74.

Kazmi, Syed Minhaj Saleem, Muhammad Junaid Munir, Yu-Fei Wu, and Indubhushan Patnaikuni. "Effect of macro-synthetic fibers on the fracture energy and mechanical behavior of recycled aggregate concrete." Construction and Building Materials 189 (2018): 857-868.

Kim, B., A. J. Boyd, H-S. Kim, and S-H. Lee. "Steel and synthetic types of fibre reinforced concrete exposed to chemical erosion." Construction and Building Materials 93 (2015): 720-728.

Kosior-Kazberuk, Marta. "Post-cracking Behaviour and Fracture Energy of Synthetic Fibre Reinforced Concrete." Materials Science 22, no. 4 (2016): 542-547.

Lameiras, Rodrigo, Joaquim Barros, Isabel B. Valente, and Miguel Azenha. "Development of fine aggregatewich panels combining fibre reinforced concrete layers and fibre reinforced polymer connectors. Part I: Conception and pull-out tests." Composite Structures 105 (2013): 446-459.

Lanzoni, Luca, Andrea Nobili, and Angelo Marcello Tarantino. "Performance evaluation of a polypropylene-based draw-wired fibre for concrete structures." Construction and building materials 28, no. 1 (2012): 798-806.

Lee, Su-Jin, and Jong-Pil Won. "Flexural behavior of precast reinforced concrete composite members reinforced with structural nano-synthetic and steel fibers." Composite Structures 118 (2014): 571-579.

Lee, Su-Jin, Se-Ho Kim, and Jong-Pil Won. "Bond-flexural behaviour of structural nano-synthetic fibre-reinforced cementitious composites." Composite Structures 152 (2016): 20-33.

Lee, Su-Jin, Yerin Hong, Ah-Hyeon Eom, and Jong-Pil Won. "Effect of steel fibres on fracture parameters of cementitious composites." Composite Structures 204 (2018): 658-663.

Lerch, J. O., H. L. Bester, A. S. Van Rooyen, R. Combrinck, W. I. de Villiers, and W. P. Boshoff. "The effect of mixing on the performance of macro synthetic fibre reinforced concrete." Cement and Concrete Research 103 (2018): 130-139.

Liu, Xingzi, Mengpei Yan, Isaac Galobardes, and Karol Sikora. "Assessing the potential of functionally graded concrete using fibre reinforced and recycled aggregate concrete." Construction and Building Materials 171 (2018): 793-801.

Llano-Torre, Aitor, Emili García-Taengua, José R. Martí-Vargas, and Pedro Serna. "Compilation and study of a database of tests and results on flexural creep behavior of fibre reinforced concrete specimens." In: FIB Symposium Proceedings. FIB Symposium Concrete Innovation and Design, 18-20 May 2015, Copenhagen, Denmark.

Llano-Torre, Aitor, Samuel Eduardo Arango, Emilio García-Taengua, José Rocío Martí-Vargas, and Pedro Serna. "Influence of fibre reinforcement on the long-term behaviour of cracked concrete." In Creep Behaviour in Cracked Sections of Fibre Reinforced Concrete, pp. 195-209. Springer, Dordrecht, 2017.

López-Buendía, Angel M., María Dolores Romero-Sánchez, Verónica Climent, and Celia Guillem. "Surface treated polypropylene (PP) fibres for reinforced concrete." Cement and Concrete Research 54 (2013): 29-35.

Meda, Alberto, Fausto Minelli, and Giovanni A. Plizzari. "Flexural behaviour of RC beams in fibre reinforced concrete." Composites Part B: Engineering 43, no. 8 (2012): 2930-2937.

Mobasher, Barzin, Mehdi Bakhshi, and Christopher Barsby. "Backcalculation of residual tensile strength of regular and high performance fiber reinforced concrete from flexural tests." Construction and Building Materials 70 (2014): 243-253.

Mohod, Milind V. "Performance of polypropylene fibre reinforced concrete." IOSR Journal of Mechanical and Civil Engineering 12, no. 1 (2015): 28-36.

Mohod, Milind V. "Performance of steel fiber reinforced concrete." International Journal of Engineering and Science 1, no. 12 (2012): 1-4.

Monetti, Diego Hernán, A. Llano-Torre, María Celeste Torrijos, G. Giaccio, Raúl Zerbino, J. R. Martí-Vargas, and P. Serna. "Long-term behavior of cracked fiber reinforced concrete under service conditions." Construction and Building Materials 196 (2019): 649-658.

Navas, F. Ortiz, Juan Navarro-Gregori, G. Leiva Herdocia, P. Serna, and E. Cuenca. "An experimental study on the shear behaviour of reinforced concrete beams with macro-synthetic fibres." Construction and Building Materials 169 (2018): 888-899.

Noushini, Amin, Bijan Samali, and Kirk Vessalas. "Flexural toughness and ductility characteristics of polyvinyl-alcohol fibre reinforced concrete (PVA-FRC)." In Proceedings of the 8th International Conference on Fracture Mechanics of Concrete and Concrete Structures, FraMCoS 2013. 2013.

Noushini, Amin, Kirk Vessalas, and Bijan Samali. "Static mechanical properties of polyvinyl alcohol fibre reinforced concrete (PVA-FRC)." Magazine of Concrete Research 66, no. 9 (2014): 465-483.

Noushini, Amin, Kirk Vessalas, Nassim Ghosni, and Bijan Samali. "Effect of polyvinyl alcohol fibre and fly ash on flexural tensile properties of concrete." In From Materials to Structures: Advancement Through Innovation-Proceedings of the 22nd Australasian Conference on the Mechanics of Structures and Materials, pp. 1165-1170. 2013.

Noushini, Amin, Max Hastings, Arnaud Castel, and Farhad Aslani. "Mechanical and flexural performance of synthetic fibre reinforced geopolymer concrete." Construction and Building Materials 186 (2018): 454-475.

Oliari Garcez, Estela, Muhammad Ikramul Kabir, Alastair MacLeod, Mahbube Subhani, and Kazem Ghabraie. "Self-Compacting Concrete Reinforced with Twisted-Bundle Macro-Synthetic Fiber." Applied Sciences 9, no. 12 (2019): 2543.

Ortega-López, V., V. Revilla-Cuesta, M. Skaf, F. Fiol, A. Santamaría, A. García-Llona, and I. Piñero. "Fracture toughness evaluation of fiber-reinforced concrete manufactured with siderurgic aggregates."

Pająk, M., and T. Ponikiewski. "Flexural behavior of self-compacting concrete reinforced with different types of steel fibers." Construction and Building Materials 47 (2013): 397-408.

Papayianni, I., and M. Papachristoforou. "Effect of high temperatures on steel fiber reinforced concrete with EAF slag aggregates."

Park, Kyoungsoo, Glaucio H. Paulino, and Jeffery Roesler. "Cohesive fracture model for functionally graded fiber reinforced concrete." Cement and concrete research 40, no. 6 (2010): 956-965.

Parmentier, Benoit, Niki Cauberg, and Lucie Vandewalle. "Shear resistance of macro-synthetic and steel fibre reinforced concrete beams without stirrups." In 8th RILEM International Symposium on Fiber Reinforced Concrete: Challenges and Opportunities. 2012.

Pelisser, Fernando, Oscar Rubem Klegues Montedo, Philippe Jean Paul Gleize, and Humberto Ramos Roman. "Mechanical properties of recycled PET fibers in concrete." Materials research 15, no. 4 (2012): 679-686.

Pešić, Ninoslav, Stana Živanović, Reyes Garcia, and Panos Papastergiou. "Mechanical properties of concrete reinforced with recycled HDPE plastic fibres." Construction and building materials 115 (2016): 362-370.

Picazo, Álvaro, Marcos G. Alberti, Jaime C. Gálvez, Alejandro Enfedaque, and Abner C. Vega. "The size effect on flexural fracture of polyolefin fibre-reinforced concrete." Applied Sciences 9, no. 9 (2019): 1762.

Ponikiewski, Tomasz, and Jacek Katzer. "X-ray computed tomography of fibre reinforced self-compacting concrete as a tool of assessing its flexural behaviour." Materials and Structures 49, no. 6 (2016): 2131-2140.

Pujadas, Pablo, Ana Blanco, Sergio Cavalaro, Albert de la Fuente, and Antonio Aguado. "Fibre distribution in macro-plastic fibre reinforced concrete slab-panels." Construction and building materials 64 (2014): 496-503.

Pujadas, Pablo, Ana Blanco, Sergio H. Cavalaro, Albert De la Fuente, and Antonio Aguado. "Flat suspended slabs reinforced only with macro-synthetic fibres." (2016).

Rana, Amit. "Some studies on steel fiber reinforced concrete." International journal of emerging technology and advanced engineering 3, no. 1 (2013): 120-127.

Rasheed, M. Abdur, S. Suriya Prakash, Gangadharan Raju, and Yuma Kawasaki. "Fracture studies on synthetic fiber reinforced cellular concrete using acoustic emission technique." Construction and Building Materials 169 (2018): 100-112.

Reddy, K. Chiranjeevi, and Kolluru VL Subramaniam. "Analysis for multi-linear stress-crack opening cohesive relationship: Application to macro-synthetic fiber reinforced concrete." Engineering Fracture Mechanics 169 (2017): 128-145.

Richardson, A. E., and P. Jackson. "Equating steel and synthetic fibre concrete post crack performance." In 2nd International Conference on Current Trends in Technology, NUiCONE, December 8–10. Nirma University Ahmedabad, India, 2011.

Richardson, Alan, and David Batey. "Impact resistance of concrete using dovetailed fibres and type 2 synthetic fibres." (2015).

Richardson, Alan, and Kathryn Coventry. "Dovetailed and hybrid synthetic fibre concrete–impact, toughness and strength performance." Construction and Building Materials 78 (2015): 439-449.

Richardson, Alan, and Rhys Ovington. "Performance of fibre concrete with regard to temperature." (2017). In 1st International Conference on Construction Materials for Sustainable Future (pp. 19-21).

Richardson, Alan, and Rhys Ovington. "Temperature related steel and synthetic fibre concrete performance." Construction and Building Materials 153 (2017): 616-621.

Richardson, Alan, Kathryn Coventry, Thomas Lamb, and David Mackenzie. "The addition of synthetic fibres to concrete to improve impact/ballistic toughness." Construction and Building Materials 121 (2016): 612-621.

Rooholamini, H., A. Hassani, and M. R. M. Aliha. "Evaluating the effect of macro-synthetic fibre on the mechanical properties of roller-compacted concrete pavement using response surface methodology." Construction and Building Materials 159 (2018): 517-529.

Sahoo, Dipti Ranjan, Kaushik Maran, and Avdhesh Kumar. "Effect of steel and synthetic fibers on shear strength of RC beams without shear stirrups." Construction and Building Materials 83 (2015): 150-158.

Sengün, E., Burhan Alam, and İ. Ö. Yaman. "Effect of synthetic fibers on flexural performance of normal and high performance concrete." In Proc., 9th RILEM Int. Symp. on Fiber Reinforced Concrete. 2016.

Shende, A. M., A. M. Pande, and M. Gulfam Pathan. "Experimental study on steel fiber reinforced concrete for M-40 grade." International Refereed Journal of Engineering and Science 1, no. 1 (2012): 043-048.

Shinde, Pravin B., Sangita V. Pawar, and V. P. Kulkarni. "Flexural behaviour of hybrid fiber reinforced concrete deep beam and effect of steel polypropylene fiber on mechanical properties of concrete." Int. J. Adv. Res. Sci. Eng 4, no. 2 (2015): 62-73.

Simões, T., H. Costa, D. Dias-da-Costa, and E. N. B. S. Júlio. "Influence of fibres on the mechanical behaviour of fibre reinforced concrete matrixes." Construction and Building Materials 137 (2017): 548-556.

Singh, S. P., A. P. Singh, and V. Bajaj. "Strength and flexural toughness of concrete reinforced with steel-polypropylene hybrid fibres." (2010): 495-507.

Soutsos, M. N., T. T. Le, and A. P. Lampropoulos. "Flexural performance of fibre reinforced concrete made with steel and synthetic fibres." Construction and building materials 36 (2012): 704-710.

Stephen, J. S., R. Gettu, and R. Raphael. "Effect of loading rate on the fracture behavior of fibre reinforced concrete." In 9th international conference on fracture mechanics of concrete

and concrete structures, Proceedings FraMCoS-9. https://doi. org/10.21012/FC9, vol. 71. 2016.

Sukontasukkul, Piti, and Pitthaya Jamsawang. "Use of steel and polypropylene fibers to improve flexural performance of deep soil–cement column." Construction and Building Materials 29 (2012): 201-205.

Tiberti, Giuseppe, Antonio Conforti, and Giovanni A. Plizzari. "Precast segments under TBM hydraulic jacks: Experimental investigation on the local splitting behavior." Tunnelling and Underground Space Technology 50 (2015): 438-450.

Vandevyvere, Brecht, Zeger Sierens, Miquel Joseph, Paul Jonckheere, Luc Decraemer, and Jiabin Li. "Effect of PP fibres on flexural behaviour of concrete with RCAs–A preliminary study." In Proceedings of The 12th fib International PhD Symposium in Civil Engineering, pp. 1259-1265. Czech Technical University in Prague, 2018.

Vrijdaghs, Rutger, Marco di Prisco, and L. Vandewalle. "Creep of cracked polymer fiber reinforced concrete under sustained tensile loading." In FRAMCOS 9, pp. 1-9. University of California, Berkeley Clark Kerr Campus, 2016.

Wang, Jun-Yan, Nemkumar Banthia, and Min-Hong Zhang. "Effect of shrinkage reducing admixture on flexural behaviors of fiber reinforced cementitious composites." Cement and Concrete Composites 34, no. 4 (2012): 443-450.

Won, Jong-Pil, Byung-Tak Hong, Tei-Joon Choi, Su-Jin Lee, and Joo-Won Kang. "Flexural behaviour of amorphous micro-steel fibre-reinforced cement composites." Composite Structures 94, no. 4 (2012): 1443-1449.

Yang, In-Hwan, Changbin Joh, and Byung-Suk Kim. "Flexural response predictions for ultra-high-performance fibre-reinforced concrete beams." Magazine of Concrete Research 64, no. 2 (2012): 113-127.

Yazdanbakhsh, Ardavan, Salah Altoubat, and Klaus-Alexander Rieder. "Analytical study on shear strength of macro synthetic fiber reinforced concrete beams." Engineering Structures 100 (2015): 622-632.

Yehia, Sherif, AlaEddin Douba, Omar Abdullahi, and Sharef Farrag. "Mechanical and durability evaluation of fiber-reinforced self-compacting concrete." Construction and Building Materials 121 (2016): 120-133.

Yew, Ming Kun, Hilmi Bin Mahmud, Bee Chin Ang, and Ming Chian Yew. "Influence of different types of polypropylene fibre on the mechanical properties of high-strength oil palm shell lightweight concrete." Construction and Building Materials 90 (2015): 36-43.

Yin, Shi, Rabin Tuladhar, Jacob Riella, David Chung, Tony Collister, Mark Combe, and Nagaratnam Sivakugan. "Comparative evaluation of virgin and recycled polypropylene fibre reinforced concrete." Construction and building materials 114 (2016): 134-141.

Yin, Shi, Rabin Tuladhar, Tony Collister, Mark Combe, Nagaratnam Sivakugan, and Zongcai Deng. "Post-cracking performance of recycled polypropylene fibre in concrete." Construction and Building Materials 101 (2015): 1069-1077.

Yu, R., P. Spiesz, and H. J. H. Brouwers. "Development of Ultra-High Performance Fibre Reinforced Concrete (UHPFRC): Towards an efficient utilization of binders and fibres." Construction and building materials 79 (2015): 273-282.

Zamanzadeh, Ziaaddin, Lúcio Lourenço, and Joaquim Barros. "Recycled steel fibre reinforced concrete failing in bending and in shear." Construction and Building Materials 85 (2015): 195-207.

Zerbino, R., Diego Hernán Monetti, and G. Giaccio. "Creep behaviour of cracked steel and macro-synthetic fibre reinforced concrete." Materials and Structures 49, no. 8 (2016): 3397-3410.

Zerbino, R., J. M. Tobes, M. E. Bossio, and G. Giaccio. "On the orientation of fibres in structural members fabricated with self compacting fibre reinforced concrete." Cement and Concrete Composites 34, no. 2 (2012): 191-200.